GEORGIA DOT RESEARCH PROJECT 12-28

FINAL REPORT

OPERATING PERFORMANCE OF DIVERGING DIAMOND INTERCHANGES

Georgia Department of Transportation

OFFICE OF PERFORMANCE-BASED MANAGEMENT AND RESEARCH

15 KENNEDY DRIVE

FOREST PARK, GA 30297-2534

GDOT Research Project 12-28

Final Report

OPERATING PERFORMANCE OF DIVERGING DIAMOND INTERCHANGES

By

Angshuman Guin, Ph.D., Principal Investigator
Michael Hunter, Ph.D., co-Principal Investigator
Michael Rodgers, Ph.D., Investigator
James Anderson, Graduate Research Assistant
Sung Jun Park, Graduate Research Assistant

School of Civil and Environmental Engineering, Georgia Institute of Technology

Contract with

Georgia Department of Transportation

In cooperation with

U.S. Department of Transportation
Federal Highway Administration

August 2018

Technical Report Documentation Page

1. Report No.: FHWA-GA-18-1228	2. Government Accession No.:	3. Recipient's Catalog No.:
4. Title and Subtitle: **Operating Performance of Diverging Diamond Interchanges**		5. Report Date: August 2018 6. Performing Organization Code:
7. Author(s): Angshuman Guin, Ph.D.; Michael Hunter, Ph.D.; Michael Rodgers, Ph.D.; James Anderson; Sung Jun Park		8. Performing Organization Report No. 2006U97
9. Performing Organization Name and Address: Georgia Institute of Technology School of Civil and Environmental Engineering Atlanta, GA 30332-0355		10. Work Unit No.: 11. Contract or Grant No.: 0011746
12. Sponsoring Organization Name and Address: Georgia Department of Transportation Office of Performance-based Management and Research 15 Kennedy Drive Forest Park, GA 30297-2534		13. Type of Report & Period Covered: Final; August 2013 – February 2018 14. Sponsoring Agency Code:
15. Supplementary Notes: Prepared in cooperation with the U.S. Department of Transportation, Federal Highway Administration.		

16. Abstract:

As the result of changing traffic patterns, many conventional intersections and interchanges can no longer accommodate growing traffic volumes and heavy turning movements. In response, there are various innovative intersection and interchange designs proposed and implemented to better accommodate these changes, and the diverging diamond interchange (DDI) is one of these alternatives. This effort conducts a sensitivity analysis of conventional diamond interchange (CDI) and DDI operational performance under various interchange lane configurations, including the selected study area of the Jimmy Carter Blvd. and I-85 interchange in Norcross, Georgia, under varying traffic demands and turn-movement ratios. The sensitivity analysis explores the detailed conditions in which one interchange configuration provides superior performance over the other. The sensitivity analysis is structured into a two-step process with a critical lane volume (CLV) analysis as the first step, followed by a VISSIM microscopic simulation study as the second step. Overall, the study found that a CDI is likely the preferred option at locations with traffic volumes well below capacity and cross-street left-turn traffic proportions below 30% of the total cross-street demand, and a DDI is likely preferred at locations with traffic volumes near capacity and cross-street left-turn proportions exceeding 50% of the total cross-street demand.

17. Key Words: Diverging Diamond Interchange, Operational Evaluation		18. Distribution Statement	
19. Security Class (This Report): Unclassified	20. Security Class (This Page): Unclassified	21. No of Pages: 71	22. Price

Form DOT F 1700.7 (8/72) Reproduction of form and completed page is authorized

TABLE OF CONTENTS

LIST OF TABLES

LIST OF FIGURES

LIST OF SYMBOLS AND ABBREVIATIONS

CAP-X	Capacity Analysis for Planning of Junctions
CDI	Conventional Diamond Interchange
CLV	Critical Lane Volume
DCD	Double Crossover Diamond Interchange
DDI	Diverging Diamond Interchange
DLT	Displaced Left-Turn Intersection
DOT	Department of Transportation
DXI	Double Crossover Interchange
FHWA	Federal Highway Administration
HCM	Highway Capacity Manual
LC	Lane Configuration
LUF	Lane Utilization Factor
MoDOT	Missouri Department of Transportation
MOE	Measure of Effectiveness
mph	Miles per Hour
MUT	Median U-Turn
ParClo	Partial Cloverleaf
ROW	Right-of-Way
SPUI	Single-Point Urban Interchange
USC	Upstream Signalized Crossover
v/c	Volume-to-Capacity

VB	Visual Basic
vph	Vehicle per Hour
vphrpln	Vehicle per Hour per Lane
XDL	Crossover Displaced Left-Turn

EXECUTIVE SUMMARY

Due to changing traffic patterns, many conventional intersections and interchanges can no longer accommodate growing traffic volumes and heavy turning movements. In response, there are various innovative intersection and interchange designs proposed and implemented to better accommodate these changes, and the diverging diamond interchange (DDI) is one of these alternatives. The DDI is designed to better accommodate heavy left-turn movements, and it provides simplified signal operations with fewer phases and reduced lost times compared to a conventional diamond interchange (CDI). Previous studies have also found safety and cost benefits of the DDI in comparison to conventional interchange designs.

To contribute to these studies, this effort aims to conduct a sensitivity analysis of CDI and DDI operational performance under various interchange lane configurations, including the selected study area of the Jimmy Carter Blvd. and I-85 interchange in Norcross, Georgia, under varying traffic demands and turn-movement ratios. The sensitivity analysis explores the detailed conditions in which one interchange configuration provides superior performance over the other. A literature review is conducted on the DDI background and concepts, the benefits and costs of a DDI in comparison to the CDI and other unconventional interchange designs, and the methodologies used in previous studies on CDI and DDI operational performance analysis.

The sensitivity analysis is structured into a two-step process. First, a critical lane volume (CLV) method calculates the volume-to-capacity (v/c) ratio of each interchange design using the capacity and volume equations from the Highway Capacity Manual (HCM

2010). This CLV method allows for a quick analysis of a large number of traffic scenarios. The second part of the analysis is a VISSIM microscopic simulation study. The simulation study is conducted for a subset of the demand scenarios to confirm the comparative performance findings of the CLV analysis. VISSIM allows users to control multiple traffic parameters and allows for more detailed analysis of the network operational performance with various operational measures, such as average delay per vehicles, throughput, queue length, and average number of stops per vehicle for individual turning movements, as well as for the entire interchange.

From the CLV analysis, the CDI is found to perform better or similar to the DDI when the cross-street left-turn proportion onto the freeway entrance ramp is below 30% of the total cross-street demand, and in most cases the DDI outperforms the CDI at left-turn proportions exceeding 50%. The CDIs and DDIs were found to have similar performance in the through/left-turn proportion ranges of 70/30 and 50/50, often dependent on cross street cross sections. As the number of cross-street lanes increases, especially left-turn lanes, the left-turn proportion required for the DDI to provide favorable performance increases. Similar results are found in the VISSIM simulation study based on the average delay per vehicle and average throughput of the CDI and DDI configurations over different through/left-turn proportions. The CDI configuration is also found to have better performance at low cross-street demands at given through/left-turn proportion, although the CDI operational performance degrades more rapidly than that of the DDI at high cross-street demands. The impact of freeway off-ramp demands on the operational performance is inconclusive.

Overall, the study found that a CDI is likely the preferred option at locations with traffic volumes well below capacity and cross-street left-turn traffic proportions below 30% of the total cross-street demand, and a DDI is likely preferred at locations with traffic volumes near capacity and cross-street left-turn proportions exceeding 50% of the total cross-street demand. Findings from this study can support planning and decision-making processes associated with the implementation of DDIs.

CHAPTER 1. INTRODUCTION

Rapidly growing traffic demand and changing traffic patterns have led to the operational failure of many segments of the existing transportation infrastructure (Chlewicki 2003). According to the 2015 Urban Mobility Scorecard, the national yearly average delay per commuter in 2014 was 42 hours, and the total cost of congestion was $160 billion. In the same year, Atlanta, Georgia, recorded a yearly delay per commuter of 52 hours, which ranked twelfth among large urban areas with population over 3 million, and had a congestion cost of $1,130 per commuter. However, conventional solutions to these problems, e.g., adding more lanes and building more infrastructure, are becoming increasingly difficult to implement. It is becoming more problematic to find sufficient funding and right-of-way to expand roadways. Consequently, traffic engineers are seeking innovative intersection and interchange designs to better accommodate these challenges. The diverging diamond interchange (DDI) is one such innovative intersection that is receiving increasing interest in the United States.

A DDI is an unconventional interchange design that eliminates the left-turn - opposing through vehicle conflict from the conventional diamond interchange (CDI). Its design may offer additional benefits compared to conventional diamond interchanges. In a DDI, the cross-street traffic is diverted to travel on the left side (as opposed to all traffic on the right) of the bridge. The changeover of sides of travel is facilitated at the bridge ends. A DDI reduces total conflict points from 30 within a traditional diamond interchange to 18, provides free-flow travel to the left-turning traffic, as well as reduces the signal to two phases. A DDI provides superior operational performance to a traditional diamond interchange under high left-turn movements onto and off a freeway.

Georgia's first diverging diamond interchange, Ashford Dunwoody DDI at I-285, opened to drivers in June 2012. Shortly afterward, two more DDIs were built on Pleasant Hill Road at I-85 and on Jimmy Carter Blvd. at I-85. This current project was undertaken during the planning stage of the Jimmy Carter Blvd. interchange to enable performance evaluation at that site to determine how operational efficiency has improved under Georgia driving conditions, to determine under what conditions a DDI may provide superior performance to a traditional diamond interchange, and to allow for potential improvements in future proposed DDIs.

1.1 Background

The DDI, also called a double crossover diamond interchange (DCD), was first introduced in the United States by Gilbert Chlewicki in 2003. A DDI has crossovers on each side of an interchange to move traffic onto the left side of the road, which is opposite to conventional traffic movement. A DDI eliminates left-turn vehicle conflicts with other movements, allowing for free-flow left-turn operation. Many studies have suggested that a DDI improves the operation of turning movements and significantly reduces the number of vehicle-to-vehicle conflict points compared to a conventional diamond interchange.

Since the first DDI opened at I-44 and MO-13 in Springfield, Missouri, on June 21, 2009, 89 DDIs have been built in the United States (as of July 2017) with many more being planned (Chlewicki 2014). There are five DDIs currently in operation in the state of Georgia.

1.2 Project Goals and Scope

Although previous studies have examined the operational performance of a DDI and compared it to other interchange designs, there currently are no guidance or criteria that specify conditions that justify the conversion of a CDI into a DDI. Therefore, the primary objective of this study is to evaluate the comparative operational performance of CDI and DDI configurations across a range of traffic demands and turn-movement ratios. To achieve this goal, a sensitivity analysis of the operational performance under CDIs and DDIs is conducted for three different lane configurations, including the before–after lane configuration at the selected Jimmy Carter Blvd. and I-85 interchange in Norcross, Georgia.

Independent variables tested in the sensitivity analysis are traffic demand and turn-movement ratio, which are two critical variables in the operation of an interchange. These independent variables are tested among different interchange lane configurations to increase the applicability of the findings. The sensitivity analysis is conducted in a two-step process: (1) a critical lane volume (CLV) analysis, and (2) a VISSIM simulation study. Primary measures of effectiveness (MOEs) collected in the study are volume-to-capacity (v/c) ratio and average delay per vehicle, with additional measures of travel time, queue length, and average number of stops per vehicle collected. The scope of the study is limited to the interchange, including off- and on-ramps, bridge segment, and cross streets entering the bridge, and does not include adjacent intersections. This scope limits the number of confounding variables, enhancing the ability to conduct the analysis in a reasonable timeframe and interpret the results.

1.3 Report Organization

This report is organized in the following manner. CHAPTER 2 presents a literature review on the DDI background and concepts, benefits, and costs of a DDI in comparison to a CDI and other unconventional interchange designs, and methodologies used in previous studies on DDI operational performance. CHAPTER 3 presents the methodology, performance measures, and analysis techniques used in this study. CHAPTER 4 highlights and evaluates the results of the sensitivity analysis using the CLV method and the VISSIM simulation study. CHAPTER 5 concludes with a results summary, study limitations, and potential future research. Operational performance–related data were collected at the beginning of the study, and analysis of the pre-deployment traffic patterns was performed. However, the study focused on providing guidance on when DDIs are more advantageous than CDIs; hence, a before–after evaluation based on field data was not performed. The pre-deployment field data analysis is provided in Appendix A.

CHAPTER 2. LITERATURE REVIEW

This literature review provides an overview and background for the diverging diamond interchange layout and operation, analyses, and methodologies, as well as published operational performance comparisons of DDIs with conventional diamond interchanges.

2.1 Diverging Diamond Interchange Design

The DDI is an innovative interchange design first introduced in the United States by Gilbert Chlewicki in 2003 at the 2nd Urban Street Symposium in Anaheim, California (Chlewicki 2003). Figure 1 shows the vehicle movement layout of a DDI. The freeway access and egress are the same for a CDI and a DDI; however, in a DDI, through and left-turn traffic on the cross streets traverse over to the opposite side (left side) of the roadway between ramp terminals (Bared et al. 2005). In this configuration, the cross-street traffic enters the freeway on-ramps uninterrupted, i.e., without a conflict point, eliminating the need for dedicated left-turn phasing from the cross street to the freeway ramp. Thus, a DDI may accommodate heavier left-turn demand than a CDI. As illustrated in Figure 1, a DDI has two traffic signal–controlled conflict points, one at each crossover. A two-phased timing plan is implemented at each crossing point with the freeway off-ramp phase simultaneous with the non-conflicting cross-street direction of traffic. As a result of the crossovers, through movements in each direction follow a split-phased timing pattern, unlike those in a CDI where through movements typically receive concurrent green indications.

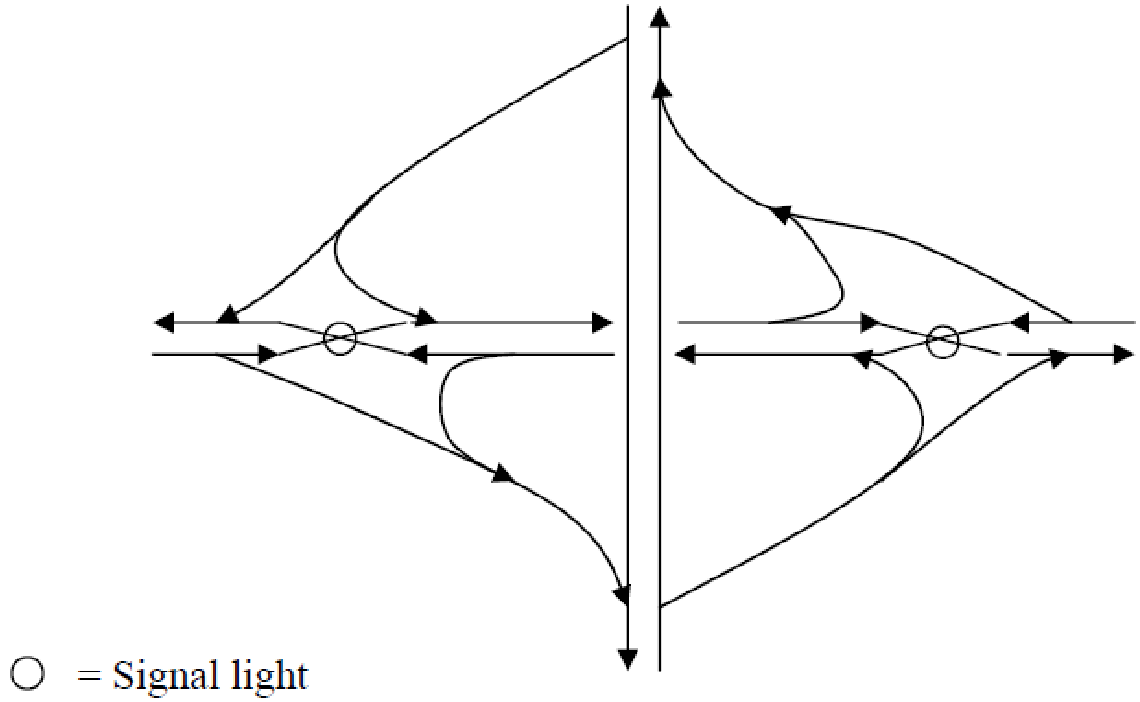

Figure 1: Layout of a diverging diamond interchange (Chlewicki 2003)

Prior to Chlewicki's introduction of the concept in the United States in 2003, the DDI configuration existed in Versailles, France, at Autoroute de Normandie and Blvd. de Jardy (Chlewicki 2014). The first DDI in the United States opened in June 2009 at the I-44 and SR-13 interchange in Springfield, Missouri. Currently there are 89 DDIs in operation in the United States with the number planned for construction increasing every year (Chlewicki 2014). DDIs are seeing increasing interest in the United States due to their low construction costs and right-of-way (ROW) needs, as well as reasonable traffic operations and safety improvements (Chlewicki 2003; Bared et al. 2005; Edara et al. 2005; Sharma and Chatterjee 2007; Speth 2008; Missouri Department of Transportation 2010; Chilukuri et al. 2011; Chlewicki 2011; Galletebeitia 2011; Khan and Anderson 2016). The following section discusses DDI benefits and costs in more detail.

2.2 Diverging Diamond Interchange Costs and Benefits

Various cost/benefit studies have explored DDI performance related to operations, safety, construction costs, etc. This section summarizes several of those studies, as well as prior research comparing DDIs to CDIs and other unconventional interchange designs.

2.2.1 Operational Performance of DDI vs. Other Interchange Designs

2.2.1.1 <u>DDI vs. CDI</u>

Chlewicki's first DDI study (2003) compared the original design of the interchange at I-695 and MD 140 in Baltimore County, Maryland, to a DDI with the same lane configurations and traffic volumes. Chlewicki found that the total number of stops, total delay, and stop delay at the CDI were two-, three-, and four-fold, respectively, that of the DDI.

Edara et al. (2005) compared DDIs having two different lane configurations (four- and six-lane) and a CDI (six-lane), for four different traffic scenarios. The study found similar performance of both DDIs and the CDI design at low-to-medium volumes, but the DDIs outperformed the CDI in all performance measures at high volumes. The DDIs also had a higher maximum off-ramp capacity of 700 vehicles per hour per lane (vphrpln) compared to the CDI with 390 vphrpln. For both DDI lane configurations tested, the capacity of the cross-street left turn to the freeway on-ramp was twice that of the CDI, a benefit of the left movement being uninterrupted (i.e., moving throughout the cycle).

Other studies conducted by Bared et al. (2005), Sharma and Chatterjee (2007), and Speth (2008) concluded that DDIs outperformed CDIs in most tested traffic scenarios, and the difference in performance was larger at high flow levels and heavy left-turn movements.

All these studies showed that DDIs operated better than CDIs despite fewer lanes on the bridge segment. Bared et al. (2005) also found that capacities of all signalized movements were higher for the DDI and that the DDI cross-street to on-ramp left-turn movement capacity was twice that of the CDI.

Chilukuri et al. (2011) conducted a before-and-after analysis of the DDI at I-44 and Route 13 in Springfield, Missouri, and concluded that overall traffic flow through the DDI improved relative to the former CDI. Despite the increase in traffic volumes after DDI implementation, the DDI had significantly lower delay and queuing for left-turn movements than the CDI. The DDI had a slight increase in the through-movement travel time due to slower speeds through the crossover intersections during off-peak periods. Chilukuri et al. also highlighted that oversized loads up to 18 ft wide and 200 ft long successfully moved through the DDI.

In addition to higher left-turn movement capacity, the DDI's operational benefits also come from its ability to combine phases that conflict in the CDI configuration. For instance, freeway on- and off-ramp phases can be combined with mainline through movements. Also, the reduction of a phase compared to a CDI reduces lost time in a cycle, and, thus, reduces delay (Chlewicki 2003). Similar findings were observed in a Missouri Department of Transportation (MoDOT) report based on MoDOT's experience with DDIs (2010). MoDOT found that signal operations were improved by converting from a CDI to a DDI, having fewer phases, a shorter cycle length, and lower lost time.

Even with those documented benefits, a DDI is not the solution for all traffic conditions. Khan and Anderson (2016) evaluated DDIs as a possible solution for existing interchanges in Athens, Alabama, by testing 83 traffic scenarios. Their results show that only four scenarios had lower delay for the DDI, likely due to relatively low turning movements relative to the through movements. Chlewicki (2011) suggested that while DDI is not the best option in each case, there is sufficient evidence to suggest that a DDI should always be considered in an interchange improvement analysis. The results from that experiment with 15,626 volume combinations show that the DDI has superior operations to the CDI when costs are similar, and the DDI is the better option if an interchange requires more lanes to accommodate higher traffic volumes.

2.2.1.2 Comparison with Other Interchange Design Alternatives

Additional studies have explored DDI performance in comparison to other unconventional interchange design alternatives. Speth (2008) was one of the first to compare the operational performance of a DDI to a single-point urban interchange (SPUI). The study found that the SPUI performs slightly better than the DDI at low-volume scenarios, but the DDI outperforms the SPUI in all other scenarios in vehicle throughput, average delay per vehicle, and average number of stops per vehicle, and it requires fewer lanes in the bridge section.

Galletebeitia (2011) conducted a study to compare and evaluate the operational performance between a DDI and partial cloverleaf (ParClo) interchanges using the microscopic simulation platform, AIMSUN. Of all U.S. interchanges, 16% are a ParClo configuration. ParClo interchanges are often selected for their accommodation of heavy left-turn movements, similar to a DDI. There are several ParClo interchange configurations, categorized as ParClo A (indicating a cloverleaf configuration on an on-ramp), ParClo B (cloverleaf configuration on an off-ramp), and ParClo AB (cloverleaf configuration on both the on- and off-ramps). In addition, a ParClo configuration may utilize from one to four quadrants for the interchange. Figure 2 shows six types of ParClo interchange (Zhang and Zong 2010). Zhang and Zong conducted a study focused on evaluating ParClo A4 and ParClo B4 interchanges, and four-lane and six-lane DDIs (DDI-4, DDI-6). The study tested 10 volume scenarios in balanced and unbalanced conditions, and found that the DDI and ParClo interchange performances are similar at low-to-medium volumes in both balanced and unbalanced conditions. In the balanced condition, ParClo interchanges experienced lower delays, stop times, and number of stops compared to the DDIs, although the difference in delay between DDI-6 and ParClo B4 decreased as the traffic flow increased. The ParClo B4 resulted in the longest maximum queue as the flow increased. In the unbalanced condition, ParClo B4 showed the best results in all measures at low-to-medium volumes, but both DDI-4 and DDI-6 resulted in better performance than the ParClo interchanges as the flow increased. The study concluded that ParClo interchanges perform better in balanced conditions with low-to-medium traffic flow, and DDIs perform better in unbalanced conditions at high flow.

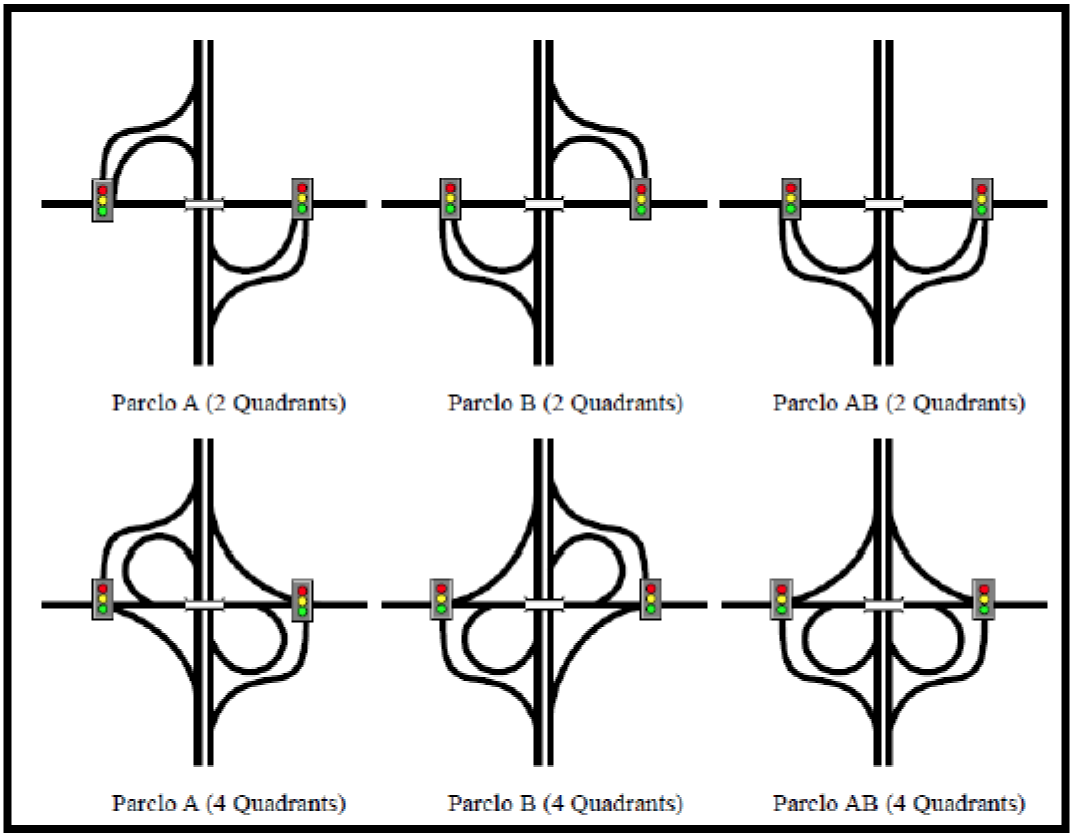

Figure 2: Six types of partial cloverleaf (Zhang and Zong 2010)

Autey et al. (2012) conducted a study to compare the operational performance of four unconventional intersection designs—crossover displaced left-turn (XDL), upstream signalized crossover (USC), double crossover intersection (DXI), and median U-turn (MUT)—as well as a conventional intersection with equal lane configurations in balanced and unbalanced volume conditions. The DXI may intuitively be thought of as the intersection form of the DDI, with mainline traffic passing through the intersection with left-hand side travel, resulting in free flow left turn movement from the mainline. The results showed that all the tested unconventional designs performed better than the conventional intersection in most cases, and the improvements became more significant at high traffic volumes. Among the tested unconventional designs, the XDL consistently outperformed other designs under both balanced and unbalanced volume conditions, especially at high volumes. In balanced traffic volumes, XDL, USC, and DXI performed equally well for moderate approach volumes (1100–1500 veh/hr), but for approach volumes higher than 1500 veh/hr, the XDL outperformed the other intersections. In unbalanced conditions, the XDL outperformed other intersection designs in all volume scenarios. The DXI performed better than the USC in most unbalanced conditions (i.e., ratio between the minor and the major street volumes less than 70%). The MUT resulted in the highest average delay per vehicle, especially with high approach volumes and heavy left-turning ratios. However, the XDL and the MUT designs require greater right-of-way to accommodate their designs, and hence, may not be appropriate alternatives to a conventional intersection in many cases.

2.2.2 Other Benefits and Costs

Numerous studies suggest that the DDI has several safety benefits over other interchange designs. Its unique design eliminates left-turn movement conflicts. With 24 and 30 conflict points, respectively, both the SPUI and the CDI have more conflict points than a DDI, which has 18 (Chlewicki 2003; Cogan 2008; MoDOT 2010; Ressel 2012). Figure 3 shows the conflict diagrams of a CDI, a DDI, and a SPUI.

A DDI also provides for easier U-turn movements on a limited-access highway, allowing a vehicle to return to a missed exit (MoDOT 2010). In a CDI, drivers must go through two signalized left turns to re-enter the highway, whereas, for a DDI, a returning vehicle must pass through only one signal as the on-ramp left-turn is uninterrupted. A DDI also eliminates wrong-way movements to and from ramps. However, in the DDI interchange configuration, the intersection crossover prohibits a vehicle's through movement from an off-ramp to an on-ramp to re-enter the highway.

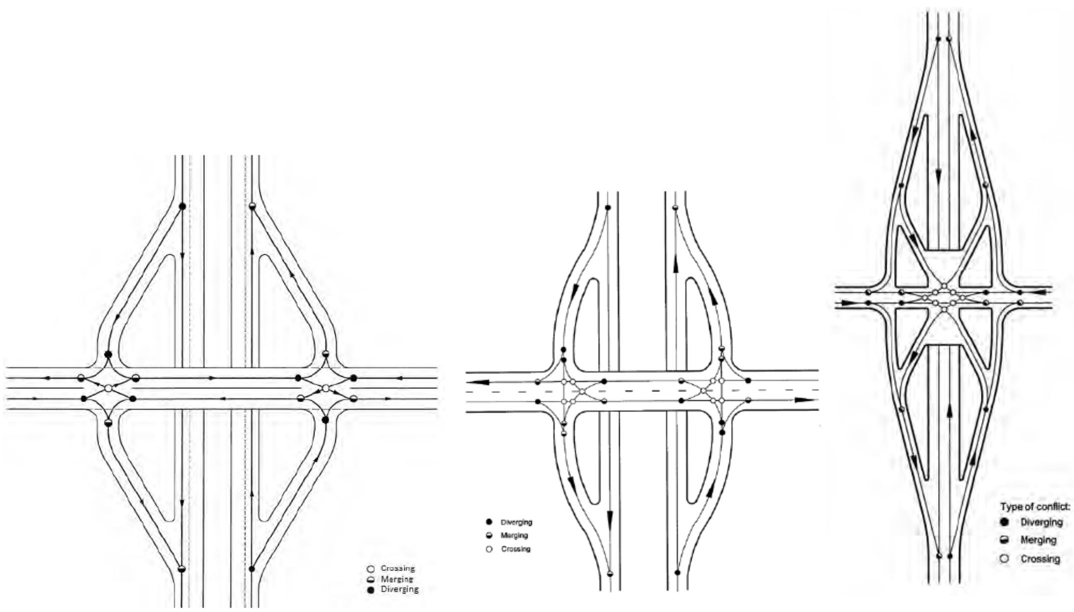

(a) (b) (c)

Figure 3: Conflict diagram of (a) DDI, (b) CDI, and (c) SPUI (MoDOT 2010)

A concern related to the DDI configuration is the potential for confusion given the unfamiliarity of drivers with the crossover intersections and driving on the left side of the road. However, this disadvantage can be mitigated through an aggressive public information campaign and appropriate education by states and cities (Chlewicki 2003; MoDOT 2010). According to an online and telephone survey conducted by Chilukuri (2011) on the DDI at I-44 and Route 13, 91% of participants expressed a good understanding of the operation of the DDI and more than 80% stated that the traffic flow had improved and delay had decreased with the DDI conversion. Several studies argued against the crossover intersection concern, stating that the driver unfamiliarity has a calming effect by encouraging slower speeds while approaching and crossing the interchange, thus serving as a potential safety benefit (MoDOT 2010; Ressel 2012). According to the MoDOT survey, 97% of drivers said they feel safer in the DDI than the previous CDI. A five-month comparison of crash data for the DDI in Springfield, Missouri, shows a 60% reduction over the previous diamond interchange (MoDOT 2010). The crash data review by Chilukuri (2011) also shows a 46% decrease in total crashes in the first year of operation of the DDI, elimination of left-turn crashes, and a decrease in angle and rear-end crashes.

A DDI is also known to have lower construction cost compared to other interchange alternatives. In many cases, an existing bridge can be used for the DDI conversion, though the DDI may require additional right-of-way compared to a CDI to allow median and ramp terminals to bend into the road. Hughes et al. (2010) found that a four-lane DDI performs at a similar level as a six-lane CDI, and a six-lane DDI performs similar to an eight-lane CDI. This reduction in lanes indicates that a DDI in many cases may provide a similar or better level of operation with little or no additional right-of-way from the existing CDI. A DDI also requires less right-of-way than a SPUI or displaced left-turn intersection (DLT), and similar right-of-way but higher capacity than a ParClo interchange (Chlewicki 2003; Stanek 2007; Hughes et al. 2010; Chlewicki 2011; Ressel 2012). The comparison of construction costs among DDIs in four locations in the United States and alternative designs, presented in Appendix B, shows that there are up to 75% cost savings from constructing DDIs over other alternatives (Chlewicki 2014).

2.3 Methodologies in Diverging Diamond Interchange Studies

The studies discussed in the previous sections used several different methodologies to evaluate and compare the operational performance of DDIs and other interchange designs. Two major methodologies are reviewed: microscopic simulation and critical lane volume method.

2.3.1 Microscopic Simulation Study

Microscopic simulation is the most popular tool used in DDI studies. While Chlewicki (2003) used Synchro (an analytic tool) to analyze the operational performance of a CDI and a DDI in his first DDI paper, many other studies have since relied on microscopic simulation, including VISSIM, AIMSUN, TSIS-CORSIM™, and Synchro with SimTraffic, to measure and compare the performance of DDIs and CDIs. These studies include Bared et al (2005), Edara et al. (2005), Schroeder et al. (2006), Sharma and Chatterjee (2007), Speth (2008), Chlewicki (2011), Chilukuri et al. (2011), Galletebeitia (2011), Ressel (2012), Yeom et al. (2014), and Khan and Anderson (2016). Microscopic simulation software has the capability to analyze the operational performance of an interchange at various traffic conditions with varying traffic volumes and turn-movement ratios, a range of vehicle types, and alternative geometric configurations. Xiao et al. (2005) and Schroeder et al. (2006) concluded in their papers that microscopic simulation tools are capable of replicating observed vehicle behaviors and meeting most of the standard traffic modeling requirements with careful calibration and validation.

The use of VISSIM is widespread among interchange operational performance studies. VISSIM is a microscopic simulation program that has the capability to replicate driver behavior, geometry, and traffic controls accurately for various roadway designs (Ressel 2012). What distinguishes VISSIM from other microscopic simulation tools is the ability to calibrate the driver behavior modeling. Other popular tools, such as Synchro with SimTraffic, have deterministic arrival patterns, lane change behaviors, and look-back distances. All of these parameters can be controlled in VISSIM, as well, which adds reliability and accuracy to the model and its outcomes (Ressel 2012).

According to Schroeder et al. (2006) and Woody (2006), calibration and field validation are essential to developing accurate VISSIM models. Schroeder et al. (2006) stated that important VISSIM model calibration factors include origin–destination volumes, route decision look-back distances, field-measured free-flow speeds, and field-implemented signal-timing schemes. Validation parameters include travel time through the network and each route, as well as average, 95^{th}, and maximum queue lengths on a per-cycle basis. Woody (2006) provided a guideline for the calibration of VISSIM models and suggested the importance of the car-following behaviors, lane-changing behavior, and standstill distance for operational calibration and study area size, analysis period, volume, route choice, traffic control, network speed, and roadway geometry for system calibration.

2.3.2 Critical Lane Volume Method

A limitation of a microscopic simulation study is that it can be costly and time-consuming depending on the length and the number of simulation inputs, and, thus, only a limited number of traffic scenarios may be analyzed. As an alternative, Chlewicki (2011) and Maji et al. (2013) used the critical lane volume method. CLV uses mathematical equations from the Highway Capacity Manual (HCM) to calculate the capacity per lane of critical movements and then compares these capacities to the demand and estimates a level of service (LOS) for the DDI (Transportation Research Board 2010). The CLV method is straightforward and less time-consuming than microscopic simulation, allowing for the analysis of a large number of alternatives in a relatively short time with reasonable reliability.

Using the CLV method, Chlewicki (2011) analyzed 15,626 volume combinations to compare the operations of a DDI and a CDI. Maji et al. (2013) found that the CLV method could provide reliable and accurate outcomes for DDI operational performance in comparison to VISSIM and Synchro. The Federal Highway Administration (FHWA) introduced the Capacity Analysis for Planning of Junctions (CAP-X) in the Diverging Diamond Interchange Information Guide (Bastian et al. 2014) as a principal planning-level tool to analyze and compare the operational performance of several interchange designs, including a DDI, using the CLV method. CAP-X uses inputs of turning-movement counts, heavy-vehicle percentages, and number of lanes on each approach to estimate v/c ratios at each crossing point of different junction designs.

However, Chlewicki (2011) pointed out several limitations of the CLV method. First, the CLV method is only capable of analyzing individual intersections. It cannot determine how signals or intersections will synchronize, which is an issue for interchanges as they typically have two or more intersections. Second, the CLV method is likely to ignore issues associated with a CDI and, thus, overestimate CDI performance relative to other alternatives. For instance, A CLV analysis may assume the same capacity for all interchange intersections regardless of interchange form. However, a DDI crossover intersection likely has a higher per-lane capacity than a CDI intersection, as the DDI has one less phase and, thus, less lost time per hour. Chlewicki also pointed out that the CLV method requires careful selection of lane adjustment factors for accurate results. Maji et al. (2013) concluded that it is better to use microscopic simulation tools for detailed operational performance analysis of interchanges, as the CLV method utilizes limited parameters. For instance, CAP-X does not use phase timings or saturation flow to calculate the capacity, but instead requires users to input the junction capacity. Also, by considering intersections in isolation, CAP-X does not capture the reduction in demand on a downstream approach as the result of upstream operational failure.

2.3.3 Other Methodologies

In addition to the microscopic simulation and the CLV method, Chilukuri et al. (2011) conducted travel-time runs, video recording, peak hour traffic volume data, crash data review, and online surveys to measure DDI operation performance. These methodologies were utilized in part to check the accuracy and reliability of the simulation results.

2.3.4 Traffic Scenario Selection Methodologies

Although many studies used similar tools for the analysis, there are differences in how each developed volume and route decision scenarios to test the operational performance of DDIs and CDIs.

2.3.4.1 Existing Volumes vs. Hypothetical Volumes

The operational performance of a DDI and a CDI can be analyzed using either existing volume data from the study area or hypothetical volumes developed by researchers. For example, Chlewicki (2003) evaluated CDI and DDI operational performance using the existing traffic volumes and turning-movement distributions for the interchange at I-695 and MD 140 in Baltimore County, Maryland. Chilukuri et al. (2011), Ressel (2012), and Maji et al. (2013) also used existing volume data for their study interchanges and projected 2035 traffic volumes based on the existing data to evaluate DDI performance. Schroeder et al. (2006) also used existing traffic volumes of four DDIs in Tennessee and Missouri to present an approach for calibrating and validating DDI models using VISSIM. Khan and Anderson (2016) developed 83 volume scenarios based on the existing volumes at a CDI in Athens, Alabama, with volume increases of 0%, 50%, 100%, 150%, and 200% of the existing.

Bared et al. (2005), Edara et al. (2005), Sharma and Chatterjee (2007), Speth (2008), Galletebeitia (2011), and Autey et al. (2012) used hypothetical combinations of volumes and turning movements to test the operational performance of interchanges. Chlewicki (2011) tested 15,626 volume combinations based on the permutation of five left-turn and through movements. Bared et al. (2005), Sharma and Chatterjee (2007), and Galletebeitia (2011) categorized the traffic volumes in peak, high, medium, and low flow rates.

2.3.5 Balanced and Unbalanced Traffic Volume

Another variable in traffic scenario selection is balanced and unbalanced traffic. Balanced traffic refers to opposing approaches (e.g., east- and westbound or north- and southbound) having equal traffic volumes and/or turning movement distributions. Unbalanced traffic refers to opposing approaches having different traffic volumes and/or turning-movement distributions. Examples of balanced and unbalanced volume conditions are illustrated in Table 1. Chlewicki (2003), Bared et al. (2005), Edara et al (2005), and Chilukuri et al. (2011) studied the operational performance of DDIs under balanced volume conditions only. Ressel (2012) and Maji et al. (2013) tested DDIs under unbalanced conditions only. Sharma and Chatterjee (2007), Speth (2008), Chlewicki (2011), Galletebeitia (2011), Autey et al. (2012), and Khan and Anderson (2016) analyzed the operations of DDIs and CDIs under both balanced and unbalanced traffic volumes. Chlewicki (2011) and Autey et al. (2012) also analyzed DDIs at different left-turn ratios to evaluate the impact of left-turn proportions on the operation of DDIs.

Table 1: Balanced and unbalanced volumes (Speth 2008)

	Northbound		Southbound		Eastbound			Westbound		
	L	R	L	R	L	T	R	L	T	R
Balanced	200	200	200	200	700	500	100	700	500	100
Unbalanced	500	200	260	70	160	400	700	330	470	300

* L: Left-turn, R: Right-turn, T: Through

CHAPTER 3. METHODOLOGY

The DDI and CDI sensitivity analysis in this study is based on the operational performance studies discussed in the literature review. The following sections describe in detail the analysis methodology, including lane configuration and traffic scenario selection, network designs, and sensitivity analysis steps and inputs.

3.1 Overview Flow Chart of the Study Procedure

The following flow chart (Figure 4) provides an overview of the step-by-step procedure of the analysis conducted in this study. Detailed descriptions of each step in the flow chart are provided in the following sections of this chapter. The study starts with a selection of CDI and DDI configurations, along with a range of demand scenarios. For each configuration and demand scenario, optimal signal-timing plans are determined using the optimization tool Synchro. A CLV analysis is then conducted for each configuration and demand scenario, allowing for a comparison of DDI and CDI performance under a wide variety of conditions. A more in-depth analysis of a subset of the scenarios is then undertaken using the VISSIM microscopic simulation tool. The CLV and VISSIM findings are then summarized to help inform the selection of a DDI or a CDI configuration in the design planning stage of a project.

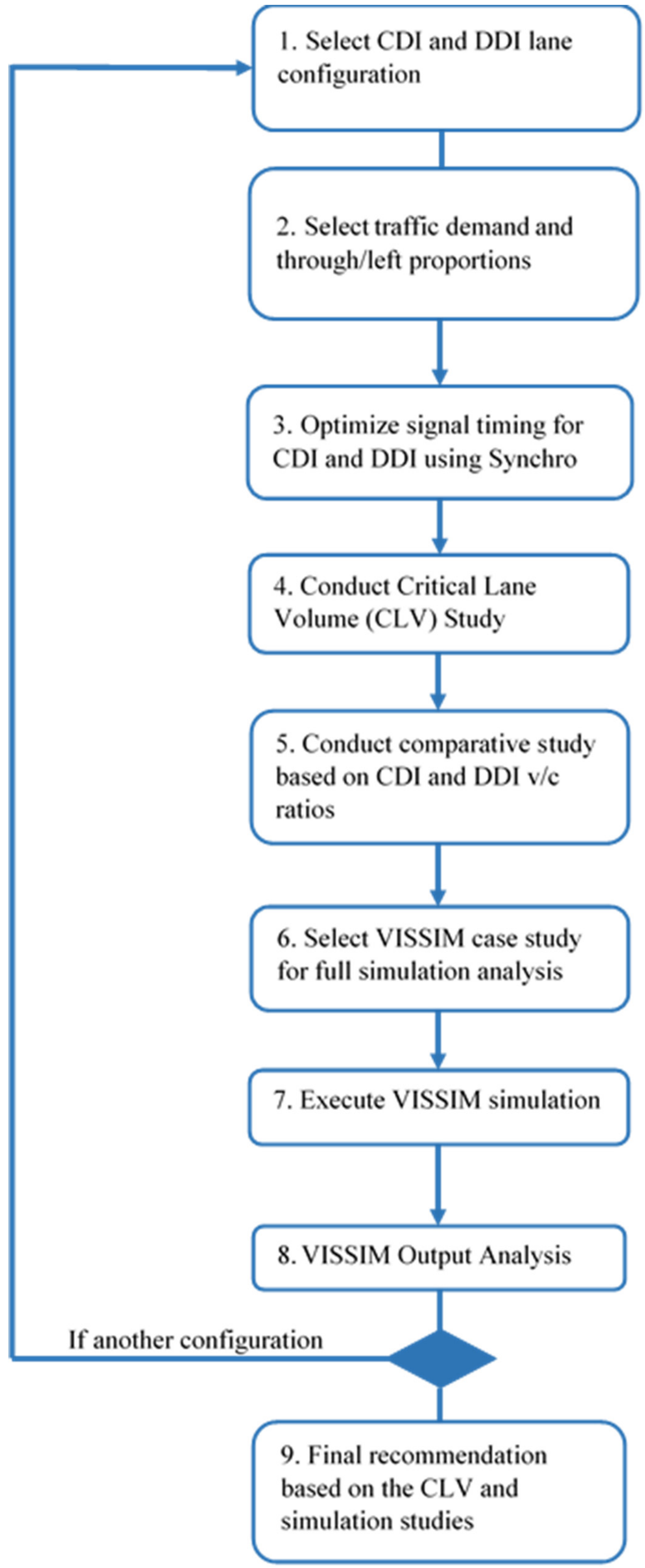

Figure 4: Flow chart of the study procedure

3.2 Lane Configuration Selection

The first step in the analysis is to select the interchange lane configurations to be tested. Analysis of various lane configurations allows for a broad application of the study findings.

The initial CDI and DDI configurations in this study are based on the before and after interchange designs at Jimmy Carter Blvd. and I-85 in Norcross, Georgia. Figure 5 and Figure 6 show aerial pictures of before-and-after configurations of the selected site. This interchange was converted to a DDI in 2015 in response to severe traffic congestion. For this report, the cross street, Jimmy Carter Blvd., is designated as north–south and the freeway, I-85, as east–west. Before the conversion, the northbound interchange approach had four through lanes with a right-turn-only lane and the southbound approach had three through lanes with a right-turn-only lane. On the bridge, there were two through lanes and two left-turn lanes northbound, and two through lanes and one left-turn lane southbound. Both I-85 off-ramps (eastbound and westbound) to Jimmy Carter Blvd. had two left-turn lanes and one right-turn lane. After the DDI conversion, the interchange has three through lanes and one right-turn lane on both the northbound and southbound approaches, and one through-only lane, one through-plus-left shared lane, and one left-turn-only lane northbound and southbound on the bridge (see Figure 7). The after off-ramp lane configurations are the same as in the before configuration. The before and after lane configurations are indicated as LC1 (Lane-Configuration-1) in subsequent analyses.

Two other CDI versus DDI lane configurations were also modeled: (1) three entering lanes on cross streets with two through lanes and one left-turn lane on the bridge in the northbound and southbound directions (indicated as LC2) as shown in Figure 8; and

(2) four entering lanes on cross streets, two through lanes and two dedicated left-turn lanes on the bridge in the northbound and southbound directions (indicated as LC3) as shown in Figure 9. The off- and on-ramps remain the same for all configurations. Unlike the first lane configuration tested, the other two lane configurations have an equal number of lanes on both the CDI and DDI southbound and northbound approaches.

Figure 5: Before configuration of the conventional diamond interchange at Jimmy Carter Blvd. and I-85 in Norcross, GA (Google Earth®, accessed 11/28/2017)

Figure 6: After configuration of the diverging diamond interchange at Jimmy Carter Blvd. and I-85 in Norcross, GA (Google Earth®, accessed 11/28/2017)

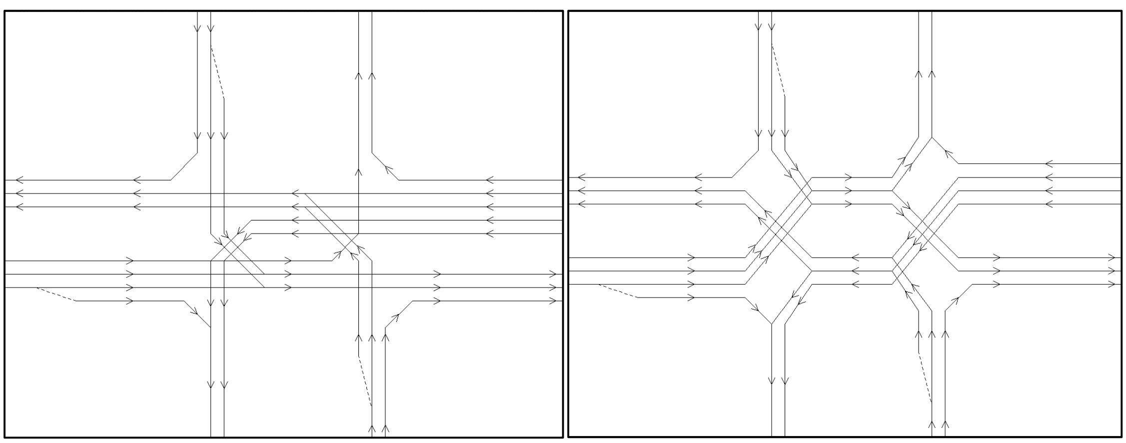

Figure 7: CDI (left) and DDI (right) in lane configuration 1

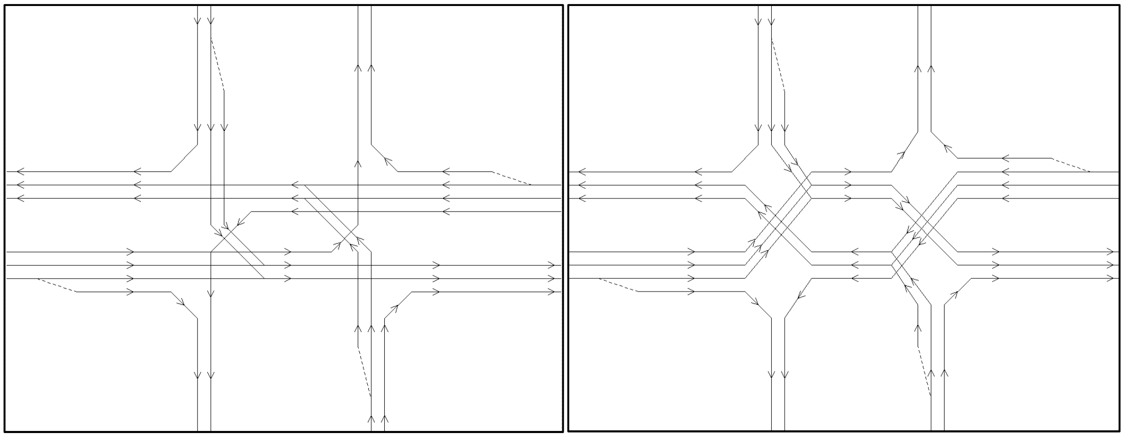

Figure 8: CDI (left) and DDI (right) in lane configuration 2

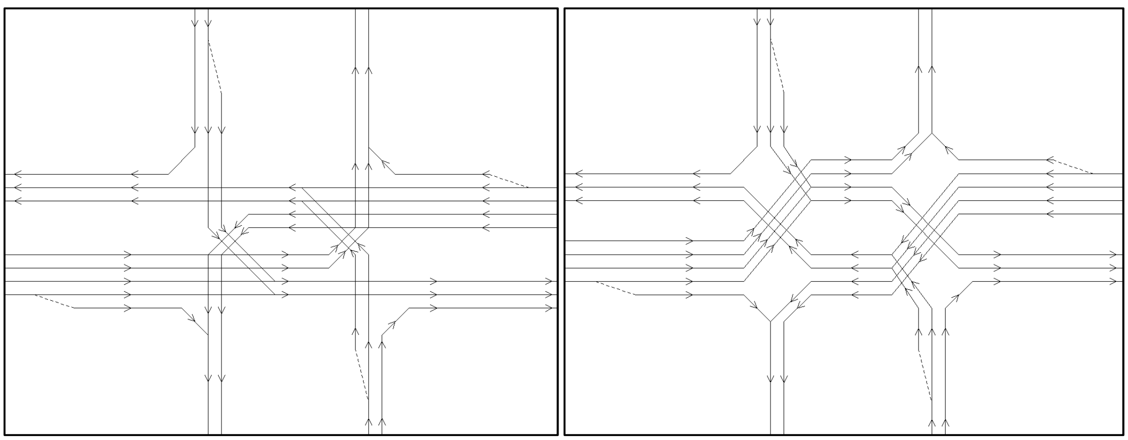

Figure 9: CDI (left) and DDI (right) in lane configuration 3

3.3 Sensitivity Analysis of DDI and CDI

Sensitivity analysis is “a technique used to determine how different values of an independent variable impact a particular dependent variable under a given set of assumptions” (Investopedia 2017). In this study, independent variables examined in the analysis are *traffic demand*, defined by number of vehicles per hour entering the network, and *turn-movement ratio*, defined by the proportion between through and left-turn movements of vehicles coming into the interchange from the cross street of Jimmy Carter Blvd.. The following subsections describe in detail the steps and parameter settings selected to perform the DDI and CDI operational performance sensitivity analysis.

3.3.1 Sensitivity Analysis Structure and Assumptions

The sensitivity analysis in this study is structured as a two-step process: a CLV analysis and a microscopic simulation study. The CLV analysis calculates and compares v/c ratios of the DDIs and CDIs for all the traffic scenarios under consideration. The CLV analysis allows for a relatively quick comparison of DDI and CDI operational performance across a large number of demand scenarios. A VISSIM simulation (a common microscopic simulation tool, see section 2.3.1) study is then conducted to confirm the comparative performance findings of the CLV analysis. Microscopic simulation allows a researcher to control various traffic elements, including vehicle volume, speed, car-following model, route decision, vehicle composition, and lane-change behavior. It also allows for a more detailed analysis of interchange operations compared to the CLV analysis through various operational measures, such as travel time, delay, number of stops, throughput, and queue length. As stated in CHAPTER 2, the drawback of microscopic simulation is that it is much more time consuming and labor intensive than CLV, and thus the VISSIM analysis focuses on a subset of the demand scenarios.

3.3.2 Traffic Scenarios Selection

Traffic scenarios consist of hourly traffic demand and turn-movement ratios. As the objective of this study is to compare interchange configurations under various demand scenarios, a large number of volume–proportion combinations are needed. Table 2 and Table 3 list all volumes and turn-movement ratios tested in this study. Each demand scenario is tested for all through/left proportions listed. These volume and turn-movement ratios result in 161 different traffic scenarios. In this study, only balanced volume conditions were tested where northbound–southbound and eastbound–westbound approaches have equal volumes and turn-movement ratios.

Table 2: Vehicle volumes tested in the study

Cross-Street Volume (vph)	Off-Ramp Volume (vph)			
	Low	Medium	High	High-2
1000	200	500	800	
1500	500	1100	1800	
1800	500	1100	1800	
2100	500	1100	1800	
2300	500	1100	1800	2100
2500	500	1100	1800	2100
2700	500	1100	1800	

Table 3: Turn-movement ratios tested in the study

Through/Left Proportions	
Through	Left
1	0
0.9	0.1
0.7	0.3
0.5	0.5
0.3	0.7
0.1	0.9
0	1

Several assumptions are included in the demand scenarios. First, vehicles exiting the freeway do not return to the freeway, that is, no vehicle from an off-ramp uses the on-ramp back to the interstate. This implies that all vehicles entering the bridge from an off-ramp make a through movement at the exiting crossover intersection. Second, the through/left proportion applies only to vehicles that enter the bridge from the cross street; vehicles from the off-ramp are not considered in the through/left volume proportion calculation. For example, the through/left proportion of 70/30 indicates 70% of vehicles entering the bridge from the cross street make a through movement at the exiting crossover intersection while the remaining 30% turn left onto the freeway on-ramp. Third, the freeway off-ramp vehicles are evenly split between left and right turns at the cross-street intersection. Finally, 20% of the arriving cross-street vehicles turn right to the freeway on-ramps, indicating 80% of vehicles enter the bridge.

3.3.3 Synchro Signal Optimization

As part of the sensitivity analysis, optimal signal timing plans for each lane configuration and traffic demand scenarios were determined. For this effort Synchro was used to optimize both the CDI and DDI signal-timing plans.

Synchro models of the DDIs and CDIs were developed based on Jimmy Carter Blvd. and I-85 aerial maps from Bing. Synchro models for both interchange configurations include the off- and on-ramps, bridge segment, and cross streets entering the bridge. The models excluded the adjacent intersections from the analysis to simplify the signal optimization.

DDI models were optimized with a pretimed setting, and CDI models were optimized with an actuated-coordinated setting with loop detectors on left-turn lanes. Cycle lengths of both interchange designs were optimized within the range of 50 seconds and 180 seconds, and the offset was referenced to the beginning of green of the northbound through (NBT) phase. These decisions were based on the existing signal implementations at the selected site provided by Gwinnett County DOT.

The basic dual ring diagrams of the DDI and CDI models were developed based on the existing timing plans from Gwinnet County DOT. Sample dual ring diagrams of the DDI and the CDI are shown in Figure 10 and Figure 11. The DDI has a split-phase configuration of the cross-street through movements, with no phase for the left-turn movements from the cross street to the on-ramps, as these are uninterrupted movements in the DDI configuration. The CDI has protected left-turn movements from the cross street to the freeway on-ramp at both bridge intersections. Based on these phase diagrams, the DDIs are expected to benefit from both free-flow left-turn movements and reduced lost time per cycle, although the DDI may have reduced cross-street capacity given the through movement split-phase timing configuration.

From the signal timing optimization using Synchro, the phase lengths, cycle lengths, and offsets on each intersection are collected.

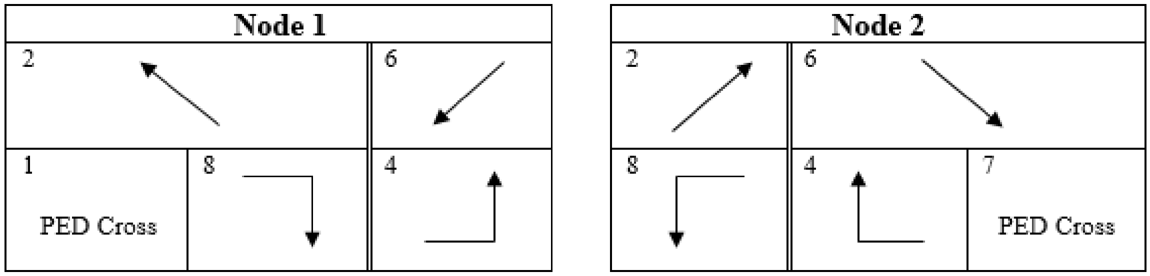

Figure 10: Sample dual ring diagram of the diverging diamond interchange

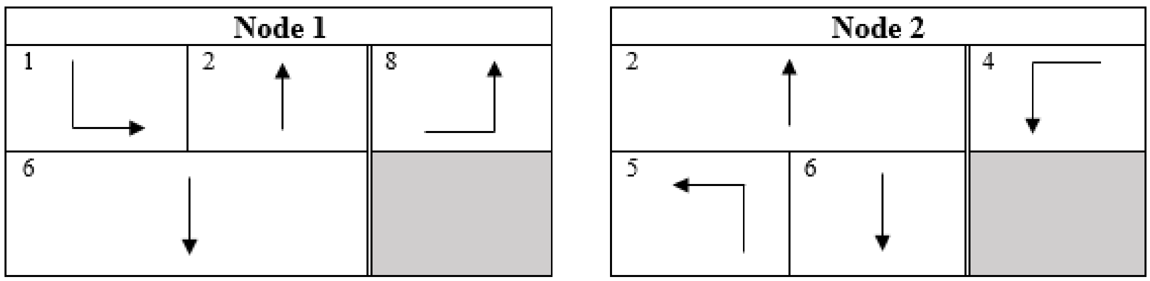

Figure 11: Sample dual ring diagram of the conventional diamond interchange

3.3.4 Critical Lane Volume Analysis

The first part of the sensitivity analysis is the CLV analysis comparing DDI and CDI critical movement v/c ratios. A critical movement (or movement pair) is defined as the movement(s) with the highest per lane demand (v/c) on each side of the ring barrier. The critical path consists of the critical movements from both sides of the dual ring diagram. Movements considered in the CLV analysis of the CDI and the DDI defined in this study are listed in Table 4. Figure 12 and Figure 13 illustrate the turning movement schematics of the CDI and the DDI. For the CLV analysis, the movements EBR1, NBR1, SBR2, and WBR2 are not considered as they are uninterrupted movements and unlikely to be capacity constrained. SBL1 and NBL2 are considered in the analysis as these are phase controlled in the CDI configuration and may be capacity constrained; however, in the DDI these movements are uninterrupted.

Table 4: DDI and CDI critical movements

Intersections	Critical Movements
Node 1	NBT1
	SBT1
	SBL1
	EBL1
Node 2	NBT2
	NBL2
	SBT2
	WBL2

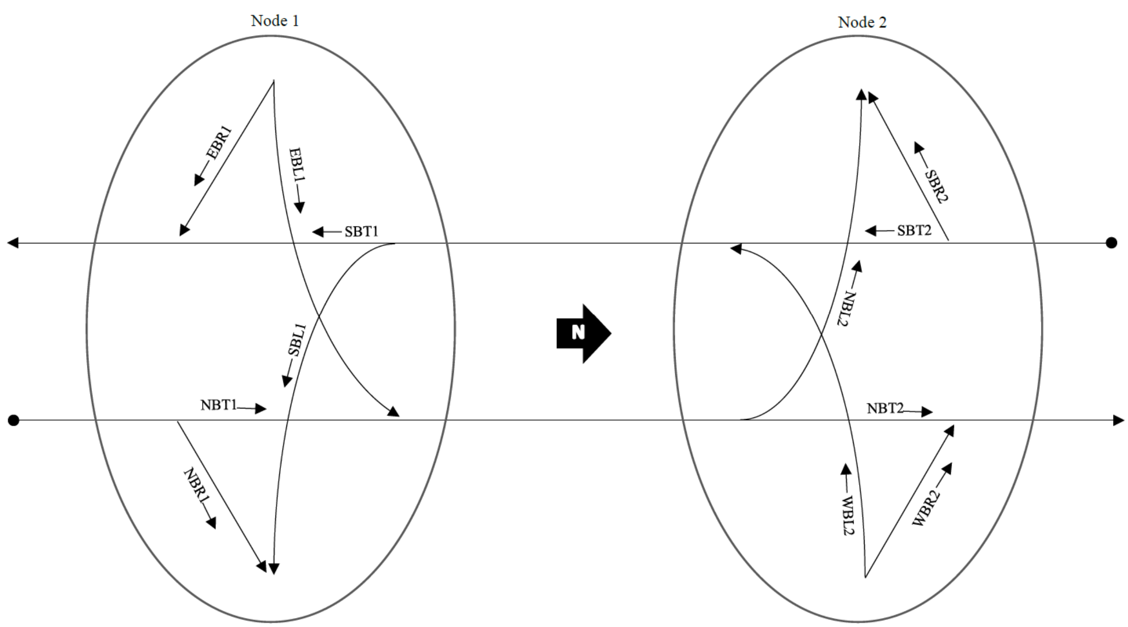

Figure 12: Turning movement schematic of the conventional diamond interchange

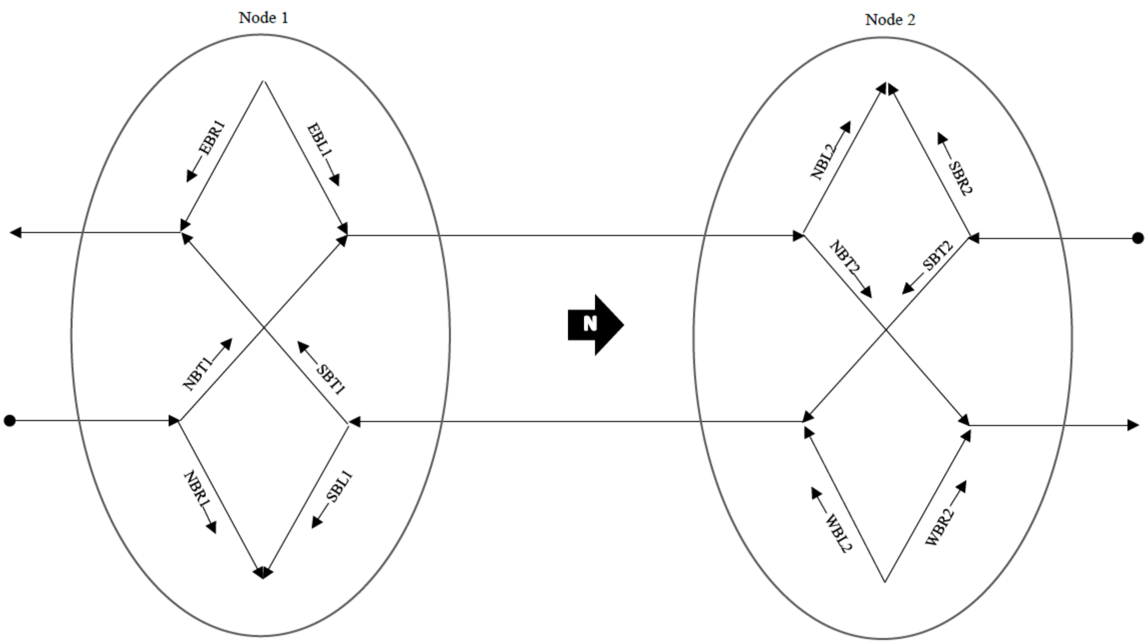

Figure 13: Turning movement schematic of the diverging diamond interchange

3.3.4.1 Volume-to-Capacity Calculations

CAP-X from FHWA is not used in this study for v/c ratio calculation, as capacity must be manually set. In addition, CAP-X does not capture the reduction in demand on a downstream approach resulting from an upstream capacity constraint. Instead, v/c ratios of CDIs and DDIs are calculated using simplified HCM 2010 methods. Equation 1 below calculates the capacity per lane for each turning movement within the interchange. Phase lengths and cycle lengths used in the CLV analysis are from Synchro signal optimization. As the CLV analysis is a planning-level analysis and, thus, intended as an approximation, saturation flow is set to be 2000 vphrpln based on VISSIM results. In addition, a 4-second lost time per phase is assumed. However, in a future iteration of the CLV analysis these values could be adjusted to reflect specific field conditions for increasingly fine-tuned results.

$$c = s \times \frac{g}{C} \tag{1}$$

c = capacity per lane (vphrpln)

s = saturation flow, assumed as 2000 vphrpln

g = effective green time, calculated as phase time minus lost time of 4 seconds

C = cycle length of the intersection in seconds

Equation 2 calculates the demand per lane for each movement using the assigned (i.e., scenario) traffic flows and lane utilization factors.

$$v = q \times LUF \tag{2}$$

v = volume per lane (vphrpln)

q = assigned movement traffic flow on each movement (vph)

LUF = lane utilization factor

Table 5 shows the calculation for the LUF for the various lane groupings. The LUFs are developed with consideration of lane assignments (left only, through only, or shared left-through), the number of lanes, and the relationship between upstream and downstream intersections. LUFs are assumed to be maximum lane utilization (i.e., distribution of vehicles across lanes) with the exception that weaving on the bridge is minimized. That is, a vehicle will not pre-position in an upstream lane that does not lead to a downstream lane allowing that movement (exclusive or shared). These assumptions tend to lead to a conservation allocation of vehicles, particularly on a DDI with a shared through-left lane, likely underutilizing the left-turn-only free-flow lane. However, as this is a planning-level analysis, the more conservative assignment was selected. Future efforts should seek to inform the selection of LUFs based on numerous DDI and CDI field observations.

Table 5: Lane utilization factor calculation* **

Turning Movements	Scenarios	Lane Utilization Factor (LUF) Calculations
Upstream Approaches: NBT1 / SBT2	LC1 (CDI), LC2, LC3	For the lanes utilized by vehicles pre-positioning to make through movement at the downstream approach: $LUF = \frac{1}{\# \; of \; lanes \; on \; SBT1 \; or \; NBT2}$, all lanes For the lanes utilized by vehicles pre-positioning to make left turn at the downstream approach: $LUF = \frac{1}{\# \; of \; lanes \; on \; SBL1 \; or \; NBL2}$, all lanes
	LC1-DDI with shared lanes (3 lanes)	Let $x_T = [number\ of\ lanes\ on\ NBT1\ or\ SBT2] \times [through\ vehicle\ proportion]$ If $x_T < 1$, then $LUF = 1$, for lane 1 $LUF = 0$, for lane 2 If $1 \leq x_T \leq 2$, then $LUF = 1/x_T$, for lane 1 $LUF = (x_T - 1)/x_T$, for lane 2 If $x_T > 2$, then $LUF = 0.5$ for both lanes
		Let $x_L = [number\ of\ lanes\ on\ NBT1\ or\ SBT2] \times [left\text{-}turn\ proportion]$ If $x_L < 1$, then $LUF = 0$, for lane 2 $LUF = 1$, for lane 3 If $1 \leq x_L \leq 2$, then $LUF = (x_L - 1)/x_T$, for lane 2 $LUF = 1/x_L$, for lane 3 If $x_L > 2$, then $LUF = 0.5$ for both lanes

* Lanes are numbered from centerline to outside edge of roadway

** Table 5 continues on the next page

Table 5: Lane utilization factor calculation (continued)*

`	LC1 (CDI), LC2, LC3	$LUF = \frac{1}{\#\ of\ lanes\ on\ SBT1\ or\ NBT2}$
	LC1-DDI with shared lanes (3 lanes)	For vehicles coming from cross street (SBT1 or NBT2): $LUF = LUF_{NBT1_{x_T}\ or\ SBT2_{x_T}}$ For vehicles coming from off-ramps (EBL1 or WBL2): $LUF = \frac{1}{\#\ of\ lanes\ on\ SBT1\ or\ NBT2}$
Downstream Approaches: SBL1 / NBL2	LC1 (CDI), LC2, LC3	$LUF = \frac{1}{\#\ of\ lanes\ on\ SBL1\ or\ NBL2}$
	LC1-DDI with shared lanes (3 lanes)	For vehicles coming from cross street (SBT1 or NBT2): $LUF = LUF_{NBT1_{x_L}\ or\ SBT2_{x_L}}$ For vehicles coming from off-ramps (EBL1 or WBL2): $LUF = \frac{1}{\#\ of\ lanes\ on\ SBL1\ or\ NBL2}$

* Lanes are numbered from centerline to outside edge of roadway

In the determination of the arriving traffic volume at an approach, potential upstream capacity constraints are considered. However, traffic volumes on downstream movements (SBT1, SBL1, NBT2, and NBL2) receive the throughputs of upstream movements (NBT1, EBL1, SBT2, and WBL2). Where the upstream intersection movement cannot process all the assigned traffic or when v/c ratios of upstream movements exceed 1, the downstream arriving volume is adjusted. It is assumed that the maximum throughput processed by the upstream approach is 95% of the capacity and, thus, the volume of downstream movements is adjusted as shown in Equation 3.

$$if\ v/c_U > 0.95, \qquad v_D = C_u \times 0.95 \times LUF \tag{3}$$

v/c_U = v/c ratio of an upstream movement

v_D = demand per lane of a downstream movement (vphrpln)

An interchange intersection v/c ratio is calculated based on the sum of the critical lane volumes in the critical path and the critical path capacity. Equation 4 calculates the critical lane volume of an intersection by summing the demand per lane of critical path phases.

$$v_{Node\ i} = \sum_{j=1}^{n} v_j \tag{4}$$

$Node\ i$ = selected intersection within the interchange

v_j = volume per lane of each movement within the critical path of the intersection (vphrpln)

n = number of phases within the critical path of the intersection

The intersection critical path capacity is calculated using Equation 5 based on the cycle length and total lost time per cycle. The DDI has two phases in a cycle critical path, and the CDI has either two or three phases in a cycle critical path depending on the phase demands.

$$c_{Node\ i} = \frac{3600 - \left[\frac{3600}{C} \times (t_L \times N)\right]}{h} \tag{5}$$

$c_{Node\ i}$ = capacity per lane of the selected intersection (vphrpln)

C = cycle length of the intersection (seconds)

t_L = total lost time per phase, assumed as 4 seconds

N = number of phases in a cycle

h = saturation headway, assumed as 1.8 s/veh (i.e., saturation flow of 2000 veh/hr/ln)

The intersection v/c ratio may then be calculated using the critical path volume and the critical path capacity. For this analysis, the interchange v/c ratio is set as the larger v/c ratio of two interchange intersections, as shown in Equation 6.

$$v/c_{interchange} = max(v/c_{Node1}, v/c_{Node2}) \quad (6)$$

3.3.4.2 Comparative Study

Calculated v/c movement and interchange ratios are populated into a tabular format and color-coded to present the difference in v/c ratios between the CDI and DDI scenarios using Microsoft Excel with Visual Basic (VB) scripts (Appendix C). The color schematics of the color-coded spreadsheet for v/c ratios are presented in Table 6. The v/c ratios are then plotted to help visualize the differences between the CDI and DDI performance over different demand and through/left proportions. Using these tables and plots, patterns in the v/c ratios and relative performance between the interchange configurations are explored.

Table 6: Color schematics of color-coded spreadsheet for v/c ratios

Cell Color	Meaning
Green	Lower v/c ratio with difference > 0.2
Yellow	Greater v/c ratio with difference > 0.2
Red	v/c ratio ≥ 0.95

3.3.5 Microscopic Simulation Study

The second step in the sensitivity analysis is the microscopic simulation study using VISSIM for selected combinations of traffic volumes and through/left proportions to confirm the observations from the CLV analysis. The CLV study alone is insufficient to evaluate the CDI and DDI operational performance, as the v/c ratio does not present a complete operational picture, as discussed in the literature review. Therefore, the VISSIM simulation study, which allows for the estimation of numerous operational parameters, is used to complement the CLV study. Similar to the CLV analysis, the signal timing plans are optimized using Synchro and are used in the VISSIM simulation network. As the simulation study is more time-consuming than the CLV analysis, only selected case studies are tested using VISSIM. Table 7 and Table 8 list the selected demand scenarios and through/left proportions tested in this microscopic simulation study for all tested lane configurations. These scenarios were selected to represent a cross section of the scenarios in the CLV study.

Table 7: Selected demand scenarios for the simulation study

Cross-Street Volume (vph)	Off-Ramp Volume (vph)		
	Low	**Medium**	**High**
1500	500	1100	1800
2100	500	1100	1800
2500	500	1100	1800

Table 8: Selected through/left proportions for the simulation study

Through/Left Proportions	
Through	**Left**
1	0
0.9	0.1
0.7	0.3
0.5	0.5
0.3	0.7
0.1	0.9
0	1

3.3.5.1 VISSIM Model

As with the CLV analysis, the CDI and DDI VISSIM lane configurations and geometric designs are developed based on the Jimmy Carter Blvd. and I-85 interchange. Cross-street grades are assumed as zero and grades on off-ramps are as measured from the field (1.5% within 300 ft of the cross-street signal and 5.0% for the rest of the segment). Single vehicle input, defined as number of vehicles input into the network per hour (vph), is used for each simulation period to minimize the variability in the data from changing traffic demands over time. Again, as with CLV analysis, the study area covers the interchange segment, including off- and on-ramps, bridge segment, and the cross-street approaches to the interchange. Figure 14 and Figure 15 show sample CDI and DDI VISSIM models with the existing lane configuration (LC1). As seen, the primary difference between the two models is the bridge segment, where the DDI model has crossovers at the two intersections. The LC2 and LC3 configurations, as discussed in the CLV section, are based on these initial VISSIM models.

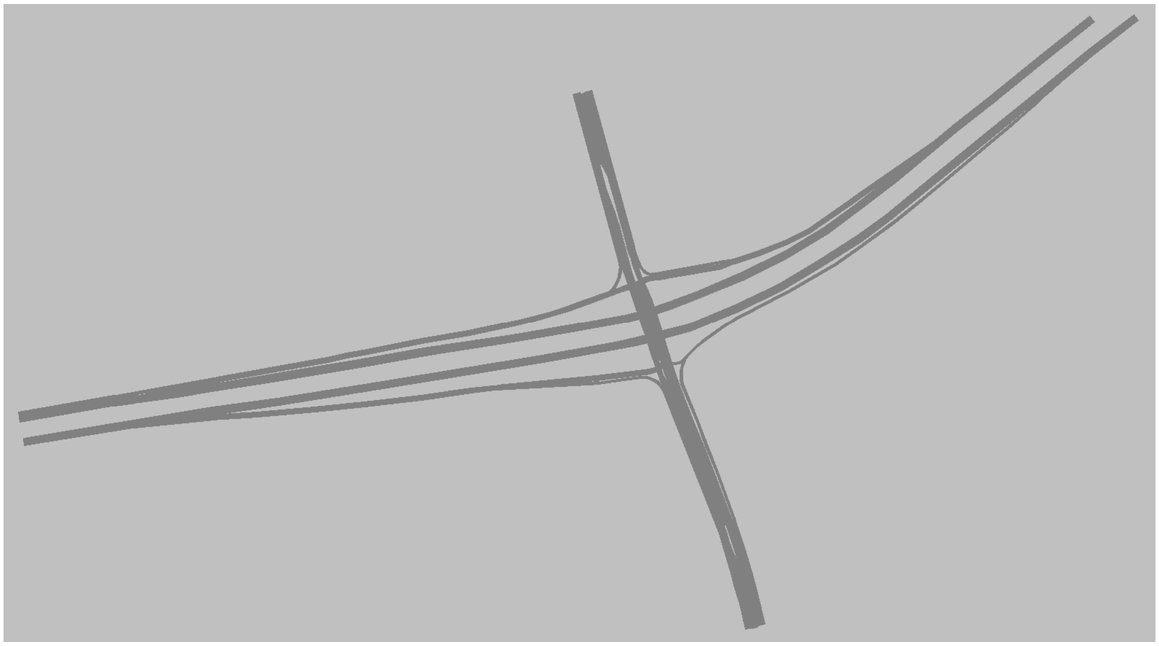

Figure 14: VISSIM model for the conventional diamond interchange (LC1)

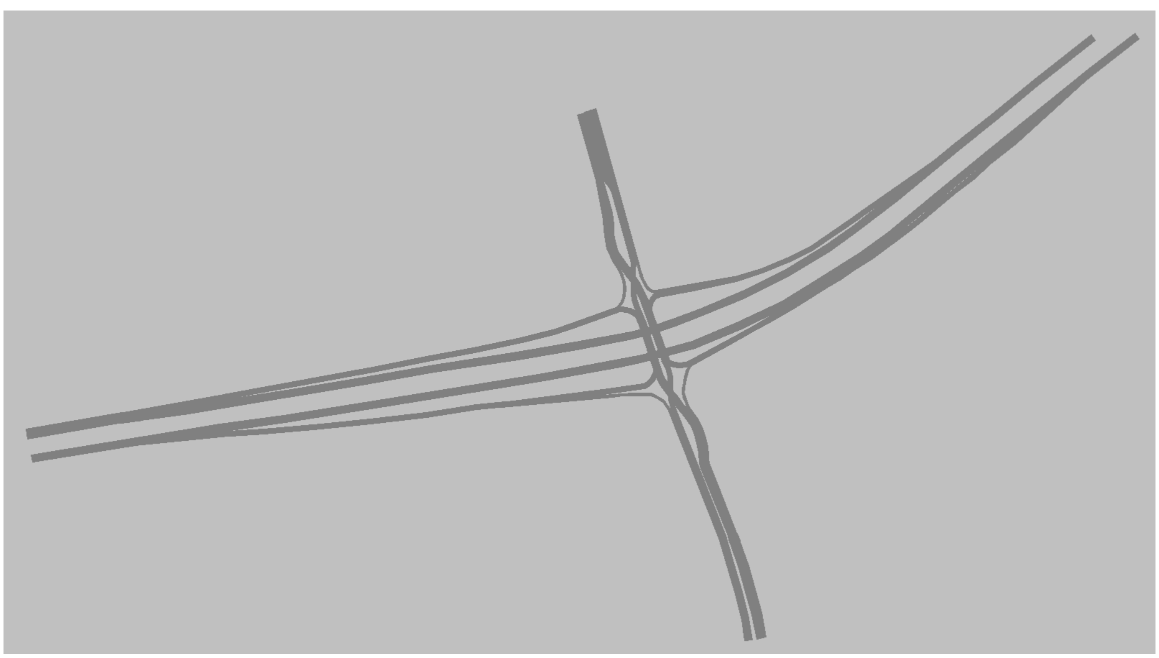

Figure 15: VISSIM model for the diverging diamond interchange (LC1)

The study uses the default VISSIM vehicle composition with 5% heavy vehicle. With the assumption of approximate turning speed of 25 mph, reduced speed zones are implemented at turning links with a speed range of 20 to 30 mph. Priority rules are implemented at the intersections to prevent vehicles from driving through other vehicles blocking the intersection. The simulation time of the VISSIM models for each traffic scenario is 4500 seconds. The first 900 seconds of the simulation is allotted to allow the model to fill and reach steady state (if possible). Performance metrics from the fill time are not included in the analysis. Therefore, data are collected for 3600 seconds, with 300-second bin aggregations. Ten simulation replications are conducted for each traffic scenario, with different seeds to provide variation in arrival patterns and network traffic flow. The simulation runs and data collection are automated using Microsoft Visual Studio with VB scripts (Appendix D).

Performance measures collected from the simulation study are average delay per vehicle, average travel time per vehicle, average number of stops per vehicle, queue length and throughput on each approach, and x- and y-coordinates of individual vehicles processed. R scripts are used to organize and summarize collected performance measures. The average delay per vehicle for each approach and the entire route are populated in Excel spreadsheets, enabling the comparisons between interchange configurations and demand scenarios.

3.4 Implementation

This section describes the sensitivity analysis implementation process, providing additional detail regarding inputs, spreadsheets, and software utilized to analyze the operational performance of the interchange configurations.

3.4.1 Synchro Signal Optimization

For each scenario of traffic demand, through/left proportion, and lane configuration, an optimal signal timing plan is determined using Synchro. Synchro exports the signal-timing parameters to a comma-separated value (CSV) file. Separate CSV files ae created for each lane configuration tested. Each timing plan of each subsequent Synchro scenario run is appended to the end of the CSV file. A screen capture of an exported signal plan in a CSV file format is shown in Figure 16. Each signal plan (PLANID) is named after the combination of cross-street and off-ramp volumes, and the left-turn proportion. For example, the PLANID of 100020050 represents a 1000-vph cross-street volume, 200-vph off-ramp volume, and 50% left-turn proportion. After all the optimized signal timings are exported to CSV files, signal plans in the CSV files are exported to the CLV spreadsheet under the “Signal Timing” tab into a format suitable for the analysis using a VB script (Appendix C). Figure 17 shows the screen capture of the signal plans reorganized in the CLV spreadsheet.

	A	B	C	D	E	F	G	H	I	J	K	L	M	N	O	P	Q	R
1	Timing Plans																	
2	PLANID	INTID	S1	S2	S3	S4	S5	S6	S7	S8	CL	OFF	LD	REF	CLR	NOTE	RUNDATE	RUNTIME
3	10002000	4		31		39		39			70	5		2		From Sync	########	########
4	10002000	6		40				30		40	70	68		2		From Sync	########	########
5	100020010	4		28		32		32			60	5		2		From Sync	########	########
6	100020010	6		33				27		33	60	0		2		From Sync	########	########
7	100020030	4		25		25		25			50	0		2		From Sync	########	########
8	100020030	6		26				24		26	50	48		2		From Sync	########	########
9	100020050	4		27		23		23			50	49		2		From Sync	########	########
10	100020050	6		24				26		24	50	0		2		From Sync	########	########
11	100020070	4		29		21		21			50	48		2		From Sync	########	########
12	100020070	6		22				28		22	50	0		2		From Sync	########	########
13	100020090	4		32		18		18			50	44		2		From Sync	########	########
14	100020090	6		19				31		19	50	0		2		From Sync	########	########
15	1000200100	4		40		20		20			60	22		2		From Sync	########	########
16	1000200100	6		21				39		21	60	0		2		From Sync	########	########

Figure 16: Optimized signal timings exported to a CSV file

	A	B	C	D	E	F	G	H	I	J	K	L
1		DDI										
2	Code	NBT1	EBL1	SBT1	EBR1	NBT2	WBR2	SBT2	WBL2	CL	Offset_NB	Offset_SB
3	10002000	31	39	39	17	40	16	30	40	70	5	68
4	100020010	28	32	32	14	33	13	27	33	60	5	0
5	100020030	25	25	25	11	26	10	24	26	50	0	48
6	100020050	27	23	23	13	24	12	26	24	50	49	0
7	100020070	29	21	21	15	22	14	28	22	50	48	0
8	100020090	32	18	18	18	19	17	31	19	50	44	0
9	1000200100	40	20	20	26	21	25	39	21	60	22	0
10	10005000	25	35	35	11	36	10	24	36	60	6	0
11	100050010	26	34	34	12	35	11	25	35	60	7	0
12	100050030	23	27	27	9	28	8	22	28	50	4	0
13	100050050	25	25	25	11	26	10	24	26	50	1	0
14	100050070	27	23	23	13	24	12	26	24	50	22	0
15	100050090	29	21	21	15	22	14	28	22	50	20	48
16	1000500100	30	20	20	16	22	14	28	22	50	21	0
17	10008000	24	36	36	10	37	9	23	37	60	7	0
18	100080010	24	36	36	10	36	10	24	36	60	6	0
19	100080030	22	28	28	8	29	7	21	29	50	5	0
20	100080050	24	26	26	10	27	9	23	27	50	2	0
21	100080070	25	25	25	11	26	10	24	26	50	24	48
22	100080090	27	23	23	13	25	11	25	25	50	25	0
23	1000800100	27	23	23	13	25	11	25	25	50	25	0
24	15005000	33	47	47	19	48	18	32	48	80	7	0
25	150050010	34	46	46	20	47	19	33	47	80	7	0
26	150050030	33	37	37	19	38	18	32	38	70	5	0
27	150050050	30	30	30	16	30	16	30	30	60	1	0
28	150050070	28	22	22	14	23	13	27	23	50	22	0
29	150050090	31	19	19	17	20	16	30	20	50	19	49

Figure 17: Signal plans reorganized in the CLV spreadsheet

3.4.2 CLV Study and Comparative Analysis

After importing the DDI and CDI interchange signal plans for all volume–proportion combinations and lane configurations in the “Signal Timing” tab of the CLV spreadsheet (each lane configuration has a separate CLV workbook), CLV analysis is conducted to calculate v/c ratios for each scenario. The v/c ratio for each volume–proportion combination is calculated in “DDI_CLV” and “CDI_CLV” worksheets in the workbook. Each sheet consists of vehicle input, through/left proportion, route decision, phase diagram, proportional phase timing, volume set for Synchro, traffic demand and lane numbers on each approach, optimized timing from Synchro, approach capacity, and v/c ratio calculation. Cells in the right-top corner of the spreadsheet contain selected cross-street and off-ramp volumes, and through/left proportions to be tested. Figure 18 below shows a screen capture of the "DDI_CLV" worksheet. A VB script (Appendix C) automatically inputs cross-street and off-ramp volumes and through/left proportions into the cells and exports calculated v/c ratios into the "Color Coded" worksheet, which contains color-coded tables and plots of the CDI and DDI v/c ratios, utilizing the color schematics described in Table 6. These tables and plots are used to analyze the conditions in which one interchange design outperforms the other.

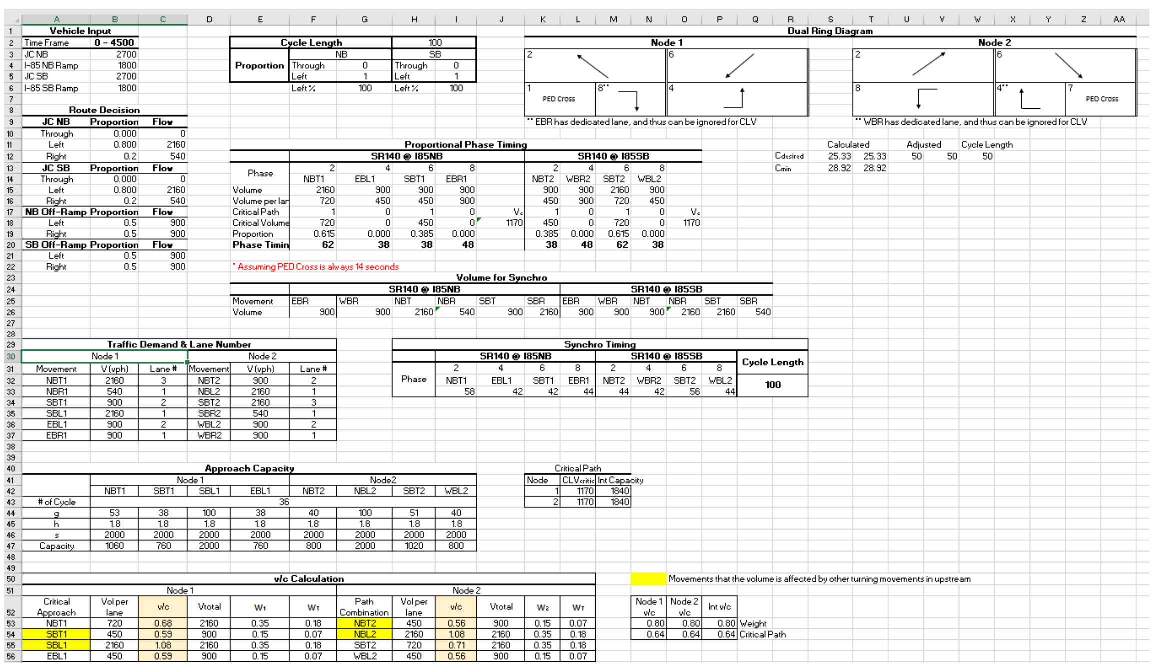

Figure 18: Spreadsheet for v/c ratio calculation for the CLV analysis

3.4.3 VISSIM Simulation Analysis

After completion of the CLV analysis, the VISSIM microscopic simulation study is undertaken. Based on the CLV findings, cross-street and off-ramp volumes representing low, medium, and high traffic-demand scenarios are selected for the simulation case study.

As stated previously, CDI and DDI VISSIM models are created based on the geometry from a Google Maps® aerial of the Jimmy Carter Blvd. and I-85 interchange. Signal timing files (Ring Barrier Control, or RBC files) are manually created for each traffic scenario using the signal plans from Synchro. The developed Microsoft Visual Studio VB script (see Appendix D) automates the process to call, input, and run VISSIM models and to collect performance measures, including delay, travel time, throughput, queue length, and x- and y-coordinates of individual vehicles. Ten simulation runs are conducted for each volume–proportion set and average delay per vehicle data are calculated based on the weighted average of these ten simulation runs using the R script as shown in Equation 7.

$$average\ delay\ per\ vehicle = \frac{\sum_{i=1}^{n}(d_i \times v_i)}{\sum_{i=1}^{n} v_i} \tag{7}$$

n = number of simulation runs conducted (10 runs)

d_i = delay per vehicle at n^{th} simulation run

v_i = throughput on an approach at n^{th} simulation run

Average delay per vehicle and average throughput data for each lane configuration are organized in the “VISSIM Output Analysis” worksheet and plotted for each turning movement to enable the comparison of CDI and DDI operational performance across the various scenarios. Each worksheet in the LC1, LC2, and LC3 workbooks contains the delay and throughput data from the simulation study of the respective configuration.

CHAPTER 4. RESULTS AND DISCUSSION

This chapter summarizes, compares, and evaluates results from the CLV analysis and the VISSIM simulation study.

4.1 CLV Analysis Results

The CLV study calculates CDI and DDI v/c ratios at different traffic demands and turn-movement ratios. Calculated v/c ratios are populated into color-coded spreadsheets and plots to present the CDI and DDI operational performance. Figure 19, Figure 20, and Figure 21 plot the difference between the CDI v/c ratio and the DDI v/c ratio for each lane-configuration (LC1, LC2, and LC3) and traffic-demand scenario. Values in the legend represent cross-street and off-ramp demands, i.e., 2100/500 is interpreted as a cross-street demand of 2100 vph and an off-ramp demand of 500 vph. See Appendix E for all detailed results of color-coded tables and plots developed using the CLV method.

For the existing lane configuration (LC1), the CDI is favored over the DDI (i.e., v/c ratios of the CDI are lower than those of the DDI, thus the difference in v/c ratios is negative) when the cross-street left-turn proportion is below 30%. The two interchange configurations experience similar v/c ratios at the proportion of 70/30, and the DDI outperforms the CDI at left-turn proportions exceeding 50% of total demand. Also, for a given through/left proportion the v/c ratio difference consistently increases as the demands increase, supporting that there are benefits of the DDI under higher demands. Thus, at the lower left-turn proportions, while the CDI may have lower v/c ratios, the relative advantage over DDI decreases as demands increase; likewise, at higher left-turn proportions, the advantage of the DDI is amplified at higher demands. For the LC2 scenario (i.e., fewer lanes than LC1) the DDI and CDI have a similar performance as that for LC1. The CDI again has superior operational performance to the DDI until the left-turn proportion reaches 30% of total demand, at which point performance is similar. At left-turn percentages of 50% and above, the DDI outperforms the CDI, although the magnitude of the difference is not as large. The LC3 plot, the largest bridge cross section (8 lanes) tested in this study, shows a slight shift, with the CDI and DDI having similar performance at the through/left ratio of 50/50 with the CDI generally providing better service at lower left-turn proportions and the DDI at higher left-turn proportions. This change is expected as the CDI capacity is more sensitive to the number of lanes; thus, when the number of lanes increases, the CDI operational performance will see greater improvements than the DDI (Hughes et al. 2010).

From the color-coded tables comparing the CDI and DDI v/c ratios by individual turning movement (see Appendix E), SBT1 and NBT2, the through movements exiting the bridge, as expected, experience better operations (lower v/c ratios) on the CDI than on the DDI, in most traffic scenarios. This is primarily due to the CDI through movement having concurrent signal timing, whereas these movements operate in a split-phase pattern on the DDI. However, the DDI provides superior service to the left-turn movements from the cross streets to the on-ramps and the left turns from the off-ramps to the bridge (SBL1, NBL2, EBL1, and WBL2) in most traffic scenarios. This derives from the DDI free-flow left-turn movements, an overall reduction in lost time, and the off-ramp movements in the DDI running concurrent with cross-street through movements, often resulting in a higher effective green for this movement than in the CDI. Overall, as expected the CDI has a tendency to favor cross-street through movements while a DDI favors left-turn movements.

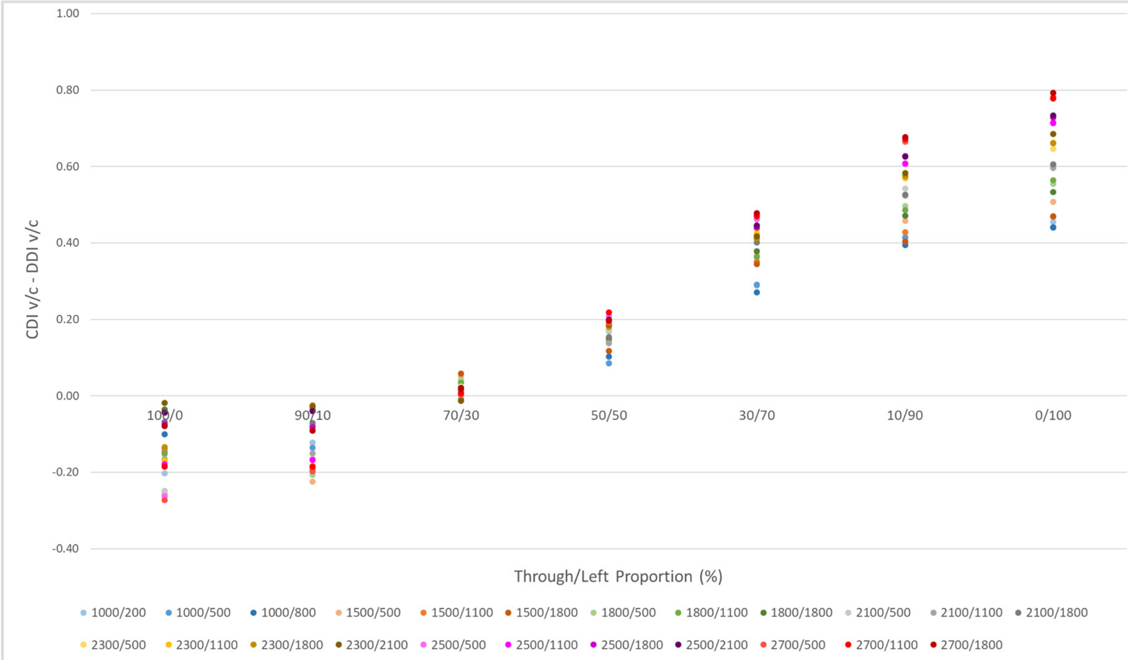

Figure 19: Difference in v/c ratios between CDI and DDI for LC1 at different traffic demands and through/left proportions

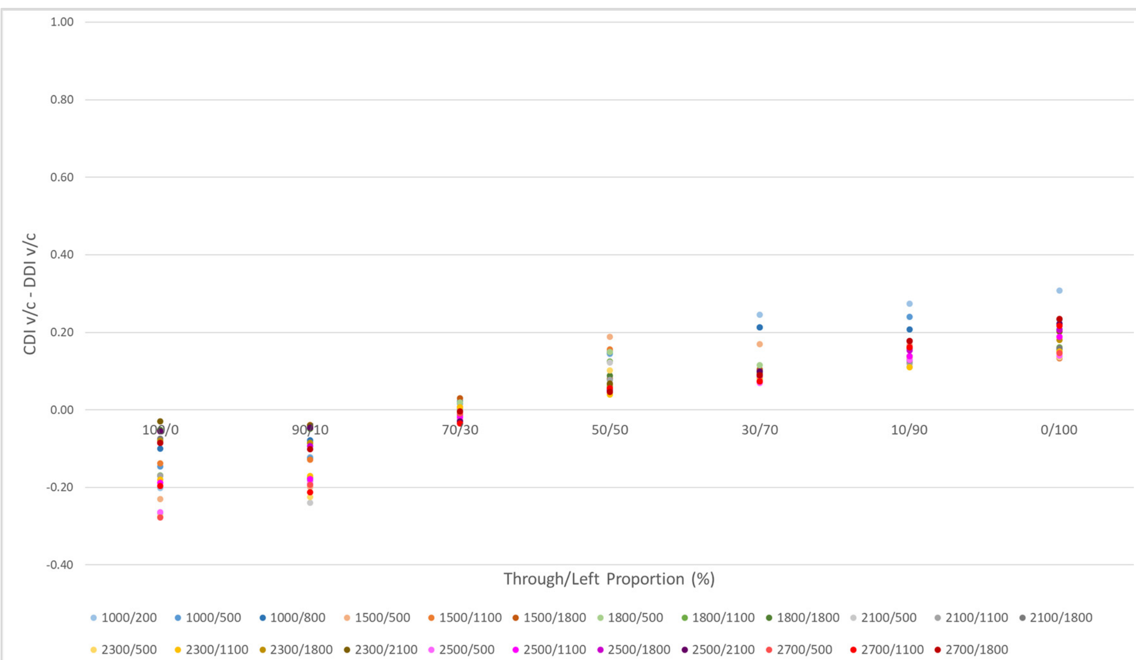

Figure 20: Difference in v/c ratios between CDI and DDI for LC2 at different traffic demands and through/left proportions

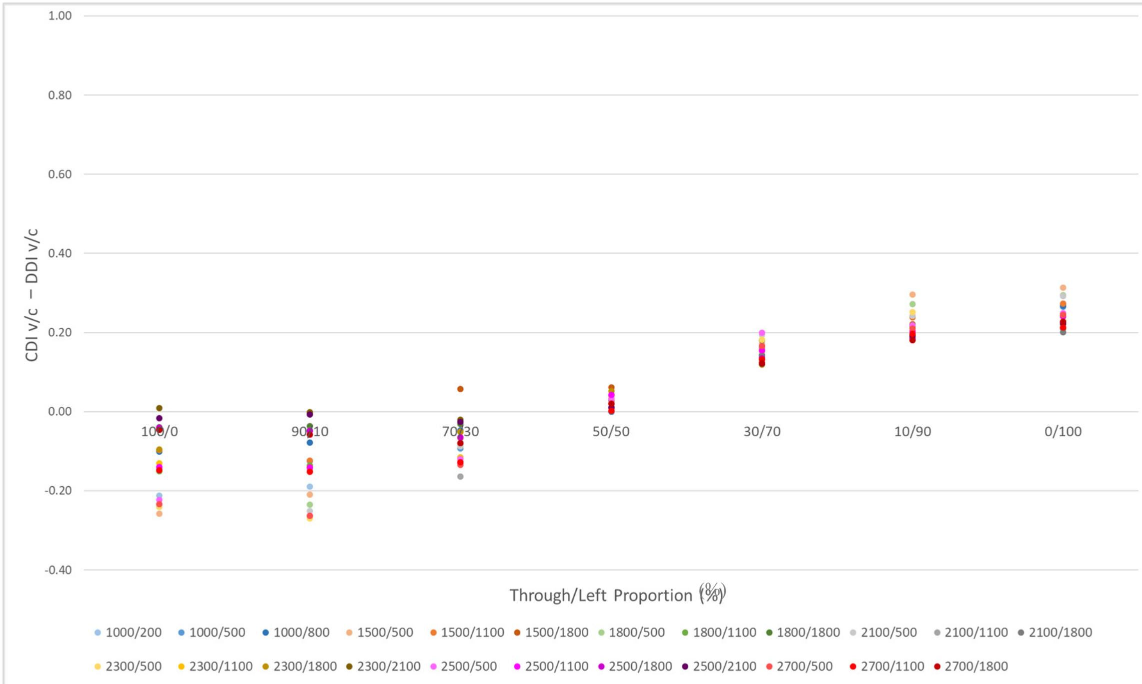

Figure 21: Difference in v/c ratios between CDI and DDI for LC3 at different traffic demands and through/left proportions

4.2 Microscopic Simulation Study Results

As part of the VISSIM simulation portion of this study, various performance measures were collected including delay, throughput volume, number of stops, and queue length on each approach. In this section, the primary performance measures discussed are the average delay per vehicle in the interchange, aggregated over all movements, and the interchange throughput, as these were found to provide the best representation of overall performance. Appendix F provides all detailed results of CDI and DDI average delay per vehicle and throughput data on individual turning movements.

4.2.1 Lane Configuration 1 (LC1)

The first lane configuration tested in this study, LC1, is the before-and-after models of the Jimmy Carter Blvd. and I-85 interchange. Figure 22, Figure 23, and Figure 24 plot the average delay per vehicle and the throughput of the CDI and the DDI for the studied traffic volumes and turn-movement ratios. Values in the legend represent the off-ramp demands tested for the cross-street demand.

From these plots, the CDI generally performs better or at a similar level to the DDI at left-turn proportions below 30% of total traffic demand, and the DDI outperforms the CDI when the left-turn proportion is 50% or greater. These results are similar to the CLV findings, although at the higher left-turn proportions, the CDI delays are significantly higher than those in any through/left proportion on the DDI. These patterns are also noted in the throughput data. At the lower left-turn proportions, the CDI tends to satisfy demand, whereas the DDI is less likely to satisfy demand, particularly at higher overall demands. When the left-turn proportion exceeds 50%, the CDI is often unable to process the demand, failing to serve a significant portion of the demand at the higher volume levels, whereas the DDI reliably processes the full demand.

The relative difference in performance between the CDI and the DDI at the through/left proportions of 50/50 or more is greater in the simulation study than those found in the CLV analysis, especially at higher cross-street demands. This is because the CLV method does not reflect the synchronization of intersections in the interchange or the complex lane utilizations seen in the VISSIM simulations. These differences are particularly exhibited on the SBT1 and NBT2 approaches, i.e., the through movements exiting the bridge. These movements tend to favor CDIs in the CLV analysis but are found to be similar between the CDI and the DDI in the simulation study. Additionally, in the simulation plots the left-turn proportion at which the DDI becomes the favored alternative is higher for lower cross-street demands.

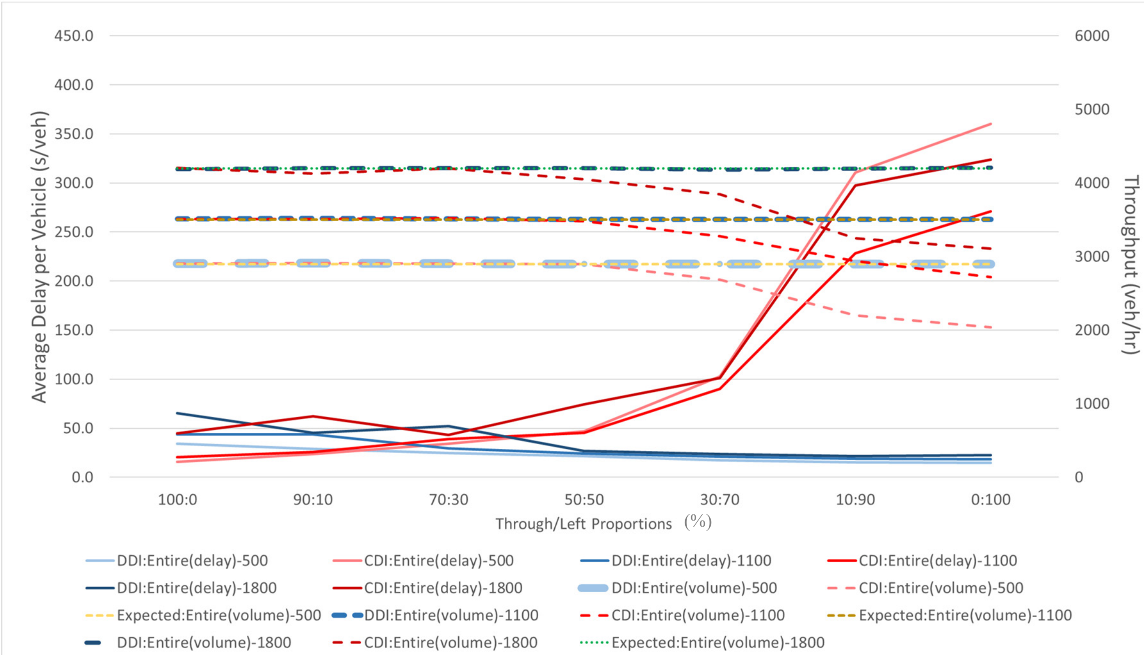

Figure 22: DDI and CDI average delay per vehicle and interchange throughput with cross-street demand of 1500 vph at different off-ramp demands and through/left proportions for LC1

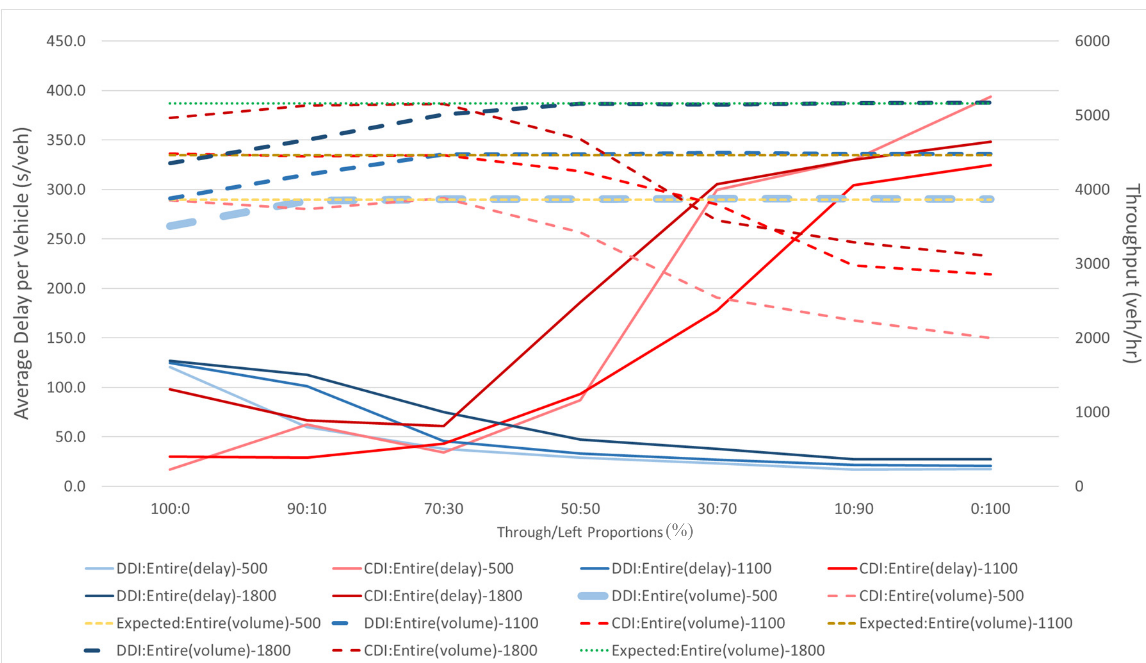

Figure 23: DDI and CDI average delay per vehicle and interchange throughput with cross-street demand of 2100 vph at different off-ramp demands and through/left proportions for LC1

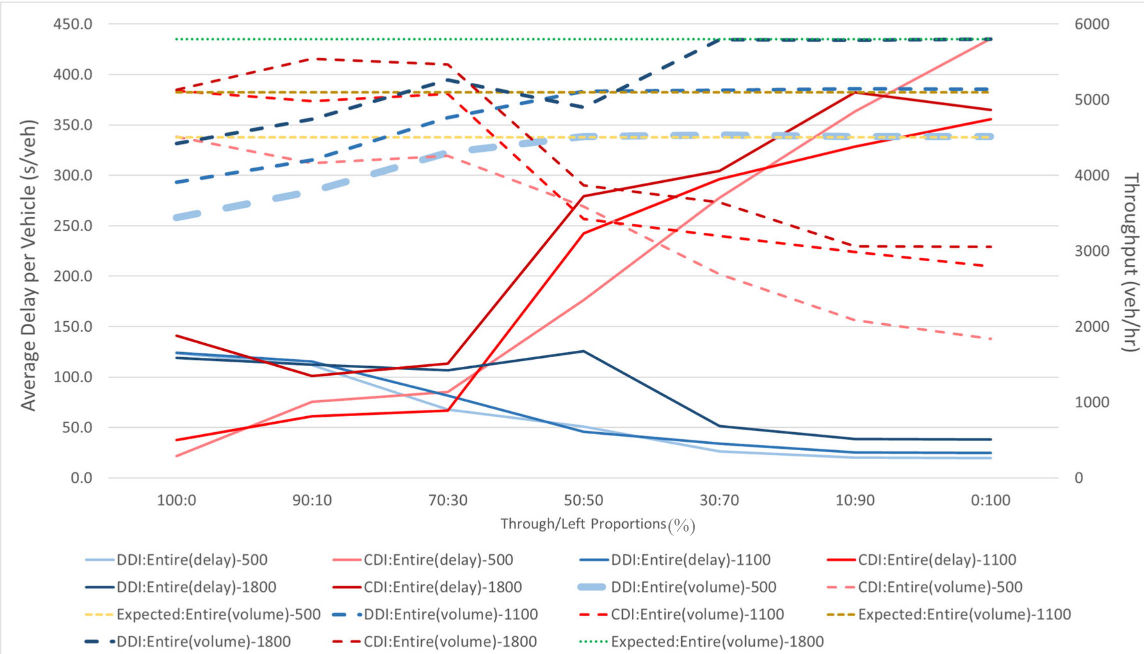

Figure 24: DDI and CDI average delay per vehicle and interchange throughput with cross-street demand of 2500 vph at different off-ramp demands and through/left proportions for LC1

4.2.2 Lane Configuration 2 (LC2)

The second lane configuration tested, LC2, has three entering lanes on the cross-street approaches and one left-turn and two through lanes on each direction of the bridge. Figure 25, Figure 26, and Figure 27 plot the average delay per vehicle and the CDI and DDI throughput at different traffic demands and turn-movement ratios. For all three cross-street demands tested, the CDI only clearly outperforms the DDI in the 10% left-turn case, and the average delay per vehicle of the CDI starts to exceed that of the DDI at the left-turn proportion of 30%. This trend is the same as that found in the CLV analysis, where the difference in CDI and DDI v/c ratios starts to turn positive (i.e., v/c ratios of CDIs are higher than that of DDIs) at through/left proportion of 70/30. As with LC1, in the simulation plots the left-turn proportion at which the DDI becomes the favored alternative is higher for lower cross-street demands.

Unlike the results found in the CLV analysis where the magnitude of difference in v/c ratios between the CDI and DDI configuration is smaller for LC2 than LC1, the results from the simulation study show no meaningful change in differences in average delay per vehicle between the LC1 and LC2 interchange configuration.

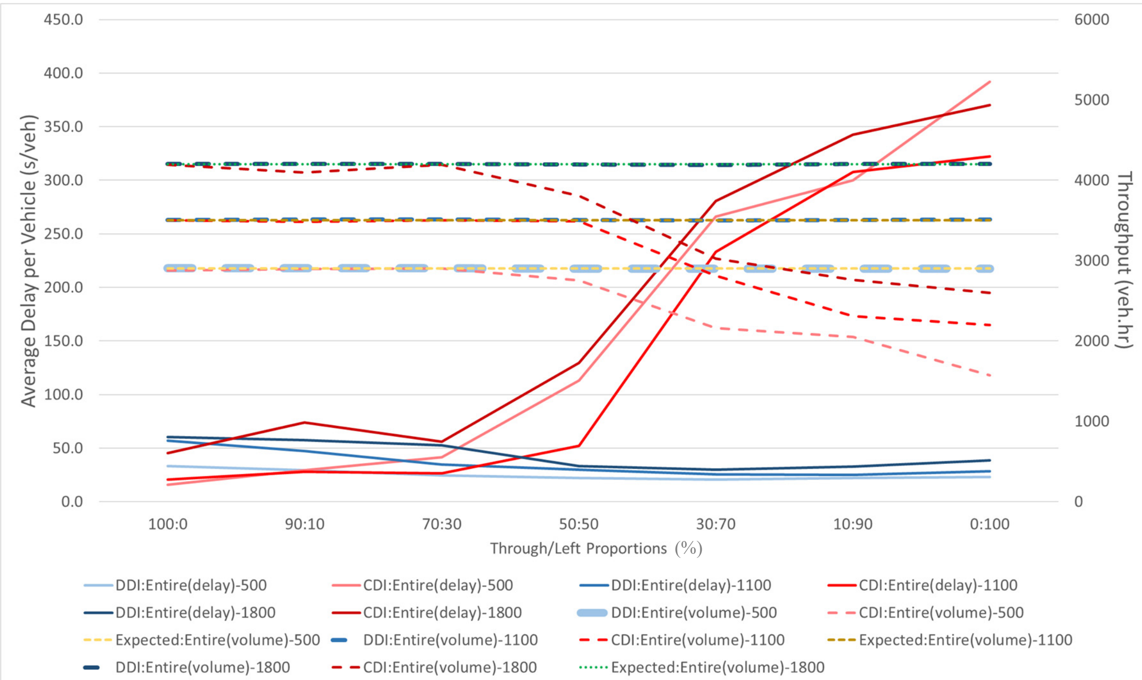

Figure 25: DDI and CDI average delay per vehicle and interchange throughput with cross-street demand of 1500 vph at different off-ramp demands and through/left proportions for LC2

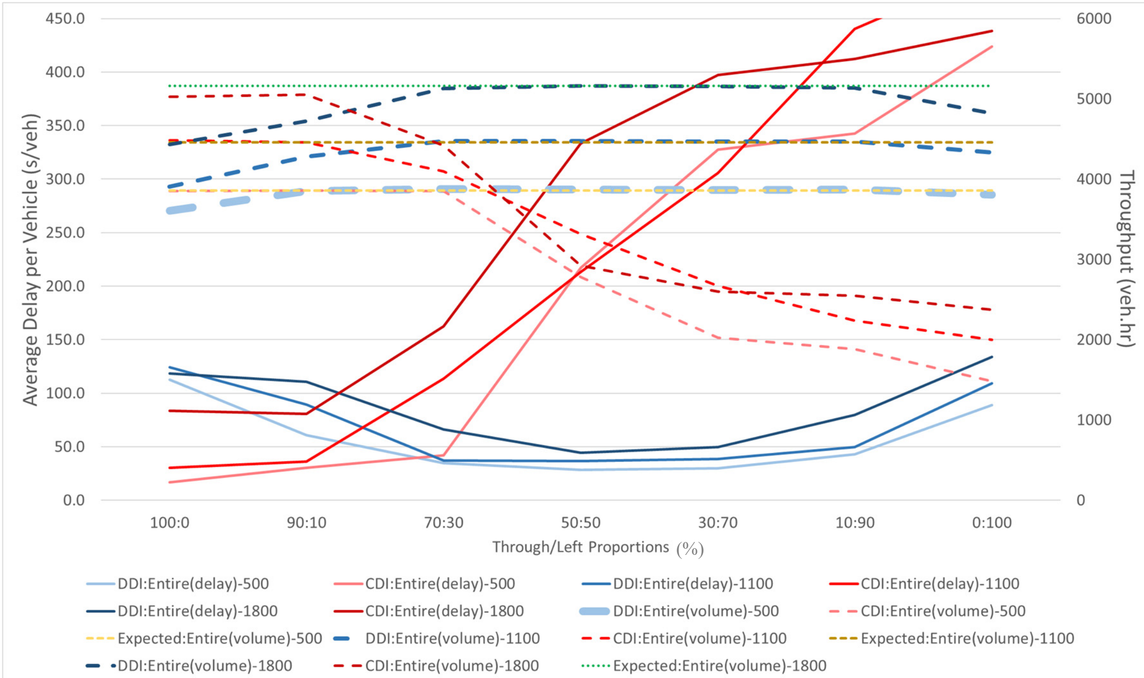

Figure 26: DDI and CDI average delay per vehicle and interchange throughput with cross-street demand of 2100 vph at different off-ramp demands and through/left proportions for LC2

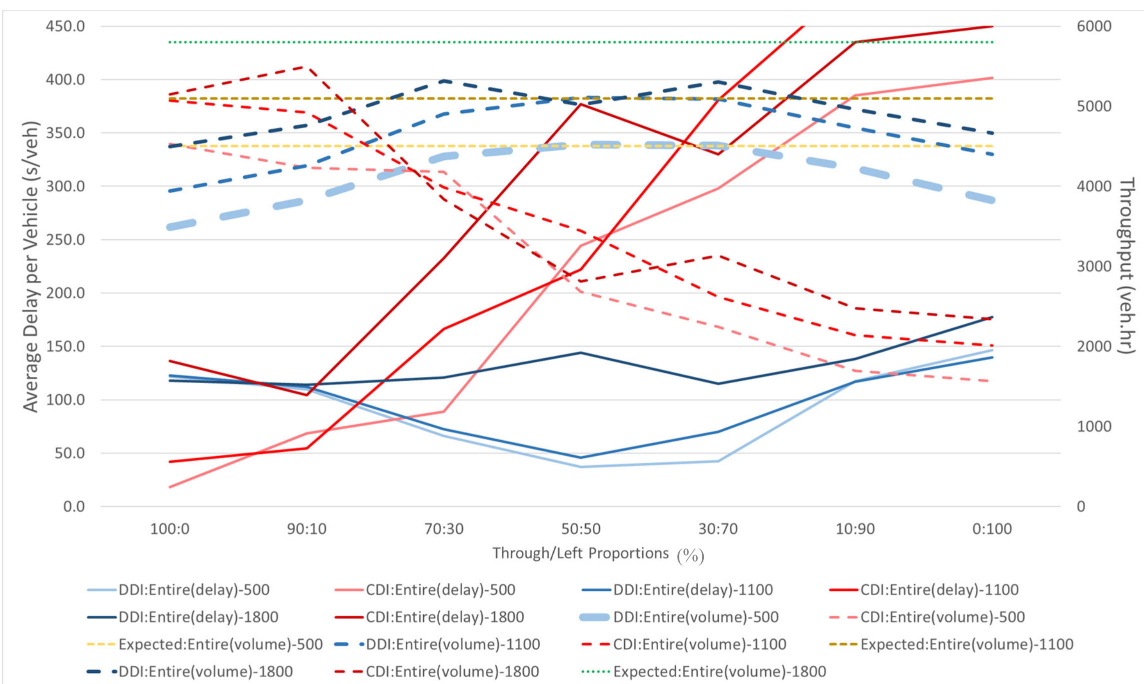

Figure 27: DDI and CDI average delay per vehicle and interchange throughput with cross-street demand of 2500 vph at different off-ramp demands and through/left proportions for LC2

4.2.3 Lane Configuration 3 (LC3)

The third lane configuration tested, LC3, has the most lanes, with four entering lanes on the cross-street approaches and two left-turn and two through lanes on the bridge. Figure 28, Figure 29, and Figure 30 plot the average delay per vehicle and the interchange throughput at different traffic volumes and turn-movement ratios. The CDI performs better or at a similar level to the DDI until the left-turn proportion reaches 50%. The DDI starts to outperform the CDI at a left-turn proportion of 70%. Similar to the CLV results, the simulation results show that the CDI and DDI v/c ratios are similar at the 50/50 through/left proportion. LC3 has the highest left-turn proportion at which the DDI becomes the favored alternative, aligning with the CLV finding that the relative operational performance of CDI and DDI are partially dependent on the total available cross section. Again, as with LC1 and LC2, in the simulation plots the left-turn proportion at which the DDI becomes the favored alternative, is higher for lower cross-street demands, indicating that the CDI performs better at lower traffic volume.

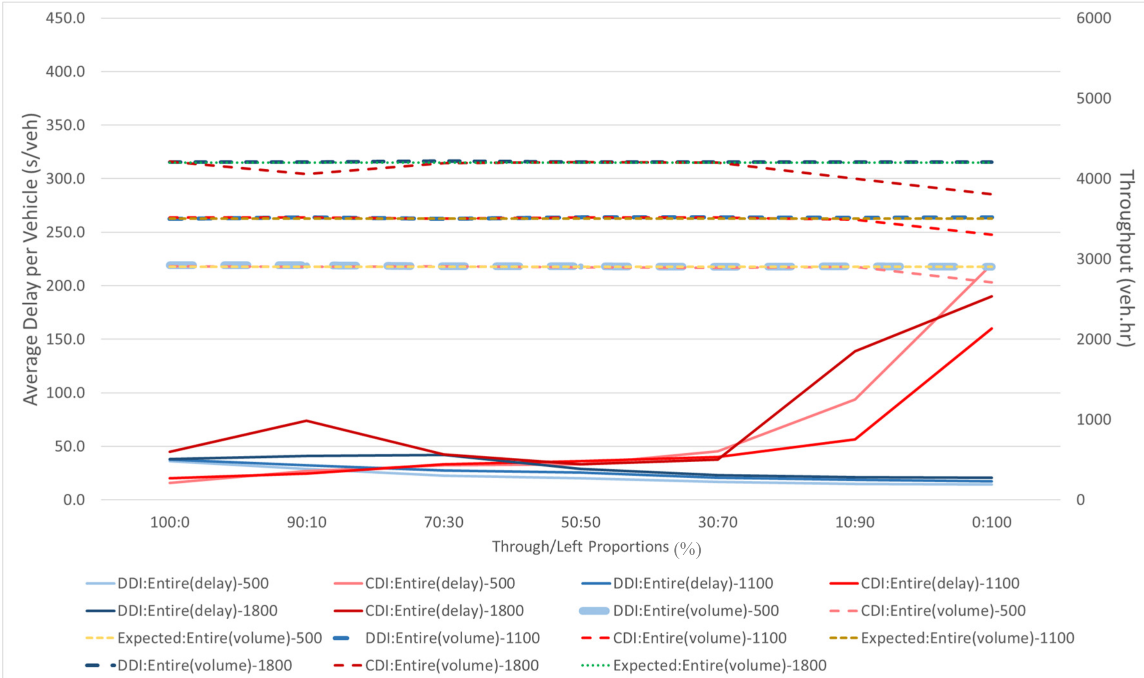

Figure 28: DDI and CDI average delay per vehicle and interchange throughput with cross-street demand of 1500 vph at different off-ramp demands and through/left proportions for LC3

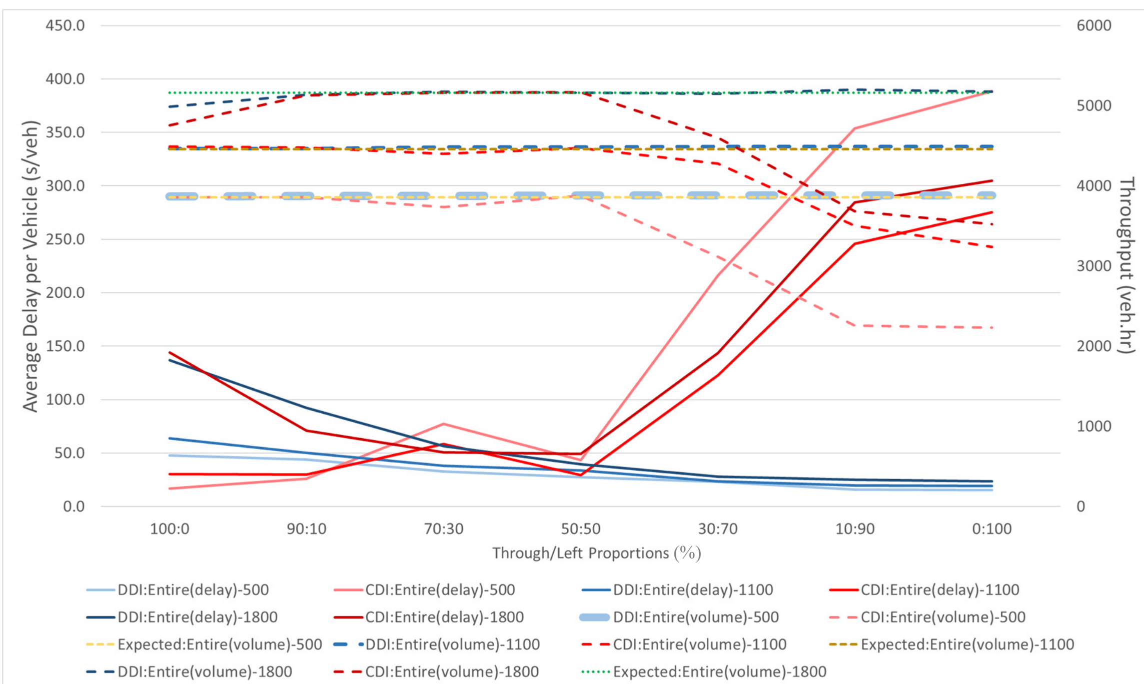

Figure 29: DDI and CDI average delay per vehicle and interchange throughput with cross-street demand of 2100 vph at different off-ramp demands and through/left proportions for LC3

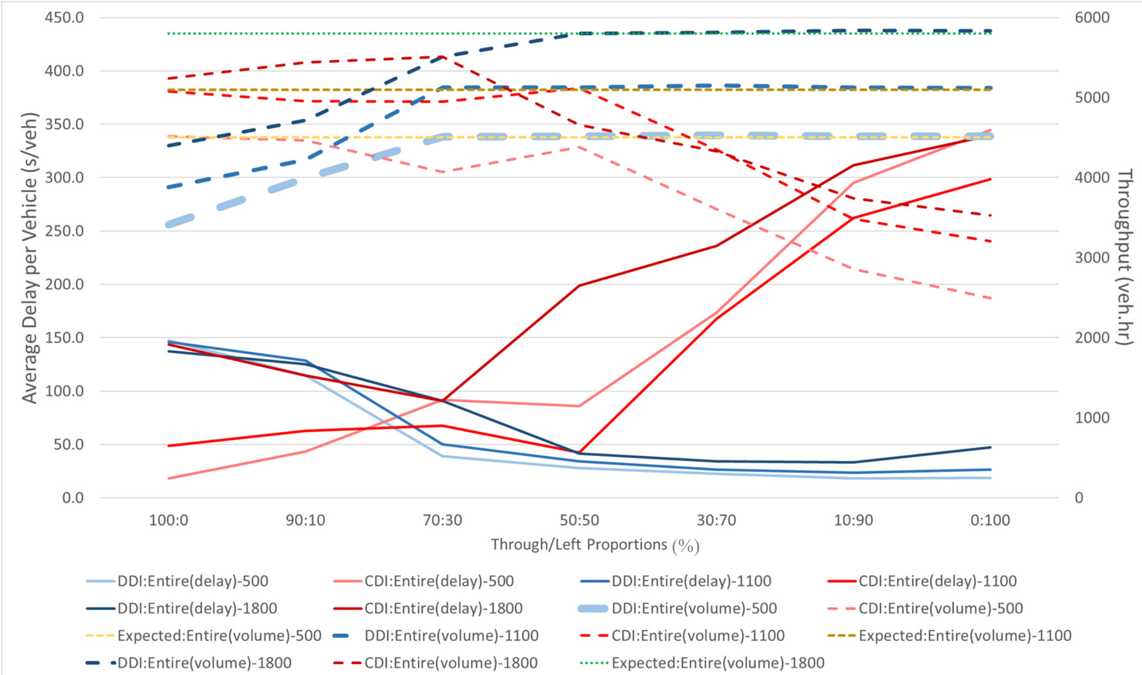

Figure 30: DDI and CDI average delay per vehicle and interchange throughput with cross-street demand of 2500 vph at different off-ramp demands and through/left proportions for LC3

4.3 Discussion and Evaluation of the Results

Based on the results from the CLV analysis and VISSIM simulation study, CDIs have better operational performance than DDIs at higher through and lower left-turn proportions, while DDIs perform better in the opposite condition. The through/left proportion at which the CDI and DDI configurations had similar performance is dependent on cross-street cross sections, and total demand. As the number of lanes on the cross street increases, especially left-turn lanes, the left-turn proportion required for the DDI to provide favorable performance increases. For the lane configurations tested in this study, the CDIs and DDIs were found to have similar performance in the through/left proportion range of 70/30 to 50/50. Where the left-turn proportion was below 30%, the CDI tended to offer better performance, and where the left-turn proportion exceeded 50% of the total traffic demand, the DDI tended to offer better performance. The most significant operational benefits of DDI configuration are found on the cross street to on-ramp left-turn movements and freeway off-ramps onto the cross-street bridge. CDI configurations tended to provide better through movement operations.

The CDI configuration also was found to perform better at lower cross-street demands at a given through/left proportion, while the operational performance of the CDI degrades faster than that of the DDI at higher cross-street demands. These results align well with findings from previous studies that the CDI performs better or similar to the DDI at low-to-medium volumes, and the DDI outperforms the CDI at higher traffic volumes (Bared et al. 2005; Edara et al. 2005; Sharma and Chatterjee 2007; Speth 2008). However, the impact of off-ramp demands on the operational performance of CDIs and DDIs is inconclusive due to the mixed results found in this study.

The overall comparative CDI and DDI operational performance trends observed are similar in both the CLV and simulation methodologies, with some difference in the observed performance-difference magnitudes and at the individual movement level. In the CLV analysis, the CDI configuration is found to have better performance on the SBT1 and NBT2 movements in most traffic scenarios. However, these movements have no meaningful operational difference in the simulation study. This is primarily due to the CLV method's inability to capture the effect of synchronization between intersections and the difference in lane utilizations between the two methods.

CHAPTER 5. CONCLUSIONS AND RECOMMENDATIONS

5.1 Conclusions

This project focused on determining the general traffic operating conditions under which a DDI is more appropriate than a CDI and vice versa, using traffic simulation and CLV analysis. While the Jimmy Carter Interchange is utilized as the base case, the simulation was not specifically calibrated to all site geometric conditions, instead constructed to provide a reasonable representation of a DDI and conventional interchange to allow for application of the results to other locations. Reflection of the specific site conditions in the model would limit the ability to apply the result more generally; however, it is recoginzied that it is critical that a designer consider the specifics of their site when considering any interchange design.

Given the preceding, the operational performance curves developed in this study for CDI and DDI interchange configurations are able to support planning and decision-making procedures for interchange improvement projects and should contribute to the development of criteria for the selection, planning, and design of CDI to DDI interchange conversions. From the sensitivity analysis of the CDI and DDI interchange configurations using both critical lane volume and microscopic simulation, the two configurations were found to provide similar performance (or alternate configuration which provided better service) at left-turn proportions between 30% and 50% of the total traffic demand, dependent on the interchange lane configuration and total demand. For instance, the left-turn proportion at which a DDI configuration outperforms the CDI configuration increases as the number of lanes on the cross-street cross section increases. The CDI also performs better at lower cross-street demands, although its operation degrades faster than that of the DDI at high cross-street demands. In the current study, the impact of off-ramp demands on the CDI and DDI operational performance is inconclusive.

5.2 Recommendations

It is recommendated that a CDI is likely the preferred alternative at locations with low traffic volumes and left-turn traffic proportions below 30% of the total traffic demand, and a DDI is likely the preferred alternative at locations with higher traffic volumes and left-turn proportions exceeding 50% of the total demand. Volumes sets that fall between these ranges will required modeling of the specific case to determine the superior alternative.

In addition, this study provides a foundation for developing more detailed standards and guidelines for the implementation of a DDI based on various lane configurations and traffic conditions. However, for a more thorough analysis the researchers recommend that future studies conduct the simulation study for both balanced and unbalanced traffic conditions and expand the study area to include adjacent intersections.

It is also recommended to study the operational impact of large trucks (exceeding 50 ft in length) with a turning radius that would require multiple lanes to enter the bridge. This will provide a better understanding of the impact of DDI geometrics in accommodating heavy trucks. Inaddition, adding ramp meters into simulation models will capture the impact of spillback from on-ramps to the bridge. This will provide more reliable performance data where freeway congestion may impact the cross-street operations.

Finally, it is recommended to develop inproved lane utilization factors. Improved lane utilization factors, in addition to left-turn and heavy-vehicle adjustment factors, will allow the CLV analysis to better replicate the potential variations in field conditions. These additions to future study will provide more reliable and accurate data in analyzing the DDI operational performance.

5.3 Limitations in the Study

There are a few limitations in this study that can be improved in future research efforts. First, as noted by Chlewicki (2011) and Schroeder et al. (2014), the CLV method oversimplifies the operational performance of an interchange and an intersection. It tends to overestimate the performance of the CDI due to its inability to account for intersection signal synchronization. As a result, some discrepancies in results between the CLV analysis and the simulation study were found, especially on the through movements exiting the bridge (i.e., SBT1 and NBT2). In both the CDI and DDI configurations, the VISSIM simulations show relatively constant, low delays on the through movements exiting the bridge with good signal coordination between the intersections. However, the CLV method does not reflect this intersection synchronization, resulting in higher v/c ratios for the same movements on DDIs.

In addition, the CLV analysis does not capture the impact of significant queuing or spillback. For instance, on the DDI configuration the freeway on-ramp from the cross street is assumed to be uninterrupted and, thus, free flow. However, it is possible the free-flow traffic could lead to downstream congestion on the ramp, either when merging with right-turning vehicles from the cross street or merging onto the freeway. Spillback, potentially to the bridge, is not reflected by the CLV method. This problem was observed during peak hours at the interchange of Jimmy Carter Boulevard and I-85. Therefore, it is important for engineers and planners to understand the potential broader impact of the improved DDI left-turn accommodation, and that bottlenecks may not be eliminated, only moved to new locations. This study also did not take into account adjacent intersections. Adjacent intersections may have significant impacts on the interchange operation. However, adjacent intersections were neglected in this study to minimize the number of confounding variables in the operational analysis.

During the field observation at the study interchange, it was observed that a large truck, exceeding 50 ft in length, occupied both off-ramp lanes while turning onto the bridge. This behavior is not replicated in the current CLV analysis or VISSIM simulation. However, when designing the interchange, consideration must be given to the potential reduction in capacity due to tight curve radii. Future efforts may expand the current VISSIM model to explore this impact.

This study only examined balanced volume conditions, i.e., similar demand from both cross-street approaches. It is desirable to expand the analysis to explore the impact of unbalanced volumes.

Lastly, this study did not consider conditions unique to the Jimmy Carter interchange. For instance, the selected 2000 (vphrpln) saturation flow is likely not realistic for the I-85 northbound off-ramp to Jimmy Carter Blvd. as the ramp approach curvature at Jimmy Carter Blvd. likely results in reduce saturation flow and performance. In addition, the opening of the shoulder usage lane added some confounding variables in the before–after analysis. However, this study has gathered the pre- and post-deployment travel-time data, and a before–after analysis should still be considered in a follow-on study to understand how traffic operations were affected at this interchange with the combination of changes that occurred.

CHAPTER 6. REFERENCES

Autey, J., T. Sayed, and M. El Esawey (2012). "Operational Performance Comparison of Four Unconventional Intersection Designs Using Micro-simulation." *Journal of Advanced Transportation* **47**(5): 17.

Bared, J., P.K. Edara, and R. Jagannathan. (2005). "Design and Operational Performance of Double Crossover Intersection and Diverging Diamond Interchange." In *Transportation Research Record: Journal of the Transportation Research Board, No. 1912*: 31–38.

Chlewicki, G. (2003). "New Interchange and Intersection Designs: The Synchronized Split-Phasing Intersection and the Diverging Diamond Interchange." Presented at 2nd Urban Street Symposium, Anaheim, Calif.

Chlewicki, G. (2011). "Should the Diverging Diamond Interchange Always Be Considered a Diamond Interchange Form?" In *Transportation Research Record: Journal of the Transportation Research Board, No. 2223*: 88–95.

Chlewicki, G. (2014). "The Diverging Diamond Interchange Website." History. Retrieved August 18, 2017. http://www.divergingdiamond.com/index.html.

Chilukuri, V., S. Siromaskul, M. Trueblood, and T. Ryan. (2011). "Diverging Diamond Interchange: Performance Evaluation (I-44 and Route 13)." National Technical Information Service, HDR Engineering, Missouri Department of Transportation, Federal Highway Administration: 62.

Cogan, C.A. (2008). "The Design and Operations of Diverging Diamond Interchange: A Case Study in Kansas City, Missouri." *Civil Engineering*. University of Missouri, Master in Science: 60.

Edara, P.K., J.G. Bared, and R. Jagannathan. (2005). "Diverging Diamond Interchange and Double Crossover Intersection—Vehicle and Pedestrian Performance." The 3rd International Symposium on Highway Geometric Design, Chicago, Illinois.

Bastian S.; C. Cunningham, B. Ray, A. Daleiden, P. Jenior, and J. Knudsen. (2014). "Diverging Diamond Interchange Informational Guide" Publication FHWA-SA-14-067. FHWA, U.S. Department of Transportation.

Galletebeitia, B. (2011). “Comparative Analysis Between the Diverging Diamond Interchange and Partial Cloverleaf Interchange Using Microsimulation Modeling.” *Civil Engineering*. ProQuest LLC, Florida Atlantic University. Master’s: 1199.

Hughes, W., R. Jagannathan, D. Sengupta, and J. Hummer. (2010). “Alternative Intersections/Interchanges Informational Report (AIIR).” Publication FHWA HRT-09-060. FHWA, U.S. Department of Transportation.

Investopedia. (2017). “Terms.” Sensitivity Analysis. Retrieved August 31, 2017. http://www.investopedia.com/terms/s/sensitivityanalysis.asp.

Khan, T., and A. Michael. (2016). “Evaluating the Application of Diverging Diamond Interchange in Athens, Alabama.” *International Journal for Traffic and Transport Engineering* **6**(1): 38–50.

Maji, A., S. Mishra, and M.K. Jha. (2013). “Critical Lane Volume-based Capacity and Level of Service Analyses for Diverging Diamond Interchange.” 92nd Annual Meeting of the Transportation Research Board, Washington, D.C.

Missouri Department of Transportation. (2010). “Missouri’s Experience with a Diverging Diamond Interchange—Lessons Learned.” Missouri Department of Transportation.

Ressel, N.R. (2012). “Insights into the First Three Diverging Diamond Interchanges in Missouri.” *Civil Engineering*. University of Missouri, Master in Science: 97.

Schroeder, B.J., K. Salamati, and J. Hummer. (2006). “Calibration and Field Validation of Four Double-Crossover Diamond Interchanges in VISSIM Microsimulation.” In *Transportation Research Record: Journal of the Transportation Research Board, No. 2404*: 49–58.

Schroeder, B., C. Cunningham, B. Ray, A. Daleiden, P. Jenior., and J. Knudsen. (2014). “Diverging Diamond Interchange Informational Guide.” Publication FHWA-SA-14-067. FHWA, U.S. Department of Transportation.

Sharma, S., and I. Chatterjee. (2007). “Performance Evaluation of the Diverging Diamond Interchange in Comparison with the Conventional Diamond Interchange.” Department of Civil and Environmental Engineering, University of Missouri-Columbia: 13.

Speth, S.B. (2008). "A Comparative Analysis of Diverging Diamond Interchange Operations." ITE 2008 Annual Meeting and Exhibit, Washington D.C., HDR Engineering.

Stanek, D. (2007). "Innovative Diamond Interchange Designs: How to Increase Capacity and Minimize Cost." Institute of Transportation Engineers Annual Meeting, Pittsburgh.

Transportation Research Board. (2010). *Highway Capacity Manual*. Transportation Research Board of the National Academies, Washington, D.C. Print.

Woody, T. (2006). "Calibrating Freeway Simulation Models in VISSIM." *Civil Engineering*. University of Washington, Master's: 20.

Xiao, H., R. Ambadipudi, J. Hourdakis, and P. Michalopoulos. (2005). "Methodology for Selecting Microscopic Simulators: Comparative Evaluation of AIMSUN and VISSIM." Intelligent Transportation Systems Institute, University of Minnesota. May.

Yeom, C., B. Schroeder, C. Cunningham, C. Vaughan, N. Rouphail, and J. Hummer. (2014). "Lane Utilization at Two-Lane Arterial Approaches to Double Crossover Diamond Interchanges." In *Transportation Research Record: Journal of the Transportaton Research Board, No. 2461*(13): 103–112.

Zhang, Z., and T. Zong. (2010). "Signal Control of Dual T-intersections and Partial Cloverleaf Interchanges with One Controller." Presented at the Technical Session of 2010 ITE Western District Conference, San Francisco.

APPENDIX A. PRE-DEPLOYMENT DATA COLLECTION AND ANALYSIS

List of Figures

List of Tables

This project focused on determining the general traffic operating conditions under which a DDI is more appropriate than a CDI and vice versa, using traffic simulation and CLV analysis. However, as part of the study, traffic operations performance data were collected at the interchange and the adjacent area. Vehicle travel-time data were collected for both the pre-deployment and post-deployment period. The following sections provide the details of the data collection and an analysis of the pre-deployment data.

A.1 Data Source, Collection Sites, and Routes

The traffic operations performance data were collected using commercial "off–the-shelf" Bluetooth® travel-time detection equipment. A total of six Bluetooth® detectors were deployed in the field by the Georgia Department of Transportation (GDOT) over the study area. These detectors recorded Bluetooth® media access control (MAC) addresses of Bluetooth®-equipped devices (in discoverable mode) within vehicles traversing the study location. MAC addresses are assigned under a scheme designed to reduce the likelihood that any two devices will have the same MAC address. Under this scheme, 48-bit MAC addresses are comprised of six sets of two alphanumeric pairs. The first three pairs are assigned to a specific hardware manufacturer, while the last three are generated by the manufacturer to be unique among all devices they manufacture (Barceló et al. 2010). Since MAC addresses are expected to be unique among all digital devices, Bluetooth® detectors can match the MAC addresses detected at different locations to generate travel times between these locations. For the before-and-after DDI analysis, 20 unique routes were defined for MAC address matching; however, only 10 of the routes were used for the analysis. The 10 routes chosen for analysis overlap the other 10 routes that were defined and cover a longer route. This serves two purposes. First, these 10 routes cover the entire coordinated signal corridor allowing evaluation of the corridor as a whole. Second, the origins and destinations on these routes are farther from each other, thereby reducing the impact of error from uncertainties in detection location of the Bluetooth® system (Colberg et al. 2014). Figure A - 1 shows the location of Jimmy Carter Blvd. with respect to Atlanta, Georgia. Figure A - 2 shows the Bluetooth® device locations in the corridor. Figure A - 3 shows five maps outlining the 10 routes through the interchange for which Bluetooth® travel times were collected for this analysis.

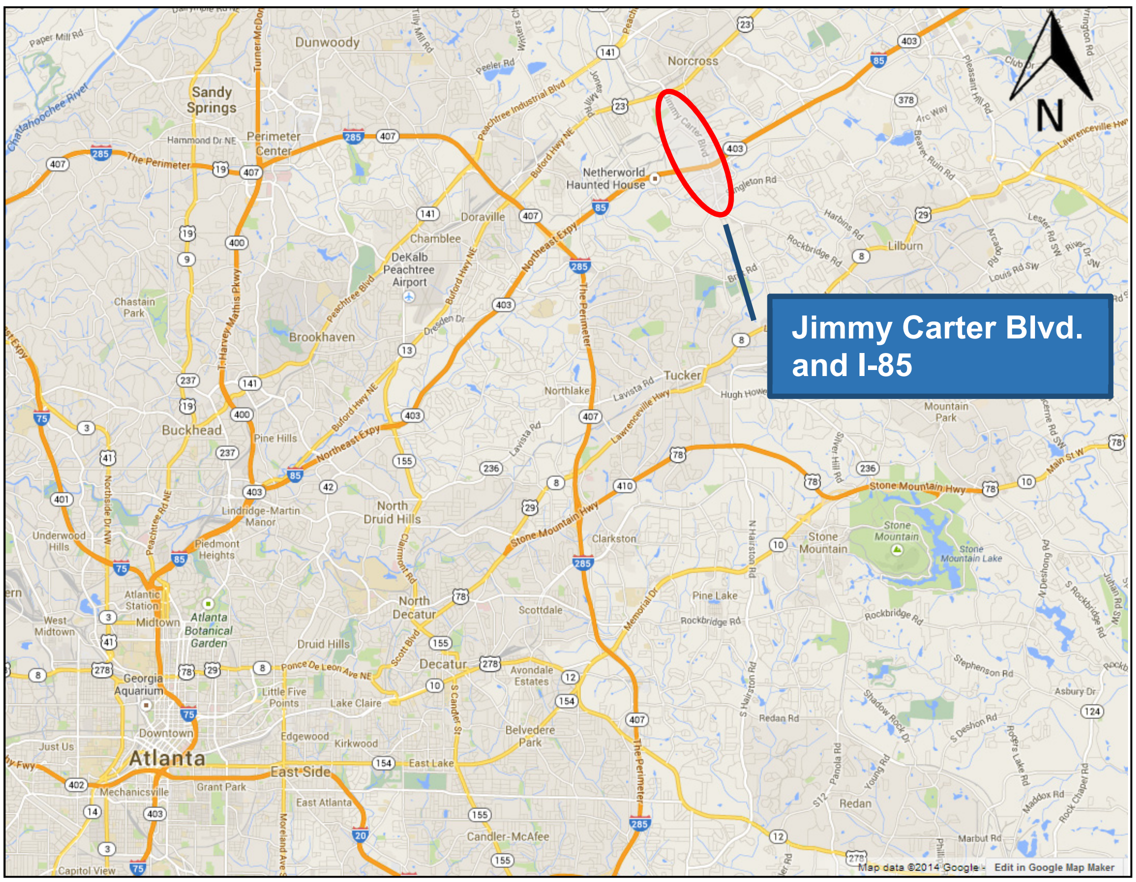

Figure A - 1: Location of Jimmy Carter Blvd. in Metro Atlanta, GA

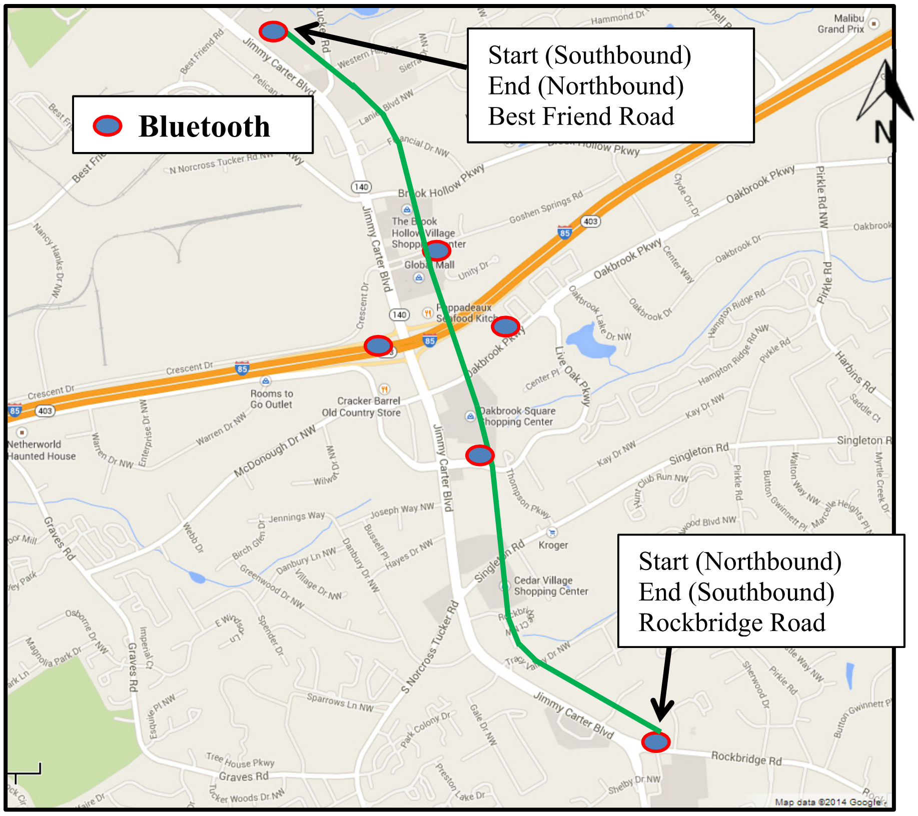

Figure A - 2: Jimmy Carter Blvd. Bluetooth® detector unit locations

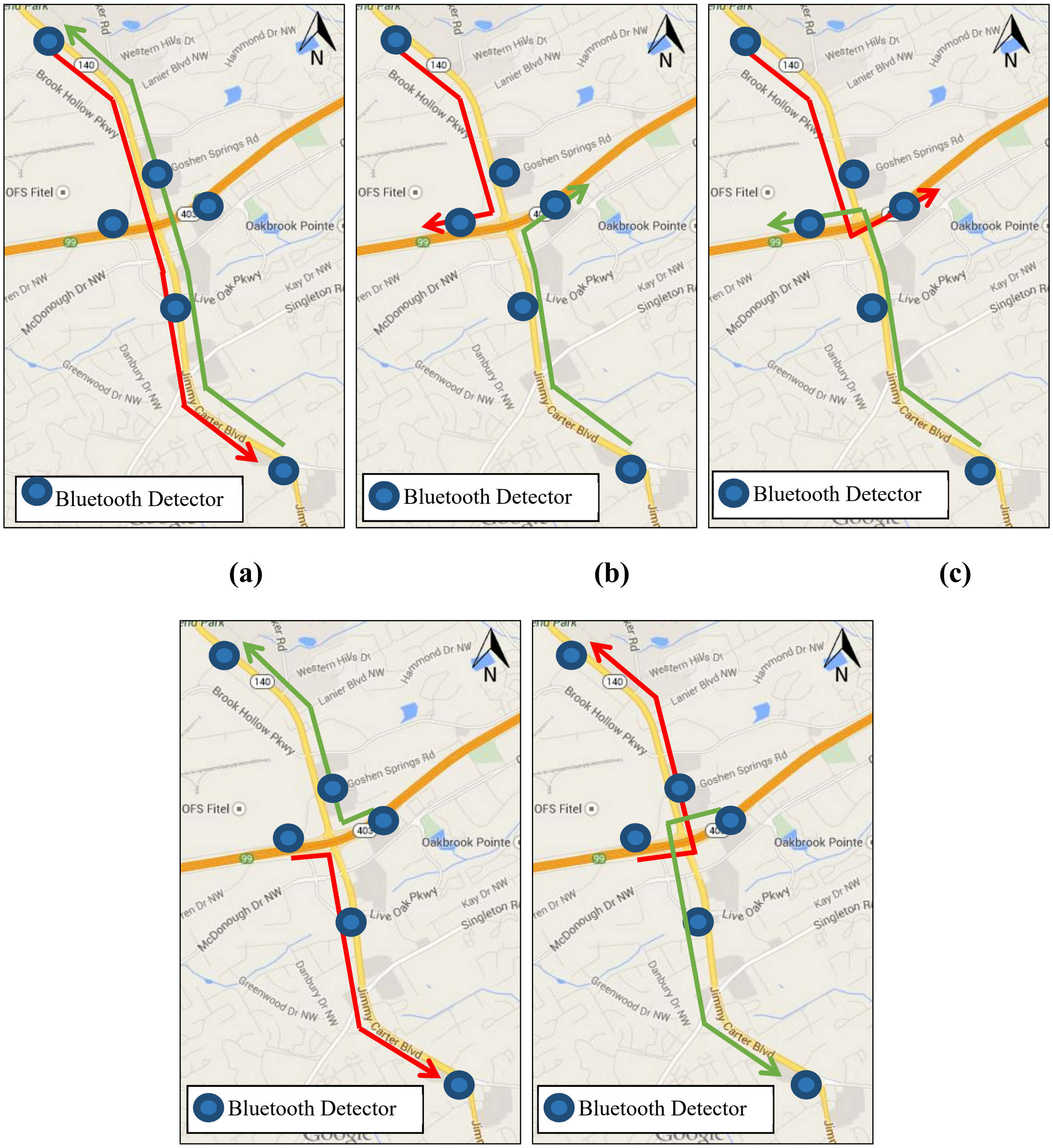

(a) **(b)** **(c)**

(d) **(e)**

Figure A - 3: The 10 Travel-time routes used for multiple distribution analysis, (a) northbound (NB) and southbound (SB) routes through the interchange, (b) NB and SB right turn onto I-85, (c) NB and SB left turn onto I-85, (d) right turns originating from I-85, and (e) left turns originating from the interchange

The 10 routes shown in Figure A - 3 are the 10 possible paths that can be taken through the interchange. The routes are shown in green or red lines/arrows, and Bluetooth®

detectors are shown as blue circles. Figure A - 3(a) shows the northbound (NB) and southbound (SB) routes through the interchange that originate and terminate at the northernmost and southernmost Bluetooth® detectors. Figure A - 3(b) shows the two routes originating at the northernmost and southernmost Bluetooth® detectors, making a right turn onto I-85, and terminating at the Bluetooth® detectors located at the interchange ramps. Figure A - 3(c) shows the two routes originating at the northernmost and southernmost Bluetooth® detectors, making a left turn onto I-85, and terminating at the Bluetooth® detectors located at the interchange ramps. Figure A - 3(d) shows the two routes originating from the I-85 exit ramps, turning right onto Jimmy Carter Blvd., and terminating at the northernmost and southernmost Bluetooth® detectors. Finally, Figure A - 3(e) shows the two routes originating from the I-85 exit ramps, turning left onto Jimmy Carter Blvd., and terminating at the northernmost and southernmost Bluetooth® detectors.

As illustrated in Figure A - 3, only one detector was being used at each origin and destination to detect both directions of travel. At each of these locations the detector was mounted on various roadside objects such as utility poles, signal support poles, or road sign gantry supports. At the interchange ramp locations, the detectors were detecting vehicles not only at the adjacent ramp but also at the ramp located on the far side of I-85 across from the detector. This large distance (approximately 220 ft at the NB on-ramp and 250 ft at the SB on-ramp) is within the 1000-ft range of the commercial Bluetooth® detectors. However, due to the larger distances, it is expected that the detection rate of routes originating at the I-85 exit ramps would be lower than that of other routes originating and terminating at locations closer to the detectors. Besides distance from the detector, several other factors can also affect the detection rate of Bluetooth® devices, as described in the following subsection.

A.1.1 Bluetooth® Characteristics Affecting Travel Times

Bluetooth® is a method of wireless communications operating in the 2.4 Gigahertz (GHz) to 2.483 GHz frequencies. The connection process between two Bluetooth® devices can take up to 10.24 seconds. Some studies have found that most devices take between 5.12 and 5.76 seconds to establish a connection (Chakraborty et al. 2006; Peterson et al. 2006). Due to the variance in delay of a connection between devices and the detector, as well as device signal strength and sensitivity, different devices may be detected at different distances from the detector. Furthermore, once a device is detected it is typically re-detected several times before the device leaves the detection zone. The detectors used in this study are proprietary and specifications of the detectors as well as their filtering processes for multiple detections are not readily available. Therefore, the exact location where each Bluetooth® device was detected is unknown, which adds some variability to the travel times used in this study.

For data verification purposes, license plate data were recorded along this corridor via automated license plate recognition (ALPR) cameras at locations approximately matching the locations of the Bluetooth® sensors' detection areas. The license plates were matched using a Visual Basic script, and travel times were derived by subtracting the time stamps of the license plate records across locations. The travel times from the ALPR system and the Bluetooth® system were then compared visually. The Bluetooth® travel times and the ALPR travel times are plotted in Figure A - 4. The blue triangles are Bluetooth® data that have been filtered via the commercial Bluetooth® systems filters, the green plus signs are the Bluetooth® raw matches, and the red circles are the ALPR travel times. Figure A - 4 shows that although ALPR generates more travel-time data, both the filtered and unfiltered Bluetooth® travel times closely match the ALPR travel-time data. Furthermore, both systems show similarities in outlying data points. Finally, this comparison also shows that with enough data points collected on a single day the multiple distribution tendency is prominent. In the ALPR data, two prominent bands are observed between 2:00 PM and 4:15 PM. As congestion sets in after 4:15 PM, the lower band begins to diminish, but does not completely disappear.

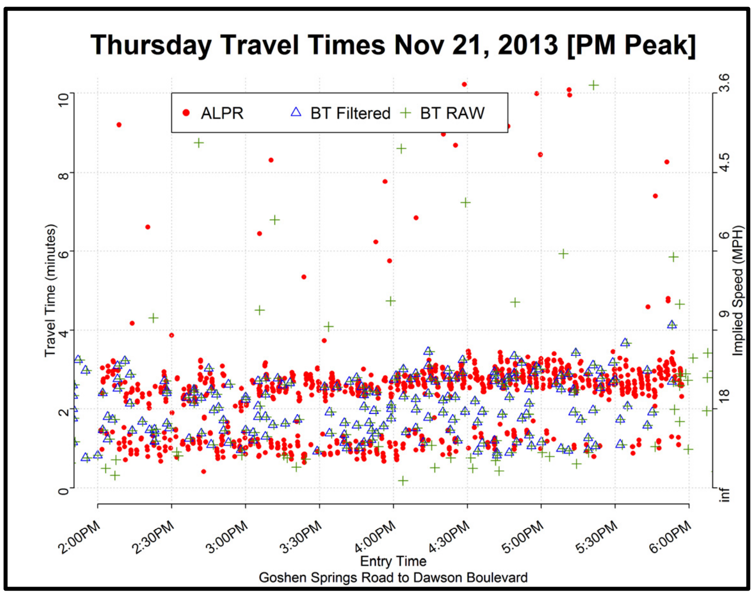

Figure A - 4: Bluetooth® raw matches, Bluetooth® filtered matches, and ALPR travel-time comparison

Besides the variability in detection location affecting travel times, previous studies of Bluetooth® travel-time technology have found detection rates ranging from 5 to 10 percent (Day et al. 2010; Brennan et al. 2010; Tarnoff et al. 2009; Wang et al. 2010). These detection rates are calculated as the number of unique MAC address detections divided by the total volume passing the detector. Due to the low detection rate of

Bluetooth® detectors (Zinner 2012; Box 2011), it is difficult to perform analyses and identify patterns over short (e.g., one-hour) intervals, and successful analysis often requires combining data from multiple days. For this study, data were segregated into five data sets, one for each day of the week. The individual datasets comprised 14 days of data, collected over a 16-week period between Monday, August 5, 2013, and Friday, November 22, 2013, and excludes data collected during the week of a major U.S. holiday (i.e., Labor Day—Monday September 2, 2013). Due to an outage in the Bluetooth® system, data were also not collected from September 13, 2013, to September 25, 2013.

The individual data points of the data across multiple days were plotted with a different color symbol for each unique day within the data set, to check whether any of the days displayed drastically different traffic patterns. A sample plot using the data for Tuesdays is provided in Figure A - 5.

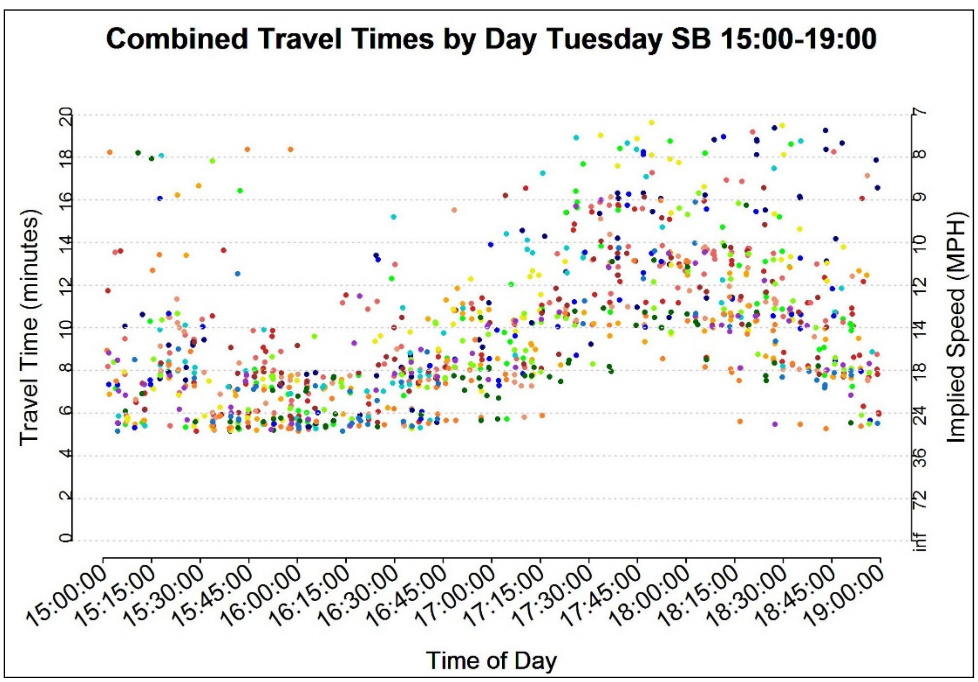

Figure A - 5: Mixed Tuesday raw data plot from 3 PM to 7 PM for the SB through route

A.2 Previous Research

As observed in Figure A - 4, the travel-time data from the study site displayed multiple bands in the data, indicating the presence of multiple distributions in the dataset. Bimodal and multimodal distributions of travel time have been previously observed in a number of settings. These include arterials (Ji and Zhang 2013; Yang et al. 2014), due to the presence of signalized intersections, and freeways (Park et al. 2010; Chalumuri and Asakura 2012; Colberg et al. 2014) when there are lane closures during construction periods or, more generally, when both congested and uncongested travel is present. These multimodal distributions reflect different subgroups of traffic that may experience different service quality along the same roadway. Previous studies have used expectation–maximization (EM) and hierarchical Bayesian mixture models to separate these distributions in order to develop travel-time reliability indices (Ji and Zhang 2013; Yang et al. 2014; Park et al. 2010; Chalumuri and Asakura 2012).

In this study, an expectation–maximization algorithm (Benaglia et al. 2010) is utilized to separate multimodal travel-time data collected on a major arterial (Jimmy Carter Blvd.) in the metropolitan Atlanta area and assign a separate corridor-level LOS rating to each distribution. This multiple LOS rating method is not intended to replace the HCM 2010 facility LOS method (TRB 2010); instead, it is being developed as a supplementary tool to provide more detailed LOS information. For example, the impact of roadway improvements (e.g., signal timing, geometric changes, etc.) on the different road user subgroups may be directly evaluated by providing a more detailed view that captures the underlying performance of each subgroup rather than a single aggregate LOS measure. This type of analysis is becoming available by the growing availability of disaggregate travel-time data by continuous data collection systems such as Bluetooth®, cell phone tracking, etc. The advantages and drawbacks of this approach are discussed later in the text.

As mentioned earlier, bimodal/multimodal travel-time distributions have been encountered on multiple roadway types (Park et al. 2010; Chalumuri and Asakura 2012; Ji and Zhang 2013; Colberg et al. 2014; Yang et al. 2014). Typically, these distributions have been studied in association with research on travel-time reliability and/or congestion detection. For example, two previous studies aimed to develop congestion detection algorithms for arterial roadways (Ji and Zhang 2013; Yang et al. 2014). Ji and Zhang successfully used bus probe data to collect travel times along an arterial roadway on the Ohio State University campus by recording from the campus bus automatic vehicle location (AVL) system. In that study, location data near bus stops were omitted in order to collect travel-time data on segments that included either one signal or no traffic signal and did not include delay from boarding and alighting. It was found that the segments with one signal consistently showed bimodality in travel times, while a segment without a signal had only a single mode. Curves were fit to the resulting data using a Bayesian mixture model assuming either a single or bimodal distribution, and then congestion-detection algorithms were applied. In the segments with a signalized intersection, the developed congestion-detection algorithms detected congestion more accurately with the mixed models than the single-mode models (Ji and Zhang 2013).

In a second study by Yang et al., similar data were collected on multiple corridors in the downtown area of Nanjing, China. The selected links were similar to Ji and Zhang's study in that each link only contained one signal. Similarly, bimodal distributions were found and an EM algorithm was used to separate the data. In this study a combination of six distribution types were tested on each data set and the best fit for each distribution was found based on the resulting R-squared values. Subsequently, the resulting distributions were applied to two methods of detecting congestion in bimodal travel-time distributions: the expected-travel-time and RATIO indices (Yang et al. 2014). Additionally, Henclewood et al. suggested that although first moment values, such as average travel time, may be sufficient to evaluate general traffic performance at an aggregated level, considering travel times at the distribution level allows for a better representation of traffic performance at an individual vehicle level (Henclewood et al. 2013).

Freeway studies have also found bimodal travel-time distributions (Park et al. 2010; Chalumuri and Asakura 2012). Park et al. created a model to predict congested and uncongested freeway travel times similar to weather forecasting. In that study, simulated data were used from a model of I-66 outside of Washington, D.C. Using this model, congested and uncongested conditions were simulated separately and data from the different simulation runs intentionally were mixed. Here, varying ratios of congested travel-time data and uncongested travel-time data were mixed and separated using EM algorithms. Travel-time data for all vehicles completing the route were available so the ratio of congested to uncongested data was known before bimodal curve fitting. After separating the data, the output ratios from the EM algorithm were found to be very similar to the known input conditions. Their conclusion was that if a sufficiently high sampling rate could be attained on freeways, the ratio of congested to uncongested travel times during periods of the day could be accurately estimated. Therefore, these ratios, developed using historical data, could be used to give drivers the probability of encountering congestion during a given time on a given route, and provide an estimate of congested and uncongested travel times (Park et al. 2010). These multimodal distributions have also been determined by Colberg et al. (2014) to occur on freeways in work zones when lane closures are present. They found that drivers in the left lanes of the study corridor (the location of the lane closures) experienced significantly shorter travel times than those in the right lanes of the same freeway. The researchers believed that vehicles in the right lanes experienced higher delays due to queue formation in the right lanes and that slower moving trucks were not permitted to travel in the left lanes (Colberg et al. 2014).

A.3 Multiple Travel-time Distribution Separation

Arterial roadway travel times often exhibit multiple travel-time distributions within the same time period. This is typically caused by the signal systems in place along these corridors (Ji and Zhang 2013; Yang et al. 2014). It is well known that coordinated signal systems may systematically enforce groupings of vehicles into different travel-time bands. For example, one group of vehicles may be able to traverse the entire corridor stopping only once due to a red signal, while another vehicle group may traverse the same corridor and encounter multiple red signals. In this scenario, the vehicles that stop multiple times will have more delay and a longer travel time than vehicles that stop only once. Furthermore, as congestion builds along signalized corridors and queueing spills back from one intersection to the next, it becomes more likely that drivers will be delayed at more than one intersection, pushing more drivers into higher travel-time bands. Another source of these multiple distributions may be congestion and delays due to lane-specific conditions. For example, spillback from left-turn lanes into through lanes may cause added delay to through vehicles traveling in the lanes adjacent to the left-turn lanes. For instance, in the corridor studied for the current research, left-turn lane spillbacks have been witnessed by the research group along the study corridor during congested periods. Additional potential causes for multiple travel-time distributions exist, such as high driveway densities, lane additions and drops, etc.

For this multiple distribution data deconvolution analysis, the paths of interest are from (1) the north end to the south end of the Jimmy Carter Blvd. corridor, a distance of 2.4 miles (4 km); and (2) the reverse path. Figure A - 6 illustrates the observed travel times over the study period for the southbound (Tuesday, 5:00 PM to 6:30 PM) and northbound (Tuesday, 5:00 PM to 6:30 PM) through movements, respectively. In this figure, data-points represent a single paired (origin–destination) observed travel time with the varying colors representing different measurement days. The time periods analyzed in this research were derived from the signal timing plan periods (e.g., before and after the 5 PM to 6:30 PM period, different signal plans are implemented). These analysis periods were chosen to eliminate the possibility of multiple travel-time distributions occurring due to signal plan changes within the analysis periods. These data sets have been pre-processed with two filters. The first filter is a "20 minute" filter that removes any travel-time observation greater than 20 minutes. The second filter is a "60 miles per hour" filter that acts to remove any observed travel time that, when converted to a speed, is greater than 60 mph. These filters removed data likely resulting from well-known issues associated with travel-time data collected using Bluetooth® technology (Wasson et al. 2010; Colberg 2013; Colberg et al. 2014) and are considered well outside the reasonable travel-time range for this corridor. In all cases the number of removed data points was minimal.

Observing Figure A - 6(a), travel-time "bands" are discernable at approximately 6, 8, and 10 minutes. Furthermore, in Figure A - 6(b) it is difficult to visually distinguish any obvious banding of travel times. However, in the histograms for these data shown in Figure A - 7, for the southbound direction there are possibly up to five discernable travel-time bands: the first centered at slightly less than 6 minutes, the second at slightly less than 8 minutes, the third (and fourth) at greater than 8 minutes, and a possible fifth band capturing data over 14 minutes. For the northbound direction there also may be up to five distributions; however, these distributions appear to be closer together, suggesting that there is possibly less congestion. These multiple distributions do appear to be centered at approximately 5.5, 6.5, 8, and 9 minutes as well as a fifth distribution encompassing data from 10 minutes onward.

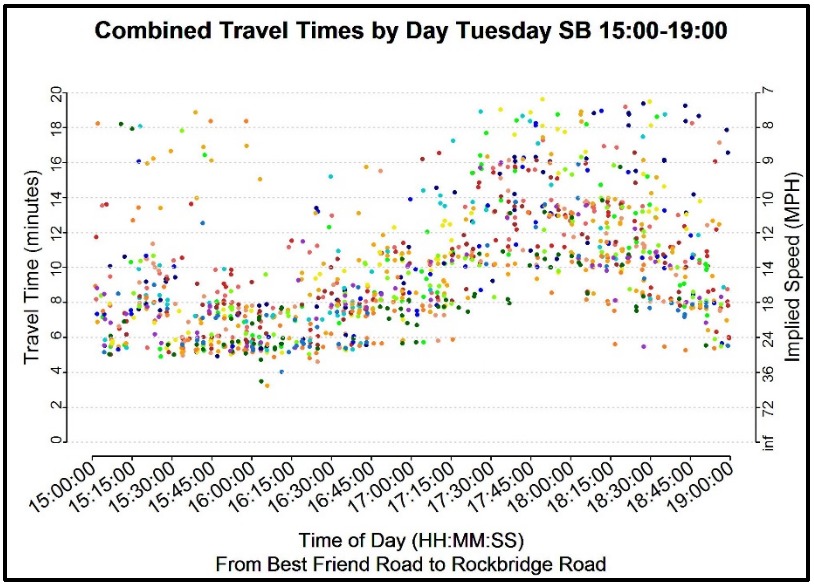

(a)

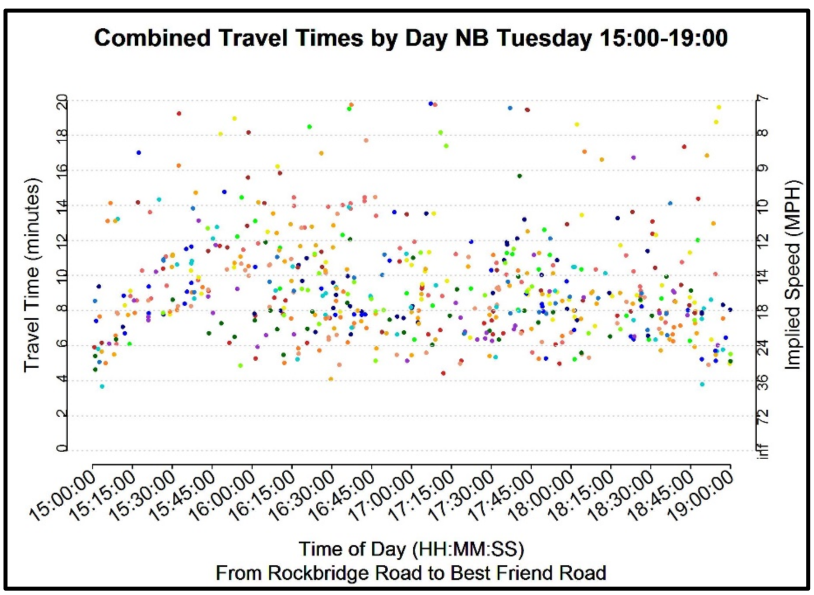

(b)

Figure A - 6: Travel times for through movements along the study corridor:
(a) southbound travel times (AM peak), (b) northbound travel times (AM Peak)

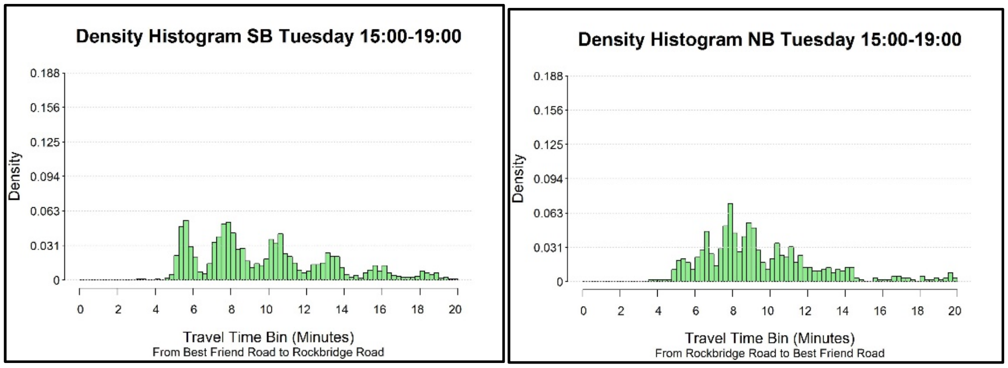

(a) **(b)**

Figure A - 7: Travel-time histogram of data in Figure 2: (a) southbound histogram, (b) northbound histogram

The multiple peaks (modes) displayed in the histograms provide strong evidence for the existence of multiple travel-time distributions. To identify the characteristics of these individual distributions, multiple gamma curves were fit to the observations. To accomplish this, an EM algorithm for multiple gamma curve fitting was used. This algorithm, named the gammamixEM function, is part of the "mixtools" package that was developed and implemented in R by Bengalia et al. (2009). This function uses the expectation–maximization iterative process to fit multiple gamma curves and provides an *a posteriori* probability for each data point (i.e., the estimated probability that the point belongs to a particular distribution). These probabilities were used, in conjunction with a random number generated between 0 and 1, to assign individual data points to a particular distribution. It should be noted that since multiple distributions were fit, multiple posterior probabilities were generated for each data point, the sum of which equals 1. Finally, Figure A - 8 shows the fitted gamma curves for each travel-time band and the histograms of the data assigned to each distribution for the southbound direction. Six distributions were fit for the southbound direction. This number of underlying distributions was chosen using an R-square value in conjunction with an Akaike information criterion (AIC) number.

In this process, multiple distributions were fit (1 to 7 distributions). To ensure that each distribution fit was an optimum fit, the multiple distribution function was run 100 times for each number of distributions and the fit with the highest R-squared value was taken to compare between number of distributions. To compare between the number of distributions, the AIC value was used. The AIC value uses the log likelihood of the fit with a modification factor for the number of parameters used in the fit. This allows a comparison between different number of fits while accounting for information lost due to increased complexity of the model.

In general, multi-distributional fit provided a meaningful improvement in information over a single distribution fit, as witnessed by the AIC values. However, based on this process some time periods did show a better fit with only a single distribution rather than multiple distributions for the northbound route. For example, for the 7:45 AM to 8:45 AM and the 3:00 PM to 5:00 PM time periods, the AIC values were lowest for a single distribution. For the data shown in Figure A - 8, a six-distribution fit was chosen. This fit's AIC value was 2188 while its respective single-distribution fit AIC value was 2295. Because the AIC value for the six-distribution fit was lower, it provides a meaningful improvement in information content.

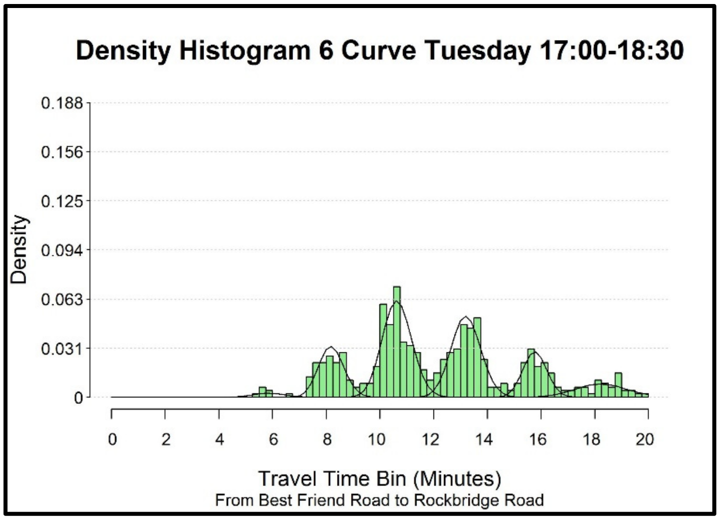

Figure A - 8: Southbound travel-time data with a 6-curve fit.

A.4 Multiple LOS Rating Assignment

After assigning multiple gamma functions to the data sets and separating the data by distribution, an LOS rating was assigned to each distribution. In order to assign an LOS rating for each distribution, a base free-flow speed for each direction was first determined. The HCM methodology for determining the facility LOS rating was followed when determining the base free-flow speed (TRB 2010). A base free-flow speed was not field measured as the given Bluetooth® data include control delays and do not allow for distinguishing free-flow speeds on a corridor (TRB 2010).

Travel speed through the corridor was derived from the travel-time data distributions. For each distribution created through the curve-fitting procedure, the average travel time was converted into a speed in miles per hour. The final step in determining facility LOS was to calculate the percent reduction of free-flow speed for each individual mode and determine which speed-reduction range included the observed reduction.

Table A - 1 shows the percentile ranges for each LOS rating according to the 2010 HCM. The multiple-facility LOS ratings for the lowest speed hour for the AM and PM periods can be found in the results section in Table A - 2. In the HCM method of analysis a v/c ratio greater than 1.0 automatically warrants an LOS of F, as shown in Table A - 1. In this study, volume counts corresponding to the travel-time data were not available. Thus, for this analysis, v/c ratio was not considered when determining LOS ratings.

Table A - 1: Percentile ranges for facility LOS ratings (TRB 2010)

Travel Speed as a Percentage of Base Free-Flow Speed (%)	LOS by Critical Volume-to-Capacity Ratio	
	≤ 1.0	≥ 1.0
>85	A	F
>67–85	B	F
>50–67	C	F
>40–50	D	F
>30–40	E	F
≤30	F	F

A.5 Results

For brevity, one day of results from the combined Tuesday dataset is shown here. Table A - 2 presents the LOS and mean speed for each modal distribution, and the overall, corresponding signal timing period of the day and direction along the corridor for the Tuesday data. LOS ratings are generally lower for the PM time periods than for the AM. Figure A - 9 and Figure A - 10 provide temporal plots and histograms for the complete data set and each of the three modal distributions (Mode 1=slowest) determined by the fitting procedures for the southbound and northbound routes, respectively.

Table A - 2: Facility LOS ratings for AM lowest mean speed hour on Jimmy Carter Blvd.

		Mean Speed							Level of Service							Avg	Avg
Direction	Time	1	2	3	4	5	6	7	1	2	3	4	5	6	7	Speed	LOS
SB	6:00 - 7:45	19.2	26.2	14.8	11.5	8.33	--	--	D	C	E	F	F	--	--	18.6373	D
SB	7:45 - 8:45	25.6	18.9	13.1	8.11	--	--	--	C	D	E	F	--	--	--	17.0666	E
SB	8:45 - 9:30	25.2	18.7	14.5	11.8	9.25	--	--	C	D	E	F	F	--	--	16.5644	E
SB	9:30 - 15:00	28.2	20.9	16.2	12	9.05	--	--	C	D	E	F	F	--	--	20.991	D
SB	15:00 - 17:00	25.2	39.4	18.4	14.1	10.8	8.25	--	C	A	D	E	F	F	--	19.4232	D
SB	17:00 - 18:30	22.8	17.2	13.3	10.7	8.93	7.71	--	C	D	E	F	F	F	--	12.2724	F
SB	18:30 - 19:00	24.8	17.7	13.4	10.9	8.18	--	--	C	D	E	F	F	--	--	15.0686	E
NB	6:00 - 7:45	22.3	11.5	--	--	--	--	--	C	F	--	--	--	--	--	20.4726	D
NB	7:45 - 8:45	16.4	--	--	--	--	--	--	E	--	--	--	--	--	--	16.3952	E
NB	8:45 - 9:30	26.9	15.5	--	--	--	--	--	C	E	--	--	--	--	--	24.8433	C
NB	9:30 - 15:00	22.4	20.8	9.7	--	--	--	--	C	D	F	--	--	--	--	20.3692	D
NB	15:00 - 17:00	15.7	--	--	--	--	--	--	E	--	--	--	--	--	--	15.6655	E
NB	17:00 - 18:30	17.1	7.77	--	--	--	--	--	E	F	--	--	--	--	--	16.6385	E
NB	18:30 - 19:00	19.7	10.7	--	--	--	--	--	D	F	--	--	--	--	--	18.3045	D

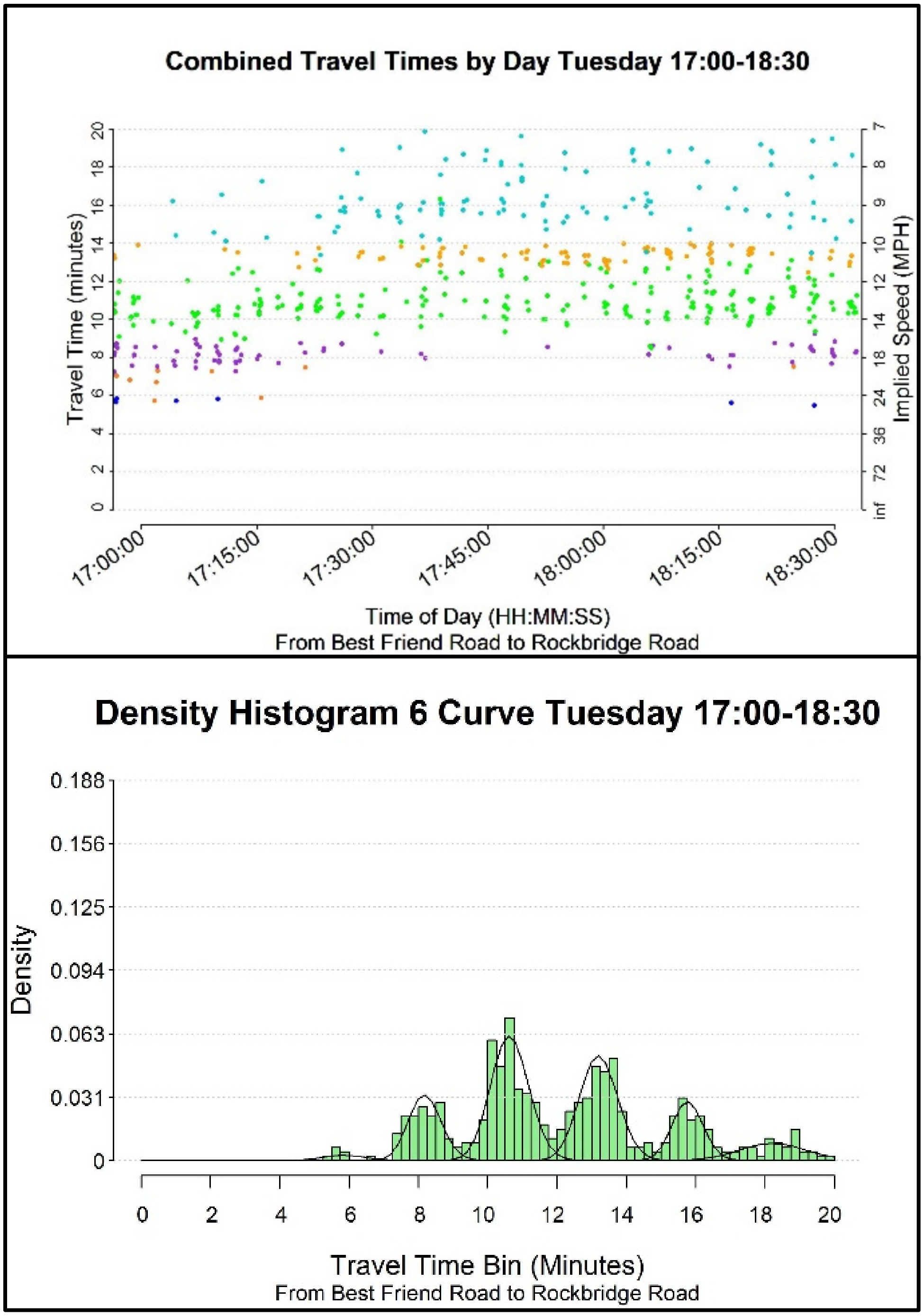

Figure A - 9: Data separated by distribution: southbound direction (PM)

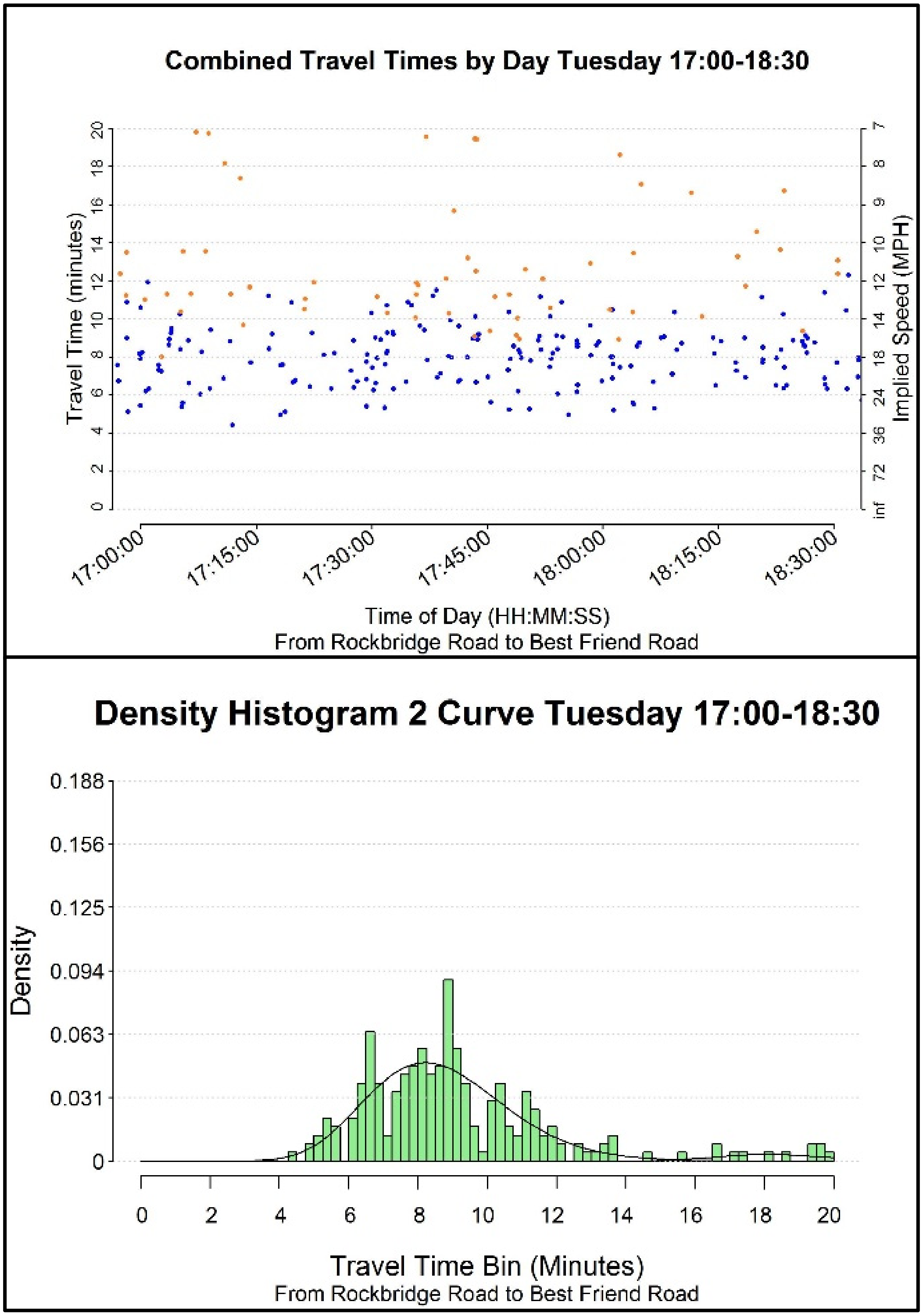

Figure A - 10: Data separated by distribution: northbound direction (AM)

A.6 Analysis and Discussion

For the Tuesday data (Table A - 2), the lowest mean speeds were observed during the 5:00 PM to 6:30 PM time periods for the southbound direction and from 3:00 PM to 5:00 PM for the northbound direction. In the southbound direction the observed number of distributions ranged from four to six distributions. The first distribution typically received an LOS of C in the southbound direction except the 6:00 AM to 7:45 AM time period. Interestingly, the second time period, in some instances, contained a higher LOS than the first distribution for the southbound direction. Typically, the LOS in the second distribution here was D, except in the case of the 6:00 AM to 7:45 AM period and the 3:00 PM to 5:00 PM period, where the LOS was C and A, respectively, for the southbound direction. This may be due to higher travel times contained in a broader first distribution for these time periods. The third distribution typically was assigned an LOS of E except during the 3:00 PM to 5:00 PM time period where it received an LOS of D for the southbound direction. The fourth distribution typically contained an LOS of F except in the 3:00 PM to 5:00 PM time period when it received an LOS of E for the southbound direction. Finally, the fifth and sixth distributions received an LOS of F for the southbound direction.

For the northbound direction the number of distributions that were determined to exist ranged from one to three. Since a lower number of distributions was fit for this direction, the LOS ratings assigned to each distribution were more mixed than for the southbound direction. Here, the first distribution was assigned an LOS of C, E, or D; the second distribution was assigned an LOS of F, E, or D; and the third distribution, existing from 9:30 AM to 3:00 PM, received an LOS of F.

Where multiple distributions were observed, drivers in the slowest groups experienced average speeds ranging from 7.71 mph to 9.25 mph for the southbound direction. For the northbound direction, drivers in the slowest groups experienced average speeds ranging from 7.77 mph to 15.5 mph. From Figure A - 9 and Figure A - 10 it can be seen that there are a number of vehicles in this slowest distribution. During peak periods it is plausible that many of these are actual travel times from vehicles that do not stop along the corridor but experience severe congestion pushing them into the slowest distribution. However, during non-congested periods of the day the slowest distributions carry fewer data points but do not disappear. There are 98 driveways and 12 signalized intersections from which a driver may access many businesses, ranging from office complexes to restaurants. Due to the high number of destinations along the corridor, it is possible that members of the slowest distributions may also have stopped for a few minutes along the corridor.

Despite this potential mix of vehicles in the slowest groups, these data remain informative. When short stops (e.g., to refuel) are the primary reason for the long travel times, which is likely during uncongested traffic, one would expect similar behavior in a before–after analysis, allowing for separation of this group in any improvement analysis. Thus, for example, where only signal timing has changed, these vehicles should not be considered when using Bluetooth® data to compare before–after results, as their behavior is likely not a function of the signal timing. During congested conditions this mode may contain a mix of vehicles that experience high delays and vehicles with short stops. Where improvements are not anticipated to impact the number of vehicles making stops, changes in these vehicles' distribution will partially reflect the impact of improvements on highly delayed vehicles. In addition, fewer samples in the mode in the post-deployment data will indicate fewer highly delayed vehicles.

The researchers believe that, where the data had multiple distributions, the fastest group (group 1 or 2) and the middle group (group 3 or 4) of drivers likely drove the corridor continuously without stopping, except where instructed to do so by traffic control devices. As seen in Figure A - 9 and Figure A - 10, approximately 73% to 78% of the data points lie within these first distributions. Although a uniform sampling rate over all road user sub-groups cannot be assumed (discussed below), it can be assumed that a proportion of vehicles traversing the corridor fall into these two distributions. For the southbound PM direction shown in Figure A - 9, these distributions are separated by a little over 2 minutes or 120 seconds. For the northbound AM direction shown in Figure A - 10, these distributions are separated by approximately 1 minute or 60 seconds. During the time period shown in Figure A - 9, the signal-timing cycle length along the corridor is 160 seconds, and for the time period shown in Figure A - 10, the signal-timing cycle length along the corridor is 140 seconds. These differences are likely related to different paths through the time–space diagram as a function of signal offsets, vehicle arrival times, and congestion (potentially lane specific). For example, significant lane-specific delays were observed in the field during the peak periods as left-turning vehicles at some signalized intersections, especially near the I-85 interchange, spill back out of the left-turn lanes into adjacent left-most through lanes. While this analysis does not conclusively determine the reason for the different behaviors, it does highlight that different road user subgroups are experiencing different LOS. Improved analysis and evaluations (e.g., before–after comparisons) may be obtained by considering these groups separately rather than as a single aggregate collection of road users.

A.7 Limitations and Future Applications

The concept of multiple LOS rating assignment can be used to give a more detailed description of traffic conditions. There are two scenarios that affect how the multiple LOS ratings can ultimately be used for public reporting. Under the first assumption, there is a uniform travel-time sampling rate over all road user subgroups of the corridor of interest, and under the second assumption, a uniform sampling rate cannot be reasonably assumed (e.g., the first assumption cannot be proven). These two situations and their future exploration are discussed in the next two subsections.

A.7.1 Scenario One: Uniform Sampling Rate Over All Road User Subgroups

This approach implicitly assumes that the sample data were collected uniformly across all road user subgroups (that is, each of the underlying gamma curves is sampled at the same rate). In the case where a uniform sampling rate across all subgroups can be assumed, proportions of vehicles in each distribution can be accurately estimated and presented along with the LOS for that distribution. Thus, the multiple LOS rating information will become more robust in describing traffic patterns and situations. Furthermore, if using the multiple LOS method as a performance measurement tool for before and after project implementations, one can see clearly not only the shifts and changes in distributions on a statistical level but a shift in the percentage of drivers belonging to each distribution.

A.7.2 Scenario Two: Cannot Assume Uniform Sampling Rate Over All Road User Sub Groups

When it cannot be reasonably assumed that there is a uniform sampling rate over all road user subgroups, the multiple LOS method is not as robust, as the percentages of drivers in each distribution cannot be assumed to be the same as the sampling proportions. In this situation it can only be assumed that the different distributions exist within the data set and that there are certain unknown proportions of vehicles experiencing different levels of service depending on combinations of red or green signals encountered while traversing the corridor. In the case of the data set used for this research project, a uniform sampling rate across road user subgroups cannot be safely assumed as the likelihood of a Bluetooth® data point is related to vehicle speed and distance from the detector as well as other factors (Colberg 2013; Colberg et al. 2014). When using multiple LOS ratings as performance measures for before and after analyses, analysts can use the separated data sets as individual distributions and run robust statistical tests to determine if changes in the distributions are statistically significant (e.g., using t-tests, chi-squared tests, etc.). Typically, statistical tests apply only to a certain distribution type assumed by the analyst. When these tests are applied to data that clearly have multiple distributions, the test results cannot be taken as accurate, as would be the case with the aggregated travel-time distributions. Using these data-separation techniques, researchers can test the significance of shifts in the separated distributions. Such a test can also be useful; while a change may not affect the LOS ratings, the statistical tests may show statistically significant changes in the distribution, proving that an improvement did occur due to changes made in the corridor.

A.8 Conclusions

Separation of the mixed distributions allows for robust statistical testing of the separated data. However, under the conditions that a uniform sampling rate can be assumed, proportions of vehicles in each distribution can be accurately estimated and shown along with the corresponding LOS ratings to give a more comprehensive picture of traffic conditions to nontransportation professionals. In the case of Jimmy Carter Blvd. in northeast Atlanta, Georgia, researchers learned that, when multiple distributions were found to exist, the highest speed distribution in the southbound direction exhibited a typical LOS C or D rating, while the northbound highest speed distribution exhibited LOS C, D, or E ratings. The second distribution in the southbound direction exhibited LOS ratings C, D, or A, while in the northbound direction D, E and F LOS ratings were experienced. Time periods that experienced three to six distributions exhibited an LOS of D, E, or F in these distributions. During the peak periods, a significant portion of travel times fell into the fourth or fifth (slowest) distribution. It is plausible that this distribution during the peak periods is composed of a portion of travel times where drivers did not make any stops in the corridor but were pushed into this distribution by severe congestion. The fourth or fifth distribution, however, is mixed with outlying data points where drivers may have stopped, as there are ample opportunities (98 total driveways) for drivers to stop along the corridor. During off-peak periods, the fifth distribution contains a much smaller proportion of the travel times, suggesting that these are mostly composed of travel times where drivers stopped at a destination along the corridor for a short period of time.

Multiple curves were fit to the travel-time data sets in this study using an EM algorithm for gamma curves. The data were separated using the posterior probabilities calculated by the R statistical package "mixtools" using the "gammamixEM" function (Benaglia et al. 2010). LOS ratings were assigned using a method based on the HCM 2010 manual (TRB 2010). In this method, the base free-flow speed was calculated according to the HCM 2010 manual (TRB 2010), and average travel times for each distribution were calculated and converted to a speed to use as the travel speed in determining the multiple LOS ratings. The HCM-recommended percentile thresholds for facility LOS ratings were used to assign each distribution an LOS (TRB 2010).

Previous studies have found usefulness in separating multiple distributions for research in travel-time reliability indices (Park et al. 2010; Chalumuri and Asakura 2012; Ji and Zhang 2013; Yang et al. 2014). This study found it useful to separate the travel-time data to assign multiple LOS ratings to the different distributions. From the analysis it was clear that different subgroups of vehicles can experience different LOS ratings on the same roadway facility during the same time period. By separating the travel times into their underlying distributions it becomes possible to consider each of these subgroups separately. Separating these distributions will allow for more robust statistical tests to be used to detect changes in the before-and-after study for the Jimmy Carter Blvd. interchange.

A.9 References

Barceló, J., L. Montero, Laura Marqués, and C. Carmona. (2010). "Travel Time Forecasting and Dynamic Origin–Destination Estimation for Freeways Based on Bluetooth Traffic Monitoring." In *Transportation Research Record: Journal of the Transportaton Research Board, No. 2175*, Accessed from http://trb.metapress.com/content/17x1v88n6p8363p1/fulltext.pdf.

Benaglia, T., D. Chauveau, D. Hunter, and D. Young. (2010). "mixtools: An R Package for Analyzing Mixture Models." In *Journal of Statistical Software*, Oct. **32**(6).

Box, S., (2011). "Arterial Travel Time Data Collection Using Bluetooth Technology." Master's Thesis, Georgia Institute of Technology.

Brennan, T., J. Ernst, C. Day, D. Bullock, J. Krogmeier, and M. Martchouk. (2010). "Influence of Vertical Sensor Placement on Data Collection Efficiency from Bluetooth MAC Address Collection Devices." *Journal of Transportation Engineering*, Dec. **136**: 1104–1109.

Chakraborty, D., G. Chakraborty, S. Naik, and N. Shiratori. (2006). "Discovery and Delay Analysis of Bluetooth Devices." 7th International Conference on Mobile Data Management, Accessed from http://ieeexplore.ieee.org/stamp/stamp.jsp?tp=&arnumber=1630650.

Chalumuri, R.S., and Y. Asakura. (2012). "Modelling Travel Time Distribution Under Various Uncertainties on Hanshin Expressway of Japan." *European Transport Research Review*. **6**: 85–92.

Colberg, K. (2013). "Investigating the Ability of Automated License Plate Recognition Camera Systems to Measure Travel Times in Work Zones." Master's Thesis, Georgia Institute of Technology.

Colberg, K., W. Suh, J. Anderson, S. Zinner, A. Guin, M. Hunter, and R. Guensler. (2014). "Lane Bias Issues in Work Zone Travel Time Measurement and Reporting." In *Transportation Research Record: Journal of the Transportation Research Board, No. 2458*: 78–87.

Day, C.M., R. Haseman, H. Premachandra, T.M. Brennan, J. Wasson, J. Sturdevant, and D. Bullock. (2010). "Evaluation of Arterial Signal Coordination: Methodologies for Visualizing High-Resolution Event Data and Measuring Travel Time." In

Transportation Research Record: Journal of the Transportation Research Board, No. 2192: 37–49, December 1, 2010.

Henclewood, D., W. Suh, M. Rodgers, and M. Hunter. (2013). "Statistical Calibration for Data-Driven Microscopic Simulation Model." In *Transportation Research Board 92nd Annual Meeting*, Transportation Research Board of the National Academies, Washington, D.C.

Ji, Y., and H.M. Zhang. (2013). "Travel Time Distributions on Urban Streets: Their Estimation with a Hierarchical Bayesian Mixture Model and Application to Traffic Analysis Using High-Resolution Bus Probe Data." In *Transportation Research Board 92nd Annual Meeting*, Transportation Research Board of the National Academies, Washington, D.C.

Park, S., H. Rakha, and F. Guo. (2010). "Calibration Issues for Multistate Model of Travel Time Reliability." In *Transportation Research Record: Journal of the Transportation Research Board, No. 2188*: 74–84.

Peterson, B., R. Baldwin, and J. Kharoufeh. (2006). "Bluetooth Inquiry Time Characterization and Selection." *IEEE Transactions on Mobile Computing* **5**(9), Accessed from http://ieeexplore.ieee.org/stamp/stamp.jsp?tp=&arnumber=1661527.

Tarnoff, P.J., D. Bullock, S. Young, J. Wasson, N. Ganig, and J. Sturdevant. (2009). "Continuing Evolution of Travel Time Data Information Collection and Processing." In *Transportation Research Board 88th Annual Meeting*, Transportation Research Board of the National Academies, Washington D.C.: 14.

Transportation Research Board. (2010). *Highway Capacity Manual*. Transportation Research Board of the National Academies, Washington, D.C.

Wang, Y., Y. Malinovskiy, Y. Wu, U. Lee, T. Bailey, and M. Neely. (2010). "Field Experiments with Bluetooth Sensors." Accessed from http://www.westernstatesforum.org/Documents/2010/UW_FINAL_Bluetooth_WSRTF_6-17-10.pdf

Wasson, J., R. Haseman, and D. Bullock. (2010). "Real-Time Measurement of Work Zone Travel Time Delay and Evaluation Metrics Using Bluetooth Probe Tracking." In *Transportation Research Board 89th Annual Meeting*, Transportation Research Board of the National Academies, Washington, D.C.

Yang, F., M. Yun, and X. Yang. (2014). "Travel Time Distributions under Interrupted Flow and Its Application to Travel Time Reliability." In *Transportation Research Board 93rd Annual Meeting*, Transportation Research Board of the National Academies, Washington, D.C.

Zinner, S. (2012). "A Methodology for Using Bluetooth to Measure Real-time Work Zone Travel Time." Master's Thesis, Georgia Institute of Technology.

APPENDIX B. COST OF CONSTRUCTION OF DIVERGING DIAMOND INTERCHANGES AND ALTERNATIVE DESIGNS AT FOUR LOCATIONS

Table B - 1 compares the construction costs of DDIs and other alternative designs at four locations in the United States (Chlewicki 2014). This table shows large cost savings in constructing DDIs over other alternatives in many cases.

Table B - 1: Cost of construction of diverging diamond interchanges and alternative designs at four locations

Interchange	Location	DDI Cost (real or estimated, $Million)	Alternative Design Cost ($Million)	Cost Saving (%)
I-44 @ Route 13	Springfield, MO	3.2	> 10	~70
I-435 @ Front Street	Kansas City, MO	6.7	CDI: 11. 4 SPUI: 25	~75
SR_265 @ SR-62	Utica, IN	52	118	~55
I-590 @ Winton Road	Brighton, NY	3~4	SPUI: 10 Triple Left Diamond: 13.6	~75

APPENDIX C. EXCEL MACRO VISUAL BASIC SCRIPTS

This appendix provides Visual Basic scripts used in the Macro functions of Microsoft Excel to automate the data analysis and organization processes for the CLV analysis.

C.1 Optimized Signal Timing Relocation

The following VB script relocates the optimized signal timing plans from Synchro to the “Signal Timing” worksheet under the CLV workbook into a format that is suitable for v/c ratio calculations.

```
Sub SynchroCDITimingFill()

Dim CLVwbk As Workbook
Dim CLVSheet As Worksheet
Dim Timingwbk As Workbook
Dim TimingSheet As Worksheet
Dim testval

Set TimingSheet = Sheets("Timing")
Set CLVwbk = Workbooks. Open("C:\Users\spark365\Documents\Sung Jun
Park\Research\DDI\After\DDI Final\CLV Method\CLV Spreadsheet LC2. xlsm")
Set CLVSheet = CLVwbk. Sheets("Signal Timing")
Dim rownumber As Long

rownumber = (TimingSheet. Range("A1", TimingSheet. Range("A1"). End(xlDown)). Rows.
Count) - 2
Planrow = 1 'count for rows of each signal plan

For PlanID = 1 To rownumber

    ICode = Cells(2 + PlanID, 1)
    IntID = Cells(2 + PlanID, 2)

    If IntID = 4 Then 'NB intersection
        Phase1 = Cells(2 + PlanID, 3) 'SBL1
        Phase2 = Cells(2 + PlanID, 4) 'NBT1
        Phase6 = Cells(2 + PlanID, 8) 'SBT1
        Phase8 = Cells(2 + PlanID, 10) 'EBL1
        CL = Cells(2 + PlanID, 11) 'cycle length
        Offset = Cells(2 + PlanID, 12)
        CLVSheet. Cells(2 + Planrow, 15) = ICode
        CLVSheet. Cells(2 + Planrow, 16) = Phase2
        CLVSheet. Cells(2 + Planrow, 17) = Phase1
        CLVSheet. Cells(2 + Planrow, 18) = Phase6
        CLVSheet. Cells(2 + Planrow, 19) = Phase8
        CLVSheet. Cells(2 + Planrow, 24) = CL
```

```
        CLVSheet. Cells(2 + Planrow, 25) = Offset

    ElseIf IntID = 6 Then 'SB intersection
        Phase2 = Cells(2 + PlanID, 4) 'NBT2
        Phase4 = Cells(2 + PlanID, 6) 'WBL2
        Phase5 = Cells(2 + PlanID, 7) 'NBL2
        Phase6 = Cells(2 + PlanID, 8) ' SBT2
        Offset = Cells(2 + PlanID, 12)
        CLVSheet. Cells(2 + Planrow, 20) = Phase2
        CLVSheet. Cells(2 + Planrow, 21) = Phase4
        CLVSheet. Cells(2 + Planrow, 22) = Phase5
        CLVSheet. Cells(2 + Planrow, 23) = Phase6
        CLVSheet. Cells(2 + Planrow, 26) = Offset
        Planrow = Planrow + 1 'add 1 to Planrow if IntID = 6

    End If

Next PlanID

End Sub
```

C.2 Volume-to-Capacity Ratio Calculation and Redistribution

The following VB scripts automatically input traffic demands and turn-movement ratios into the “DDI_CLV” and “CDI_CLV” worksheets in the CLV workbook and relocate calculated v/c ratios to “Color Coded” worksheets, where calculated DDI and CDI v/c ratios are color-coded and plotted for comparison.

C.2.1 DDI_CLV script

```
Sub CLVTableFillDDI()

Dim JCEnterVol As Integer
Dim I85OffVol As Integer
For VolumeCase = 1 To 7
    JCEnterVol = Cells(3 + VolumeCase, 30)

    For RampCase = 1 To 4
        I85OffVol = Cells(3 + VolumeCase, 30 + RampCase)

        If I85OffVol >= 1 Then

            For PropLeft = 1 To 7
                Prop = Cells(3 + PropLeft, 37)
                Cells(3, 2) = JCEnterVol
                Cells(4, 2) = I85OffVol
                Cells(5, 7) = Prop
                VCNBT1 = Cells(56, 3)
                VCSBT1 = Cells(57, 3)
```

```
                VCSBL1 = Cells(58, 3)
                VCEBL1 = Cells(59, 3)
                VCNBT2 = Cells(54, 6)
                VCNBL2 = Cells(55, 6)
                VCSBT2 = Cells(58, 6)
                VCWBL2 = Cells(59, 6)
                Intvc = Cells(59, 10)
                Sheets("Color Coded"). Cells(7 + PropLeft, 2 + (((VolumeCase - 1) *
11) + (RampCase * 2))) = VCNBT1
                Sheets("Color Coded"). Cells(14 + PropLeft, 2 + (((VolumeCase - 1)
* 11) + (RampCase * 2))) = VCSBT1
                Sheets("Color Coded"). Cells(21 + PropLeft, 2 + (((VolumeCase - 1)
* 11) + (RampCase * 2))) = VCSBL1
                Sheets("Color Coded"). Cells(28 + PropLeft, 2 + (((VolumeCase - 1)
* 11) + (RampCase * 2))) = VCEBL1
                Sheets("Color Coded"). Cells(35 + PropLeft, 2 + (((VolumeCase - 1)
* 11) + (RampCase * 2))) = VCNBT2
                Sheets("Color Coded"). Cells(42 + PropLeft, 2 + (((VolumeCase - 1)
* 11) + (RampCase * 2))) = VCNBL2
                Sheets("Color Coded"). Cells(49 + PropLeft, 2 + (((VolumeCase - 1)
* 11) + (RampCase * 2))) = VCSBT2
                Sheets("Color Coded"). Cells(56 + PropLeft, 2 + (((VolumeCase - 1)
* 11) + (RampCase * 2))) = VCWBL2
                Sheets("Color Coded"). Cells(63 + PropLeft, 2 + (((VolumeCase - 1)
* 11) + (RampCase * 2))) = Intvc

           Next PropLeft

        End If

    Next RampCase

Next VolumeCase

End Sub
```

C.2.2 CDI_CLV script

```
Sub CLVTableFillCDI()

Dim JCEnterVol As Integer
Dim I85OffVol As Integer

For VolumeCase = 1 To 7
    JCEnterVol = Cells(3 + VolumeCase, 30)

    For RampCase = 1 To 4
        I85OffVol = Cells(3 + VolumeCase, 30 + RampCase)

        If I85OffVol >= 1 Then

            For PropLeft = 1 To 7 'Can be up to 7
                Prop = Cells(3 + PropLeft, 37)
                'Enter Volumes to be test into calculator
                Cells(3, 2) = JCEnterVol
                Cells(4, 2) = I85OffVol
```

```
                Cells(5, 7) = Prop
                VCNBT1 = Cells(56, 3)
                VCSBT1 = Cells(57, 3)
                VCSBL1 = Cells(58, 3)
                VCEBL1 = Cells(59, 3)
                VCNBT2 = Cells(54, 6)
                VCNBL2 = Cells(55, 6)
                VCSBT2 = Cells(58, 6)
                VCWBL2 = Cells(59, 6)
                Intvc = Cells(59, 10)
                Sheets("Color Coded"). Cells(7 + PropLeft, 1 + (((VolumeCase - 1) *
11) + (RampCase * 2))) = VCNBT1
                Sheets("Color Coded"). Cells(14 + PropLeft, 1 + (((VolumeCase - 1)
* 11) + (RampCase * 2))) = VCSBT1
                Sheets("Color Coded"). Cells(21 + PropLeft, 1 + (((VolumeCase - 1)
* 11) + (RampCase * 2))) = VCSBL1
                Sheets("Color Coded"). Cells(28 + PropLeft, 1 + (((VolumeCase - 1)
* 11) + (RampCase * 2))) = VCEBL1
                Sheets("Color Coded"). Cells(35 + PropLeft, 1 + (((VolumeCase - 1)
* 11) + (RampCase * 2))) = VCNBT2
                Sheets("Color Coded"). Cells(42 + PropLeft, 1 + (((VolumeCase - 1)
* 11) + (RampCase * 2))) = VCNBL2
                Sheets("Color Coded"). Cells(49 + PropLeft, 1 + (((VolumeCase - 1)
* 11) + (RampCase * 2))) = VCSBT2
                Sheets("Color Coded"). Cells(56 + PropLeft, 1 + (((VolumeCase - 1)
* 11) + (RampCase * 2))) = VCWBL2
                Sheets("Color Coded"). Cells(63 + PropLeft, 1 + (((VolumeCase - 1)
* 11) + (RampCase * 2))) = Intvc

             Next PropLeft

        End If

    Next RampCase

Next VolumeCase

End Sub
```

APPENDIX D. MICROSOFT VISUAL STUDIO VISUAL BASIC SCRIPTS

This appendix provides the VB script in Microsoft Visual Studio that automates the procedure for inputting and assigning variables, and collecting and relocating output files from the VISSIM simulation study. This script allows the user to collect the necessary output files from the VISSIM simulation with varying traffic scenarios and lane configurations without having to manually open and run individual input files.

```
'Imports System. Text'
Imports System. Convert
Imports System. Math
Imports System
Imports System. IO
Imports System. Threading

Imports VISSIM_COMSERVERLib
Module Module1
    Dim vissim As Vissim
    Dim net As Net
    Dim simulation As Simulation
    Dim vehicles As Vehicles
    Dim vehicle As Vehicle
    Dim links As Links
    Dim link As Link
    Dim evaluation As Evaluation
    Dim vehinps As VehicleInputs
    Dim decisions As RoutingDecisions
    Dim decision As RoutingDecision
    Dim JC As Integer
    Dim Off As Integer
    Dim m As Integer
    Dim simtime = 4500
    Dim resolution = 10
    Sub Main()
        'set groups of arrays that contain vehicle inputs
        Dim vehinp1() As Integer = New Integer() {1500, 2100, 2500} 'Jimmy Carter
NB1
        Dim vehinp2() As Integer = New Integer() {1500, 2100, 2500} 'Jimmy Carter
SB2
        Dim vehinp3() As Integer = New Integer() {500, 1100, 1800} 'I-85 off-ramp
NB
        Dim vehinp4() As Integer = New Integer() {500, 1100, 1800} 'I-85 off-ramp
SB

        'set groups of arrays that contain different route decisions
        Dim decision1_1() As Double = New Double() {0. 8, 0. 72, 0. 56, 0. 4, 0.
24, 0. 08, 0} 'NBT2
```

```
        Dim decision1_2() As Double = New Double() {0, 0. 08, 0. 24, 0. 4, 0. 56,
0. 72, 0. 8} 'NBL2
        Dim decision1_3() As Double = New Double() {0. 2} 'NBR1
        Dim decision2_1() As Double = New Double() {0. 8, 0. 72, 0. 56, 0. 4, 0.
24, 0. 08, 0} 'SBT1
        Dim decision2_2() As Double = New Double() {0, 0. 08, 0. 24, 0. 4, 0. 56,
0. 72, 0. 8} 'SBL1
        Dim decision2_3() As Double = New Double() {0. 2} 'SBR2
        Dim decision3_1() As Double = New Double() {0. 5} 'EBL1
        Dim decision3_2() As Double = New Double() {0. 5} 'EBR1
        Dim decision4_1() As Double = New Double() {0. 5} 'WBL2
        Dim decision4_2() As Double = New Double() {0. 5} 'WBR2

        For l As Integer = 1 To 3 'For loop for lane configuration

            'For-loop to insert desired routing decision into the model
            JC = 0 'counter for Jimmy Carter volumes

            'For-loop to run through different traffic volumes and turn movement
ratios
            For i As Integer = 1 To 3 'For loop for JC volumes (1: 1500, 2: 2100,
3: 2500)

                Off = 0 'counter for Off-ramp volumes

                For j As Integer = 1 To 3 'For loop for Off-ramp volumes (1: 500,
2: 1100, 3: 1800)

                    m = 0 'counter for route decisions

                    For k As Integer = 1 To 7 '7 different turning movement
proportions (1: 100/0, 2: 90/10, 3: 70/30, 4: 50/50, 5: 30/70, 6: 10/90, 7: 0:100)

                        For n As Integer = 1 To 2

                            'Initializing a new instance of Vissim'
                            vissim = New Vissim

                            If n = 1 Then 'running DDI models
                                'loading Vissim network model ". inp" file and ".
ini" file for offset test
                                'this is to call DDI files
                                vissim. LoadNet("C:\Users\spark365\Documents\Sung
Jun Park\Research\DDI\After\DDI Final\VISSIM\LC" & l & "\After\" & i & "_" & j &
"\DDI_PM_" & k & ". inp")
                                vissim.
LoadLayout("C:\Users\spark365\Documents\Sung Jun Park\Research\DDI\After\DDI
Final\VISSIM\LC" & l & "\After\" & i & "_" & j & "\vissim. ini")

                                'you may minimize the VISSIM window if you want'
                                vissim. ShowMinimized()

                                'initiate route decision and vehicle input
variable
                                Dim vehinps = vissim. Net. VehicleInputs
                                Dim decisions = vissim. Net. RoutingDecisions

                                'initiate vehicle nput for each approach
```

```
                                Dim vehinpNB = vissim. Net. VehicleInputs.
GetVehicleInputByNumber(26) 'number in the bracket is link/connector number in
VISSIM
                                Dim vehinpSB = vissim. Net. VehicleInputs.
GetVehicleInputByNumber(1)
                                Dim vehinpNBRamp = vissim. Net. VehicleInputs.
GetVehicleInputByNumber(10)
                                Dim vehinpSBRamp = vissim. Net. VehicleInputs.
GetVehicleInputByNumber(24)

                                'initiate route decisions for each approach
                                Dim decisionNB = decisions.
GetRoutingDecisionByNumber(1) 'number in the bracket is route decision number in
VISSIM
                                Dim decisionSB = decisions.
GetRoutingDecisionByNumber(2)
                                Dim decisionNBR = decisions.
GetRoutingDecisionByNumber(3)
                                Dim decisionSBR = decisions.
GetRoutingDecisionByNumber(4)

                                'add vehicle input from desired vehicle input
group for each time frame
                                vehinpNB = vehinps. AddVehicleInput(26, 0, 4500)
'vehinps. AddVehincleInput(link/connector #, start time, end time)
                                vehinpNB. AttValue("Volume") = vehinp1(JC) 'this
calls the first number from the array of vehinp1 (the first number in the array is
0th position)
                                vehinpNB. AttValue("TrafficComposition") = 1 '1
for Default, 2 for DDI (currently no difference between the two)

                                vehinpSB = vehinps. AddVehicleInput(1, 0, 4500)
                                vehinpSB. AttValue("Volume") = vehinp2(JC)
                                vehinpSB. AttValue("TrafficComposition") = 1

                                vehinpNBRamp = vehinps. AddVehicleInput(10, 0,
4500)
                                vehinpNBRamp. AttValue("Volume") = vehinp3(Off)
                                vehinpNBRamp. AttValue("TrafficComposition") = 1

                                vehinpSBRamp = vehinps. AddVehicleInput(24, 0,
4500)
                                vehinpSBRamp. AttValue("Volume") = vehinp4(Off)
                                vehinpSBRamp. AttValue("TrafficComposition") = 1

                                'add route decision from desired route decision
group for each time frame
                                'DDI NB:
                                decisionNB. AttValue2("RelativeFlow", 1, 4500) =
decision1_1(m) 'decisionX. AttValue2("RelativeFlow, Decision #, end time) =
decision1_X(position of proportion that you want to call)
                                decisionNB. AttValue2("RelativeFlow", 2, 4500) =
decision1_2(m)
                                decisionNB. AttValue2("RelativeFlow", 3, 4500) =
decision1_3(0)
                                'DDI SB:
                                decisionSB. AttValue2("RelativeFlow", 1, 4500) =
decision2_1(m)
```

```
                                decisionSB. AttValue2("RelativeFlow", 2, 4500) =
decision2_2(m)
                                decisionSB. AttValue2("RelativeFlow", 3, 4500) =
decision2_3(0)
                                'NB Ramp:
                                decisionNBR. AttValue2("RelativeFlow", 1, 4500) =
decision3_1(0)
                                decisionNBR. AttValue2("RelativeFlow", 2, 4500) =
decision3_2(0)
                                'SB Ramp:
                                decisionSBR. AttValue2("RelativeFlow", 1, 4500) =
decision4_1(0)
                                decisionSBR. AttValue2("RelativeFlow", 2, 4500) =
decision4_2(0)

                                Dim randseed = 1 'this allows you to change random
seed in VISSIM in each run, and thus you get some variable flows in each run

                                For randcount = 1 To 10 'number of runs for a
particular traffic volume and route decision combinations with different seeds in
each run

                                    'activating evaluation tools in the file'
                                    evaluation = vissim. Evaluation
                                    evaluation. AttValue("traveltime") = True
                                    evaluation. AttValue("delay") = True
                                    evaluation. AttValue("datacollection") = True
                                    evaluation. AttValue("queuecounter") = True
                                    evaluation. AttValue("vehiclerecord") = True

                                    'assigning simulation propoerties'
                                    simulation = vissim. Simulation
                                    simulation. Period = simtime
                                    simulation. Resolution = resolution
                                    simulation. RandomSeed = randseed
                                    simulation. RunContinuous()

                                    Thread. Sleep(5000)

                                    'rename and move output files into separate
folder
                                    'relocate output file - Data Collection Raw(.
mer), Data Collection Compiled(. mes), Delay Raw(. vlr), Delay Compiled(. vlz),
Travel Time Raw(. rsr), Travel Time Compiled(. rsz), and Error files(. err)'
                                    'for DDI model
                                    My. Computer. FileSystem.
CopyFile("C:\Users\spark365\Documents\Sung Jun Park\Research\DDI\After\DDI
Final\VISSIM\LC" & l & "\After\" & i & "_" & j & "\DDI_PM_" & k & ". mer",
"C:\Users\spark365\Documents\Sung Jun Park\Research\DDI\After\DDI Final\Data\LC" &
l & "\After\dc\raw\volume" & i & "_" & j & "\proportion" & k & "\run" & randcount
& ". txt", True)
                                    My. Computer. FileSystem.
CopyFile("C:\Users\spark365\Documents\Sung Jun Park\Research\DDI\After\DDI
Final\VISSIM\LC" & l & "\After\" & i & "_" & j & "\DDI_PM_" & k & ". mes",
"C:\Users\spark365\Documents\Sung Jun Park\Research\DDI\After\DDI Final\Data\LC" &
l & "\After\dc\comp\volume" & i & "_" & j & "\proportion" & k & "\run" & randcount
& ". txt", True)
```

```
                                    My. Computer. FileSystem.
CopyFile("C:\Users\spark365\Documents\Sung Jun Park\Research\DDI\After\DDI
Final\VISSIM\LC" & l & "\After\" & i & "_" & j & "\DDI_PM_" & k & ". vlr",
"C:\Users\spark365\Documents\Sung Jun Park\Research\DDI\After\DDI Final\Data\LC" &
l & "\After\delay\raw\volume" & i & "_" & j & "\proportion" & k & "\run" &
randcount & ". txt", True)
                                    My. Computer. FileSystem.
CopyFile("C:\Users\spark365\Documents\Sung Jun Park\Research\DDI\After\DDI
Final\VISSIM\LC" & l & "\After\" & i & "_" & j & "\DDI_PM_" & k & ". vlz",
"C:\Users\spark365\Documents\Sung Jun Park\Research\DDI\After\DDI Final\Data\LC" &
l & "\After\delay\comp\volume" & i & "_" & j & "\proportion" & k & "\run" &
randcount & ". txt", True)
                                    My. Computer. FileSystem.
CopyFile("C:\Users\spark365\Documents\Sung Jun Park\Research\DDI\After\DDI
Final\VISSIM\LC" & l & "\After\" & i & "_" & j & "\DDI_PM_" & k & ". rsr",
"C:\Users\spark365\Documents\Sung Jun Park\Research\DDI\After\DDI Final\Data\LC" &
l & "\After\tt\raw\volume" & i & "_" & j & "\proportion" & k & "\run" & randcount
& ". txt", True)
                                    My. Computer. FileSystem.
CopyFile("C:\Users\spark365\Documents\Sung Jun Park\Research\DDI\After\DDI
Final\VISSIM\LC" & l & "\After\" & i & "_" & j & "\DDI_PM_" & k & ". rsz",
"C:\Users\spark365\Documents\Sung Jun Park\Research\DDI\After\DDI Final\Data\LC" &
l & "\After\tt\comp\volume" & i & "_" & j & "\proportion" & k & "\run" & randcount
& ". txt", True)
                                    My. Computer. FileSystem.
CopyFile("C:\Users\spark365\Documents\Sung Jun Park\Research\DDI\After\DDI
Final\VISSIM\LC" & l & "\After\" & i & "_" & j & "\DDI_PM_" & k & ". stz",
"C:\Users\spark365\Documents\Sung Jun Park\Research\DDI\After\DDI Final\Data\LC" &
l & "\After\queue\volume" & i & "_" & j & "\proportion" & k & "\run" & randcount &
". txt", True)
                                    My. Computer. FileSystem.
CopyFile("C:\Users\spark365\Documents\Sung Jun Park\Research\DDI\After\DDI
Final\VISSIM\LC" & l & "\After\" & i & "_" & j & "\DDI_PM_" & k & ". fzp",
"C:\Users\spark365\Documents\Sung Jun Park\Research\DDI\After\DDI Final\Data\LC" &
l & "\After\vr\volume" & i & "_" & j & "\proportion" & k & "\run" & randcount & ".
txt", True)

                                    randseed = randseed + 11 'add 11 to random
seed after each run

                                Next
                                vissim. Exit() 'exit currently opened VISSIM file

                            ElseIf n = 2 Then 'running CDI models
                                'this is to call CDI files
                                vissim. LoadNet("C:\Users\spark365\Documents\Sung
Jun Park\Research\DDI\After\DDI Final\VISSIM\LC" & l & "\Before\" & i & "_" & j &
"\Before_PM_" & k & ". inp")
                                vissim.
LoadLayout("C:\Users\spark365\Documents\Sung Jun Park\Research\DDI\After\DDI
Final\VISSIM\LC" & l & "\Before\" & i & "_" & j & "\vissim. ini")

                                'you may minimize the VISSIM window if you want'
                                vissim. ShowMinimized()

                                'initiate route decision and vehicle input
variable
                                Dim vehinps = vissim. Net. VehicleInputs
```

```
                                Dim decisions = vissim. Net. RoutingDecisions

                                'initiate vehicle nput for each approach
                                Dim vehinpNB = vissim. Net. VehicleInputs.
GetVehicleInputByNumber(26) 'number in the bracket is link/connector number in
VISSIM
                                Dim vehinpSB = vissim. Net. VehicleInputs.
GetVehicleInputByNumber(1)
                                Dim vehinpNBRamp = vissim. Net. VehicleInputs.
GetVehicleInputByNumber(10)
                                Dim vehinpSBRamp = vissim. Net. VehicleInputs.
GetVehicleInputByNumber(24)

                                'initiate route decisions for each approach
                                Dim decisionNB = decisions.
GetRoutingDecisionByNumber(1) 'number in the bracket is route decision number in
VISSIM
                                Dim decisionSB = decisions.
GetRoutingDecisionByNumber(2)
                                Dim decisionNBR = decisions.
GetRoutingDecisionByNumber(3)
                                Dim decisionSBR = decisions.
GetRoutingDecisionByNumber(4)

                                'add vehicle input from desired vehicle input
group for each time frame
                                vehinpNB = vehinps. AddVehicleInput(26, 0, 4500)
'vehinps. AddVehincleInput(link/connector #, start time, end time)
                                vehinpNB. AttValue("Volume") = vehinp1(JC) 'this
calls the first number from the array of vehinp1 (the first number in the array is
0th position)
                                vehinpNB. AttValue("TrafficComposition") = 1 '1
for Default, 2 for DDI (currently no difference between the two)

                                vehinpSB = vehinps. AddVehicleInput(1, 0, 4500)
                                vehinpSB. AttValue("Volume") = vehinp2(JC)
                                vehinpSB. AttValue("TrafficComposition") = 1

                                vehinpNBRamp = vehinps. AddVehicleInput(10, 0,
4500)
                                vehinpNBRamp. AttValue("Volume") = vehinp3(Off)
                                vehinpNBRamp. AttValue("TrafficComposition") = 1

                                vehinpSBRamp = vehinps. AddVehicleInput(24, 0,
4500)
                                vehinpSBRamp. AttValue("Volume") = vehinp4(Off)
                                vehinpSBRamp. AttValue("TrafficComposition") = 1

                                'add route decision from desired route decision
group for each time frame
                                'DDI NB:
                                decisionNB. AttValue2("RelativeFlow", 1, 4500) =
decision1_1(m) 'decisionX. AttValue2("RelativeFlow, Decision #, end time) =
decision1_X(position of proportion that you want to call)
                                decisionNB. AttValue2("RelativeFlow", 2, 4500) =
decision1_2(m)
                                decisionNB. AttValue2("RelativeFlow", 3, 4500) =
decision1_3(0)
```

```
                                'DDI SB:
                                decisionSB. AttValue2("RelativeFlow", 1, 4500) =
decision2_1(m)
                                decisionSB. AttValue2("RelativeFlow", 2, 4500) =
decision2_2(m)
                                decisionSB. AttValue2("RelativeFlow", 3, 4500) =
decision2_3(0)
                                'NB Ramp:
                                decisionNBR. AttValue2("RelativeFlow", 1, 4500) =
decision3_1(0)
                                decisionNBR. AttValue2("RelativeFlow", 2, 4500) =
decision3_2(0)
                                'SB Ramp:
                                decisionSBR. AttValue2("RelativeFlow", 1, 4500) =
decision4_1(0)
                                decisionSBR. AttValue2("RelativeFlow", 2, 4500) =
decision4_2(0)

                                Dim randseed = 1 'this allows you to change random
seed in VISSIM in each run, and thus you get some variable flows in each run

                                For randcount = 1 To 10 'number of runs for a
particular traffic volume and route decision combinations with different seeds in
each run

                                    'activating evaluation tools in the file'
                                    evaluation = vissim. Evaluation
                                    evaluation. AttValue("traveltime") = True
                                    evaluation. AttValue("delay") = True
                                    evaluation. AttValue("datacollection") = True
                                    evaluation. AttValue("queuecounter") = True
                                    evaluation. AttValue("vehiclerecord") = True

                                    'assigning simulation propoerties'
                                    simulation = vissim. Simulation
                                    simulation. Period = simtime
                                    simulation. Resolution = resolution
                                    simulation. RandomSeed = randseed
                                    simulation. RunContinuous()

                                    Thread. Sleep(5000)

                                    'rename and move output files into separate
folder
                                    'relocate output file - Data Collection Raw(.
mer), Data Collection Compiled(. mes), Delay Raw(. vlr), Delay Compiled(. vlz),
Travel Time Raw(. rsr), Travel Time Compiled(. rsz), and Error files(. err)'
                                    'for CDI model
                                    My. Computer. FileSystem.
CopyFile("C:\Users\spark365\Documents\Sung Jun Park\Research\DDI\After\DDI
Final\VISSIM\LC" & l & "\Before\" & i & "_" & j & "\Before_PM_" & k & ". mer",
"C:\Users\spark365\Documents\Sung Jun Park\Research\DDI\After\DDI Final\Data\LC" &
l & "\Before\dc\raw\volume" & i & "_" & j & "\proportion" & k & "\run" & randcount
& ". txt", True)
                                    My. Computer. FileSystem.
CopyFile("C:\Users\spark365\Documents\Sung Jun Park\Research\DDI\After\DDI
Final\VISSIM\LC" & l & "\Before\" & i & "_" & j & "\Before_PM_" & k & ". mes",
"C:\Users\spark365\Documents\Sung Jun Park\Research\DDI\After\DDI Final\Data\LC" &
```

```
l & "\Before\dc\comp\volume" & i & "_" & j & "\proportion" & k & "\run" &
randcount & ". txt", True)
                                    My. Computer. FileSystem.
CopyFile("C:\Users\spark365\Documents\Sung Jun Park\Research\DDI\After\DDI
Final\VISSIM\LC" & l & "\Before\" & i & "_" & j & "\Before_PM_" & k & ". vlr",
"C:\Users\spark365\Documents\Sung Jun Park\Research\DDI\After\DDI Final\Data\LC" &
l & "\Before\delay\raw\volume" & i & "_" & j & "\proportion" & k & "\run" &
randcount & ". txt", True)
                                    My. Computer. FileSystem.
CopyFile("C:\Users\spark365\Documents\Sung Jun Park\Research\DDI\After\DDI
Final\VISSIM\LC" & l & "\Before\" & i & "_" & j & "\Before_PM_" & k & ". vlz",
"C:\Users\spark365\Documents\Sung Jun Park\Research\DDI\After\DDI Final\Data\LC" &
l & "\Before\delay\comp\volume" & i & "_" & j & "\proportion" & k & "\run" &
randcount & ". txt", True)
                                    My. Computer. FileSystem.
CopyFile("C:\Users\spark365\Documents\Sung Jun Park\Research\DDI\After\DDI
Final\VISSIM\LC" & l & "\Before\" & i & "_" & j & "\Before_PM_" & k & ". rsr",
"C:\Users\spark365\Documents\Sung Jun Park\Research\DDI\After\DDI Final\Data\LC" &
l & "\Before\tt\raw\volume" & i & "_" & j & "\proportion" & k & "\run" & randcount
& ". txt", True)
                                    My. Computer. FileSystem.
CopyFile("C:\Users\spark365\Documents\Sung Jun Park\Research\DDI\After\DDI
Final\VISSIM\LC" & l & "\Before\" & i & "_" & j & "\Before_PM_" & k & ". rsz",
"C:\Users\spark365\Documents\Sung Jun Park\Research\DDI\After\DDI Final\Data\LC" &
l & "\Before\tt\comp\volume" & i & "_" & j & "\proportion" & k & "\run" &
randcount & ". txt", True)
                                    My. Computer. FileSystem.
CopyFile("C:\Users\spark365\Documents\Sung Jun Park\Research\DDI\After\DDI
Final\VISSIM\LC" & l & "\Before\" & i & "_" & j & "\Before_PM_" & k & ". stz",
"C:\Users\spark365\Documents\Sung Jun Park\Research\DDI\After\DDI Final\Data\LC" &
l & "\Before\queue\volume" & i & "_" & j & "\proportion" & k & "\run" & randcount
& ". txt", True)
                                    My. Computer. FileSystem.
CopyFile("C:\Users\spark365\Documents\Sung Jun Park\Research\DDI\After\DDI
Final\VISSIM\LC" & l & "\Before\" & i & "_" & j & "\Before_PM_" & k & ". fzp",
"C:\Users\spark365\Documents\Sung Jun Park\Research\DDI\After\DDI Final\Data\LC" &
l & "\Before\vr\volume" & i & "_" & j & "\proportion" & k & "\run" & randcount &
". txt", True)

                                    randseed = randseed + 11 'add 11 to random
seed after each run

                                Next
                                vissim. Exit() 'exit currently opened VISSIM file

                            End If

                        Next
                        m = m + 1 'add 1 to move to next routing proportion

                    Next
                    Off = Off + 1 'add 1 to move to next off-ramp volume

                Next
                JC = JC + 1 'add 1 to move to next JC volume

            Next
```

```
        Next

    End Sub

End Module
```

APPENDIX E. CRITICAL LANE VOLUME ANALYSIS RESULTS

List of Tables

List of Figures

This appendix provides the resultant color-coded tables and plots showing the difference in the CDI and DDI v/c ratios at different through/left proportions, traffic demands, and lane configurations.

E.1 Lane Configuration 1

E.1.1 Color-Coded Tables of CDI and DDI v/c Ratios

The following color-coded tables show the comparison of the CDI and DDI v/c ratios calculated using the CLV method for LC1. The color schematics of these tables are described in Table 6 in Chapter 3.

Table E - 1: Color-coded tables of the CDI and DDI turning movement and interchange v/c ratios at (a) cross-street demand of 1000 vph, and (b) cross-street demand of 1500 vph with different off-ramp demands and through/left proportions for LC1

(a)

JC Volume 1000 vph							
Proportion	Approach	CDI	DDI	CDI	DDI	CDI	DDI
		200 vph		500 vph		800 vph	
100:0	NBT1	0.28	0.56	0.33	0.60	0.34	0.63
90:10		0.50	0.49	0.51	0.54	0.56	0.57
70:30		0.50	0.35	0.50	0.39	0.54	0.41
50:50		0.37	0.32	0.41	0.35	0.43	0.37
30:70		0.65	0.30	0.60	0.33	0.70	0.37
10:90		0.84	0.36	0.90	0.39	1.05	0.43
0:100		1.00	0.38	1.07	0.42	1.07	0.45
100:0	SBT1	0.32	0.44	0.44	0.51	0.52	0.56
90:10		0.31	0.42	0.39	0.47	0.48	0.53
70:30		0.24	0.37	0.31	0.44	0.39	0.50
50:50		0.16	0.31	0.23	0.37	0.30	0.43
30:70		0.11	0.24	0.17	0.31	0.23	0.36
10:90		0.06	0.14	0.11	0.23	0.17	0.30
0:100		0.03	0.08	0.08	0.18	0.13	0.26
100:0	SBL1	0.00	0.00	0.00	0.00	0.00	0.00
90:10		0.18	0.02	0.20	0.02	0.22	0.02
70:30		0.35	0.06	0.40	0.06	0.43	0.06
50:50		0.45	0.10	0.48	0.10	0.55	0.10
30:70		0.58	0.14	0.65	0.14	0.63	0.14
10:90		0.55	0.18	0.53	0.18	0.53	0.18
0:100		0.52	0.20	0.50	0.20	0.49	0.20
100:0	EBL1	0.13	0.05	0.26	0.12	0.38	0.19
90:10		0.14	0.05	0.25	0.12	0.38	0.19
70:30		0.18	0.06	0.35	0.14	0.45	0.21
50:50		0.22	0.06	0.36	0.14	0.50	0.22
30:70		0.25	0.07	0.47	0.16	0.54	0.23
10:90		0.35	0.08	0.55	0.17	0.58	0.25
0:100		0.33	0.08	0.56	0.18	0.67	0.26
100:0	NBT2	0.32	0.43	0.44	0.49	0.52	0.55
90:10		0.31	0.41	0.39	0.47	0.48	0.51
70:30		0.24	0.35	0.32	0.42	0.40	0.48
50:50		0.17	0.30	0.24	0.35	0.32	0.42
30:70		0.11	0.22	0.18	0.29	0.24	0.35
10:90		0.06	0.13	0.12	0.22	0.18	0.29
0:100		0.03	0.08	0.08	0.17	0.15	0.24
100:0	NBL2	0.00	0.00	0.00	0.00	0.00	0.00
90:10		0.13	0.02	0.13	0.02	0.17	0.02
70:30		0.25	0.06	0.27	0.06	0.30	0.06
50:50		0.32	0.10	0.35	0.10	0.40	0.10
30:70		0.40	0.14	0.42	0.14	0.45	0.14
10:90		0.45	0.18	0.48	0.18	0.48	0.18
0:100		0.43	0.20	0.45	0.20	0.48	0.20
100:0	SBT2	0.28	0.58	0.33	0.63	0.34	0.67
90:10		0.43	0.51	0.45	0.54	0.47	0.60
70:30		0.37	0.37	0.41	0.41	0.44	0.44
50:50		0.54	0.33	0.58	0.37	0.67	0.39
30:70		0.84	0.32	0.99	0.35	0.98	0.39
10:90		1.15	0.38	1.26	0.41	1.33	0.45
0:100		1.28	0.40	1.39	0.43	1.52	0.50
100:0	WBL2	0.13	0.05	0.26	0.12	0.38	0.18
90:10		0.14	0.05	0.25	0.12	0.38	0.18
70:30		0.18	0.05	0.31	0.13	0.42	0.20
50:50		0.18	0.06	0.31	0.16	0.40	0.21
30:70		0.21	0.07	0.34	0.15	0.44	0.22
10:90		0.22	0.07	0.36	0.14	0.47	0.24
0:100		0.25	0.08	0.38	0.17	0.47	0.24
100:0	Int v/c	0.28	0.48	0.39	0.53	0.48	0.58
90:10		0.32	0.44	0.35	0.49	0.45	0.53
70:30		0.38	0.35	0.42	0.41	0.47	0.45
50:50		0.39	0.31	0.44	0.35	0.50	0.40
30:70		0.56	0.27	0.60	0.31	0.63	0.36
10:90		0.68	0.27	0.73	0.31	0.75	0.36
0:100		0.72	0.27	0.75	0.31	0.80	0.36

(b)

JC Volume 1500 vph							
Proportion	Approach	CDI	DDI	CDI	DDI	CDI	DDI
		500 vph		1100 vph		1800 vph	
100:0	NBT1	0.44	0.88	0.47	0.97	0.48	1.06
90:10		0.70	0.76	0.77	0.84	0.68	0.92
70:30		0.70	0.54	0.74	0.62	0.80	0.66
50:50		0.55	0.48	0.62	0.55	0.68	0.64
30:70		0.90	0.48	0.95	0.55	1.05	0.57
10:90		1.25	0.56	1.35	0.64	1.48	0.70
0:100		1.50	0.60	1.60	0.68	1.76	0.72
100:0	SBT1	0.53	0.69	0.69	0.70	0.83	0.75
90:10		0.50	0.65	0.66	0.66	0.81	0.78
70:30		0.39	0.56	0.55	0.63	0.76	0.69
50:50		0.28	0.49	0.42	0.59	0.60	0.67
30:70		0.19	0.40	0.31	0.52	0.47	0.63
10:90		0.11	0.27	0.21	0.42	0.35	0.55
0:100		0.07	0.20	0.17	0.36	0.31	0.49
100:0	SBL1	0.00	0.00	0.00	0.00	0.00	0.00
90:10		0.28	0.03	0.30	0.03	0.36	0.03
70:30		0.56	0.09	0.64	0.09	0.69	0.09
50:50		0.70	0.15	0.78	0.15	0.81	0.15
30:70		0.65	0.21	0.63	0.21	0.61	0.21
10:90		0.53	0.27	0.51	0.27	0.51	0.27
0:100		0.49	0.30	0.48	0.30	0.45	0.30
100:0	EBL1	0.34	0.12	0.59	0.23	0.78	0.35
90:10		0.31	0.12	0.55	0.22	0.75	0.35
70:30		0.45	0.13	0.59	0.25	0.69	0.36
50:50		0.49	0.14	0.69	0.28	0.78	0.40
30:70		0.56	0.16	0.76	0.31	0.88	0.45
10:90		0.74	0.18	0.88	0.34	0.98	0.48
0:100		0.74	0.20	0.92	0.36	1.03	0.49
100:0	NBT2	0.53	0.67	0.69	0.72	0.83	0.75
90:10		0.50	0.63	0.66	0.66	0.81	0.76
70:30		0.40	0.55	0.56	0.63	0.76	0.68
50:50		0.29	0.47	0.44	0.58	0.64	0.67
30:70		0.20	0.38	0.33	0.52	0.51	0.60
10:90		0.11	0.26	0.23	0.40	0.39	0.53
0:100		0.08	0.18	0.18	0.34	0.31	0.45
100:0	NBL2	0.00	0.00	0.00	0.00	0.00	0.00
90:10		0.20	0.03	0.23	0.03	0.27	0.03
70:30		0.41	0.09	0.45	0.09	0.51	0.09
50:50		0.50	0.15	0.58	0.15	0.63	0.15
30:70		0.57	0.21	0.64	0.21	0.63	0.21
10:90		0.47	0.27	0.48	0.27	0.48	0.27
0:100		0.41	0.30	0.42	0.30	0.42	0.30
100:0	SBT2	0.44	0.91	0.47	1.00	0.48	1.13
90:10		0.60	0.79	0.65	0.84	0.59	0.98
70:30		0.55	0.57	0.60	0.62	0.60	0.69
50:50		0.81	0.50	0.88	0.57	0.97	0.64
30:70		1.18	0.50	1.31	0.55	1.49	0.61
10:90		1.60	0.59	1.80	0.68	1.95	0.74
0:100		1.86	0.63	2.04	0.71	2.32	0.81
100:0	WBL2	0.34	0.12	0.59	0.23	0.78	0.34
90:10		0.31	0.12	0.55	0.22	0.75	0.34
70:30		0.39	0.13	0.55	0.25	0.69	0.35
50:50		0.40	0.14	0.60	0.28	0.68	0.40
30:70		0.43	0.16	0.60	0.31	0.73	0.43
10:90		0.48	0.17	0.64	0.33	0.77	0.47
0:100		0.51	0.18	0.67	0.34	0.78	0.45
100:0	Int v/c	0.49	0.75	0.66	0.80	0.82	0.85
90:10		0.46	0.68	0.63	0.72	0.79	0.82
70:30		0.60	0.54	0.66	0.62	0.73	0.68
50:50		0.62	0.48	0.71	0.56	0.77	0.65
30:70		0.80	0.43	0.87	0.52	0.94	0.59
10:90		0.89	0.43	0.95	0.52	1.01	0.61
0:100		0.94	0.43	0.99	0.52	1.06	0.59

Table E - 2: Color-coded tables of the CDI and DDI turning movement and interchange v/c ratios at (a) cross-street demand of 1800 vph, and (b) cross-street demand of 2100 vph with different off-ramp demands and through/left proportions for LC1

(a)

JC Volume 1800 vph							
Proportion	Approach	CDI	DDI	CDI	DDI	CDI	DDI
		500 vph		1100 vph		1800 vph	
100:0	NBT1	0.51	1.03	0.52	1.11	0.54	1.25
90:10		0.85	0.91	0.84	0.97	0.77	1.08
70:30		0.76	0.63	0.84	0.70	0.91	0.78
50:50		0.65	0.56	0.68	0.62	0.76	0.70
30:70		0.99	0.54	1.08	0.60	1.17	0.67
10:90		1.47	0.65	1.62	0.72	1.72	0.78
0:100		1.75	0.69	1.87	0.77	2.03	0.84
100:0	SBT1	0.60	0.67	0.72	0.72	0.87	0.75
90:10		0.57	0.71	0.70	0.78	0.86	0.78
70:30		0.43	0.63	0.58	0.71	0.78	0.80
50:50		0.30	0.55	0.43	0.62	0.61	0.73
30:70		0.20	0.44	0.31	0.57	0.47	0.65
10:90		0.11	0.31	0.22	0.43	0.35	0.57
0:100		0.07	0.21	0.17	0.36	0.29	0.51
100:0	SBL1	0.00	0.00	0.00	0.00	0.00	0.00
90:10		0.31	0.04	0.34	0.04	0.40	0.04
70:30		0.65	0.11	0.69	0.11	0.75	0.11
50:50		0.75	0.18	0.85	0.18	0.82	0.18
30:70		0.64	0.25	0.64	0.25	0.64	0.25
10:90		0.54	0.32	0.52	0.32	0.52	0.32
0:100		0.49	0.36	0.48	0.36	0.48	0.36
100:0	EBL1	0.38	0.11	0.65	0.23	0.84	0.34
90:10		0.34	0.11	0.60	0.24	0.80	0.35
70:30		0.47	0.13	0.64	0.25	0.75	0.38
50:50		0.56	0.14	0.77	0.27	0.85	0.41
30:70		0.74	0.16	0.86	0.32	1.01	0.44
10:90		0.85	0.20	0.98	0.34	1.13	0.49
0:100		0.91	0.21	1.07	0.36	1.19	0.51
100:0	NBT2	0.60	0.68	0.72	0.72	0.87	0.75
90:10		0.57	0.71	0.70	0.80	0.86	0.78
70:30		0.44	0.62	0.59	0.70	0.78	0.78
50:50		0.31	0.53	0.45	0.62	0.65	0.73
30:70		0.21	0.43	0.33	0.55	0.48	0.63
10:90		0.12	0.29	0.23	0.42	0.33	0.54
0:100		0.07	0.20	0.16	0.34	0.25	0.48
100:0	NBL2	0.00	0.00	0.00	0.00	0.00	0.00
90:10		0.24	0.04	0.25	0.04	0.30	0.04
70:30		0.46	0.11	0.54	0.11	0.61	0.11
50:50		0.56	0.18	0.65	0.18	0.71	0.18
30:70		0.63	0.25	0.62	0.25	0.65	0.25
10:90		0.45	0.32	0.46	0.32	0.48	0.32
0:100		0.40	0.36	0.42	0.36	0.42	0.36
100:0	SBT2	0.51	1.05	0.52	1.14	0.54	1.27
90:10		0.69	0.91	0.71	1.01	0.68	1.10
70:30		0.60	0.65	0.63	0.72	0.65	0.80
50:50		0.88	0.58	0.95	0.62	1.07	0.70
30:70		1.31	0.56	1.43	0.63	1.60	0.70
10:90		1.83	0.68	2.03	0.75	2.20	0.84
0:100		2.13	0.72	2.40	0.80	2.54	0.90
100:0	WBL2	0.38	0.11	0.65	0.22	0.84	0.34
90:10		0.34	0.11	0.60	0.24	0.80	0.35
70:30		0.42	0.12	0.60	0.25	0.75	0.37
50:50		0.47	0.14	0.65	0.27	0.75	0.41
30:70		0.51	0.16	0.67	0.31	0.81	0.43
10:90		0.59	0.18	0.74	0.33	0.87	0.46
0:100		0.63	0.20	0.77	0.34	0.90	0.48
100:0	Int v/c	0.56	0.81	0.71	0.86	0.86	0.90
90:10		0.57	0.78	0.68	0.86	0.84	0.88
70:30		0.66	0.62	0.73	0.70	0.77	0.78
50:50		0.70	0.54	0.78	0.61	0.86	0.71
30:70		0.90	0.49	0.94	0.57	1.03	0.65
10:90		1.00	0.50	1.06	0.57	1.13	0.66
0:100		1.06	0.50	1.14	0.57	1.19	0.66

(b)

JC Volume 2100 vph							
Proportion	Approach	CDI	DDI	CDI	DDI	CDI	DDI
		500 vph		1100 vph		1800 vph	
100:0	NBT1	0.57	1.20	0.58	1.26	0.60	1.37
90:10		0.95	1.01	0.85	1.09	0.81	1.19
70:30		0.84	0.72	0.91	0.80	0.98	0.87
50:50		0.72	0.63	0.75	0.70	0.81	0.76
30:70		1.15	0.61	1.25	0.69	1.32	0.74
10:90		1.72	0.73	1.84	0.81	2.00	0.86
0:100		2.04	0.78	2.22	0.84	2.36	0.93
100:0	SBT1	0.65	0.67	0.77	0.73	0.92	0.79
90:10		0.65	0.75	0.75	0.77	0.89	0.82
70:30		0.46	0.69	0.61	0.77	0.80	0.85
50:50		0.33	0.60	0.45	0.71	0.61	0.78
30:70		0.22	0.49	0.33	0.60	0.47	0.68
10:90		0.12	0.35	0.22	0.47	0.35	0.59
0:100		0.07	0.22	0.16	0.39	0.29	0.51
100:0	SBL1	0.00	0.00	0.00	0.00	0.00	0.00
90:10		0.42	0.04	0.45	0.04	0.45	0.04
70:30		0.67	0.13	0.73	0.13	0.82	0.13
50:50		0.84	0.21	0.82	0.21	0.81	0.21
30:70		0.64	0.29	0.65	0.29	0.63	0.29
10:90		0.55	0.38	0.52	0.38	0.51	0.38
0:100		0.49	0.42	0.49	0.42	0.47	0.42
100:0	EBL1	0.44	0.11	0.69	0.22	0.88	0.35
90:10		0.39	0.11	0.69	0.23	0.84	0.36
70:30		0.50	0.12	0.69	0.24	0.80	0.37
50:50		0.63	0.14	0.83	0.28	0.93	0.40
30:70		0.83	0.16	0.96	0.31	1.09	0.43
10:90		0.94	0.21	1.13	0.36	1.23	0.50
0:100		1.02	0.22	1.18	0.39	1.31	0.51
100:0	NBT2	0.65	0.67	0.77	0.73	0.92	0.79
90:10		0.65	0.75	0.77	0.77	0.89	0.82
70:30		0.47	0.68	0.63	0.76	0.82	0.84
50:50		0.34	0.60	0.47	0.70	0.65	0.77
30:70		0.22	0.47	0.34	0.60	0.46	0.67
10:90		0.12	0.33	0.20	0.45	0.30	0.58
0:100		0.07	0.21	0.14	0.38	0.22	0.51
100:0	NBL2	0.00	0.00	0.00	0.00	0.00	0.00
90:10		0.30	0.04	0.37	0.04	0.39	0.04
70:30		0.50	0.13	0.60	0.13	0.66	0.13
50:50		0.62	0.21	0.68	0.21	0.76	0.21
30:70		0.58	0.29	0.60	0.29	0.62	0.29
10:90		0.45	0.38	0.45	0.38	0.45	0.38
0:100		0.39	0.42	0.39	0.42	0.41	0.42
100:0	SBT2	0.57	1.20	0.58	1.28	0.60	1.40
90:10		0.82	1.03	0.76	1.11	0.69	1.22
70:30		0.64	0.74	0.68	0.81	0.72	0.88
50:50		0.96	0.63	1.03	0.72	1.15	0.78
30:70		1.47	0.62	1.61	0.69	1.76	0.75
10:90		2.06	0.76	2.27	0.84	2.52	0.89
0:100		2.44	0.81	2.61	0.87	2.91	0.93
100:0	WBL2	0.44	0.11	0.69	0.22	0.88	0.35
90:10		0.39	0.11	0.64	0.23	0.84	0.35
70:30		0.45	0.12	0.62	0.24	0.77	0.36
50:50		0.53	0.14	0.67	0.28	0.78	0.40
30:70		0.59	0.16	0.77	0.31	0.86	0.43
10:90		0.72	0.20	0.83	0.34	0.94	0.49
0:100		0.70	0.21	0.88	0.38	0.99	0.51
100:0	Int v/c	0.62	0.86	0.75	0.91	0.91	0.98
90:10		0.69	0.85	0.74	0.89	0.87	0.95
70:30		0.72	0.70	0.79	0.77	0.87	0.85
50:50		0.78	0.61	0.83	0.70	0.92	0.77
30:70		0.97	0.54	1.04	0.63	1.10	0.70
10:90		1.12	0.57	1.17	0.64	1.24	0.72
0:100		1.18	0.57	1.24	0.64	1.32	0.72

Table E - 3: Color-coded tables of the CDI and DDI turning movement and interchange v/c ratios at cross-street demand of 2300 vph with different off-ramp demands and through/left proportions for LC1

JC Volume 2300 vph									
Proportion	Approach	CDI	DDI	CDI	DDI	CDI	DDI	CDI	DDI
		500 vph		1100 vph		1800 vph		2100 vph	
100:0	NBT1	0.59	1.27	0.62	1.38	0.65	1.24	0.67	1.56
90:10		0.88	1.10	0.86	1.18	0.87	0.99	0.89	1.35
70:30		0.89	0.78	0.95	0.84	1.04	0.93	1.03	0.97
50:50		0.75	0.67	0.81	0.75	0.88	0.84	0.91	0.84
30:70		1.24	0.66	1.35	0.71	1.45	0.79	1.49	0.82
10:90		1.86	0.78	2.01	0.83	2.13	0.91	2.18	0.95
0:100		2.18	0.82	2.30	0.89	2.51	0.96	2.44	1.01
100:0	SBT1	0.67	0.68	0.81	0.73	0.96	0.88	1.05	0.82
90:10		0.64	0.73	0.76	0.77	0.92	0.98	1.00	0.85
70:30		0.49	0.75	0.63	0.81	0.83	0.90	0.90	0.95
50:50		0.34	0.63	0.47	0.74	0.63	0.78	0.70	0.85
30:70		0.23	0.52	0.34	0.62	0.48	0.73	0.54	0.75
10:90		0.12	0.34	0.22	0.49	0.33	0.61	0.36	0.64
0:100		0.07	0.24	0.16	0.39	0.25	0.53	0.29	0.57
100:0	SBL1	0.00	0.00	0.00	0.00	0.00	0.00	0.00	0.00
90:10		0.43	0.05	0.44	0.05	0.47	0.05	0.49	0.05
70:30		0.74	0.14	0.79	0.14	0.87	0.14	0.90	0.14
50:50		0.82	0.23	0.84	0.23	0.81	0.23	0.80	0.23
30:70		0.65	0.32	0.63	0.32	0.62	0.32	0.62	0.32
10:90		0.54	0.41	0.53	0.41	0.52	0.41	0.52	0.41
0:100		0.50	0.46	0.49	0.46	0.48	0.46	0.49	0.42
100:0	EBL1	0.47	0.11	0.72	0.22	0.92	0.39	0.98	0.40
90:10		0.44	0.11	0.69	0.23	0.88	0.42	0.95	0.41
70:30		0.56	0.12	0.72	0.24	0.82	0.37	0.88	0.43
50:50		0.74	0.13	0.89	0.28	0.99	0.39	1.04	0.45
30:70		0.89	0.16	1.03	0.31	1.16	0.45	1.21	0.49
10:90		1.02	0.20	1.18	0.37	1.35	0.51	1.38	0.54
0:100		1.02	0.24	1.24	0.39	1.35	0.53	1.44	0.57
100:0	NBT2	0.67	0.68	0.81	0.73	0.96	0.89	1.05	0.82
90:10		0.64	0.73	0.76	0.78	0.92	1.00	0.99	0.85
70:30		0.50	0.74	0.65	0.81	0.80	0.90	0.87	0.94
50:50		0.36	0.62	0.49	0.72	0.67	0.77	0.72	0.84
30:70		0.23	0.50	0.34	0.60	0.45	0.71	0.50	0.75
10:90		0.12	0.33	0.20	0.48	0.28	0.59	0.32	0.63
0:100		0.07	0.22	0.13	0.39	0.21	0.52	0.24	0.56
100:0	NBL2	0.00	0.00	0.00	0.00	0.00	0.00	0.00	0.00
90:10		0.36	0.05	0.36	0.05	0.41	0.05	0.44	0.05
70:30		0.55	0.14	0.63	0.14	0.72	0.14	0.74	0.14
50:50		0.66	0.23	0.75	0.23	0.81	0.23	0.85	0.23
30:70		0.58	0.32	0.58	0.32	0.60	0.32	0.62	0.32
10:90		0.44	0.41	0.44	0.41	0.46	0.41	0.46	0.41
0:100		0.40	0.46	0.41	0.46	0.41	0.46	0.44	0.43
100:0	SBT2	0.59	1.29	0.62	1.40	0.65	1.53	0.67	1.59
90:10		0.74	1.12	0.73	1.20	0.74	1.33	0.75	1.38
70:30		0.70	0.79	0.72	0.86	0.77	0.95	0.74	0.98
50:50		1.03	0.69	1.11	0.77	1.22	0.85	1.28	0.85
30:70		1.56	0.68	1.73	0.72	1.90	0.81	1.96	0.82
10:90		2.26	0.80	2.44	0.85	2.66	0.93	2.74	0.97
0:100		2.63	0.85	2.86	0.89	3.12	0.99	3.19	1.03
100:0	WBL2	0.47	0.11	0.72	0.22	0.92	0.35	0.98	0.40
90:10		0.44	0.11	0.69	0.23	0.88	0.35	0.96	0.40
70:30		0.45	0.12	0.65	0.24	0.79	0.37	0.88	0.42
50:50		0.54	0.13	0.74	0.27	0.83	0.38	0.88	0.45
30:70		0.66	0.16	0.80	0.30	0.92	0.44	0.96	0.49
10:90		0.75	0.19	0.88	0.36	1.01	0.49	1.07	0.53
0:100		0.80	0.22	0.95	0.39	1.07	0.52	1.12	0.56
100:0	Int v/c	0.64	0.91	0.79	0.96	0.95	1.09	1.03	1.05
90:10		0.69	0.88	0.74	0.93	0.91	1.10	0.98	1.01
70:30		0.78	0.75	0.84	0.82	0.91	0.91	0.94	0.95
50:50		0.83	0.65	0.91	0.73	0.98	0.80	1.02	0.84
30:70		1.02	0.59	1.08	0.66	1.16	0.74	1.19	0.77
10:90		1.18	0.60	1.24	0.67	1.33	0.75	1.36	0.78
0:100		1.27	0.62	1.34	0.67	1.41	0.75	1.46	0.78

Table E - 4: Color-coded tables of the CDI and DDI turning movement and interchange v/c ratios at cross-street demand of 2500 vph with different off-ramp demands and through/left proportions for LC1

JC Volume 2500 vph									
Proportion	Approach	CDI	DDI	CDI	DDI	CDI	DDI	CDI	DDI
		500 vph		1100 vph		1800 vph		2100 vph	
100:0		0.64	1.38	0.66	1.48	0.70	1.61	0.71	1.67
90:10		0.90	1.17	0.92	1.29	0.93	1.40	0.96	1.42
70:30		0.95	0.83	1.01	0.90	1.11	0.98	1.14	1.03
50:50	NBT1	0.80	0.71	0.88	0.78	0.94	0.86	0.98	0.90
30:70		1.35	0.70	1.47	0.77	1.58	0.82	1.62	0.86
10:90		2.03	0.84	2.13	0.90	2.25	0.97	2.31	1.00
0:100		2.25	0.86	2.37	0.95	2.50	1.02	2.57	1.05
100:0		0.72	0.69	0.84	0.74	1.01	0.81	1.06	0.83
90:10		0.67	0.74	0.81	0.78	0.96	0.84	1.03	0.88
70:30		0.51	0.79	0.65	0.87	0.85	0.94	0.93	0.95
50:50	SBT1	0.36	0.66	0.49	0.78	0.64	0.85	0.72	0.89
30:70		0.24	0.57	0.35	0.65	0.49	0.75	0.52	0.77
10:90		0.13	0.36	0.22	0.50	0.32	0.61	0.35	0.66
0:100		0.07	0.23	0.16	0.40	0.24	0.54	0.27	0.58
100:0		0.00	0.00	0.00	0.00	0.00	0.00	0.00	0.00
90:10		0.47	0.05	0.53	0.05	0.50	0.05	0.50	0.05
70:30		0.75	0.15	0.83	0.15	0.92	0.15	0.93	0.15
50:50	SBL1	0.85	0.25	0.84	0.25	0.82	0.25	0.81	0.25
30:70		0.65	0.35	0.64	0.35	0.63	0.35	0.62	0.35
10:90		0.54	0.45	0.54	0.45	0.52	0.45	0.52	0.42
0:100		0.52	0.50	0.50	0.50	0.50	0.46	0.50	0.44
100:0		0.47	0.11	0.78	0.23	0.94	0.35	1.03	0.40
90:10		0.45	0.11	0.73	0.23	0.91	0.36	0.98	0.41
70:30		0.57	0.12	0.76	0.25	0.87	0.38	0.92	0.43
50:50	EBL1	0.80	0.13	0.92	0.28	1.04	0.40	1.10	0.45
30:70		0.94	0.17	1.08	0.31	1.23	0.45	1.28	0.49
10:90		1.02	0.20	1.24	0.37	1.40	0.50	1.43	0.55
0:100		1.02	0.23	1.24	0.40	1.40	0.54	1.43	0.58
100:0		0.72	0.69	0.84	0.75	1.01	0.81	1.06	0.84
90:10		0.67	0.75	0.83	0.78	0.96	0.84	1.03	0.88
70:30		0.52	0.78	0.64	0.86	0.80	0.96	0.85	0.95
50:50	NBT2	0.37	0.65	0.51	0.76	0.65	0.84	0.71	0.88
30:70		0.25	0.55	0.34	0.65	0.45	0.74	0.49	0.76
10:90		0.12	0.36	0.19	0.50	0.27	0.61	0.31	0.65
0:100		0.07	0.22	0.13	0.40	0.20	0.52	0.24	0.57
100:0		0.00	0.00	0.00	0.00	0.00	0.00	0.00	0.00
90:10		0.40	0.05	0.45	0.05	0.43	0.05	0.45	0.05
70:30		0.60	0.15	0.69	0.15	0.75	0.15	0.78	0.15
50:50	NBL2	0.71	0.25	0.80	0.25	0.87	0.25	0.90	0.25
30:70		0.59	0.35	0.58	0.35	0.59	0.35	0.60	0.35
10:90		0.44	0.45	0.45	0.45	0.46	0.45	0.47	0.43
0:100		0.42	0.50	0.42	0.50	0.44	0.47	0.44	0.45
100:0		0.64	1.38	0.66	1.50	0.70	1.64	0.71	1.70
90:10		0.77	1.19	0.81	1.29	0.80	1.42	0.81	1.45
70:30		0.69	0.84	0.74	0.91	0.82	1.00	0.82	1.05
50:50	SBT2	1.08	0.72	1.19	0.80	1.29	0.87	1.34	0.91
30:70		1.72	0.72	1.83	0.77	2.00	0.84	2.10	0.88
10:90		2.42	0.84	2.61	0.90	2.89	0.97	2.95	1.02
0:100		2.81	0.88	3.10	0.95	3.33	1.04	3.40	1.07
100:0		0.47	0.11	0.78	0.22	0.94	0.35	1.03	0.40
90:10		0.45	0.11	0.69	0.23	0.91	0.36	0.98	0.41
70:30		0.52	0.12	0.69	0.24	0.82	0.38	0.90	0.43
50:50	WBL2	0.63	0.13	0.77	0.27	0.88	0.40	0.93	0.45
30:70		0.72	0.16	0.85	0.31	0.99	0.44	1.03	0.49
10:90		0.80	0.20	0.95	0.37	1.07	0.50	1.13	0.54
0:100		0.87	0.22	0.99	0.40	1.13	0.52	1.18	0.57
100:0		0.69	0.95	0.83	1.00	0.99	1.07	1.05	1.10
90:10		0.72	0.92	0.80	0.96	0.94	1.03	1.02	1.06
70:30		0.81	0.80	0.88	0.88	0.97	0.97	1.00	0.98
50:50	Int v/c	0.89	0.68	0.97	0.77	1.04	0.85	1.08	0.89
30:70		1.10	0.64	1.14	0.70	1.22	0.78	1.25	0.81
10:90		1.26	0.65	1.33	0.72	1.41	0.78	1.44	0.82
0:100		1.36	0.65	1.43	0.72	1.52	0.79	1.55	0.82

Table E - 5: Color-coded tables of the CDI and DDI turning movement and interchange v/c ratios at cross-street volume of 2700 vph with different off-ramp demands and through/left proportions for LC1

JC Volume 2700 vph							
Proportion	Approach	CDI	DDI	CDI	DDI	CDI	DDI
		500 vph		1100 vph		1800 vph	
100:0	NBT1	0.67	1.47	0.70	1.59	0.74	1.71
90:10		0.91	1.27	0.94	1.37	1.01	1.48
70:30		0.99	0.90	1.07	0.97	1.13	1.05
50:50		0.86	0.78	0.92	0.83	1.01	0.91
30:70		1.45	0.74	1.55	0.80	1.66	0.86
10:90		2.08	0.87	2.19	0.91	2.30	1.01
0:100		2.31	0.88	2.43	0.96	2.56	1.05
100:0	SBT1	0.74	0.70	0.88	0.74	1.05	0.82
90:10		0.71	0.74	0.84	0.79	0.99	0.85
70:30		0.53	0.83	0.68	0.92	0.86	0.96
50:50		0.38	0.74	0.50	0.80	0.66	0.89
30:70		0.25	0.60	0.36	0.68	0.47	0.76
10:90		0.13	0.37	0.21	0.52	0.30	0.63
0:100		0.07	0.24	0.14	0.42	0.23	0.55
100:0	SBL1	0.00	0.00	0.00	0.00	0.00	0.00
90:10		0.54	0.05	0.57	0.05	0.51	0.05
70:30		0.79	0.16	0.89	0.16	0.95	0.16
50:50		0.84	0.27	0.83	0.27	0.81	0.27
30:70		0.66	0.38	0.65	0.38	0.63	0.38
10:90		0.55	0.49	0.55	0.49	0.55	0.45
0:100		0.53	0.54	0.53	0.54	0.52	0.48
100:0	EBL1	0.57	0.11	0.79	0.23	0.99	0.36
90:10		0.47	0.11	0.76	0.23	0.94	0.36
70:30		0.63	0.12	0.80	0.25	0.91	0.38
50:50		0.83	0.14	1.00	0.27	1.09	0.41
30:70		1.02	0.17	1.18	0.31	1.31	0.44
10:90		1.02	0.20	1.24	0.38	1.40	0.51
0:100		1.02	0.24	1.24	0.42	1.40	0.55
100:0	NBT2	0.74	0.70	0.88	0.75	1.05	0.82
90:10		0.71	0.75	0.84	0.79	0.95	0.85
70:30		0.54	0.83	0.64	0.92	0.80	0.96
50:50		0.39	0.72	0.51	0.79	0.63	0.88
30:70		0.25	0.58	0.34	0.67	0.44	0.76
10:90		0.13	0.39	0.19	0.51	0.27	0.62
0:100		0.07	0.23	0.13	0.41	0.20	0.54
100:0	NBL2	0.00	0.00	0.00	0.00	0.00	0.00
90:10		0.44	0.05	0.46	0.05	0.44	0.05
70:30		0.64	0.16	0.71	0.16	0.81	0.16
50:50		0.76	0.27	0.83	0.27	0.86	0.27
30:70		0.57	0.38	0.59	0.38	0.60	0.38
10:90		0.45	0.49	0.47	0.49	0.48	0.46
0:100		0.43	0.54	0.45	0.54	0.46	0.49
100:0	SBT2	0.67	1.50	0.70	1.62	0.74	1.74
90:10		0.80	1.29	0.82	1.39	0.85	1.51
70:30		0.72	0.90	0.80	0.97	0.83	1.06
50:50		1.14	0.80	1.25	0.84	1.37	0.93
30:70		1.79	0.76	1.94	0.82	2.13	0.88
10:90		2.61	0.85	2.78	0.93	3.02	1.02
0:100		3.04	0.90	3.24	0.98	3.53	1.06
100:0	WBL2	0.57	0.11	0.79	0.22	0.99	0.35
90:10		0.47	0.11	0.76	0.23	0.94	0.36
70:30		0.57	0.12	0.72	0.25	0.84	0.38
50:50		0.67	0.14	0.81	0.27	0.92	0.40
30:70		0.80	0.16	0.92	0.31	1.04	0.44
10:90		0.87	0.21	1.03	0.36	1.16	0.50
0:100		0.94	0.23	1.08	0.41	1.19	0.54
100:0	Int v/c	0.72	1.00	0.86	1.05	1.04	1.12
90:10		0.76	0.96	0.82	1.01	0.98	1.07
70:30		0.86	0.86	0.94	0.94	1.01	0.99
50:50		0.94	0.75	1.02	0.81	1.09	0.89
30:70		1.14	0.67	1.21	0.74	1.28	0.81
10:90		1.35	0.68	1.41	0.74	1.50	0.82
0:100		1.46	0.68	1.53	0.75	1.61	0.82

E.1.2 Plots of Difference between CDI and DDI v/c Ratios

The following plots present the difference in the CDI and DDI v/c ratios on different turning movements, traffic demands, and through/left proportions for LC1. The numbers in the legend represent different cross-street and off-ramp volumes, i.e., 2300/1100 means cross-street demand of 2300 vph and off-ramp volume of 1100 vph.

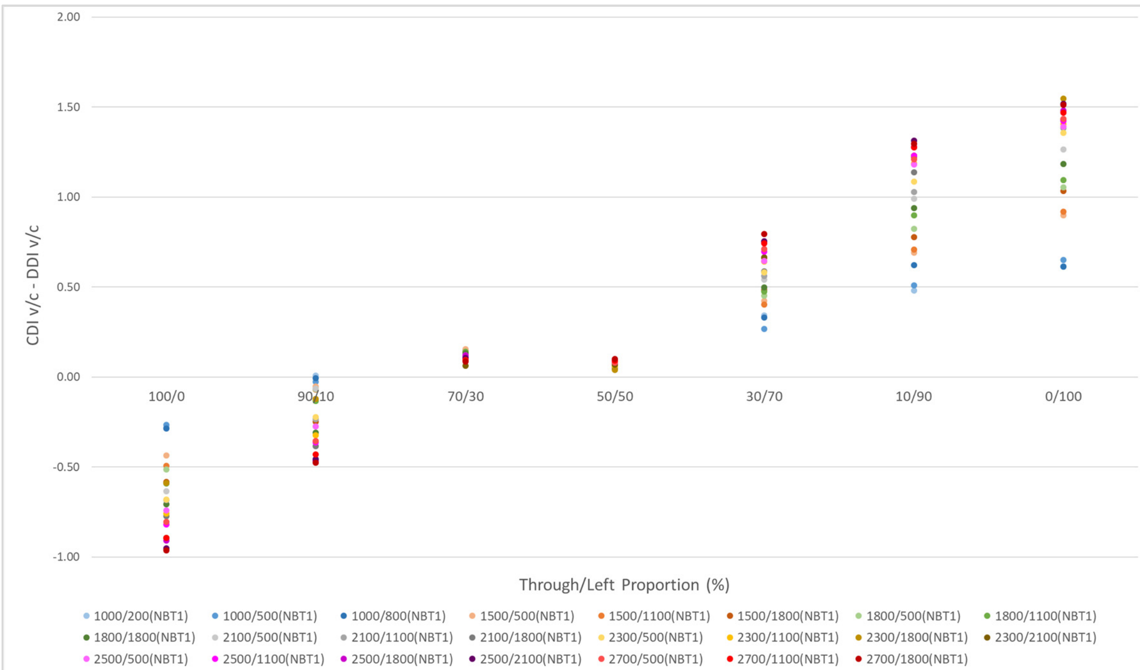

Figure E - 1: Difference in v/c ratios between CDI and DDI on NBT1 at different traffic demands and through/left proportions for LC1

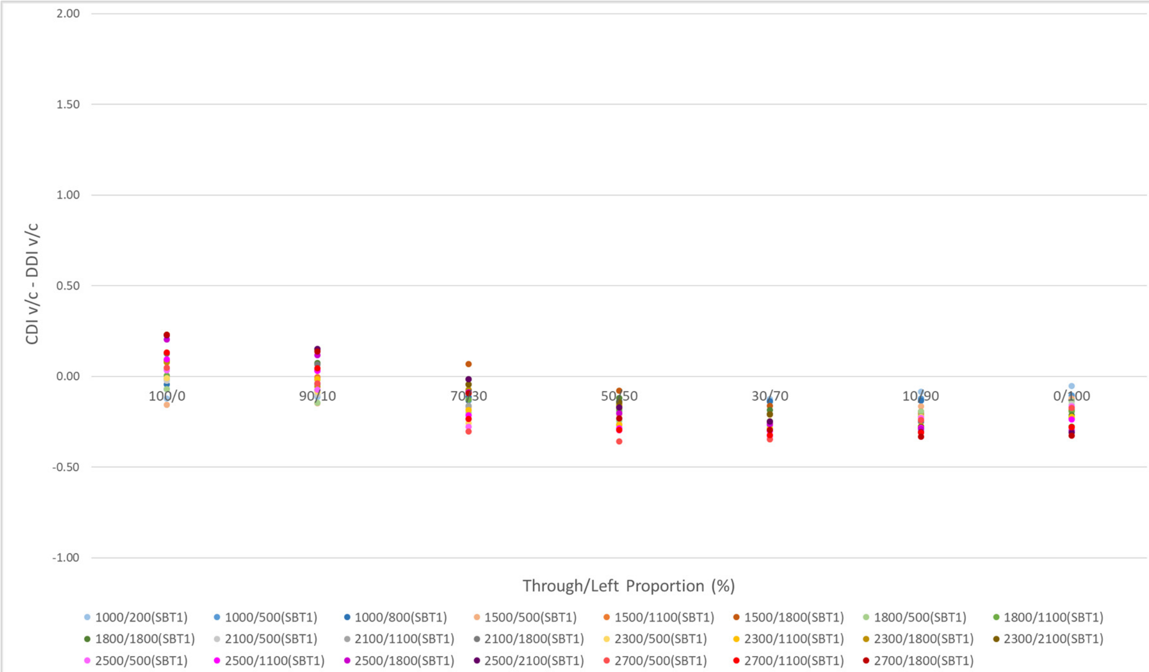

Figure E - 2: Difference in v/c ratios between CDI and DDI on SBT1 at different traffic demands and through/left proportions for LC1

Figure E - 3: Difference in v/c ratios between CDI and DDI on SBL1 at different traffic demands and through/left proportions for LC1

Figure E - 4: Difference in v/c ratios between CDI and DDI on EBL1 at different traffic demands and through/left proportions for LC1

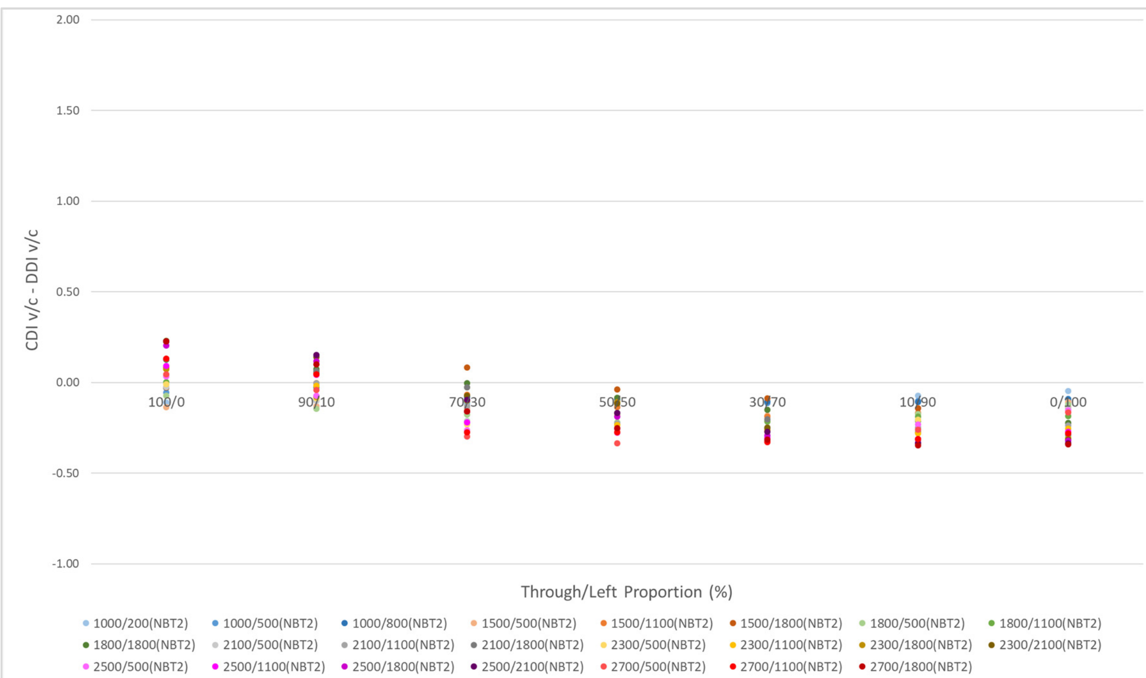

Figure E - 5: Difference in v/c ratios between CDI and DDI on NBT2 at different traffic demands and through/left proportions for LC1

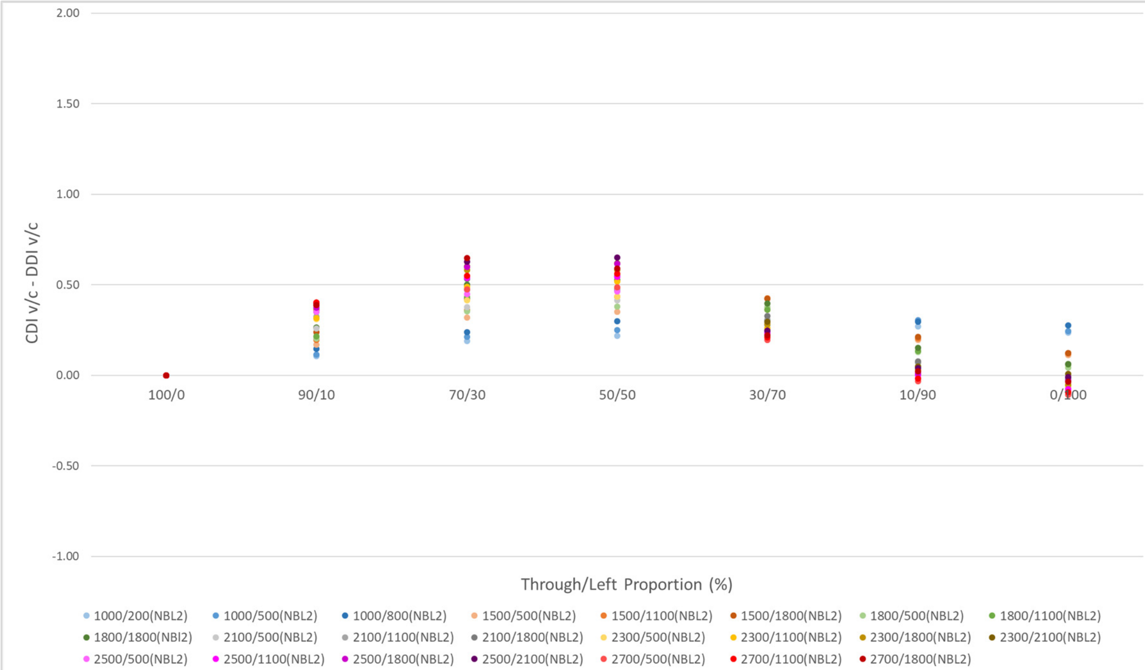

Figure E - 6: Difference in v/c ratios between CDI and DDI on NBL2 at different traffic demands and through/left proportions for LC1

Figure E - 7: Difference in v/c ratios between CDI and DDI on SBT2 at different traffic demands and through/left proportions for LC1

Figure E - 8: Difference in v/c ratios between CDI and DDI on WBL2 at different traffic demands and through/left proportions for LC1

E.2 Lane Configuration 2

The following tables and plots present the difference in the CDI and DDI v/c ratios on different turning movements, traffic demands, and through/left proportions for LC2.

E.2.1 Color-Coded Tables of v/c Ratios of CDIs and DDIs

Table E - 6: Color-coded tables of the CDI and DDI turning movement and interchange v/c ratios at (a) cross-street demand of 1000 vph, and (b) cross-street demand of 1500 vph with different off-ramp demands and through/left proportions for LC2

(a)

JC Volume 1000 vph							
Proportion	Approach	CDI	DDI	CDI	DDI	CDI	DDI
		200 vph		500 vph		800 vph	
100:0	NBT1	0.28	0.54	0.33	0.60	0.35	0.63
90:10		0.45	0.47	0.50	0.51	0.56	0.56
70:30		0.42	0.35	0.47	0.39	0.50	0.41
50:50		0.67	0.45	0.71	0.50	0.79	0.53
30:70		1.03	0.58	1.15	0.64	1.15	0.70
10:90		1.55	0.67	1.61	0.75	1.71	0.82
0:100		1.78	0.69	1.92	0.80	1.96	0.91
100:0	SBT1	0.32	0.45	0.44	0.51	0.52	0.56
90:10		0.30	0.44	0.39	0.49	0.49	0.53
70:30		0.23	0.39	0.31	0.44	0.39	0.50
50:50		0.16	0.33	0.23	0.39	0.30	0.45
30:70		0.11	0.25	0.16	0.32	0.22	0.38
10:90		0.06	0.16	0.11	0.24	0.16	0.32
0:100		0.03	0.09	0.08	0.20	0.13	0.26
100:0	SBL1	0.00	0.00	0.00	0.00	0.00	0.00
90:10		0.20	0.04	0.22	0.04	0.23	0.04
70:30		0.36	0.12	0.43	0.12	0.46	0.12
50:50		0.50	0.20	0.55	0.20	0.58	0.20
30:70		0.52	0.28	0.50	0.28	0.56	0.28
10:90		0.43	0.36	0.43	0.36	0.42	0.36
0:100		0.40	0.40	0.39	0.40	0.38	0.38
100:0	EBL1	0.13	0.05	0.26	0.12	0.38	0.19
90:10		0.16	0.05	0.28	0.13	0.38	0.19
70:30		0.19	0.06	0.35	0.14	0.45	0.21
50:50		0.25	0.07	0.42	0.15	0.50	0.23
30:70		0.29	0.07	0.45	0.16	0.58	0.24
10:90		0.32	0.09	0.53	0.18	0.62	0.26
0:100		0.33	0.09	0.55	0.20	0.66	0.26
100:0	NBT2	0.32	0.44	0.44	0.49	0.52	0.55
90:10		0.30	0.42	0.39	0.47	0.48	0.53
70:30		0.22	0.38	0.30	0.42	0.38	0.49
50:50		0.16	0.31	0.23	0.37	0.30	0.43
30:70		0.11	0.24	0.16	0.31	0.22	0.36
10:90		0.06	0.15	0.11	0.23	0.16	0.29
0:100		0.03	0.09	0.08	0.17	0.13	0.24
100:0	NBL2	0.00	0.00	0.00	0.00	0.00	0.00
90:10		0.18	0.04	0.20	0.04	0.22	0.04
70:30		0.36	0.12	0.40	0.12	0.45	0.12
50:50		0.48	0.20	0.52	0.20	0.56	0.20
30:70		0.53	0.28	0.51	0.28	0.56	0.28
10:90		0.44	0.36	0.43	0.36	0.42	0.36
0:100		0.41	0.40	0.38	0.40	0.38	0.40
100:0	SBT2	0.28	0.56	0.33	0.63	0.35	0.67
90:10		0.47	0.49	0.53	0.54	0.57	0.57
70:30		0.40	0.37	0.47	0.41	0.50	0.43
50:50		0.71	0.48	0.75	0.53	0.82	0.56
30:70		1.09	0.61	1.19	0.67	1.15	0.74
10:90		1.61	0.69	1.65	0.78	1.69	0.90
0:100		1.90	0.71	1.86	0.87	1.95	1.00
100:0	WBL2	0.13	0.05	0.26	0.12	0.38	0.18
90:10		0.16	0.05	0.28	0.12	0.38	0.19
70:30		0.21	0.06	0.39	0.13	0.47	0.20
50:50		0.25	0.06	0.42	0.14	0.50	0.22
30:70		0.29	0.07	0.46	0.16	0.58	0.23
10:90		0.33	0.08	0.53	0.17	0.63	0.24
0:100		0.34	0.09	0.57	0.17	0.67	0.24
100:0	Int v/c	0.28	0.48	0.39	0.53	0.48	0.58
90:10		0.32	0.44	0.36	0.49	0.45	0.53
70:30		0.36	0.36	0.42	0.41	0.47	0.45
50:50		0.53	0.39	0.58	0.43	0.63	0.48
30:70		0.68	0.43	0.69	0.48	0.74	0.52
10:90		0.76	0.48	0.77	0.53	0.78	0.57
0:100		0.80	0.49	0.78	0.55	0.80	0.60

(b)

JC Volume 1500 vph							
Proportion	Approach	CDI	DDI	CDI	DDI	CDI	DDI
		500 vph		1100 vph		1800 vph	
100:0	NBT1	0.45	0.86	0.47	0.94	0.48	1.07
90:10		0.68	0.74	0.63	0.81	0.64	0.90
70:30		0.59	0.53	0.67	0.60	0.68	0.64
50:50		0.96	0.71	1.06	0.78	1.15	0.90
30:70		1.50	0.91	1.67	1.05	1.76	1.09
10:90		2.19	1.04	2.37	1.23	2.56	1.30
0:100		2.55	1.06	2.77	1.36	3.00	1.44
100:0	SBT1	0.55	0.67	0.69	0.74	0.83	0.79
90:10		0.50	0.63	0.65	0.72	0.81	0.83
70:30		0.37	0.58	0.53	0.67	0.72	0.70
50:50		0.27	0.50	0.41	0.62	0.57	0.73
30:70		0.19	0.42	0.30	0.54	0.45	0.65
10:90		0.11	0.31	0.21	0.44	0.33	0.56
0:100		0.07	0.22	0.17	0.36	0.27	0.52
100:0	SBL1	0.00	0.00	0.00	0.00	0.00	0.00
90:10		0.33	0.06	0.41	0.06	0.43	0.06
70:30		0.55	0.18	0.63	0.18	0.68	0.18
50:50		0.71	0.30	0.72	0.30	0.69	0.30
30:70		0.51	0.42	0.49	0.36	0.50	0.34
10:90		0.41	0.48	0.40	0.40	0.39	0.35
0:100		0.36	0.51	0.36	0.40	0.35	0.35
100:0	EBL1	0.35	0.12	0.59	0.23	0.78	0.36
90:10		0.35	0.12	0.53	0.24	0.77	0.38
70:30		0.44	0.13	0.60	0.26	0.69	0.36
50:50		0.55	0.15	0.72	0.29	0.80	0.44
30:70		0.63	0.17	0.78	0.33	0.90	0.46
10:90		0.74	0.21	0.88	0.36	1.01	0.49
0:100		0.82	0.22	0.95	0.36	1.07	0.52
100:0	NBT2	0.55	0.66	0.69	0.73	0.83	0.79
90:10		0.49	0.62	0.65	0.71	0.81	0.81
70:30		0.37	0.56	0.52	0.66	0.72	0.69
50:50		0.27	0.49	0.40	0.59	0.57	0.72
30:70		0.19	0.40	0.30	0.52	0.45	0.61
10:90		0.11	0.29	0.21	0.42	0.33	0.51
0:100		0.07	0.20	0.17	0.34	0.27	0.47
100:0	NBL2	0.00	0.00	0.00	0.00	0.00	0.00
90:10		0.30	0.06	0.35	0.06	0.42	0.06
70:30		0.55	0.18	0.63	0.18	0.65	0.18
50:50		0.71	0.30	0.72	0.30	0.69	0.30
30:70		0.52	0.42	0.49	0.38	0.50	0.37
10:90		0.41	0.49	0.39	0.42	0.40	0.39
0:100		0.36	0.54	0.36	0.42	0.36	0.40
100:0	SBT2	0.45	0.89	0.47	0.97	0.48	1.07
90:10		0.68	0.77	0.68	0.84	0.65	0.93
70:30		0.59	0.54	0.64	0.61	0.70	0.66
50:50		0.96	0.72	1.05	0.82	1.15	0.91
30:70		1.56	0.95	1.68	1.11	1.80	1.18
10:90		2.19	1.08	2.31	1.29	2.63	1.45
0:100		2.55	1.13	2.77	1.43	3.09	1.64
100:0	WBL2	0.35	0.11	0.59	0.23	0.78	0.36
90:10		0.39	0.12	0.53	0.24	0.78	0.37
70:30		0.44	0.13	0.64	0.26	0.69	0.36
50:50		0.56	0.14	0.72	0.28	0.81	0.43
30:70		0.63	0.16	0.78	0.31	0.90	0.44
10:90		0.74	0.20	0.92	0.34	1.01	0.45
0:100		0.82	0.20	0.95	0.34	1.07	0.47
100:0	Int v/c	0.51	0.74	0.66	0.80	0.82	0.87
90:10		0.47	0.67	0.62	0.74	0.80	0.84
70:30		0.55	0.54	0.64	0.63	0.71	0.68
50:50		0.78	0.59	0.83	0.68	0.86	0.78
30:70		0.85	0.68	0.87	0.77	0.93	0.83
10:90		0.92	0.75	0.96	0.84	1.03	0.90
0:100		0.95	0.76	1.01	0.88	1.09	0.95

Table E - 7: Color-coded tables of the CDI and DDI turning movement and interchange v/c ratios at (a) cross-street demand of 1800 vph, and (b) cross-street demand of 2100 vph with different off-ramp demands and through/left proportions for LC2

(a)

JC Volume 1800 vph							
Proportion	Approach	CDI	DDI	CDI	DDI	CDI	DDI
		500 vph		1100 vph		1800 vph	
100:0	NBT1	0.51	1.01	0.52	1.11	0.54	1.20
90:10		0.77	0.86	0.70	0.95	0.78	1.04
70:30		0.68	0.61	0.71	0.69	0.79	0.76
50:50		1.05	0.81	1.17	0.90	1.28	0.99
30:70		1.72	1.05	1.85	1.16	2.06	1.26
10:90		2.56	1.20	2.78	1.35	2.99	1.51
0:100		3.01	1.24	3.22	1.49	3.50	1.68
100:0	SBT1	0.60	0.71	0.72	0.75	0.87	0.78
90:10		0.57	0.74	0.70	0.79	0.86	0.82
70:30		0.42	0.64	0.56	0.73	0.76	0.82
50:50		0.29	0.57	0.42	0.65	0.58	0.75
30:70		0.20	0.50	0.30	0.59	0.44	0.71
10:90		0.11	0.35	0.20	0.47	0.29	0.59
0:100		0.07	0.26	0.14	0.38	0.23	0.51
100:0	SBL1	0.00	0.00	0.00	0.00	0.00	0.00
90:10		0.40	0.07	0.48	0.07	0.39	0.07
70:30		0.66	0.22	0.72	0.22	0.80	0.22
50:50		0.69	0.36	0.70	0.36	0.70	0.34
30:70		0.51	0.44	0.51	0.40	0.50	0.37
10:90		0.40	0.49	0.39	0.44	0.39	0.38
0:100		0.35	0.51	0.36	0.44	0.36	0.38
100:0	EBL1	0.38	0.11	0.65	0.23	0.83	0.35
90:10		0.39	0.12	0.58	0.24	0.79	0.36
70:30		0.49	0.13	0.65	0.26	0.78	0.39
50:50		0.63	0.15	0.79	0.28	0.88	0.42
30:70		0.78	0.18	0.92	0.33	1.01	0.48
10:90		0.89	0.22	1.03	0.37	1.16	0.51
0:100		0.94	0.26	1.11	0.38	1.23	0.51
100:0	NBT2	0.60	0.72	0.72	0.75	0.88	0.78
90:10		0.57	0.72	0.70	0.78	0.86	0.82
70:30		0.41	0.63	0.55	0.72	0.75	0.81
50:50		0.29	0.55	0.42	0.65	0.58	0.74
30:70		0.20	0.47	0.30	0.57	0.44	0.69
10:90		0.11	0.33	0.20	0.45	0.29	0.56
0:100		0.07	0.22	0.14	0.36	0.23	0.48
100:0	NBL2	0.00	0.00	0.00	0.00	0.00	0.00
90:10		0.38	0.07	0.45	0.07	0.49	0.07
70:30		0.66	0.22	0.69	0.22	0.79	0.22
50:50		0.70	0.36	0.70	0.36	0.69	0.36
30:70		0.51	0.46	0.51	0.41	0.50	0.38
10:90		0.40	0.51	0.39	0.46	0.39	0.41
0:100		0.36	0.55	0.36	0.46	0.36	0.41
100:0	SBT2	0.51	1.03	0.52	1.13	0.54	1.22
90:10		0.79	0.88	0.71	0.97	0.72	1.06
70:30		0.66	0.63	0.72	0.71	0.78	0.79
50:50		1.08	0.84	1.17	0.90	1.25	1.01
30:70		1.72	1.10	1.85	1.21	2.06	1.31
10:90		2.56	1.25	2.78	1.39	2.99	1.61
0:100		3.09	1.33	3.22	1.54	3.50	1.79
100:0	WBL2	0.38	0.11	0.65	0.23	0.82	0.34
90:10		0.39	0.12	0.58	0.23	0.80	0.35
70:30		0.53	0.13	0.67	0.25	0.80	0.38
50:50		0.63	0.14	0.79	0.28	0.90	0.41
30:70		0.78	0.17	0.92	0.32	1.01	0.46
10:90		0.89	0.21	1.03	0.36	1.16	0.48
0:100		0.94	0.22	1.11	0.36	1.23	0.48
100:0	Int v/c	0.56	0.83	0.71	0.88	0.86	0.91
90:10		0.60	0.78	0.67	0.84	0.84	0.89
70:30		0.64	0.62	0.70	0.70	0.76	0.79
50:50		0.83	0.68	0.88	0.75	0.93	0.84
30:70		0.92	0.80	0.96	0.86	1.03	0.95
10:90		1.02	0.89	1.08	0.95	1.16	1.03
0:100		1.08	0.93	1.15	0.99	1.22	1.07

(b)

JC Volume 2100 vph							
Proportion	Approach	CDI	DDI	CDI	DDI	CDI	DDI
		500 vph		1100 vph		1800 vph	
100:0	NBT1	0.57	1.16	0.58	1.24	0.60	1.35
90:10		0.78	0.98	0.77	1.07	0.79	1.15
70:30		0.72	0.69	0.80	0.77	0.84	0.84
50:50		1.20	0.91	1.30	1.01	1.40	1.11
30:70		1.96	1.18	2.12	1.29	2.35	1.43
10:90		3.02	1.35	3.16	1.46	3.32	1.65
0:100		3.52	1.45	3.69	1.63	3.88	1.84
100:0	SBT1	0.65	0.70	0.77	0.74	0.92	0.81
90:10		0.59	0.77	0.74	0.80	0.89	0.85
70:30		0.44	0.73	0.60	0.81	0.77	0.87
50:50		0.32	0.64	0.44	0.74	0.60	0.83
30:70		0.21	0.59	0.31	0.63	0.41	0.74
10:90		0.11	0.40	0.18	0.54	0.26	0.64
0:100		0.06	0.26	0.13	0.41	0.19	0.54
100:0	SBL1	0.00	0.00	0.00	0.00	0.00	0.00
90:10		0.42	0.08	0.51	0.08	0.47	0.08
70:30		0.70	0.25	0.81	0.25	0.86	0.25
50:50		0.69	0.42	0.69	0.39	0.69	0.35
30:70		0.50	0.46	0.50	0.43	0.50	0.39
10:90		0.39	0.51	0.39	0.48	0.40	0.41
0:100		0.35	0.53	0.36	0.48	0.36	0.41
100:0	EBL1	0.44	0.11	0.69	0.23	0.88	0.35
90:10		0.44	0.11	0.65	0.23	0.84	0.36
70:30		0.57	0.13	0.73	0.26	0.83	0.38
50:50		0.73	0.15	0.87	0.29	0.99	0.43
30:70		0.89	0.20	1.03	0.33	1.13	0.47
10:90		0.94	0.24	1.18	0.41	1.31	0.54
0:100		1.02	0.26	1.24	0.41	1.40	0.54
100:0	NBT2	0.65	0.71	0.77	0.75	0.92	0.81
90:10		0.59	0.80	0.74	0.80	0.89	0.85
70:30		0.44	0.71	0.60	0.80	0.77	0.87
50:50		0.32	0.62	0.44	0.73	0.60	0.82
30:70		0.21	0.55	0.31	0.64	0.42	0.74
10:90		0.12	0.37	0.18	0.51	0.26	0.60
0:100		0.06	0.24	0.13	0.39	0.19	0.51
100:0	NBL2	0.00	0.00	0.00	0.00	0.00	0.00
90:10		0.39	0.08	0.49	0.08	0.46	0.08
70:30		0.70	0.25	0.79	0.25	0.84	0.25
50:50		0.69	0.42	0.69	0.39	0.69	0.36
30:70		0.50	0.48	0.50	0.43	0.49	0.39
10:90		0.39	0.53	0.39	0.49	0.40	0.43
0:100		0.36	0.55	0.36	0.49	0.37	0.43
100:0	SBT2	0.57	1.18	0.58	1.26	0.60	1.35
90:10		0.80	1.00	0.78	1.09	0.80	1.17
70:30		0.72	0.70	0.81	0.79	0.86	0.86
50:50		1.20	0.93	1.30	1.02	1.43	1.13
30:70		2.00	1.23	2.16	1.29	2.30	1.43
10:90		2.96	1.40	3.16	1.51	3.40	1.76
0:100		3.60	1.50	3.78	1.68	3.98	1.96
100:0	WBL2	0.44	0.11	0.69	0.22	0.88	0.35
90:10		0.44	0.11	0.65	0.23	0.84	0.36
70:30		0.57	0.13	0.74	0.25	0.83	0.38
50:50		0.73	0.14	0.87	0.29	0.99	0.43
30:70		0.89	0.18	1.03	0.33	1.16	0.47
10:90		1.02	0.22	1.18	0.39	1.31	0.51
0:100		1.02	0.24	1.24	0.39	1.40	0.51
100:0	Int v/c	0.62	0.88	0.75	0.92	0.91	0.98
90:10		0.63	0.87	0.72	0.90	0.87	0.96
70:30		0.69	0.70	0.79	0.79	0.84	0.86
50:50		0.89	0.77	0.93	0.85	1.00	0.94
30:70		1.01	0.92	1.06	0.96	1.13	1.04
10:90		1.14	1.02	1.20	1.08	1.28	1.16
0:100		1.21	1.07	1.28	1.13	1.36	1.20

Table E - 8: Color-coded tables of the CDI and DDI turning movement and interchange v/c ratios at cross-street demand of 2300 vph with different off-ramp demands and through/left proportions for LC2

		JC Volume 2300 vph							
Proportion	Approach	CDI	DDI	CDI	DDI	CDI	DDI	CDI	DDI
		500 vph		1100 vph		1800 vph		2100 vph	
100:0		0.59	1.24	0.62	1.34	0.65	1.45	0.67	1.51
90:10		0.81	1.07	0.83	1.15	0.80	1.26	0.82	1.31
70:30		0.74	0.74	0.83	0.82	0.88	0.89	0.93	0.92
50:50	NBT1	1.27	0.96	1.40	1.11	1.53	1.20	1.56	1.21
30:70		2.15	1.28	2.32	1.37	2.49	1.49	2.58	1.53
10:90		3.24	1.43	3.47	1.57	3.64	1.74	3.73	1.80
0:100		3.68	1.53	3.94	1.67	4.14	1.89	4.25	2.00
100:0		0.67	0.71	0.81	0.76	0.96	0.82	1.05	0.85
90:10		0.62	0.77	0.79	0.81	0.92	0.85	1.00	0.88
70:30		0.46	0.76	0.61	0.85	0.79	0.93	0.88	0.97
50:50	SBT1	0.33	0.69	0.46	0.80	0.59	0.83	0.64	0.88
30:70		0.23	0.58	0.31	0.69	0.40	0.78	0.44	0.82
10:90		0.12	0.40	0.18	0.57	0.25	0.66	0.29	0.69
0:100		0.06	0.28	0.12	0.46	0.18	0.56	0.22	0.58
100:0		0.00	0.00	0.00	0.00	0.00	0.00	0.00	0.00
90:10		0.46	0.09	0.62	0.09	0.60	0.09	0.61	0.09
70:30		0.75	0.28	0.86	0.28	0.90	0.28	0.94	0.28
50:50	SBL1	0.68	0.46	0.68	0.39	0.68	0.36	0.69	0.35
30:70		0.49	0.48	0.49	0.43	0.50	0.40	0.50	0.39
10:90		0.39	0.54	0.39	0.49	0.40	0.44	0.39	0.42
0:100		0.38	0.55	0.37	0.49	0.38	0.44	0.37	0.42
100:0		0.47	0.11	0.72	0.23	0.92	0.36	0.98	0.41
90:10		0.45	0.11	0.69	0.23	0.88	0.36	0.95	0.41
70:30		0.62	0.12	0.81	0.25	0.87	0.38	0.91	0.44
50:50	EBL1	0.80	0.15	0.92	0.30	1.04	0.41	1.10	0.47
30:70		0.94	0.18	1.08	0.34	1.23	0.48	1.28	0.54
10:90		1.02	0.23	1.24	0.43	1.40	0.55	1.43	0.58
0:100		1.13	0.28	1.30	0.46	1.45	0.56	1.48	0.58
100:0		0.67	0.71	0.81	0.76	0.96	0.82	1.05	0.85
90:10		0.62	0.77	0.79	0.81	0.92	0.85	0.99	0.88
70:30		0.46	0.75	0.61	0.84	0.79	0.92	0.88	0.97
50:50	NBT2	0.33	0.68	0.46	0.81	0.59	0.82	0.64	0.87
30:70		0.23	0.58	0.31	0.67	0.40	0.76	0.44	0.80
10:90		0.12	0.39	0.18	0.55	0.25	0.64	0.29	0.66
0:100		0.06	0.26	0.12	0.41	0.18	0.53	0.22	0.56
100:0		0.00	0.00	0.00	0.00	0.00	0.00	0.00	0.00
90:10		0.46	0.09	0.59	0.09	0.58	0.09	0.60	0.09
70:30		0.73	0.28	0.84	0.28	0.89	0.28	0.94	0.28
50:50	NBL2	0.69	0.46	0.68	0.39	0.68	0.37	0.69	0.36
30:70		0.50	0.48	0.49	0.45	0.50	0.41	0.50	0.40
10:90		0.39	0.55	0.39	0.50	0.40	0.45	0.40	0.44
0:100		0.38	0.57	0.37	0.52	0.38	0.46	0.38	0.44
100:0		0.59	1.25	0.62	1.36	0.65	1.48	0.67	1.53
90:10		0.81	1.09	0.84	1.16	0.81	1.28	0.82	1.33
70:30		0.75	0.75	0.85	0.83	0.90	0.91	0.93	0.93
50:50	SBT2	1.29	0.99	1.40	1.11	1.53	1.22	1.59	1.23
30:70		2.19	1.28	2.37	1.41	2.49	1.53	2.58	1.57
10:90		3.31	1.44	3.47	1.60	3.64	1.79	3.82	1.88
0:100		3.68	1.59	3.94	1.78	4.14	1.99	4.36	2.09
100:0		0.47	0.11	0.72	0.23	0.92	0.35	0.98	0.40
90:10		0.45	0.11	0.69	0.23	0.88	0.36	0.96	0.41
70:30		0.63	0.12	0.81	0.25	0.87	0.38	0.91	0.43
50:50	WBL2	0.80	0.14	0.92	0.30	1.04	0.41	1.10	0.46
30:70		0.94	0.18	1.08	0.33	1.23	0.47	1.28	0.53
10:90		1.02	0.23	1.24	0.41	1.40	0.53	1.43	0.56
0:100		1.13	0.26	1.30	0.41	1.45	0.53	1.48	0.56
100:0		0.64	0.92	0.79	0.97	0.95	1.03	1.03	1.06
90:10		0.67	0.89	0.77	0.94	0.91	0.99	0.98	1.02
70:30		0.73	0.75	0.84	0.83	0.89	0.91	0.93	0.95
50:50	Int v/c	0.93	0.83	0.97	0.93	1.04	0.98	1.07	1.01
30:70		1.06	0.97	1.12	1.04	1.20	1.11	1.23	1.14
10:90		1.21	1.08	1.28	1.17	1.36	1.22	1.39	1.24
0:100		1.31	1.17	1.37	1.22	1.45	1.27	1.49	1.29

Table E - 9: Color-coded tables of the CDI and DDI turning movement and interchange v/c ratios at cross-street demand of 2500 vph with different off-ramp demands and through/left proportions for LC2

Proportion	Approach	JC Volume 2500 vph							
		500 vph		1100 vph		1800 vph		2100 vph	
		CDI	DDI	CDI	DDI	CDI	DDI	CDI	DDI
100:0	NBT1	0.65	1.34	0.65	1.45	0.70	1.55	0.71	1.61
90:10	NBT1	0.88	1.14	0.86	1.25	0.87	1.35	0.89	1.40
70:30	NBT1	0.78	0.80	0.88	0.88	0.94	0.95	0.97	0.98
50:50	NBT1	1.41	1.06	1.50	1.16	1.64	1.23	1.70	1.27
30:70	NBT1	2.38	1.35	2.47	1.44	2.68	1.56	2.74	1.62
10:90	NBT1	3.45	1.50	3.60	1.66	3.86	1.80	3.95	1.86
0:100	NBT1	3.83	1.61	4.00	1.75	4.29	2.00	4.39	2.08
100:0	SBT1	0.73	0.71	0.83	0.76	1.01	0.84	1.06	0.87
90:10	SBT1	0.68	0.78	0.81	0.82	0.96	0.87	1.03	0.90
70:30	SBT1	0.48	0.81	0.63	0.89	0.81	0.99	0.90	1.00
50:50	SBT1	0.36	0.78	0.47	0.83	0.59	0.91	0.64	0.93
30:70	SBT1	0.23	0.64	0.31	0.72	0.40	0.82	0.44	0.84
10:90	SBT1	0.11	0.45	0.18	0.57	0.25	0.69	0.27	0.71
0:100	SBT1	0.06	0.31	0.12	0.46	0.18	0.56	0.21	0.60
100:0	SBL1	0.00	0.00	0.00	0.00	0.00	0.00	0.00	0.00
90:10	SBL1	0.54	0.10	0.65	0.10	0.61	0.10	0.62	0.10
70:30	SBL1	0.79	0.30	0.88	0.30	0.95	0.30	1.00	0.30
50:50	SBL1	0.69	0.43	0.69	0.41	0.69	0.38	0.68	0.37
30:70	SBL1	0.50	0.48	0.49	0.46	0.50	0.42	0.50	0.40
10:90	SBL1	0.40	0.55	0.40	0.50	0.41	0.46	0.41	0.44
0:100	SBL1	0.40	0.55	0.40	0.52	0.41	0.46	0.41	0.44
100:0	EBL1	0.50	0.11	0.77	0.23	0.94	0.36	1.03	0.41
90:10	EBL1	0.49	0.11	0.73	0.23	0.91	0.36	0.98	0.42
70:30	EBL1	0.66	0.12	0.80	0.25	0.92	0.39	0.96	0.44
50:50	EBL1	0.80	0.16	0.99	0.29	1.09	0.43	1.15	0.48
30:70	EBL1	0.94	0.19	1.18	0.34	1.31	0.49	1.35	0.53
10:90	EBL1	1.13	0.25	1.30	0.42	1.45	0.56	1.52	0.59
0:100	EBL1	1.13	0.31	1.30	0.46	1.45	0.56	1.52	0.60
100:0	NBT2	0.73	0.71	0.83	0.76	1.01	0.84	1.06	0.87
90:10	NBT2	0.68	0.78	0.82	0.82	0.96	0.87	1.03	0.90
70:30	NBT2	0.48	0.81	0.63	0.89	0.81	0.98	0.90	1.02
50:50	NBT2	0.35	0.75	0.47	0.83	0.59	0.89	0.64	0.92
30:70	NBT2	0.24	0.61	0.31	0.71	0.40	0.80	0.44	0.83
10:90	NBT2	0.11	0.42	0.18	0.55	0.25	0.67	0.27	0.68
0:100	NBT2	0.06	0.26	0.12	0.42	0.18	0.55	0.21	0.58
100:0	NBL2	0.00	0.00	0.00	0.00	0.00	0.00	0.00	0.00
90:10	NBL2	0.54	0.10	0.62	0.10	0.60	0.10	0.61	0.10
70:30	NBL2	0.79	0.30	0.88	0.30	0.95	0.30	0.98	0.30
50:50	NBL2	0.68	0.45	0.69	0.41	0.68	0.39	0.68	0.37
30:70	NBL2	0.49	0.49	0.50	0.46	0.50	0.43	0.50	0.41
10:90	NBL2	0.40	0.57	0.41	0.52	0.41	0.48	0.41	0.46
0:100	NBL2	0.40	0.59	0.41	0.54	0.41	0.48	0.41	0.46
100:0	SBT2	0.65	1.36	0.65	1.48	0.70	1.58	0.71	1.64
90:10	SBT2	0.88	1.16	0.88	1.25	0.87	1.37	0.90	1.42
70:30	SBT2	0.78	0.80	0.88	0.88	0.94	0.97	0.98	1.00
50:50	SBT2	1.38	1.09	1.50	1.16	1.64	1.25	1.70	1.29
30:70	SBT2	2.33	1.40	2.52	1.45	2.68	1.59	2.74	1.65
10:90	SBT2	3.45	1.54	3.68	1.70	3.86	1.84	3.95	1.93
0:100	SBT2	3.83	1.72	4.09	1.84	4.29	2.05	4.39	2.14
100:0	WBL2	0.50	0.11	0.77	0.23	0.94	0.36	1.03	0.41
90:10	WBL2	0.49	0.11	0.70	0.23	0.91	0.36	0.98	0.41
70:30	WBL2	0.67	0.12	0.80	0.25	0.92	0.38	0.96	0.44
50:50	WBL2	0.87	0.15	0.99	0.29	1.13	0.42	1.15	0.47
30:70	WBL2	1.02	0.18	1.18	0.34	1.31	0.48	1.35	0.53
10:90	WBL2	1.13	0.23	1.30	0.40	1.45	0.55	1.52	0.57
0:100	WBL2	1.13	0.26	1.30	0.42	1.45	0.55	1.52	0.58
100:0	Int v/c	0.69	0.96	0.82	1.01	0.99	1.08	1.05	1.11
90:10	Int v/c	0.74	0.93	0.80	0.97	0.94	1.04	1.02	1.07
70:30	Int v/c	0.77	0.80	0.86	0.88	0.94	0.97	0.98	1.01
50:50	Int v/c	0.97	0.92	1.02	0.97	1.09	1.04	1.12	1.07
30:70	Int v/c	1.12	1.05	1.19	1.10	1.26	1.17	1.29	1.19
10:90	Int v/c	1.30	1.17	1.37	1.23	1.44	1.29	1.48	1.30
0:100	Int v/c	1.40	1.26	1.47	1.28	1.55	1.34	1.58	1.36

Table E - 10: Color-coded tables of the CDI and DDI turning movement and interchange v/c ratios at cross-street demand of 2700 vph with different off-ramp demands and through/left proportions for LC2

JC Volume 2700 vph							
Proportion	Approach	CDI	DDI	CDI	DDI	CDI	DDI
		500 vph		1100 vph		1800 vph	
100:0	NBT1	0.67	1.45	0.70	1.54	0.74	1.68
90:10		0.90	1.23	0.88	1.33	0.93	1.43
70:30		0.86	0.86	0.91	0.92	0.99	1.02
50:50		1.50	1.10	1.62	1.20	1.74	1.29
30:70		2.52	1.39	2.67	1.54	2.84	1.65
10:90		3.50	1.58	3.72	1.69	3.89	1.87
0:100		3.89	1.69	4.14	1.84	4.32	2.04
100:0	SBT1	0.74	0.71	0.88	0.77	1.05	0.85
90:10		0.71	0.78	0.82	0.82	0.99	0.89
70:30		0.52	0.87	0.65	0.96	0.81	0.99
50:50		0.38	0.81	0.48	0.86	0.59	0.94
30:70		0.25	0.68	0.32	0.76	0.40	0.84
10:90		0.12	0.45	0.18	0.61	0.24	0.72
0:100		0.06	0.35	0.11	0.46	0.18	0.59
100:0	SBL1	0.00	0.00	0.00	0.00	0.00	0.00
90:10		0.58	0.11	0.61	0.11	0.63	0.11
70:30		0.88	0.32	0.91	0.32	1.02	0.32
50:50		0.68	0.45	0.69	0.42	0.69	0.39
30:70		0.49	0.50	0.50	0.47	0.50	0.43
10:90		0.43	0.58	0.44	0.53	0.45	0.48
0:100		0.43	0.57	0.44	0.55	0.45	0.48
100:0	EBL1	0.57	0.11	0.78	0.23	0.99	0.36
90:10		0.50	0.11	0.74	0.24	0.94	0.37
70:30		0.68	0.12	0.85	0.26	0.98	0.39
50:50		0.87	0.15	1.03	0.29	1.16	0.43
30:70		1.02	0.19	1.24	0.35	1.40	0.49
10:90		1.13	0.24	1.30	0.44	1.50	0.58
0:100		1.13	0.35	1.30	0.46	1.50	0.59
100:0	NBT2	0.74	0.71	0.88	0.78	1.05	0.85
90:10		0.71	0.78	0.82	0.83	0.99	0.89
70:30		0.52	0.86	0.65	0.95	0.83	0.99
50:50		0.38	0.79	0.48	0.84	0.59	0.93
30:70		0.25	0.65	0.32	0.76	0.40	0.83
10:90		0.12	0.45	0.18	0.59	0.24	0.70
0:100		0.06	0.28	0.12	0.44	0.18	0.56
100:0	NBL2	0.00	0.00	0.00	0.00	0.00	0.00
90:10		0.58	0.11	0.59	0.11	0.61	0.11
70:30		0.86	0.32	0.91	0.32	1.00	0.32
50:50		0.68	0.46	0.68	0.43	0.68	0.40
30:70		0.49	0.52	0.50	0.47	0.50	0.43
10:90		0.44	0.58	0.43	0.55	0.45	0.49
0:100		0.44	0.61	0.43	0.56	0.45	0.50
100:0	SBT2	0.67	1.47	0.70	1.57	0.74	1.68
90:10		0.90	1.25	0.88	1.35	0.94	1.46
70:30		0.87	0.86	0.91	0.93	1.00	1.03
50:50		1.52	1.13	1.59	1.22	1.74	1.31
30:70		2.57	1.43	2.67	1.54	2.84	1.66
10:90		3.57	1.58	3.72	1.73	3.89	1.91
0:100		3.97	1.80	4.14	1.88	4.32	2.12
100:0	WBL2	0.57	0.11	0.79	0.23	0.99	0.36
90:10		0.50	0.11	0.75	0.23	0.94	0.36
70:30		0.68	0.12	0.85	0.25	0.98	0.39
50:50		0.87	0.15	1.08	0.28	1.19	0.42
30:70		1.02	0.18	1.24	0.35	1.40	0.49
10:90		1.13	0.24	1.38	0.42	1.50	0.56
0:100		1.13	0.28	1.38	0.44	1.50	0.56
100:0	Int v/c	0.72	1.00	0.86	1.06	1.04	1.12
90:10		0.77	0.97	0.80	1.02	0.98	1.08
70:30		0.85	0.86	0.90	0.94	1.00	1.00
50:50		1.01	0.96	1.07	1.02	1.14	1.09
30:70		1.18	1.11	1.25	1.17	1.32	1.23
10:90		1.39	1.23	1.45	1.29	1.54	1.36
0:100		1.51	1.36	1.57	1.35	1.65	1.42

E.2.2 Plots of Difference between CDI and DDI v/c Ratios

Figure E - 9: Difference in v/c ratios between CDI and DDI on NBT1 at different traffic demands and through/left proportions for LC2

Figure E - 10: Difference in v/c ratios between CDI and DDI on SBT1 at different traffic demands and through/left proportions for LC2

Figure E - 11: Difference in v/c ratios between CDI and DDI on SBL1 at different traffic demands and through/left proportions for LC2

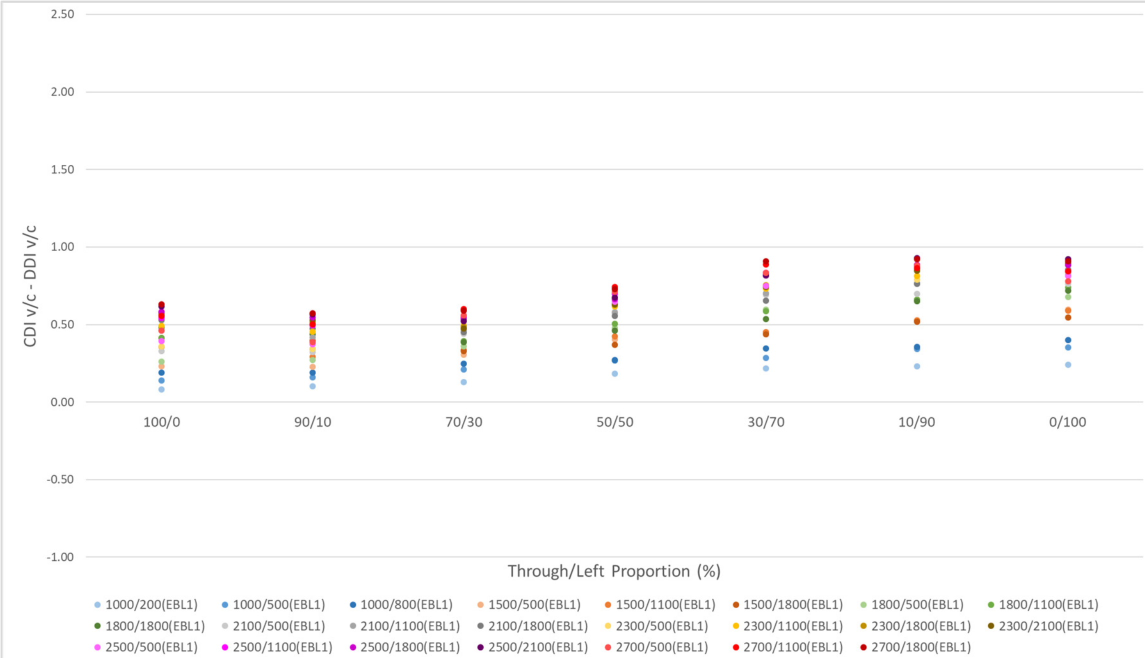

Figure E - 12: Difference in v/c ratios between CDI and DDI on EBL1 at different traffic demands and through/left proportions for LC2

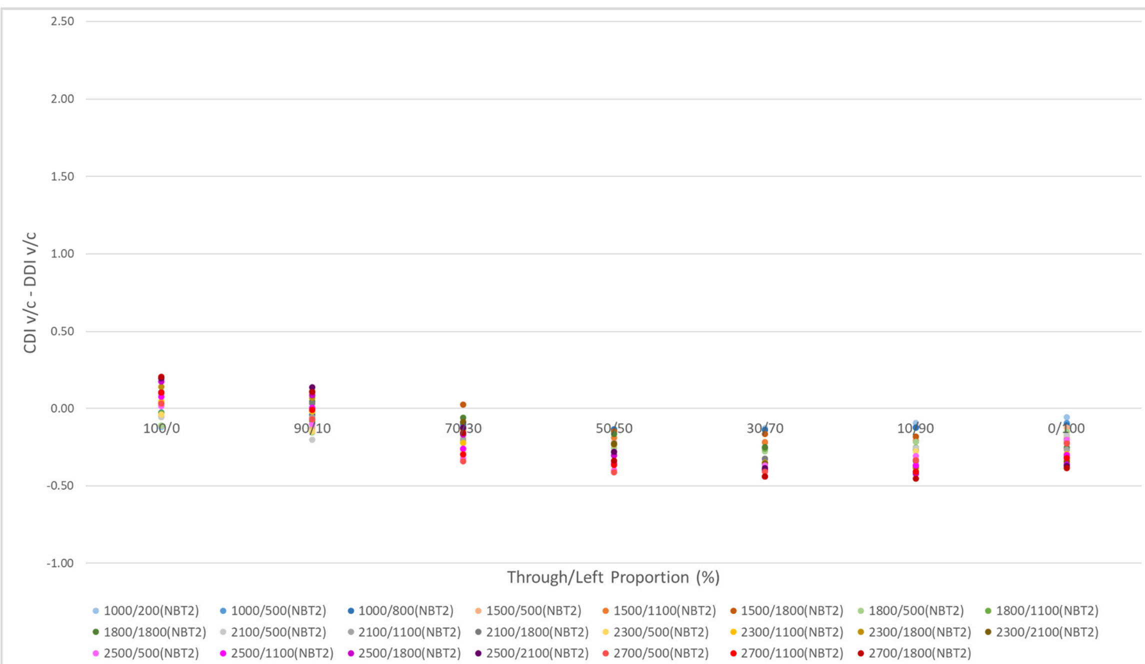

Figure E - 13: Difference in v/c ratios between CDI and DDI on NBT2 at different traffic demands and through/left proportions for LC2

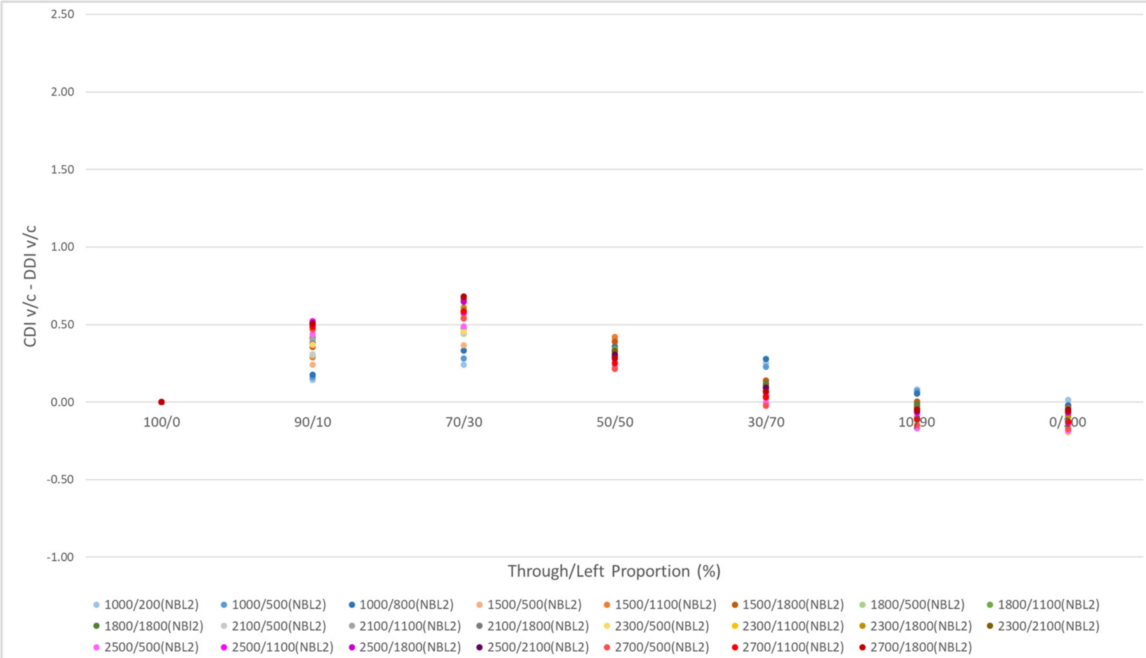

Figure E - 14: Difference in v/c ratios between CDI and DDI on NBL2 at different traffic demands and through/left proportions for LC2

Figure E - 15: Difference in v/c ratios between CDI and DDI on SBT2 at different traffic demands and through/left proportions for LC2

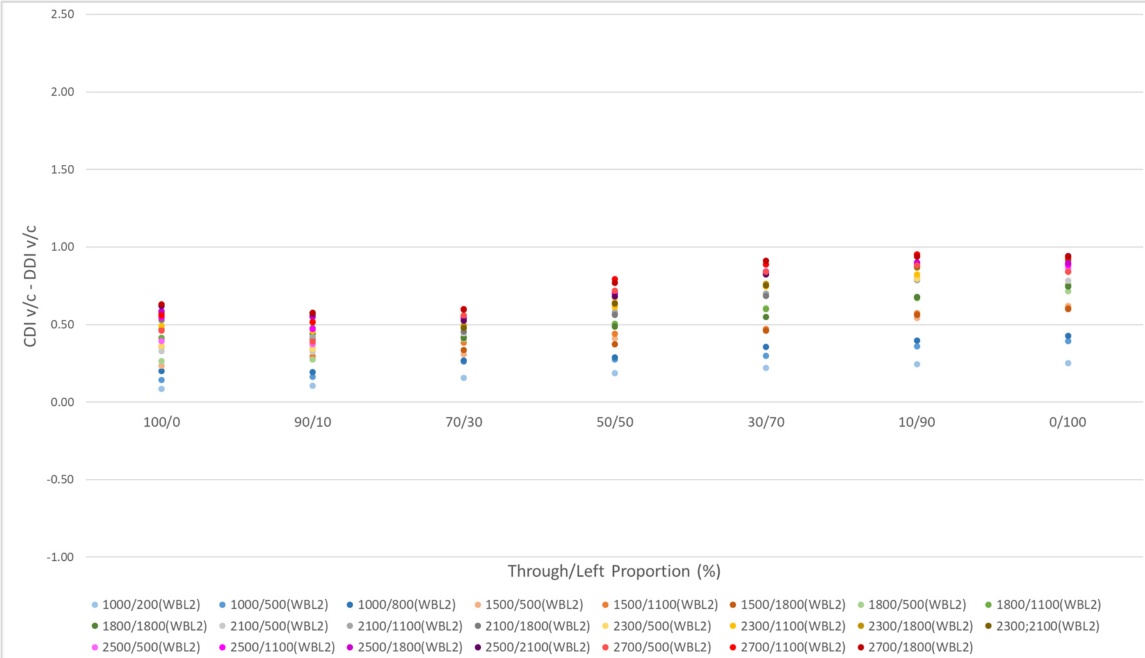

Figure E - 16: Difference in v/c ratios between CDI and DDI on WBL2 at different traffic demands and through/left proportions for LC2

E.3 Lane Configuration 3

The following tables and plots present the difference in the CDI and DDI v/c ratios on different turning movements, traffic demands, and through/left proportions for LC3.

E.3.1 Color-Coded Tables of v/c Ratios of CDIs and DDIs

Table E - 11: Color-coded tables of the CDI and DDI turning movement and interchange v/c ratios at (a) cross-street demand of 1000 vph, and (b) cross-street demand of 1500 vph with different off-ramp demands and through/left proportions for LC3

(a)

JC Volume 1000 vph							
Proportion	Approach	CDI	DDI	CDI	DDI	CDI	DDI
		200 vph		500 vph		800 vph	
100:0	NBT1	0.28	0.60	0.33	0.67	0.35	0.68
90:10		0.39	0.51	0.47	0.57	0.48	0.57
70:30		0.39	0.39	0.44	0.41	0.48	0.44
50:50		0.31	0.25	0.34	0.28	0.36	0.28
30:70		0.50	0.32	0.50	0.35	0.54	0.37
10:90		0.64	0.36	0.72	0.39	0.72	0.41
0:100		0.75	0.35	0.80	0.43	0.80	0.45
100:0	SBT1	0.32	0.44	0.44	0.48	0.52	0.54
90:10		0.29	0.41	0.40	0.45	0.49	0.53
70:30		0.24	0.36	0.33	0.42	0.42	0.48
50:50		0.18	0.30	0.25	0.35	0.33	0.43
30:70		0.12	0.22	0.19	0.29	0.26	0.36
10:90		0.06	0.14	0.12	0.23	0.18	0.32
0:100		0.03	0.09	0.09	0.17	0.15	0.26
100:0	SBL1	0.00	0.00	0.00	0.00	0.00	0.00
90:10		0.11	0.02	0.14	0.02	0.17	0.02
70:30		0.25	0.06	0.27	0.06	0.30	0.06
50:50		0.33	0.10	0.38	0.10	0.42	0.10
30:70		0.41	0.14	0.47	0.14	0.50	0.14
10:90		0.45	0.18	0.49	0.18	0.54	0.18
0:100		0.48	0.20	0.52	0.20	0.57	0.20
100:0	EBL1	0.13	0.05	0.26	0.11	0.38	0.18
90:10		0.13	0.05	0.26	0.12	0.38	0.19
70:30		0.16	0.05	0.28	0.13	0.38	0.20
50:50		0.18	0.06	0.31	0.14	0.42	0.22
30:70		0.18	0.07	0.35	0.15	0.45	0.23
10:90		0.21	0.08	0.34	0.17	0.46	0.26
0:100		0.21	0.09	0.38	0.17	0.50	0.26
100:0	NBT2	0.32	0.42	0.44	0.46	0.52	0.51
90:10		0.29	0.40	0.40	0.44	0.48	0.49
70:30		0.24	0.34	0.33	0.41	0.42	0.46
50:50		0.18	0.28	0.25	0.34	0.33	0.40
30:70		0.12	0.22	0.19	0.28	0.26	0.33
10:90		0.06	0.13	0.12	0.21	0.18	0.27
0:100		0.03	0.08	0.09	0.16	0.15	0.23
100:0	NBL2	0.00	0.00	0.00	0.00	0.00	0.00
90:10		0.10	0.02	0.13	0.02	0.16	0.02
70:30		0.23	0.06	0.25	0.06	0.27	0.06
50:50		0.33	0.10	0.36	0.10	0.38	0.10
30:70		0.41	0.14	0.44	0.14	0.47	0.14
10:90		0.45	0.18	0.49	0.18	0.51	0.18
0:100		0.46	0.20	0.52	0.20	0.55	0.20
100:0	SBT2	0.28	0.63	0.33	0.71	0.35	0.75
90:10		0.40	0.54	0.50	0.60	0.49	0.64
70:30		0.41	0.41	0.47	0.44	0.50	0.47
50:50		0.31	0.26	0.36	0.29	0.38	0.31
30:70		0.49	0.32	0.54	0.37	0.58	0.41
10:90		0.64	0.38	0.68	0.43	0.77	0.47
0:100		0.80	0.38	0.80	0.48	0.86	0.53
100:0	WBL2	0.13	0.05	0.26	0.11	0.38	0.17
90:10		0.13	0.05	0.26	0.11	0.38	0.18
70:30		0.16	0.05	0.28	0.13	0.38	0.19
50:50		0.18	0.06	0.31	0.13	0.42	0.20
30:70		0.19	0.07	0.35	0.14	0.45	0.21
10:90		0.21	0.07	0.38	0.16	0.46	0.23
0:100		0.21	0.08	0.38	0.16	0.50	0.23
100:0	Int v/c	0.28	0.49	0.39	0.53	0.48	0.58
90:10		0.26	0.44	0.36	0.49	0.45	0.53
70:30		0.30	0.36	0.32	0.41	0.40	0.45
50:50		0.30	0.27	0.35	0.31	0.36	0.36
30:70		0.40	0.27	0.45	0.31	0.50	0.36
10:90		0.48	0.27	0.53	0.31	0.58	0.36
0:100		0.53	0.26	0.58	0.31	0.63	0.36

(b)

JC Volume 1500 vph							
Proportion	Approach	CDI	DDI	CDI	DDI	CDI	DDI
		500 vph		1100 vph		1800 vph	
100:0	NBT1	0.44	0.95	0.47	1.06	0.48	1.14
90:10		0.65	0.86	0.64	0.92	0.60	1.01
70:30		0.58	0.60	0.71	0.67	0.63	0.72
50:50		0.45	0.41	0.53	0.43	0.55	0.47
30:70		0.71	0.50	0.77	0.55	0.86	0.60
10:90		0.95	0.56	1.08	0.64	1.16	0.68
0:100		1.17	0.60	1.20	0.68	1.35	0.75
100:0	SBT1	0.53	0.62	0.69	0.62	0.83	0.73
90:10		0.52	0.60	0.67	0.69	0.81	0.70
70:30		0.41	0.55	0.61	0.65	0.76	0.68
50:50		0.30	0.47	0.47	0.58	0.67	0.70
30:70		0.21	0.38	0.35	0.52	0.53	0.63
10:90		0.12	0.27	0.24	0.42	0.41	0.57
0:100		0.08	0.20	0.20	0.36	0.36	0.50
100:0	SBL1	0.00	0.00	0.00	0.00	0.00	0.00
90:10		0.21	0.03	0.24	0.03	0.27	0.03
70:30		0.41	0.09	0.45	0.09	0.50	0.09
50:50		0.50	0.15	0.56	0.15	0.63	0.15
30:70		0.59	0.21	0.64	0.21	0.70	0.21
10:90		0.65	0.27	0.61	0.27	0.64	0.27
0:100		0.58	0.30	0.56	0.30	0.58	0.30
100:0	EBL1	0.33	0.11	0.59	0.22	0.78	0.36
90:10		0.31	0.11	0.54	0.23	0.77	0.34
70:30		0.35	0.13	0.52	0.26	0.72	0.35
50:50		0.38	0.14	0.55	0.28	0.67	0.42
30:70		0.42	0.16	0.60	0.31	0.70	0.45
10:90		0.49	0.18	0.65	0.34	0.78	0.50
0:100		0.49	0.20	0.69	0.36	0.81	0.50
100:0	NBT2	0.53	0.63	0.69	0.63	0.83	0.73
90:10		0.52	0.60	0.66	0.67	0.81	0.71
70:30		0.41	0.53	0.60	0.64	0.76	0.67
50:50		0.30	0.47	0.45	0.56	0.67	0.66
30:70		0.21	0.36	0.35	0.49	0.53	0.59
10:90		0.12	0.26	0.24	0.38	0.41	0.49
0:100		0.08	0.18	0.20	0.31	0.36	0.44
100:0	NBL2	0.00	0.00	0.00	0.00	0.00	0.00
90:10		0.19	0.03	0.22	0.03	0.26	0.03
70:30		0.38	0.09	0.44	0.09	0.48	0.09
50:50		0.47	0.15	0.56	0.15	0.60	0.15
30:70		0.57	0.21	0.64	0.21	0.69	0.21
10:90		0.63	0.27	0.61	0.27	0.64	0.27
0:100		0.55	0.30	0.58	0.30	0.58	0.30
100:0	SBT2	0.44	1.00	0.47	1.10	0.48	1.24
90:10		0.67	0.86	0.66	0.96	0.61	1.08
70:30		0.62	0.63	0.72	0.69	0.64	0.76
50:50		0.47	0.41	0.50	0.45	0.57	0.53
30:70		0.73	0.53	0.77	0.58	0.85	0.66
10:90		0.99	0.59	1.08	0.71	1.17	0.81
0:100		1.12	0.63	1.26	0.79	1.35	0.90
100:0	WBL2	0.34	0.11	0.59	0.21	0.78	0.35
90:10		0.31	0.11	0.54	0.23	0.78	0.33
70:30		0.35	0.12	0.52	0.25	0.72	0.34
50:50		0.38	0.14	0.59	0.27	0.67	0.40
30:70		0.43	0.15	0.60	0.30	0.72	0.42
10:90		0.49	0.17	0.65	0.31	0.78	0.44
0:100		0.53	0.18	0.69	0.31	0.81	0.44
100:0	Int v/c	0.49	0.75	0.66	0.76	0.82	0.86
90:10		0.47	0.68	0.63	0.75	0.80	0.80
70:30		0.48	0.56	0.58	0.64	0.75	0.69
50:50		0.45	0.43	0.55	0.50	0.67	0.61
30:70		0.60	0.43	0.67	0.52	0.74	0.61
10:90		0.73	0.43	0.76	0.52	0.83	0.61
0:100		0.75	0.43	0.79	0.52	0.85	0.61

Table E - 12: Color-coded tables of the CDI and DDI turning movement and interchange v/c ratios at (a) cross-street demand of 1800 vph, and (b) cross-street demand of 2100 vph with different off-ramp demands and through/left proportions for LC3

(a)

JC Volume 1800 vph							
Proportion	Approach	CDI	DDI	CDI	DDI	CDI	DDI
		500 vph		1100 vph		1800 vph	
100:0		0.51	1.15	0.52	1.25	0.54	1.35
90:10		0.75	1.01	0.69	1.10	0.64	1.19
70:30		0.70	0.71	0.77	0.77	0.72	0.86
50:50	NBT1	0.54	0.45	0.57	0.50	0.62	0.56
30:70		0.80	0.58	0.88	0.66	0.99	0.71
10:90		1.08	0.65	1.19	0.75	1.28	0.81
0:100		1.28	0.67	1.37	0.82	1.53	0.90
100:0		0.60	0.60	0.72	0.66	0.87	0.70
90:10		0.59	0.65	0.70	0.68	0.85	0.74
70:30		0.46	0.61	0.64	0.72	0.81	0.83
50:50	SBT1	0.34	0.54	0.48	0.62	0.68	0.74
30:70		0.22	0.44	0.36	0.56	0.54	0.65
10:90		0.12	0.31	0.24	0.44	0.39	0.58
0:100		0.08	0.22	0.18	0.36	0.33	0.50
100:0		0.00	0.00	0.00	0.00	0.00	0.00
90:10		0.24	0.04	0.28	0.04	0.34	0.04
70:30		0.45	0.11	0.50	0.11	0.60	0.11
50:50	SBL1	0.57	0.18	0.63	0.18	0.69	0.18
30:70		0.63	0.25	0.71	0.25	0.78	0.25
10:90		0.63	0.32	0.61	0.32	0.61	0.32
0:100		0.56	0.36	0.56	0.36	0.54	0.33
100:0		0.38	0.11	0.65	0.23	0.83	0.34
90:10		0.35	0.11	0.60	0.23	0.80	0.35
70:30		0.39	0.12	0.54	0.25	0.75	0.39
50:50	EBL1	0.42	0.14	0.60	0.27	0.71	0.41
30:70		0.46	0.16	0.66	0.31	0.78	0.44
10:90		0.56	0.20	0.72	0.35	0.84	0.50
0:100		0.59	0.22	0.76	0.36	0.85	0.50
100:0		0.60	0.61	0.72	0.67	0.88	0.71
90:10		0.59	0.65	0.70	0.68	0.85	0.74
70:30		0.46	0.60	0.64	0.70	0.81	0.81
50:50	NBT2	0.34	0.52	0.48	0.60	0.68	0.72
30:70		0.22	0.43	0.35	0.54	0.53	0.63
10:90		0.12	0.29	0.24	0.43	0.39	0.52
0:100		0.08	0.20	0.18	0.34	0.33	0.45
100:0		0.00	0.00	0.00	0.00	0.00	0.00
90:10		0.26	0.04	0.26	0.04	0.32	0.04
70:30		0.45	0.11	0.48	0.11	0.58	0.11
50:50	NBL2	0.55	0.18	0.63	0.18	0.68	0.18
30:70		0.63	0.25	0.70	0.25	0.77	0.25
10:90		0.63	0.32	0.61	0.32	0.61	0.32
0:100		0.56	0.36	0.56	0.36	0.54	0.36
100:0		0.51	1.20	0.52	1.31	0.54	1.44
90:10		0.74	1.00	0.70	1.11	0.65	1.23
70:30		0.70	0.74	0.78	0.80	0.74	0.89
50:50	SBT2	0.55	0.47	0.57	0.53	0.63	0.58
30:70		0.80	0.60	0.90	0.70	0.99	0.74
10:90		1.08	0.68	1.19	0.78	1.32	0.93
0:100		1.27	0.72	1.37	0.87	1.53	1.03
100:0		0.38	0.11	0.65	0.22	0.82	0.33
90:10		0.35	0.11	0.60	0.23	0.80	0.34
70:30		0.39	0.12	0.54	0.25	0.75	0.38
50:50	WBL2	0.43	0.13	0.60	0.26	0.72	0.40
30:70		0.47	0.16	0.66	0.30	0.78	0.43
10:90		0.56	0.18	0.72	0.34	0.84	0.45
0:100		0.59	0.20	0.76	0.34	0.85	0.45
100:0		0.56	0.80	0.71	0.86	0.86	0.90
90:10		0.53	0.77	0.68	0.81	0.83	0.87
70:30		0.56	0.64	0.61	0.72	0.79	0.82
50:50	Int v/c	0.53	0.49	0.60	0.56	0.69	0.66
30:70		0.67	0.50	0.75	0.59	0.84	0.66
10:90		0.77	0.50	0.81	0.59	0.87	0.68
0:100		0.80	0.50	0.84	0.59	0.88	0.68

(b)

JC Volume 2100 vph							
Proportion	Approach	CDI	DDI	CDI	DDI	CDI	DDI
		500 vph		1100 vph		1800 vph	
100:0		0.57	1.33	0.58	1.44	0.60	1.52
90:10		0.72	1.15	0.75	1.22	0.69	1.31
70:30		0.77	0.78	0.82	0.87	0.82	0.93
50:50	NBT1	0.57	0.51	0.63	0.57	0.69	0.63
30:70		0.85	0.65	0.93	0.71	1.03	0.76
10:90		1.23	0.73	1.30	0.82	1.45	0.91
0:100		1.42	0.74	1.53	0.91	1.68	1.01
100:0		0.65	0.60	0.77	0.64	0.92	0.71
90:10		0.60	0.65	0.75	0.69	0.89	0.74
70:30		0.51	0.70	0.67	0.78	0.83	0.84
50:50	SBT1	0.36	0.60	0.51	0.67	0.69	0.79
30:70		0.24	0.47	0.36	0.61	0.52	0.72
10:90		0.13	0.35	0.23	0.50	0.38	0.58
0:100		0.07	0.22	0.18	0.38	0.32	0.52
100:0		0.00	0.00	0.00	0.00	0.00	0.00
90:10		0.29	0.04	0.32	0.04	0.40	0.04
70:30		0.53	0.13	0.55	0.13	0.58	0.13
50:50	SBL1	0.64	0.21	0.69	0.21	0.75	0.21
30:70		0.72	0.29	0.75	0.29	0.76	0.29
10:90		0.60	0.38	0.60	0.38	0.61	0.38
0:100		0.54	0.42	0.53	0.42	0.54	0.37
100:0		0.44	0.11	0.69	0.22	0.88	0.34
90:10		0.40	0.11	0.65	0.23	0.84	0.34
70:30		0.45	0.12	0.57	0.25	0.78	0.37
50:50	EBL1	0.49	0.14	0.65	0.27	0.77	0.41
30:70		0.56	0.16	0.72	0.32	0.84	0.46
10:90		0.63	0.21	0.78	0.38	0.88	0.49
0:100		0.66	0.22	0.81	0.38	0.92	0.52
100:0		0.65	0.60	0.77	0.64	0.92	0.71
90:10		0.60	0.65	0.75	0.70	0.89	0.74
70:30		0.51	0.68	0.66	0.77	0.83	0.82
50:50	NBT2	0.36	0.58	0.50	0.67	0.69	0.77
30:70		0.24	0.46	0.36	0.59	0.52	0.68
10:90		0.13	0.33	0.23	0.47	0.38	0.55
0:100		0.07	0.21	0.18	0.36	0.31	0.49
100:0		0.00	0.00	0.00	0.00	0.00	0.00
90:10		0.28	0.04	0.30	0.04	0.39	0.04
70:30		0.53	0.13	0.55	0.13	0.63	0.13
50:50	NBL2	0.61	0.21	0.67	0.21	0.75	0.21
30:70		0.70	0.29	0.75	0.29	0.76	0.29
10:90		0.60	0.38	0.60	0.38	0.60	0.38
0:100		0.55	0.42	0.54	0.42	0.53	0.40
100:0		0.57	1.35	0.58	1.48	0.60	1.59
90:10		0.73	1.15	0.76	1.26	0.69	1.37
70:30		0.77	0.81	0.79	0.90	0.78	0.98
50:50	SBT2	0.59	0.53	0.64	0.57	0.68	0.65
30:70		0.88	0.67	0.93	0.74	1.03	0.82
10:90		1.22	0.76	1.32	0.86	1.42	0.98
0:100		1.45	0.76	1.56	0.95	1.68	1.08
100:0		0.44	0.10	0.69	0.21	0.88	0.33
90:10		0.40	0.11	0.65	0.22	0.84	0.34
70:30		0.45	0.12	0.60	0.24	0.78	0.36
50:50	WBL2	0.49	0.13	0.66	0.26	0.78	0.40
30:70		0.56	0.15	0.72	0.31	0.84	0.44
10:90		0.64	0.20	0.79	0.36	0.90	0.46
0:100		0.66	0.21	0.81	0.36	0.94	0.49
100:0		0.62	0.85	0.75	0.89	0.91	0.95
90:10		0.57	0.82	0.73	0.87	0.87	0.92
70:30		0.63	0.72	0.64	0.81	0.82	0.87
50:50	Int v/c	0.58	0.54	0.66	0.62	0.72	0.72
30:70		0.75	0.56	0.81	0.64	0.87	0.73
10:90		0.82	0.57	0.86	0.66	0.92	0.73
0:100		0.85	0.56	0.89	0.66	0.95	0.74

Table E - 13: Color-coded tables of the CDI and DDI turning movement and interchange v/c ratios at cross-street demand of 2300 vph with different off-ramp demands and through/left proportions for LC3

JC Volume 2300 vph									
Proportion	Approach	CDI	DDI	CDI	DDI	CDI	DDI	CDI	DDI
		500 vph		1100 vph		1800 vph		2100 vph	
100:0	NBT1	0.59	1.45	0.62	1.56	0.65	1.38	0.67	1.73
90:10		0.73	1.22	0.77	1.32	0.74	1.08	0.75	1.49
70:30		0.82	0.85	0.87	0.92	0.82	1.03	0.80	1.05
50:50		0.61	0.54	0.65	0.59	0.71	0.68	0.74	0.70
30:70		0.91	0.69	1.02	0.77	1.10	0.86	1.12	0.88
10:90		1.32	0.75	1.41	0.90	1.55	0.97	1.62	1.00
0:100		1.53	0.79	1.62	0.95	1.80	1.07	1.84	1.12
100:0	SBT1	0.67	0.60	0.81	0.64	0.96	0.78	1.05	0.74
90:10		0.64	0.66	0.78	0.68	0.92	0.86	1.00	0.77
70:30		0.54	0.74	0.70	0.80	0.86	0.83	0.90	0.84
50:50		0.38	0.63	0.52	0.72	0.71	0.78	0.80	0.85
30:70		0.24	0.52	0.37	0.64	0.53	0.73	0.60	0.75
10:90		0.13	0.36	0.23	0.51	0.38	0.61	0.43	0.65
0:100		0.07	0.26	0.17	0.38	0.31	0.51	0.34	0.55
100:0	SBL1	0.00	0.00	0.00	0.00	0.00	0.00	0.00	0.00
90:10		0.34	0.05	0.35	0.05	0.43	0.05	0.44	0.05
70:30		0.54	0.14	0.60	0.14	0.68	0.14	0.64	0.14
50:50		0.66	0.23	0.74	0.23	0.83	0.23	0.84	0.23
30:70		0.73	0.32	0.75	0.32	0.76	0.32	0.76	0.32
10:90		0.60	0.41	0.59	0.41	0.59	0.38	0.60	0.37
0:100		0.52	0.46	0.53	0.46	0.53	0.38	0.54	0.37
100:0	EBL1	0.47	0.10	0.72	0.21	0.92	0.36	0.98	0.38
90:10		0.42	0.11	0.69	0.22	0.88	0.40	0.95	0.39
70:30		0.42	0.12	0.60	0.24	0.79	0.36	0.88	0.41
50:50		0.50	0.14	0.69	0.27	0.84	0.39	0.85	0.45
30:70		0.60	0.16	0.75	0.32	0.86	0.45	0.91	0.49
10:90		0.67	0.21	0.83	0.38	0.94	0.51	0.98	0.55
0:100		0.71	0.26	0.88	0.38	0.99	0.51	1.05	0.55
100:0	NBT2	0.67	0.60	0.81	0.64	0.96	0.79	1.05	0.74
90:10		0.64	0.66	0.78	0.69	0.92	0.88	0.99	0.77
70:30		0.52	0.72	0.68	0.79	0.86	0.83	0.90	0.84
50:50		0.38	0.62	0.52	0.70	0.71	0.77	0.80	0.84
30:70		0.24	0.50	0.37	0.61	0.53	0.73	0.60	0.74
10:90		0.13	0.34	0.23	0.48	0.38	0.58	0.44	0.62
0:100		0.07	0.22	0.17	0.36	0.31	0.48	0.34	0.53
100:0	NBL2	0.00	0.00	0.00	0.00	0.00	0.00	0.00	0.00
90:10		0.32	0.05	0.33	0.05	0.41	0.05	0.43	0.05
70:30		0.55	0.14	0.60	0.14	0.66	0.14	0.63	0.14
50:50		0.66	0.23	0.71	0.23	0.80	0.23	0.82	0.23
30:70		0.73	0.32	0.75	0.32	0.76	0.32	0.76	0.32
10:90		0.60	0.41	0.59	0.41	0.59	0.41	0.59	0.39
0:100		0.52	0.46	0.54	0.46	0.53	0.41	0.54	0.39
100:0	SBT2	0.59	1.45	0.62	1.56	0.65	1.73	0.67	1.80
90:10		0.74	1.25	0.78	1.35	0.74	1.49	0.75	1.55
70:30		0.77	0.88	0.83	0.94	0.83	1.04	0.80	1.09
50:50		0.61	0.56	0.67	0.61	0.74	0.70	0.77	0.71
30:70		0.90	0.72	1.02	0.81	1.10	0.86	1.14	0.89
10:90		1.31	0.78	1.41	0.94	1.55	1.03	1.59	1.07
0:100		1.55	0.85	1.66	0.99	1.84	1.14	1.88	1.19
100:0	WBL2	0.47	0.10	0.72	0.21	0.92	0.33	0.98	0.38
90:10		0.42	0.11	0.69	0.22	0.88	0.33	0.96	0.38
70:30		0.47	0.12	0.64	0.24	0.80	0.36	0.88	0.40
50:50		0.50	0.13	0.69	0.26	0.84	0.38	0.85	0.45
30:70		0.61	0.16	0.75	0.31	0.86	0.45	0.91	0.49
10:90		0.68	0.20	0.83	0.36	0.94	0.48	1.01	0.53
0:100		0.72	0.22	0.88	0.36	0.99	0.48	1.05	0.53
100:0	Int v/c	0.64	0.88	0.79	0.92	0.95	1.05	1.03	1.02
90:10		0.60	0.87	0.76	0.90	0.91	1.05	0.98	0.98
70:30		0.65	0.78	0.72	0.84	0.84	0.89	0.89	0.92
50:50		0.61	0.58	0.69	0.66	0.79	0.74	0.81	0.79
30:70		0.79	0.60	0.84	0.69	0.89	0.77	0.92	0.79
10:90		0.86	0.60	0.89	0.71	0.96	0.77	0.99	0.80
0:100		0.87	0.62	0.93	0.69	0.99	0.77	1.03	0.80

Table E - 14: Color-coded tables of the CDI and DDI turning movement and interchange v/c ratios at cross-street demand of 2500 vph with different off-ramp demands and through/left proportions for LC3

JC Volume 2500 vph									
Proportion	Approach	CDI	DDI	CDI	DDI	CDI	DDI	CDI	DDI
		500 vph		1100 vph		1800 vph		2100 vph	
100:0	NBT1	0.64	1.55	0.66	1.67	0.70	1.80	0.71	1.84
90:10		0.74	1.33	0.81	1.42	0.79	1.56	0.81	1.59
70:30		0.84	0.92	0.88	1.00	0.85	1.09	0.89	1.13
50:50		0.63	0.58	0.70	0.64	0.76	0.71	0.78	0.73
30:70		0.97	0.72	1.07	0.82	1.14	0.88	1.21	0.90
10:90		1.41	0.86	1.50	0.93	1.62	1.02	1.72	1.04
0:100		1.61	0.86	1.73	1.00	1.91	1.13	2.00	1.14
100:0	SBT1	0.72	0.59	0.84	0.64	1.01	0.72	1.06	0.75
90:10		0.66	0.64	0.81	0.68	0.96	0.75	1.03	0.78
70:30		0.56	0.77	0.71	0.80	0.87	0.84	0.94	0.87
50:50		0.39	0.67	0.54	0.75	0.71	0.84	0.80	0.86
30:70		0.25	0.55	0.37	0.65	0.53	0.75	0.61	0.79
10:90		0.13	0.38	0.23	0.51	0.36	0.64	0.41	0.67
0:100		0.07	0.26	0.17	0.39	0.27	0.53	0.32	0.58
100:0	SBL1	0.00	0.00	0.00	0.00	0.00	0.00	0.00	0.00
90:10		0.38	0.05	0.38	0.05	0.45	0.05	0.45	0.05
70:30		0.60	0.15	0.63	0.15	0.70	0.15	0.65	0.15
50:50		0.70	0.25	0.78	0.25	0.81	0.25	0.85	0.25
30:70		0.77	0.35	0.75	0.35	0.76	0.35	0.75	0.35
10:90		0.59	0.45	0.60	0.45	0.60	0.39	0.59	0.39
0:100		0.53	0.50	0.54	0.46	0.54	0.39	0.53	0.38
100:0	EBL1	0.48	0.10	0.77	0.21	0.94	0.33	1.03	0.39
90:10		0.45	0.11	0.71	0.22	0.91	0.34	0.98	0.39
70:30		0.47	0.12	0.65	0.24	0.82	0.36	0.89	0.41
50:50		0.56	0.13	0.73	0.26	0.81	0.40	0.86	0.44
30:70		0.66	0.16	0.80	0.31	0.91	0.45	0.95	0.50
10:90		0.72	0.21	0.90	0.38	1.01	0.52	1.05	0.56
0:100		0.80	0.26	0.95	0.39	1.07	0.53	1.10	0.58
100:0	NBT2	0.72	0.59	0.84	0.64	1.01	0.72	1.06	0.76
90:10		0.66	0.64	0.81	0.69	0.96	0.75	1.03	0.78
70:30		0.56	0.76	0.71	0.81	0.87	0.84	0.94	0.87
50:50		0.39	0.65	0.54	0.73	0.71	0.83	0.80	0.85
30:70		0.25	0.53	0.37	0.65	0.53	0.73	0.61	0.76
10:90		0.13	0.38	0.23	0.49	0.36	0.60	0.41	0.64
0:100		0.07	0.22	0.17	0.38	0.27	0.49	0.32	0.54
100:0	NBL2	0.00	0.00	0.00	0.00	0.00	0.00	0.00	0.00
90:10		0.36	0.05	0.36	0.05	0.43	0.05	0.44	0.05
70:30		0.60	0.15	0.63	0.15	0.68	0.15	0.64	0.15
50:50		0.68	0.25	0.77	0.25	0.81	0.25	0.85	0.25
30:70		0.77	0.35	0.75	0.35	0.76	0.35	0.75	0.35
10:90		0.59	0.45	0.60	0.45	0.60	0.42	0.59	0.41
0:100		0.54	0.50	0.54	0.48	0.54	0.42	0.53	0.42
100:0	SBT2	0.64	1.55	0.66	1.70	0.70	1.84	0.71	1.91
90:10		0.75	1.36	0.82	1.45	0.79	1.59	0.81	1.65
70:30		0.84	0.93	0.88	1.02	0.86	1.11	0.89	1.15
50:50		0.64	0.59	0.71	0.65	0.76	0.72	0.78	0.74
30:70		0.96	0.74	1.07	0.82	1.17	0.90	1.21	0.95
10:90		1.41	0.86	1.50	0.96	1.65	1.09	1.72	1.09
0:100		1.64	0.93	1.76	1.03	1.91	1.21	2.00	1.25
100:0	WBL2	0.49	0.10	0.77	0.21	0.94	0.33	1.03	0.38
90:10		0.45	0.10	0.72	0.22	0.91	0.34	0.98	0.39
70:30		0.47	0.12	0.65	0.24	0.82	0.36	0.89	0.41
50:50		0.56	0.13	0.73	0.26	0.82	0.39	0.86	0.44
30:70		0.66	0.16	0.80	0.31	0.91	0.44	0.95	0.49
10:90		0.72	0.21	0.90	0.36	1.01	0.49	1.05	0.54
0:100		0.80	0.22	0.95	0.38	1.07	0.49	1.10	0.54
100:0	Int v/c	0.69	0.91	0.83	0.97	0.99	1.03	1.05	1.07
90:10		0.63	0.89	0.79	0.93	0.94	0.99	1.02	1.03
70:30		0.70	0.82	0.75	0.88	0.86	0.92	0.92	0.95
50:50		0.65	0.62	0.74	0.69	0.79	0.78	0.82	0.81
30:70		0.83	0.64	0.87	0.72	0.93	0.80	0.95	0.83
10:90		0.89	0.67	0.94	0.74	1.01	0.82	1.03	0.84
0:100		0.92	0.67	0.98	0.74	1.04	0.82	1.07	0.85

Table E - 15: Color-coded tables of the CDI and DDI turning movement and interchange v/c ratios at cross-street demand of 2700 vph with different off-ramp demands and through/left proportions for LC3

JC Volume 2700 vph							
Proportion	Approach	CDI	DDI	CDI	DDI	CDI	DDI
		500 vph		1100 vph		1800 vph	
100:0	NBT1	0.67	1.65	0.70	1.77	0.74	1.91
90:10		0.77	1.40	0.85	1.51	0.84	1.65
70:30		0.85	0.96	0.90	1.05	0.89	1.15
50:50		0.66	0.61	0.70	0.68	0.78	0.74
30:70		1.02	0.80	1.12	0.85	1.24	0.93
10:90		1.48	0.90	1.59	0.97	1.75	1.06
0:100		1.74	0.93	1.87	1.04	2.03	1.18
100:0	SBT1	0.74	0.59	0.88	0.66	1.05	0.73
90:10		0.69	0.64	0.84	0.70	0.99	0.76
70:30		0.58	0.80	0.73	0.81	0.89	0.85
50:50		0.41	0.71	0.53	0.79	0.72	0.86
30:70		0.26	0.60	0.38	0.70	0.54	0.79
10:90		0.13	0.42	0.24	0.55	0.34	0.67
0:100		0.07	0.26	0.17	0.46	0.25	0.54
100:0	SBL1	0.00	0.00	0.00	0.00	0.00	0.00
90:10		0.40	0.05	0.40	0.05	0.46	0.05
70:30		0.63	0.16	0.65	0.16	0.72	0.16
50:50		0.72	0.27	0.77	0.27	0.86	0.27
30:70		0.75	0.38	0.75	0.38	0.76	0.38
10:90		0.60	0.49	0.59	0.46	0.59	0.42
0:100		0.54	0.54	0.53	0.47	0.54	0.42
100:0	EBL1	0.57	0.10	0.80	0.21	0.99	0.34
90:10		0.49	0.10	0.76	0.22	0.94	0.34
70:30		0.49	0.11	0.65	0.23	0.85	0.36
50:50		0.57	0.13	0.73	0.27	0.87	0.39
30:70		0.69	0.17	0.83	0.32	0.94	0.46
10:90		0.82	0.22	0.95	0.39	1.07	0.54
0:100		0.87	0.26	0.99	0.46	1.13	0.54
100:0	NBT2	0.74	0.60	0.88	0.66	1.05	0.74
90:10		0.69	0.65	0.84	0.70	0.99	0.76
70:30		0.58	0.79	0.73	0.81	0.89	0.85
50:50		0.40	0.69	0.53	0.77	0.72	0.86
30:70		0.26	0.60	0.38	0.68	0.54	0.77
10:90		0.13	0.39	0.24	0.52	0.34	0.65
0:100		0.07	0.24	0.17	0.42	0.25	0.53
100:0	NBL2	0.00	0.00	0.00	0.00	0.00	0.00
90:10		0.39	0.05	0.39	0.05	0.45	0.05
70:30		0.60	0.16	0.65	0.16	0.70	0.16
50:50		0.71	0.27	0.76	0.27	0.86	0.27
30:70		0.75	0.38	0.74	0.38	0.75	0.38
10:90		0.60	0.49	0.59	0.49	0.59	0.43
0:100		0.54	0.54	0.54	0.49	0.54	0.43
100:0	SBT2	0.67	1.68	0.70	1.80	0.74	1.94
90:10		0.78	1.42	0.85	1.53	0.85	1.68
70:30		0.88	0.98	0.90	1.06	0.90	1.17
50:50		0.67	0.63	0.71	0.69	0.78	0.75
30:70		1.04	0.80	1.12	0.88	1.22	0.95
10:90		1.48	0.93	1.62	1.01	1.75	1.10
0:100		1.74	0.96	1.91	1.10	2.03	1.22
100:0	WBL2	0.57	0.10	0.80	0.21	0.99	0.33
90:10		0.49	0.10	0.76	0.22	0.94	0.34
70:30		0.49	0.11	0.65	0.23	0.85	0.36
50:50		0.60	0.13	0.73	0.26	0.87	0.39
30:70		0.70	0.17	0.85	0.31	0.96	0.45
10:90		0.82	0.21	0.95	0.38	1.07	0.53
0:100		0.87	0.24	0.99	0.42	1.13	0.53
100:0	Int v/c	0.72	0.96	0.86	1.01	1.04	1.08
90:10		0.66	0.92	0.82	0.97	0.98	1.04
70:30		0.73	0.86	0.77	0.90	0.88	0.96
50:50		0.68	0.65	0.73	0.73	0.83	0.81
30:70		0.86	0.70	0.90	0.76	0.96	0.84
10:90		0.93	0.72	0.98	0.78	1.04	0.86
0:100		0.96	0.72	1.02	0.81	1.09	0.86

E.3.2 Plots of Difference between CDI and DDI v/c Ratios

Figure E - 17: Difference in v/c ratios between CDI and DDI on NBT1 at different traffic demands and through/left proportions for LC3

Figure E - 18: Difference in v/c ratios between CDI and DDI on SBT1 at different traffic demands and through/left proportions for LC3

Figure E - 19: Difference in v/c ratios between CDI and DDI on SBL1 at different traffic demands and through/left proportions for LC3

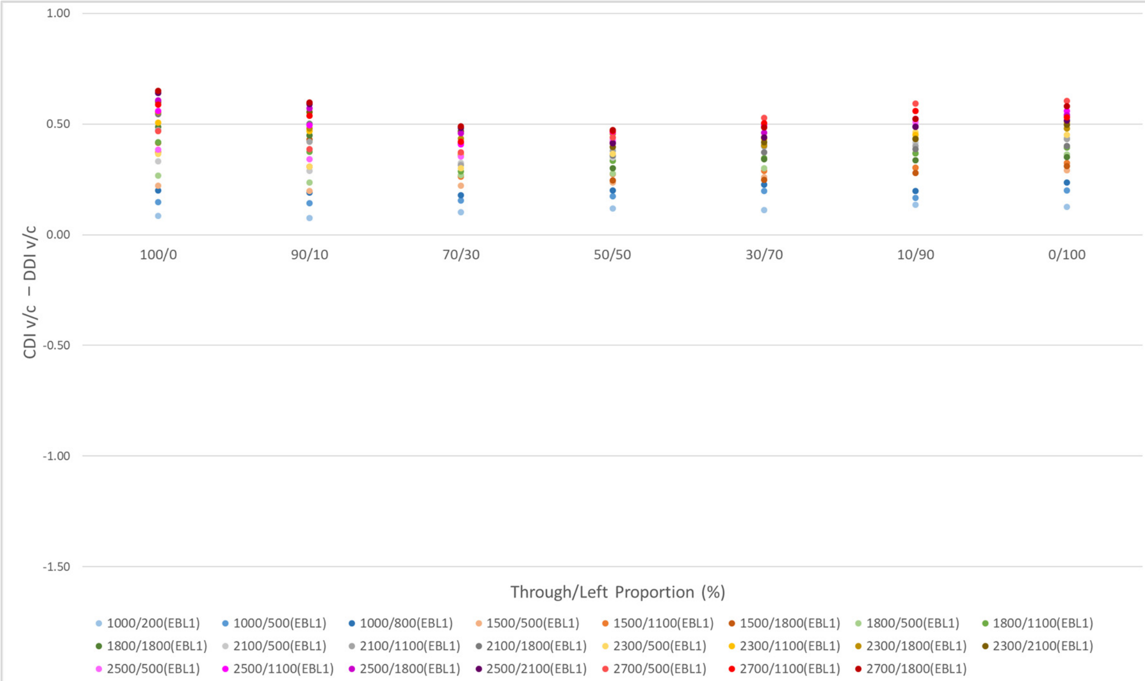

Figure E - 20: Difference in v/c ratios between CDI and DDI on EBL1 at different traffic demands and through/left proportions for LC3

Figure E - 21: Difference in v/c ratios between CDI and DDI on NBT2 at different traffic demands and through/left proportions for LC3

Figure E - 22: Difference in v/c ratios between CDI and DDI on NBL2 at different traffic demands and through/left proportions for LC3

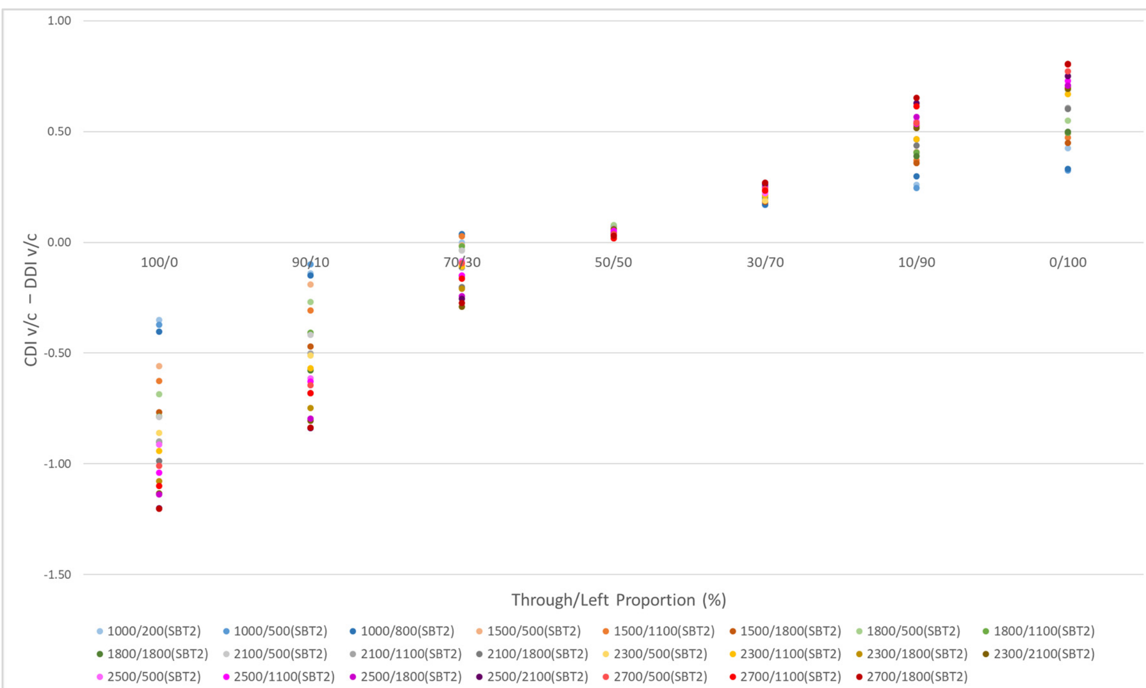

Figure E - 23: Difference in v/c ratios between CDI and DDI on SBT2 at different traffic demands and through/left proportions for LC3

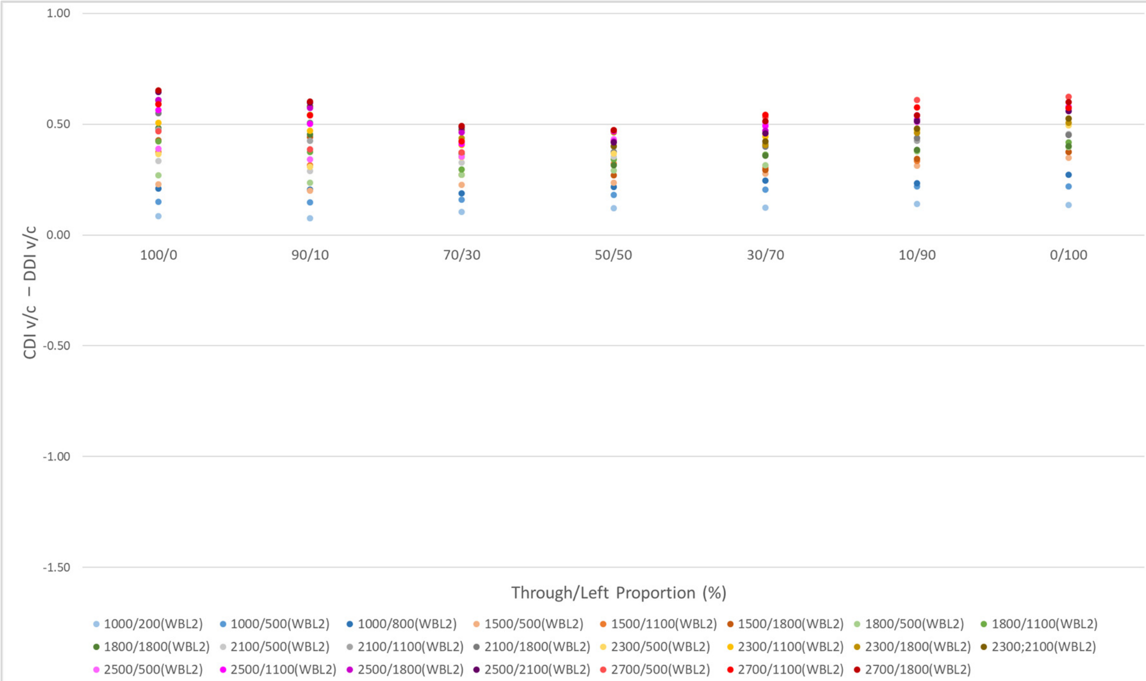

Figure E - 24: Difference in v/c ratios between CDI and DDI on WBL2 at different traffic demands and through/left proportions for LC3

APPENDIX F. MICROSCOPIC SIMULATION STUDY RESULTS

List of Figures

This appendix provides resultant plots of average delay per vehicle and throughput at different through/left proportions from the VISSIM simulation study. Each plot illustrates the performance measures of individual turning movements. Numbers in the legend represent different off-ramp demands tested in the simulation.

F.1 Lane Configuration 1

F.1.1 Cross-Street Demand: 1500 vph

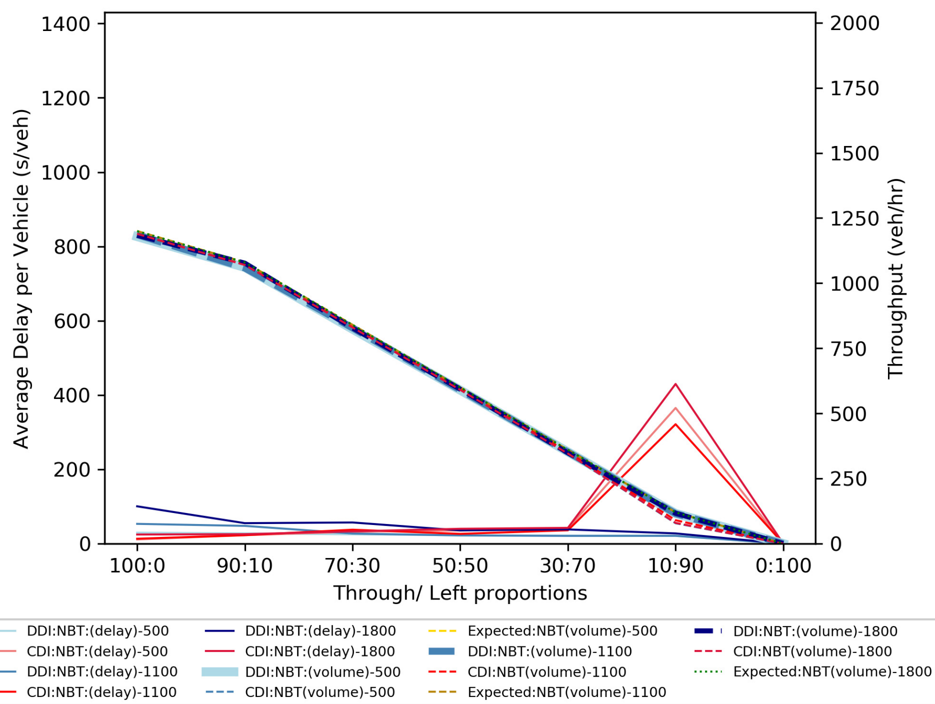

Figure F - 1: DDI and CDI average delay per vehicle and throughput on NBT with cross-street demand of 1500 vph at different off-ramp demands and through/left proportions for LC1

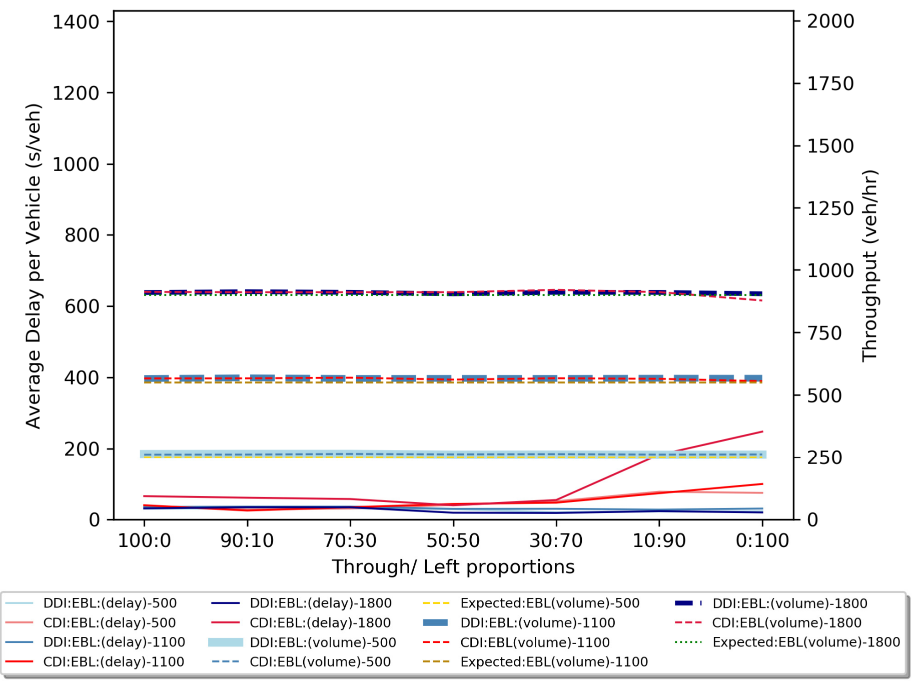

Figure F - 2: DDI and CDI average delay per vehicle and throughput on EBL with cross-street demand of 1500 vph at different off-ramp demands and through/left proportions for LC1

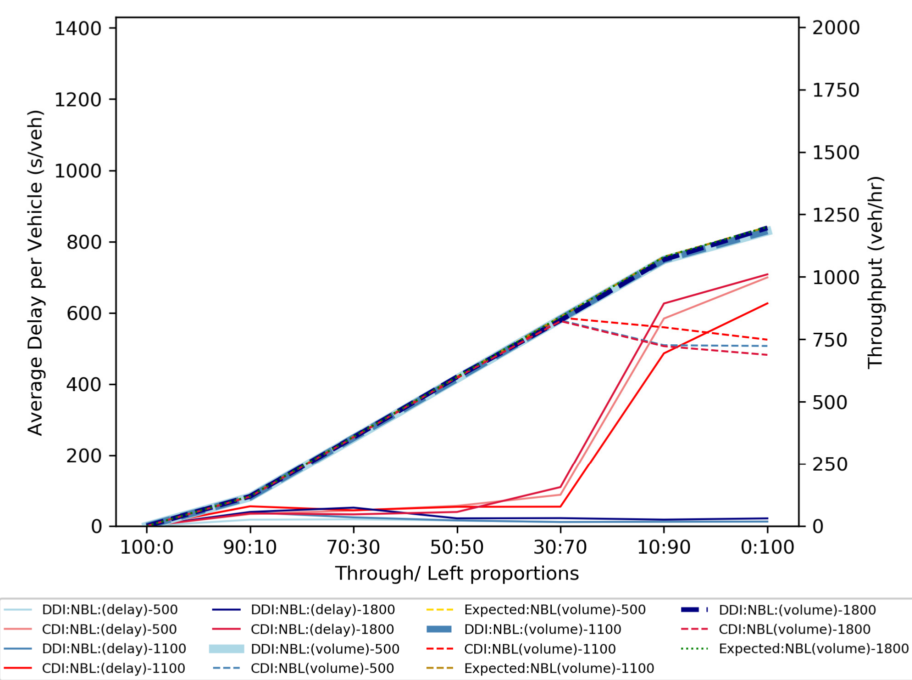

Figure F - 3: DDI and CDI average delay per vehicle and throughput on NBL with cross-street demand of 1500 vph at different off-ramp demands and through/left proportions for LC1

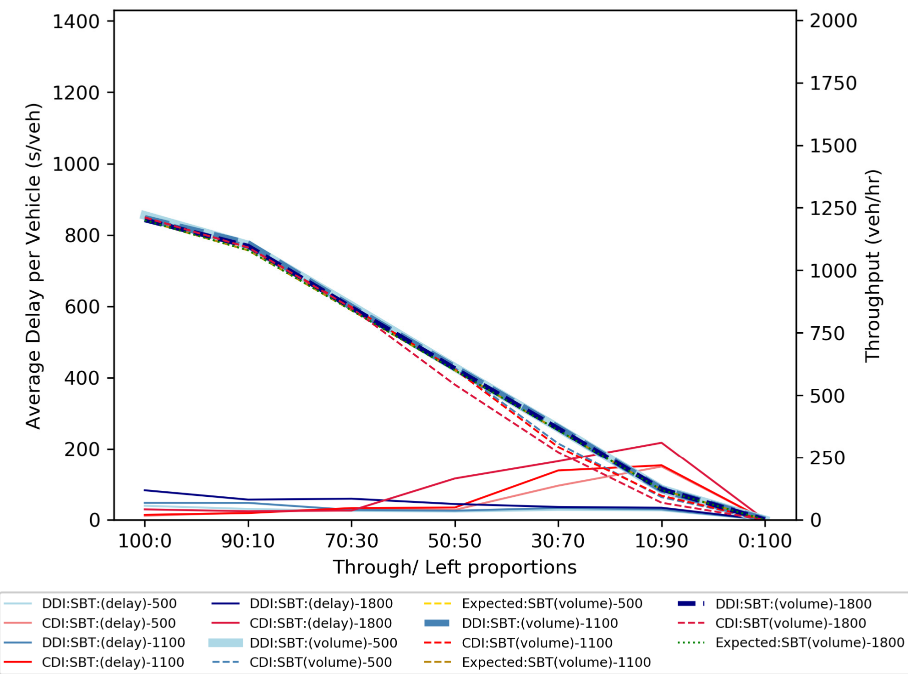

Figure F - 4: DDI and CDI average delay per vehicle and throughput on SBT with cross-street demand of 1500 vph at different off-ramp demands and through/left proportions for LC1

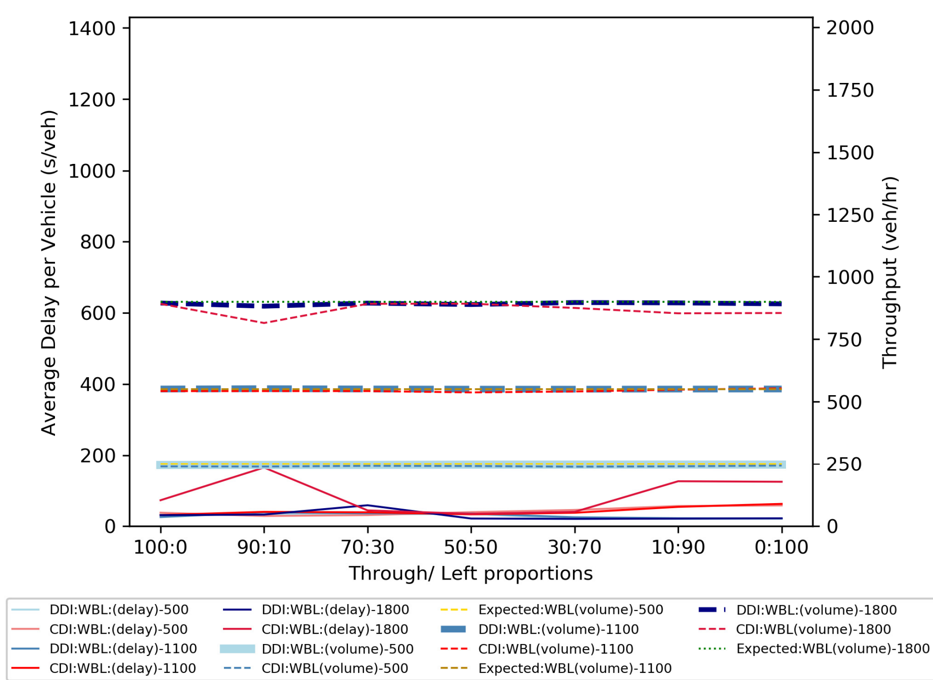

Figure F - 5: DDI and CDI average delay per vehicle and throughput on WBL with cross-street demand of 1500 vph at different off-ramp demands and through/left proportions for LC1

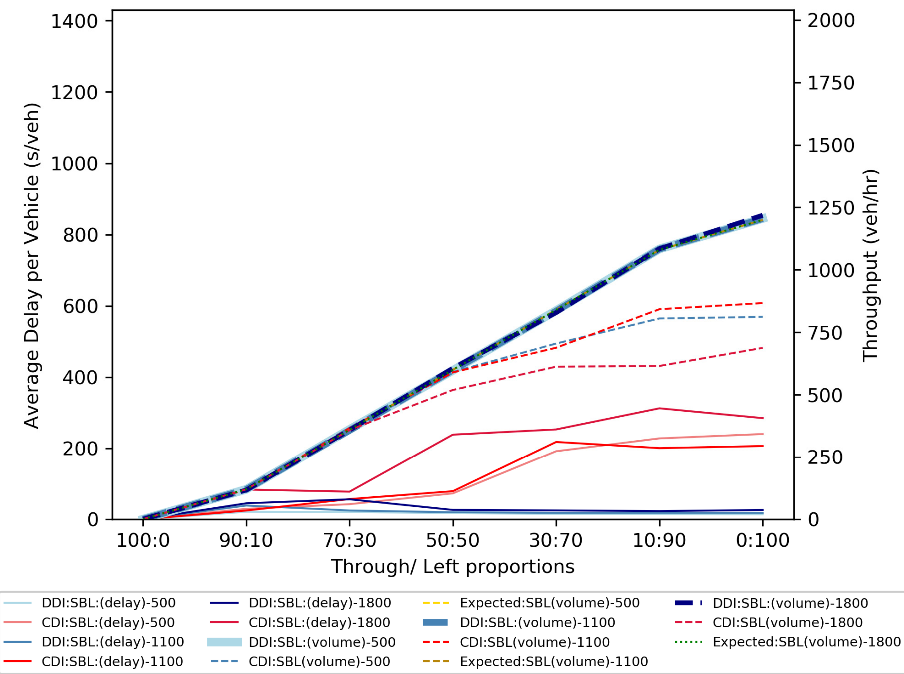

Figure F - 6: DDI and CDI average delay per vehicle and throughput on SBL with cross-street demand of 1500 vph at different off-ramp demands and through/left proportions for LC1

F.1.2 Cross-Street Demand: 2100 vph

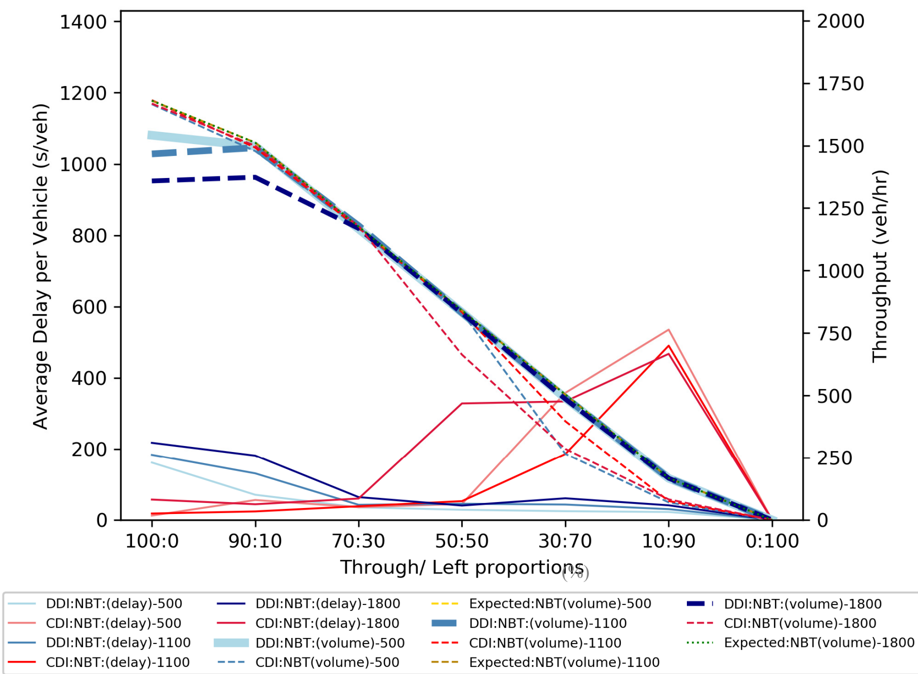

Figure F - 7: DDI and CDI average delay per vehicle and throughput on NBT with cross-street demand of 2100 vph at different off-ramp demands and through/left proportions for LC1

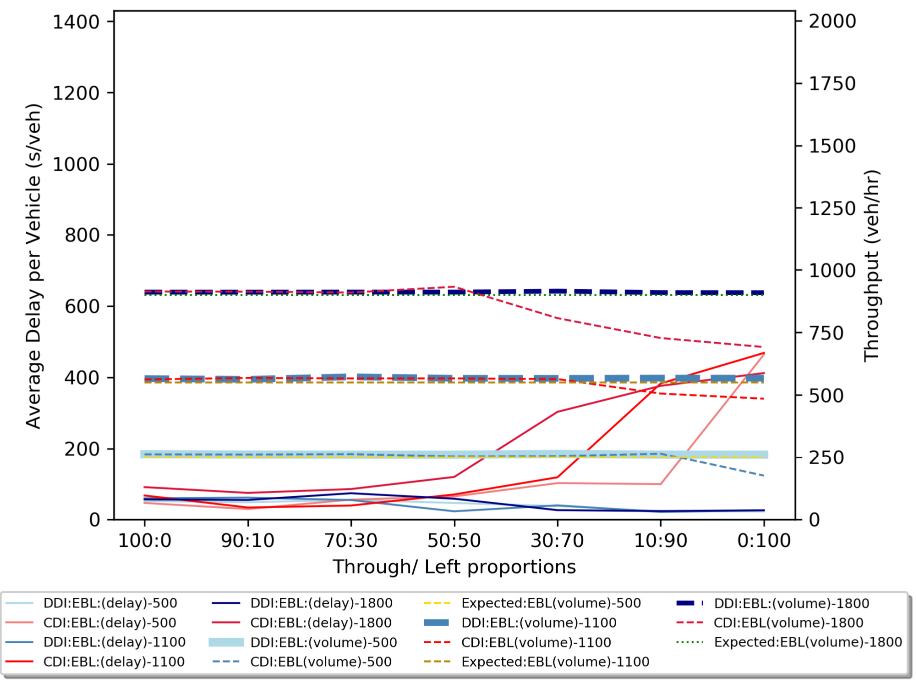

Figure F - 8: DDI and CDI average delay per vehicle and throughput on EBL with cross-street demand of 2100 vph at different off-ramp demands and through/left proportions for LC1

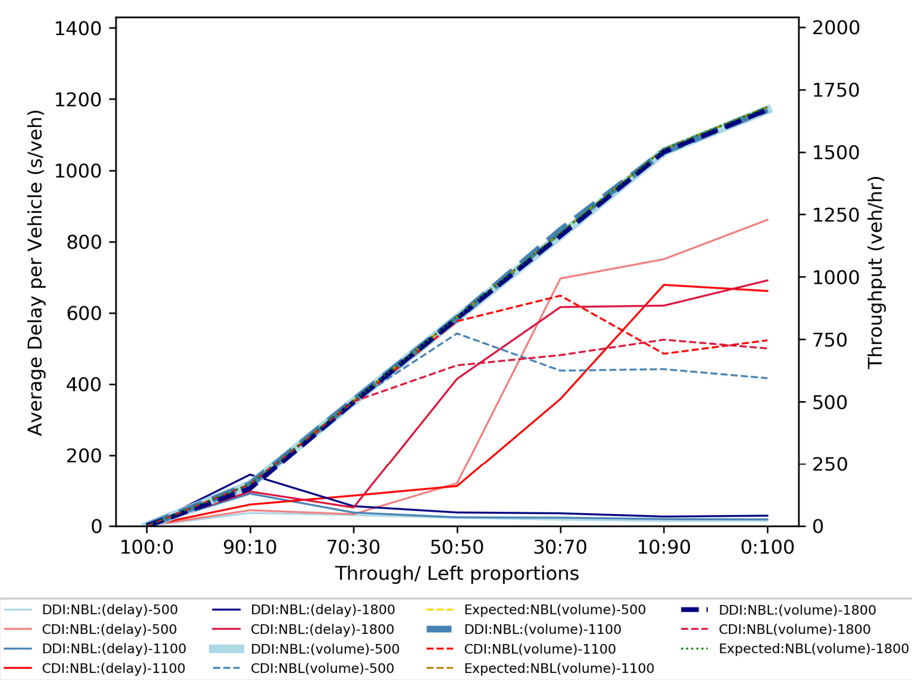

Figure F - 9: DDI and CDI average delay per vehicle and throughput on NBL with cross-street demand of 2100 vph at different off-ramp demands and through/left proportions for LC1

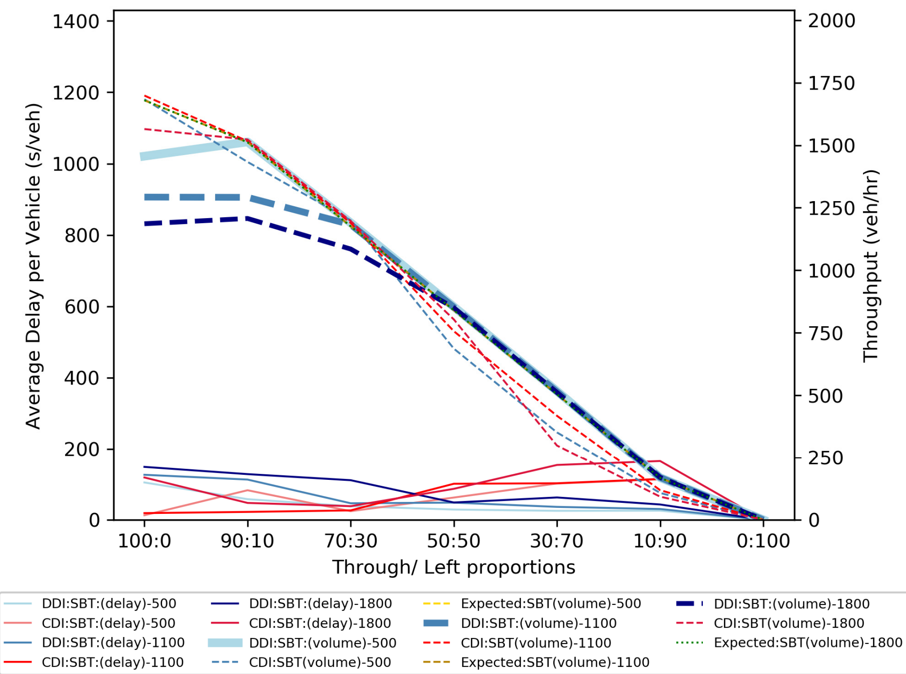

Figure F - 10: DDI and CDI average delay per vehicle and throughput on SBT with cross-street demand of 2100 vph at different off-ramp demands and through/left proportions for LC1

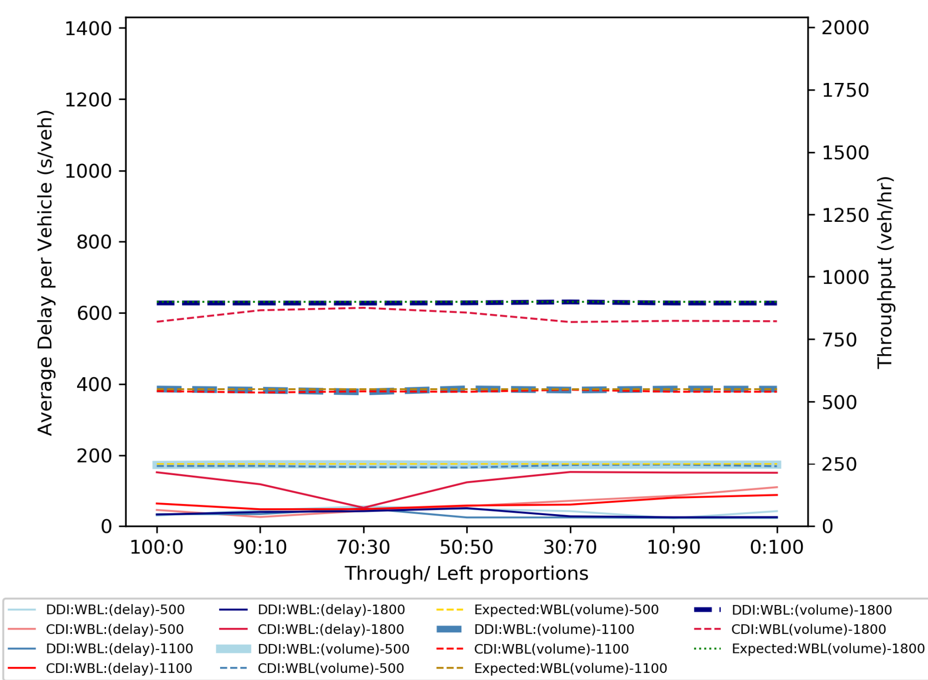

Figure F - 11: DDI and CDI average delay per vehicle and throughput on WBL with cross-street demand of 2100 vph at different off-ramp demands and through/left proportions for LC1

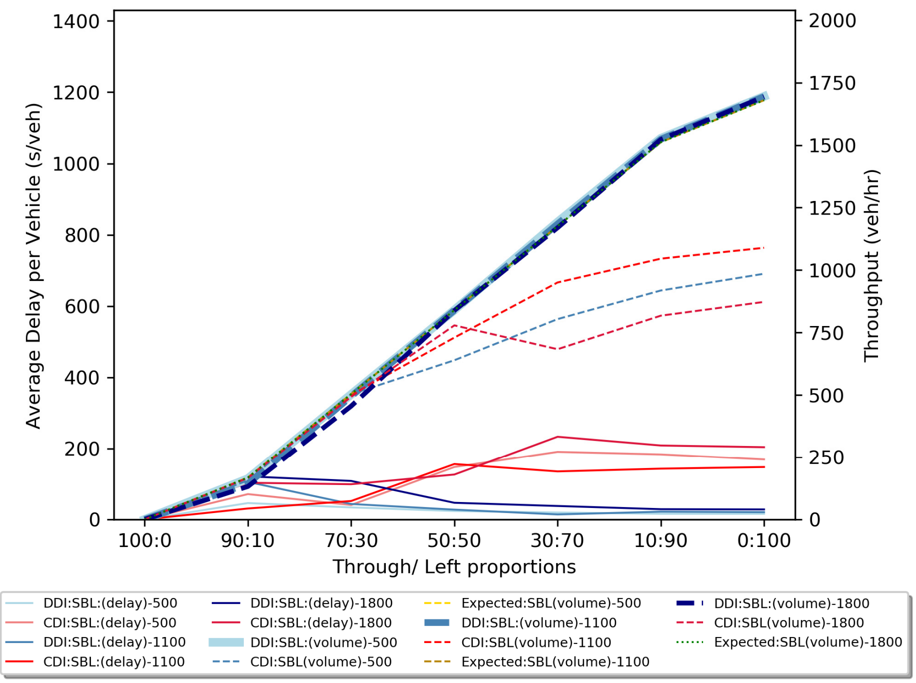

Figure F - 12: DDI and CDI average delay per vehicle and throughput on SBL with cross-street demand of 2100 vph at different off-ramp demands and through/left proportions for LC1

F.1.3 Cross-Street Demand: 2500 vph

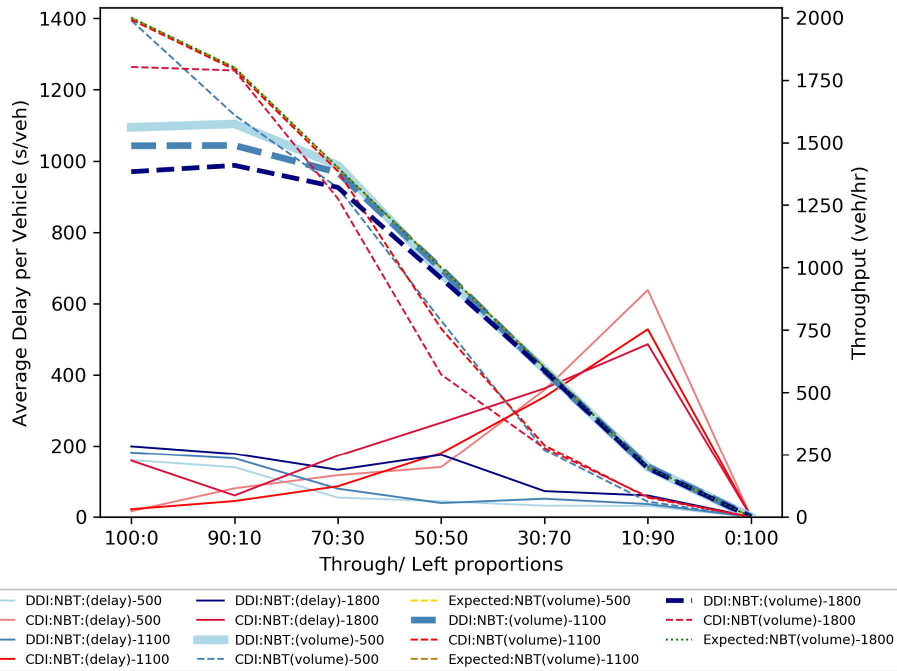

Figure F - 13: DDI and CDI average delay per vehicle and throughput on NBT with cross-street demand of 2500 vph at different off-ramp demands and through/left proportions for LC1

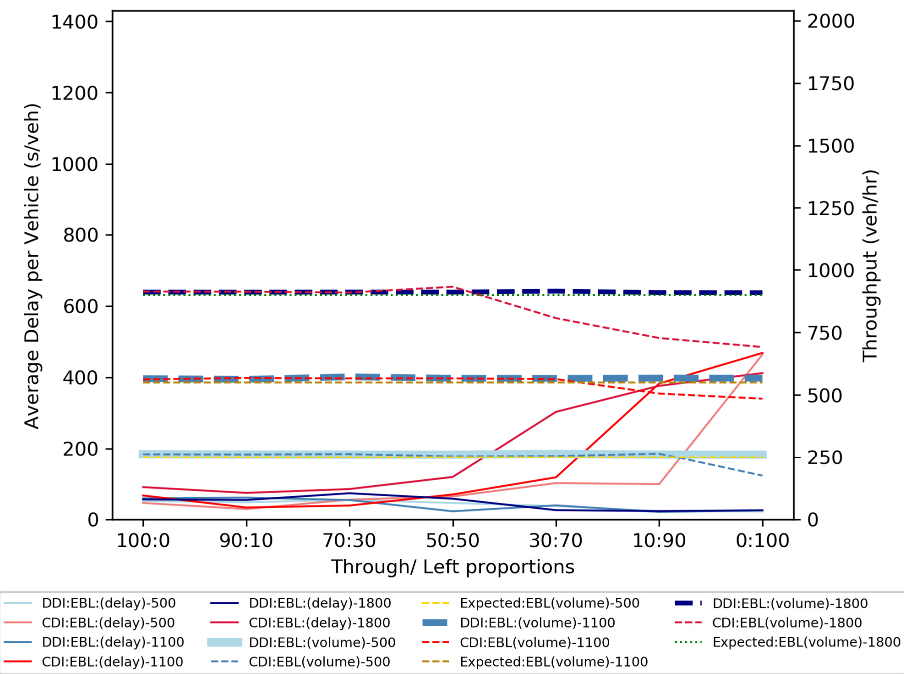

Figure F - 14: DDI and CDI average delay per vehicle and throughput on EBL with cross-street demand of 2500 vph at different off-ramp demands and through/left proportions for LC1

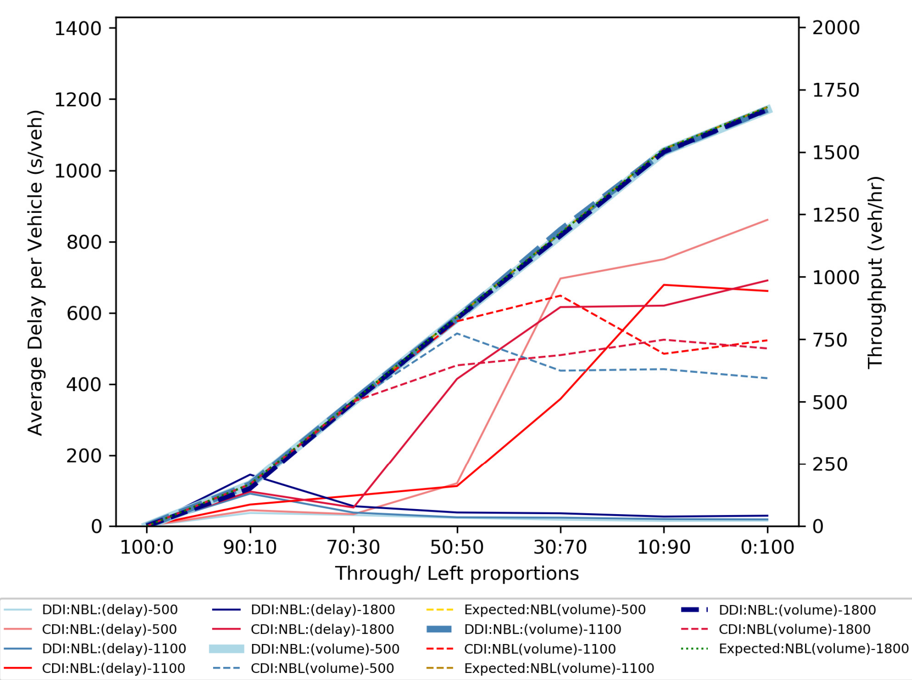

Figure F - 15: DDI and CDI average delay per vehicle and throughput on NBL with cross-street demand of 2500 vph at different off-ramp demands and through/left proportions for LC1

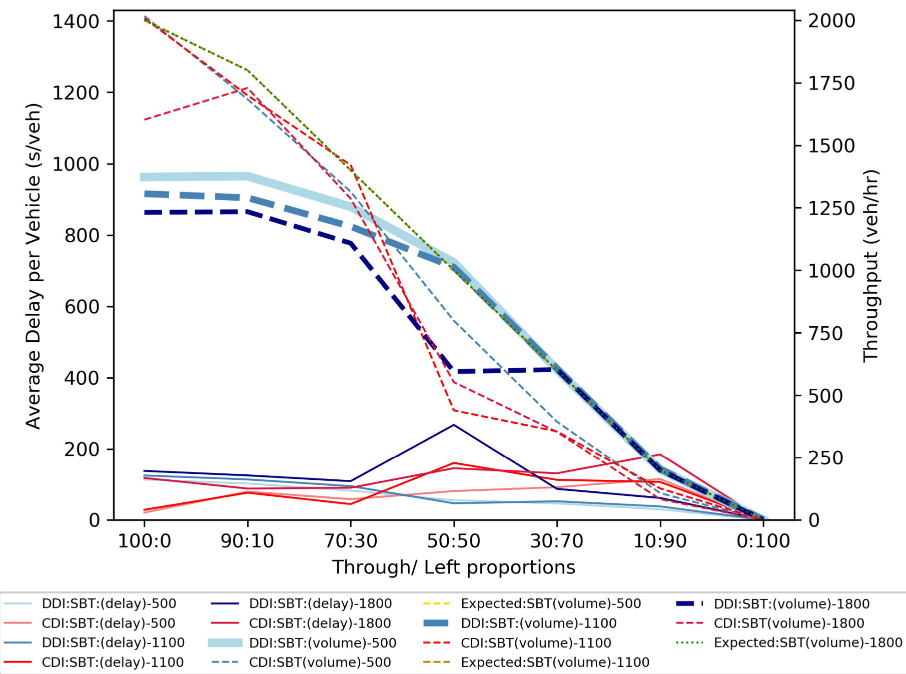

Figure F - 16: DDI and CDI average delay per vehicle and throughput on SBT with cross-street demand of 2500 vph at different off-ramp demands and through/left proportions for LC1

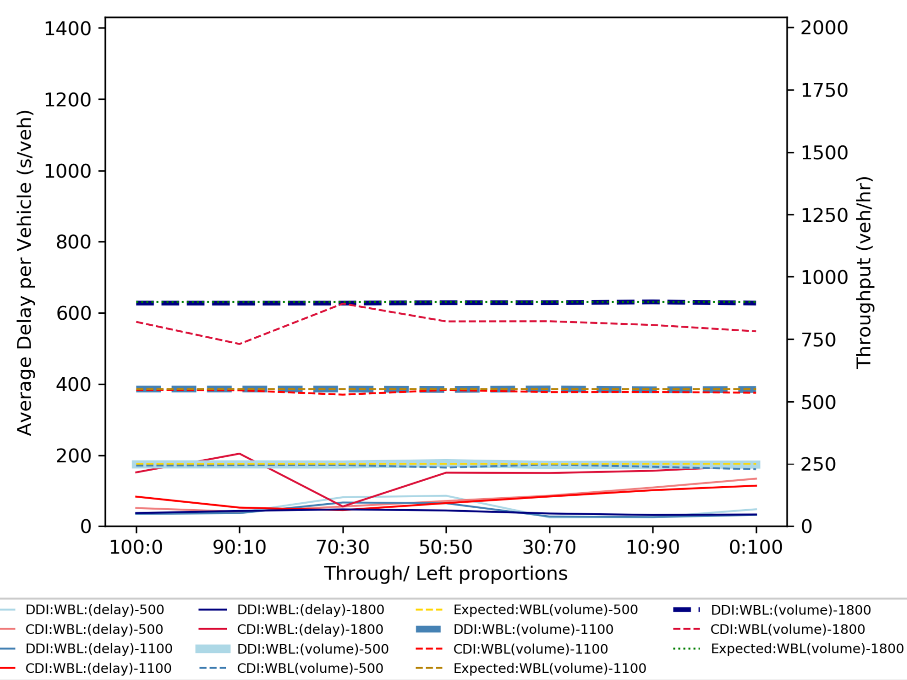

Figure F - 17: DDI and CDI average delay per vehicle and throughput on WBL with cross-street demand of 2500 vph at different off-ramp demands and through/left proportions for LC1

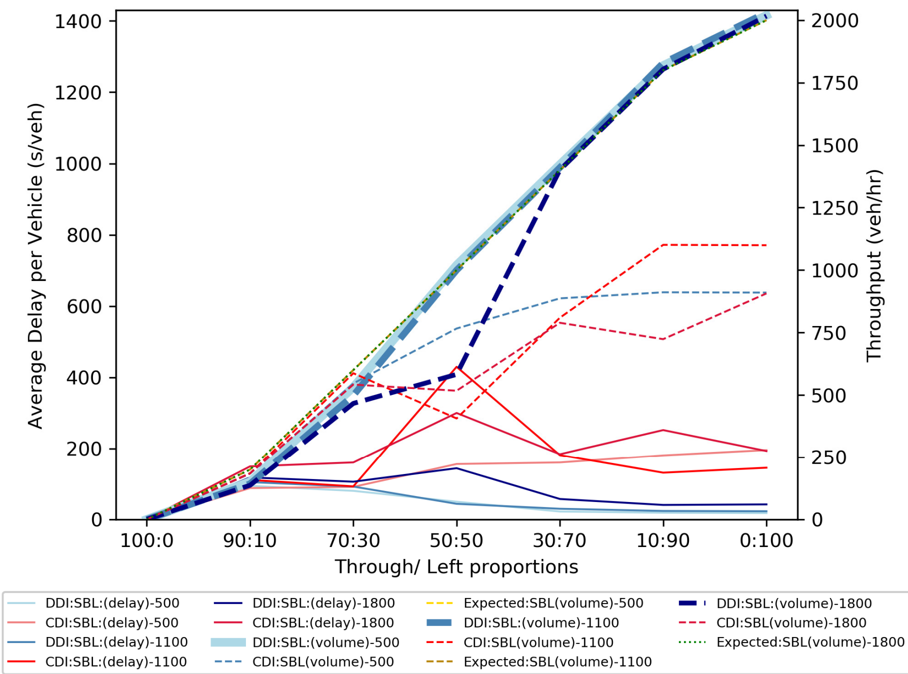

Figure F - 18: DDI and CDI average delay per vehicle and throughput on SBL with cross-street demand of 2500 vph at different off-ramp demands and through/left proportions for LC1

F.2 Lane Configuration 2

F.2.1 Cross-Street Demand: 1500 vph

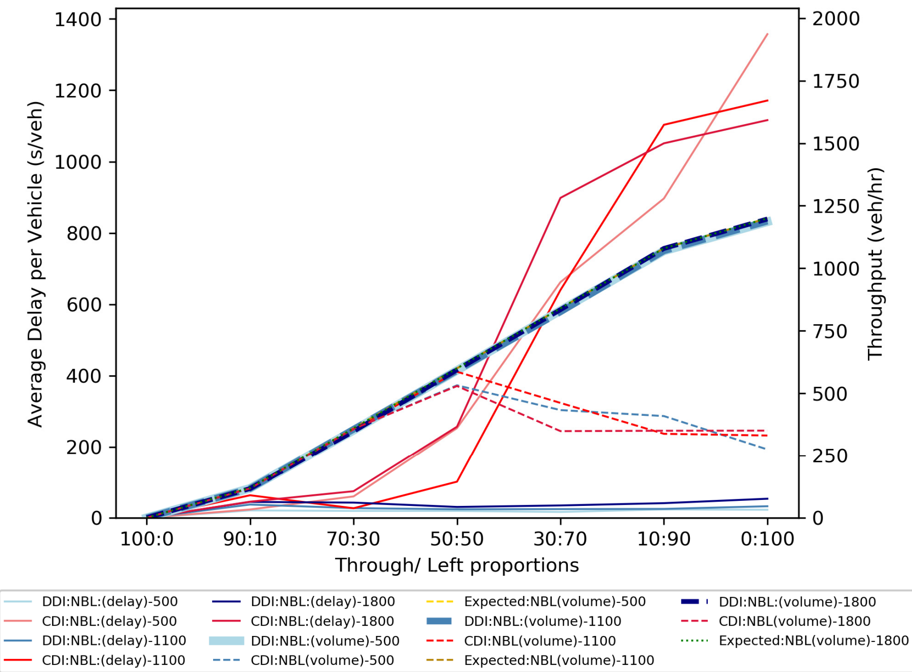

Figure F - 19: DDI and CDI average delay per vehicle and throughput on NBT with cross-street demand of 1500 vph at different off-ramp demands and through/left proportions for LC2

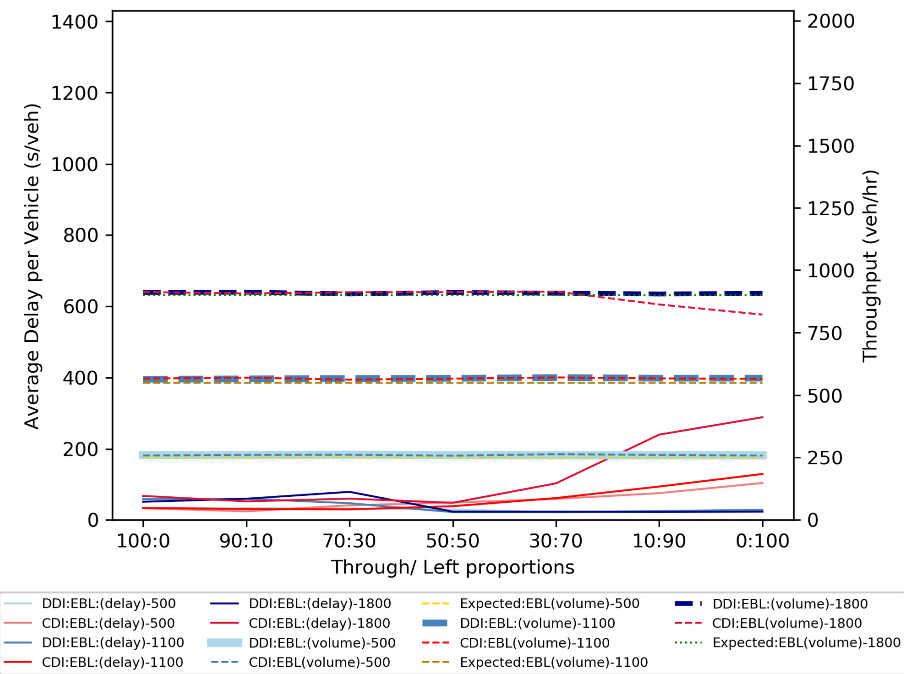

Figure F - 20: DDI and CDI average delay per vehicle and throughput on EBL with cross-street demand of 1500 vph at different off-ramp demands and through/left proportions for LC2

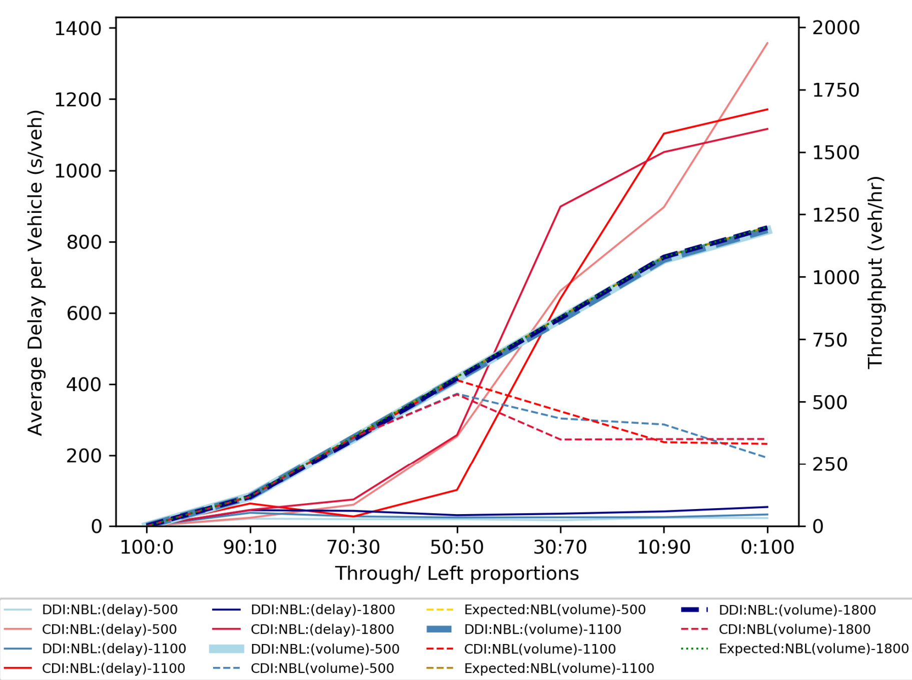

Figure F - 21: DDI and CDI average delay per vehicle and throughput on NBL with cross-street demand of 1500 vph at different off-ramp demands and through/left proportions for LC2

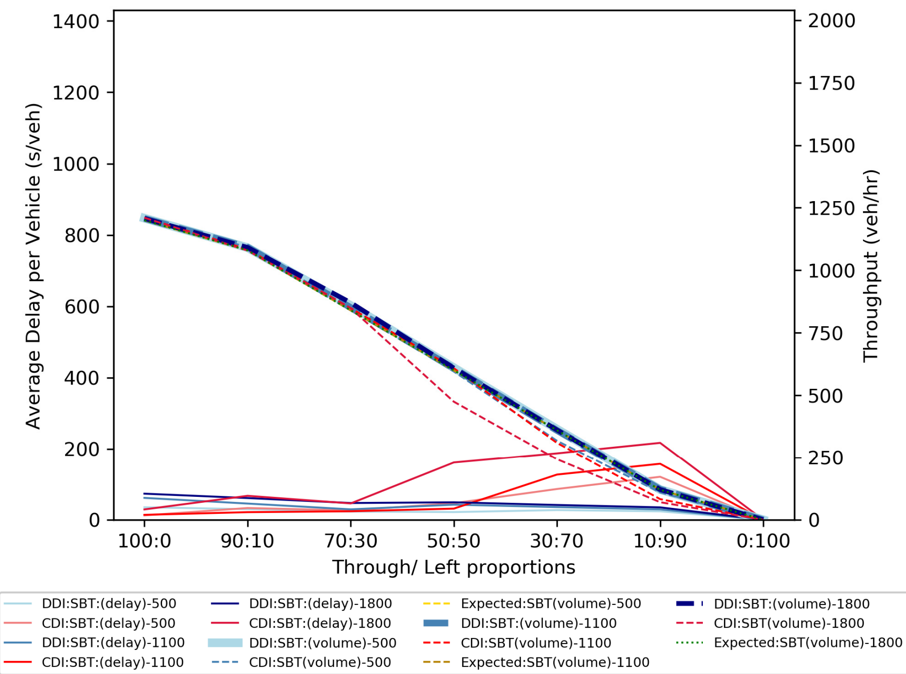

Figure F - 22: DDI and CDI average delay per vehicle and throughput on SBT with cross-street demand of 1500 vph at different off-ramp demands and through/left proportions for LC2

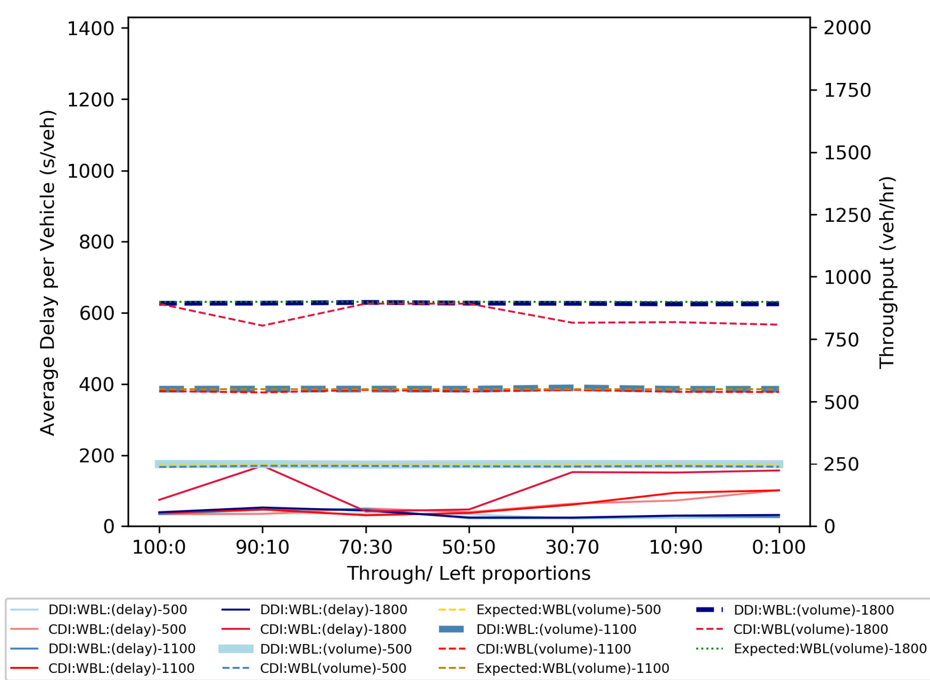

Figure F - 23: DDI and CDI average delay per vehicle and throughput on WBL with cross-street demand of 1500 vph at different off-ramp demands and through/left proportions for LC2

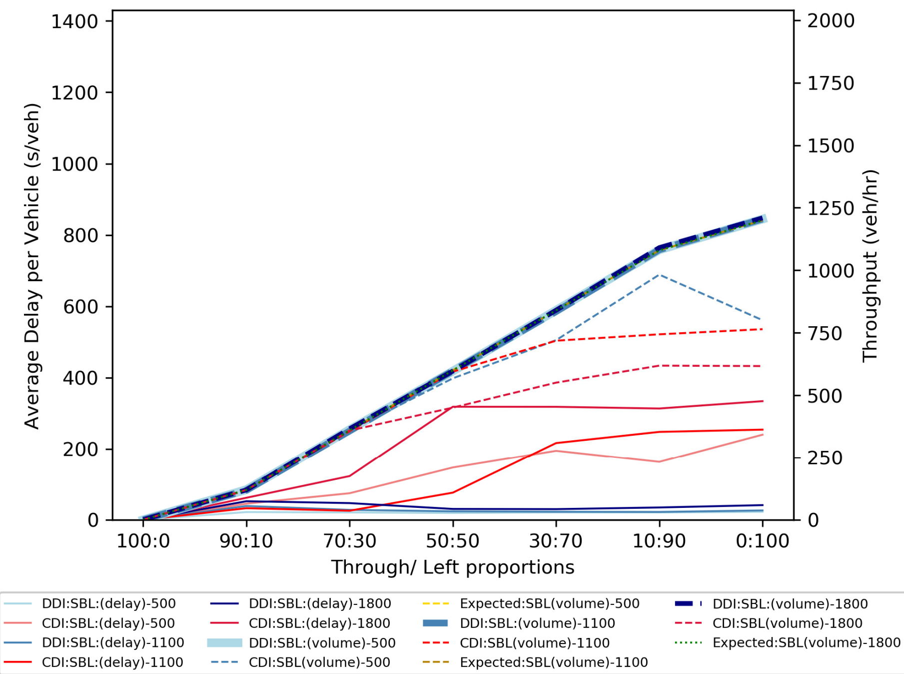

Figure F - 24: DDI and CDI average delay per vehicle and throughput on SBL with cross-street demand of 1500 vph at different off-ramp demands and through/left proportions for LC2

F.2.2 Cross-Street Demand: 2100 vph

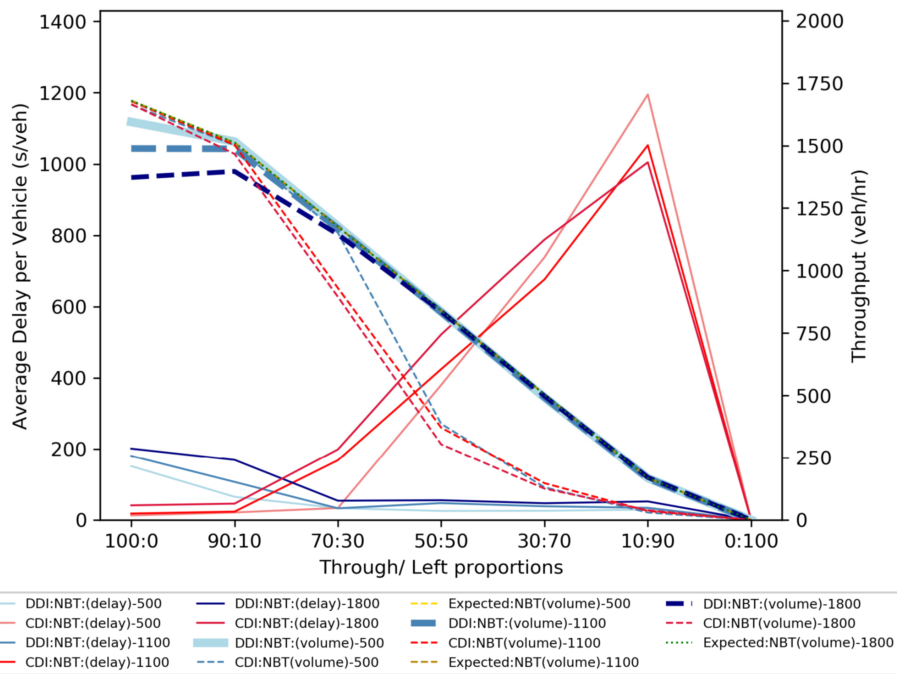

Figure F - 25: DDI and CDI average delay per vehicle and throughput on NBT with cross-street demand of 2100 vph at different off-ramp demands and through/left proportions for LC2

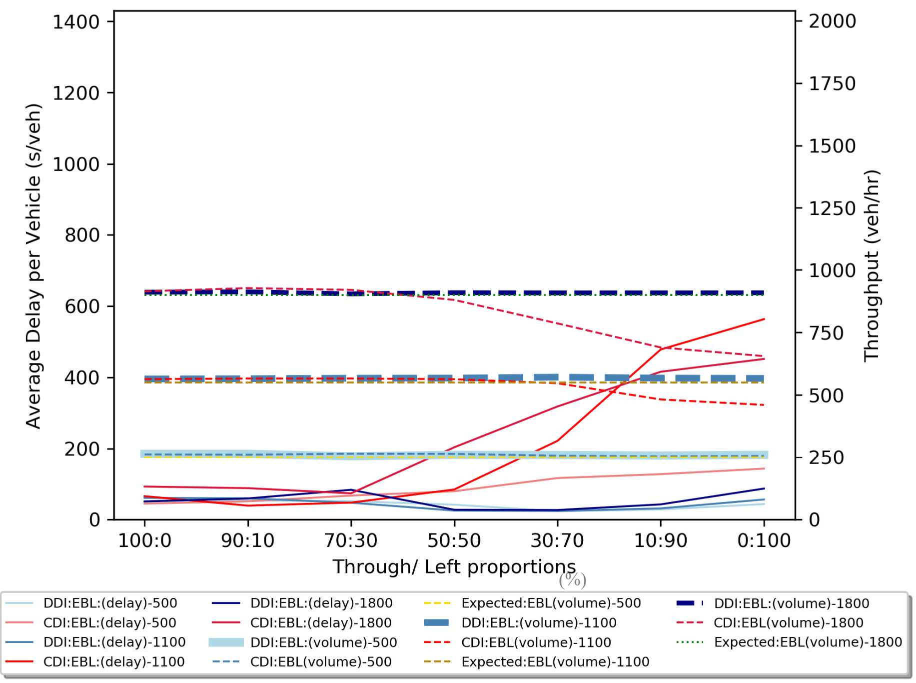

Figure F - 26: DDI and CDI average delay per vehicle and throughput on EBL with cross-street demand of 2100 vph at different off-ramp demands and through/left proportions for LC2

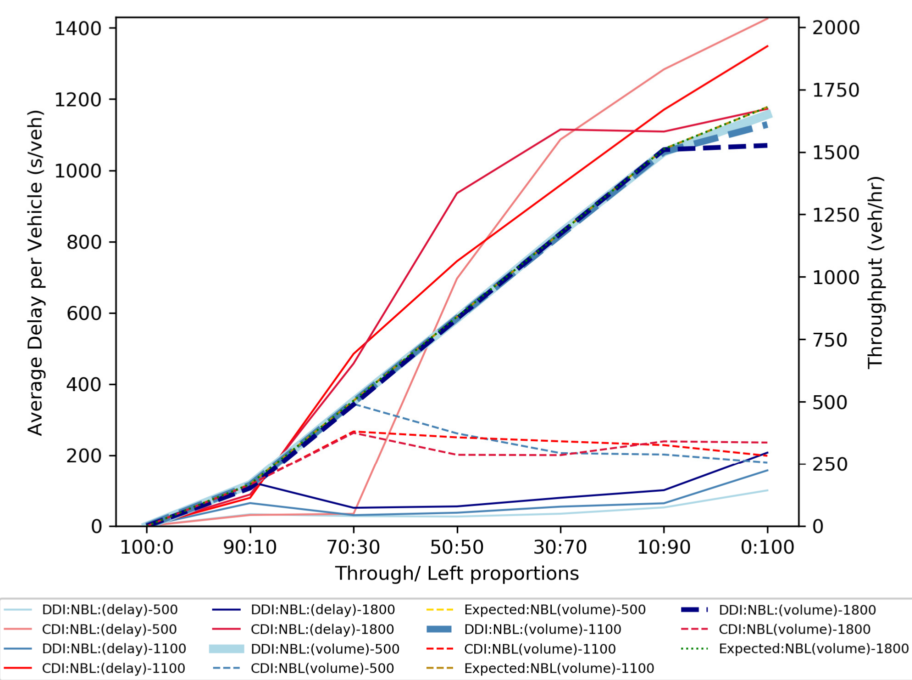

Figure F - 27: DDI and CDI average delay per vehicle and throughput on NBL with cross-street demand of 2100 vph at different off-ramp demands and through/left proportions for LC2

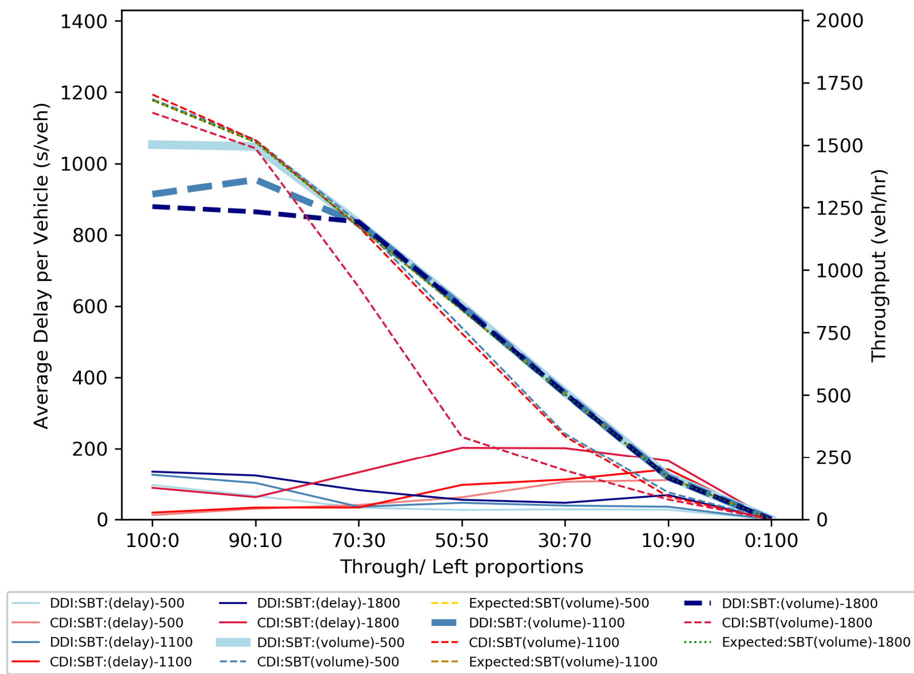

Figure F - 28: DDI and CDI average delay per vehicle and throughput on SBT with cross-street demand of 2100 vph at different off-ramp demands and through/left proportions for LC2

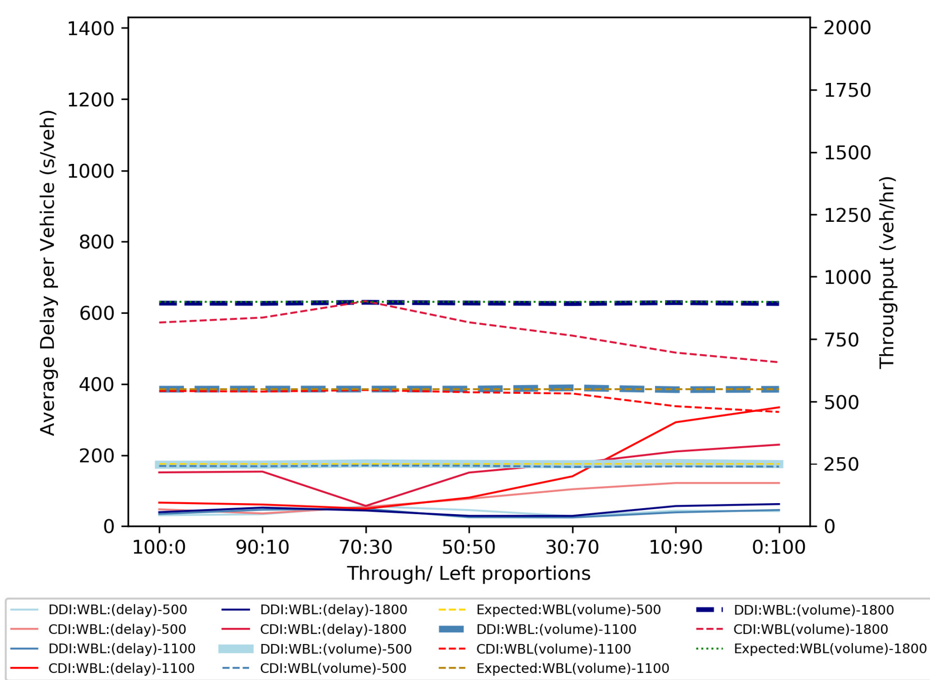

Figure F - 29: DDI and CDI average delay per vehicle and throughput on WBL with cross-street demand of 2100 vph at different off-ramp demands and through/left proportions for LC2

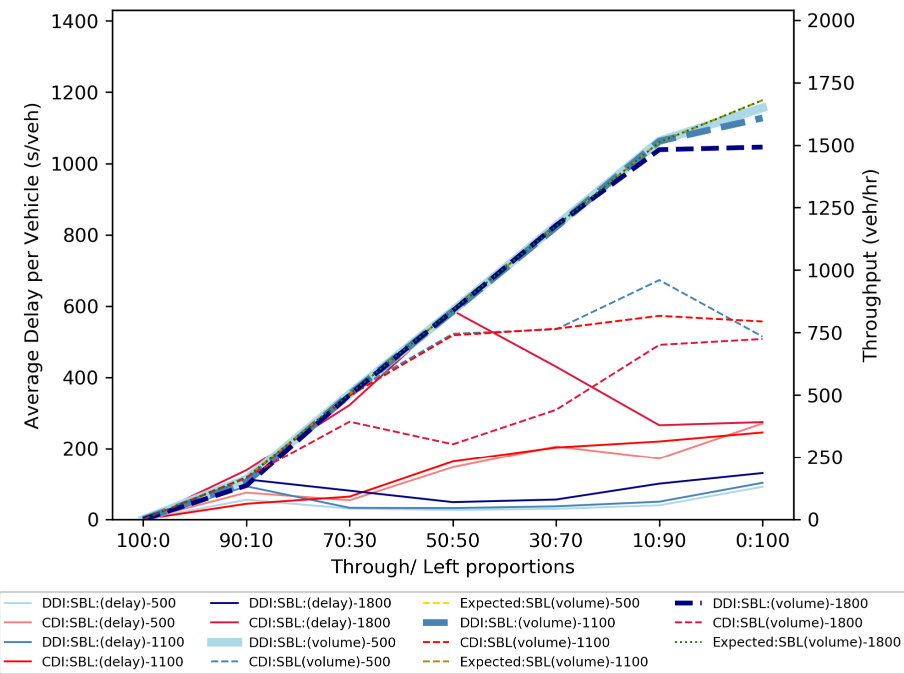

Figure F - 30: DDI and CDI average delay per vehicle and throughput on SBL with cross-street demand of 2100 vph at different off-ramp demands and through/left proportions for LC2

F.2.3 Cross-Street Demand: 2500 vph

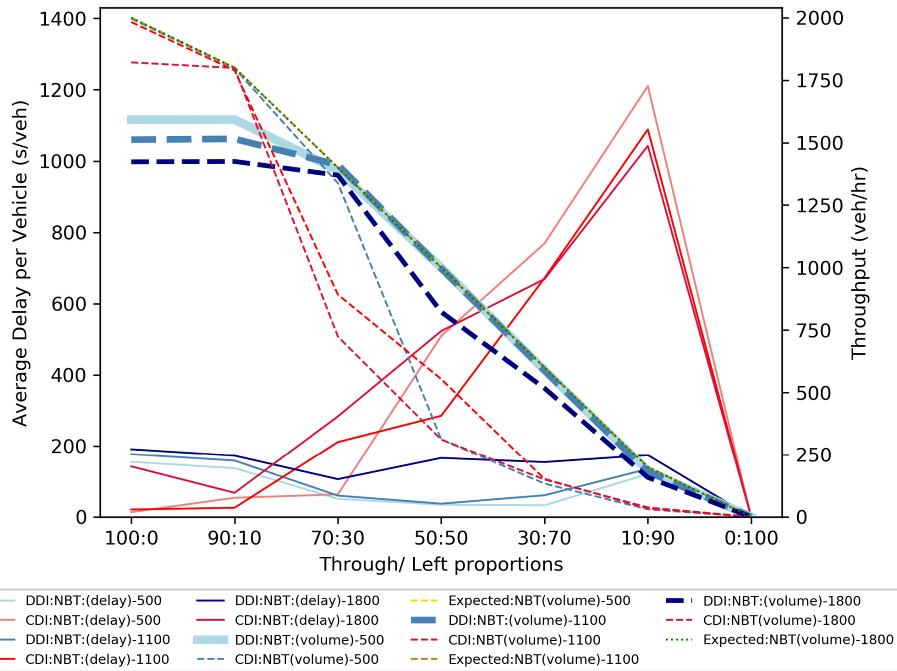

Figure F - 31: DDI and CDI average delay per vehicle and throughput on NBT with cross-street demand of 2500 vph at different off-ramp demands and through/left proportions for LC2

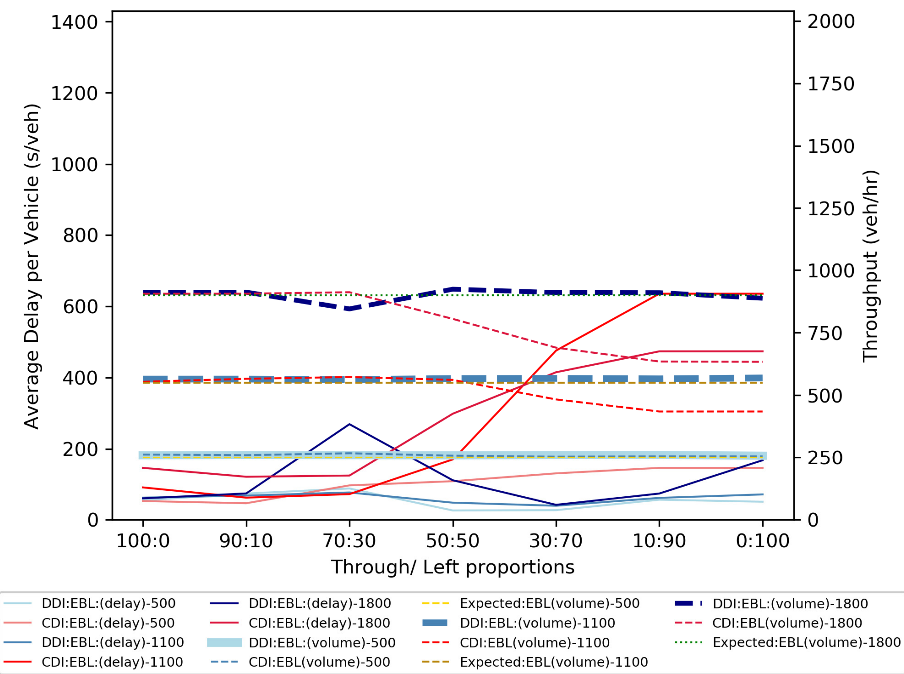

Figure F - 32: DDI and CDI average delay per vehicle and throughput on EBL with cross-street demand of 2500 vph at different off-ramp demands and through/left proportions for LC2

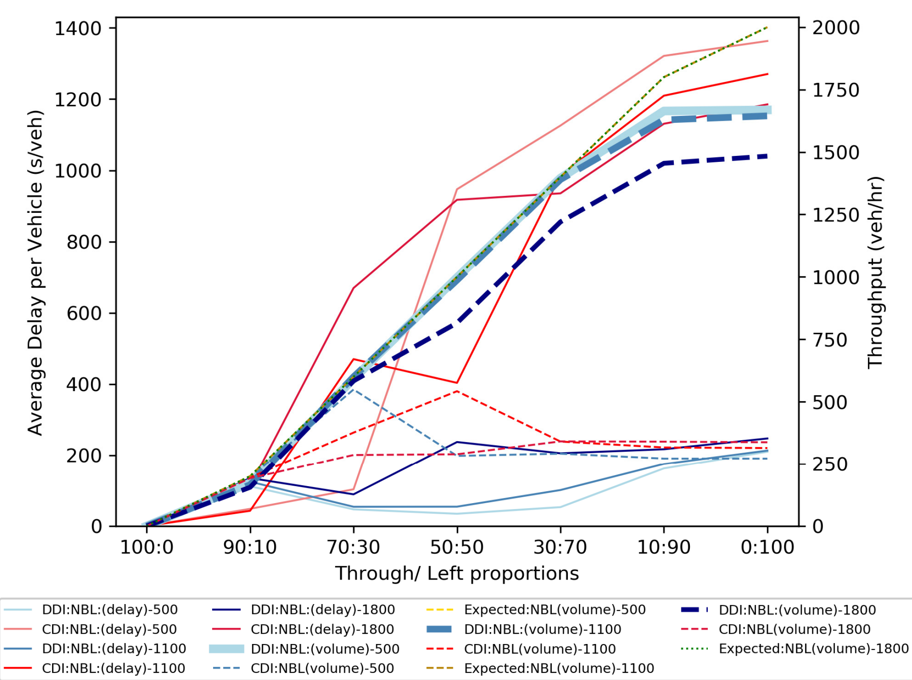

Figure F - 33: DDI and CDI average delay per vehicle and throughput on NBL with cross-street demand of 2500 vph at different off-ramp demands and through/left proportions for LC2

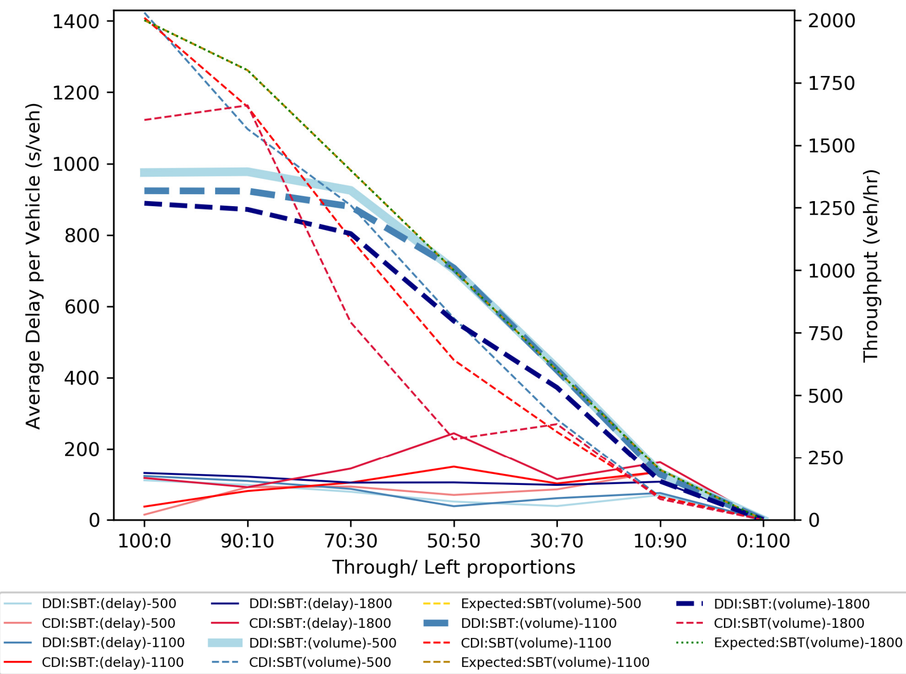

Figure F - 34: DDI and CDI average delay per vehicle and throughput on SBT with cross-street demand of 2500 vph at different off-ramp demands and through/left proportions for LC2

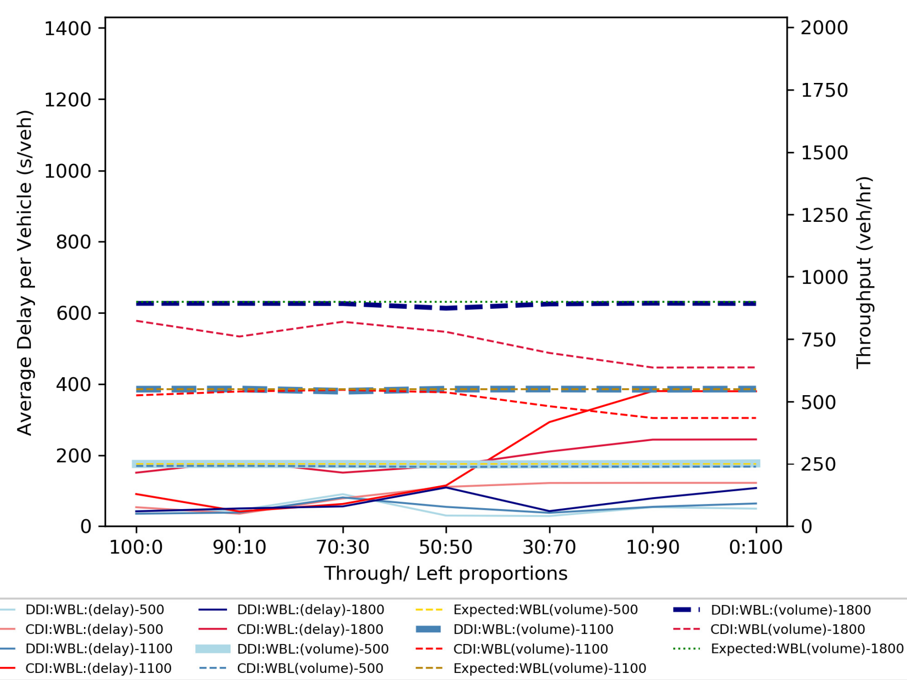

Figure F - 35: DDI and CDI average delay per vehicle and throughput on WBL with cross-street demand of 2500 vph at different off-ramp demands and through/left proportions for LC2

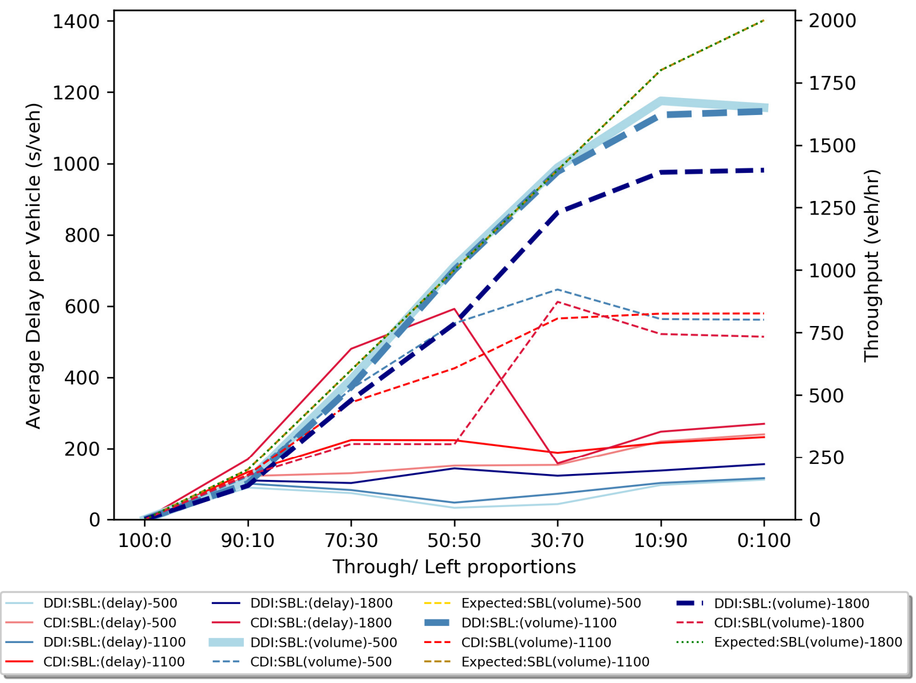

Figure F - 36: DDI and CDI average delay per vehicle and throughput on SBL with cross-street demand of 2500 vph at different off-ramp demands and through/left proportions for LC2

F.3 Lane Configuration 3

F.3.1 Cross-Street Demand: 1500 vph

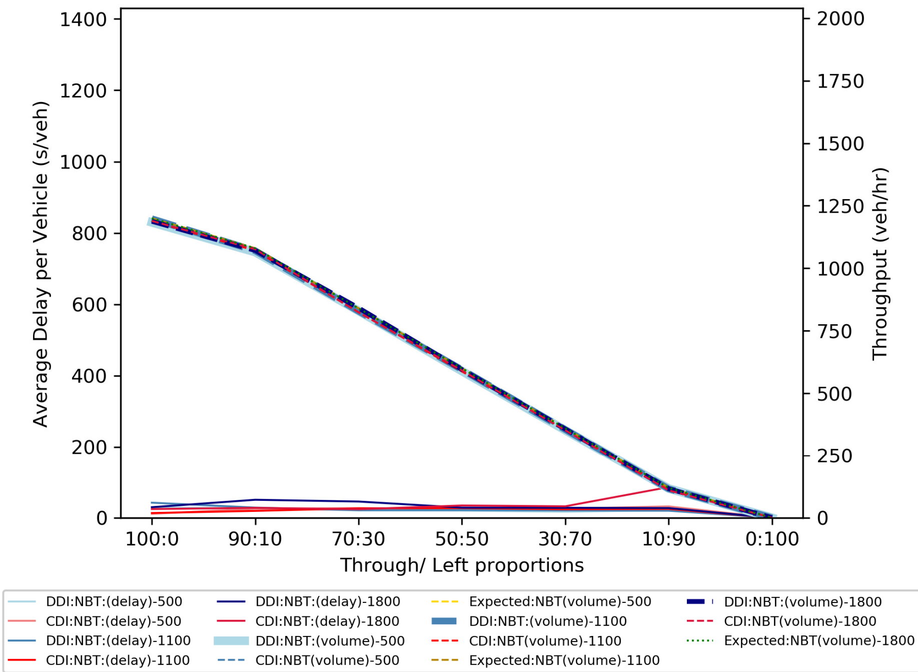

Figure F - 37: DDI and CDI average delay per vehicle and throughput on NBT with cross-street demand of 1500 vph at different off-ramp demands and through/left proportions for LC3

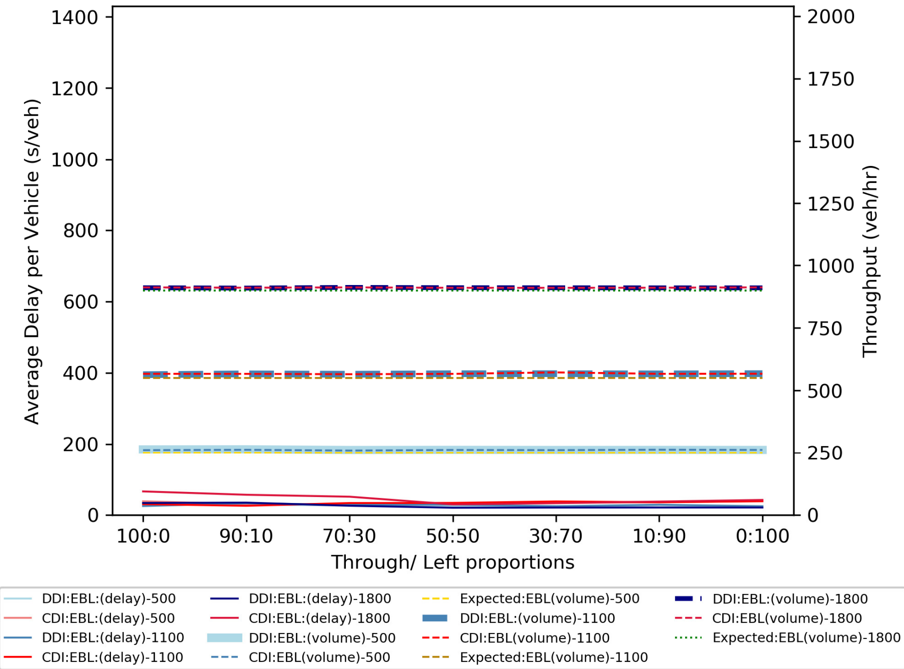

Figure F - 38: DDI and CDI average delay per vehicle and throughput on EBL with cross-street demand of 1500 vph at different off-ramp demands and through/left proportions for LC3

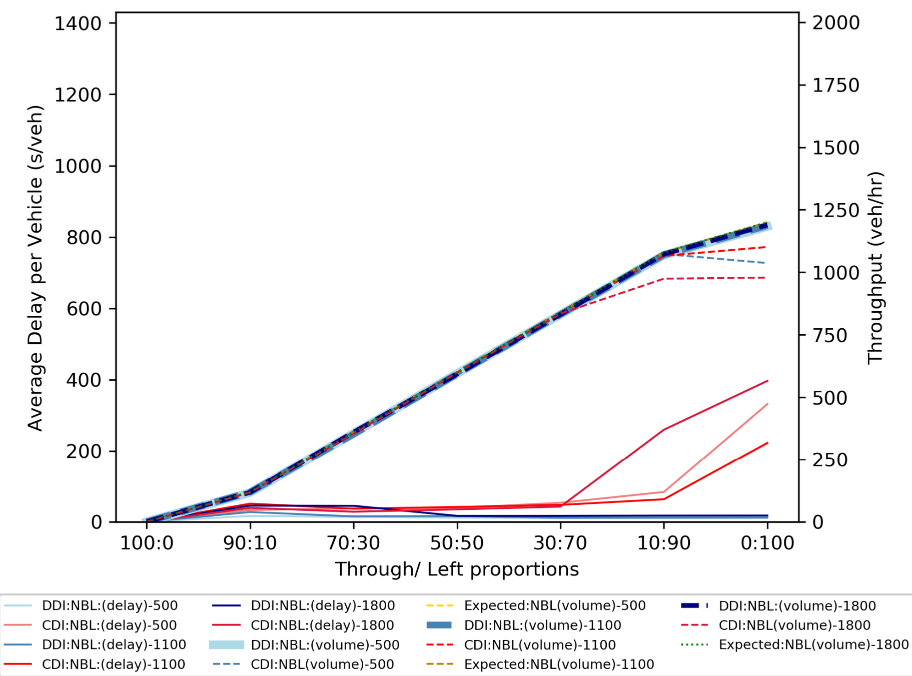

Figure F - 39: DDI and CDI average delay per vehicle and throughput on NBL with cross-street demand of 1500 vph at different off-ramp demands and through/left proportions for LC3

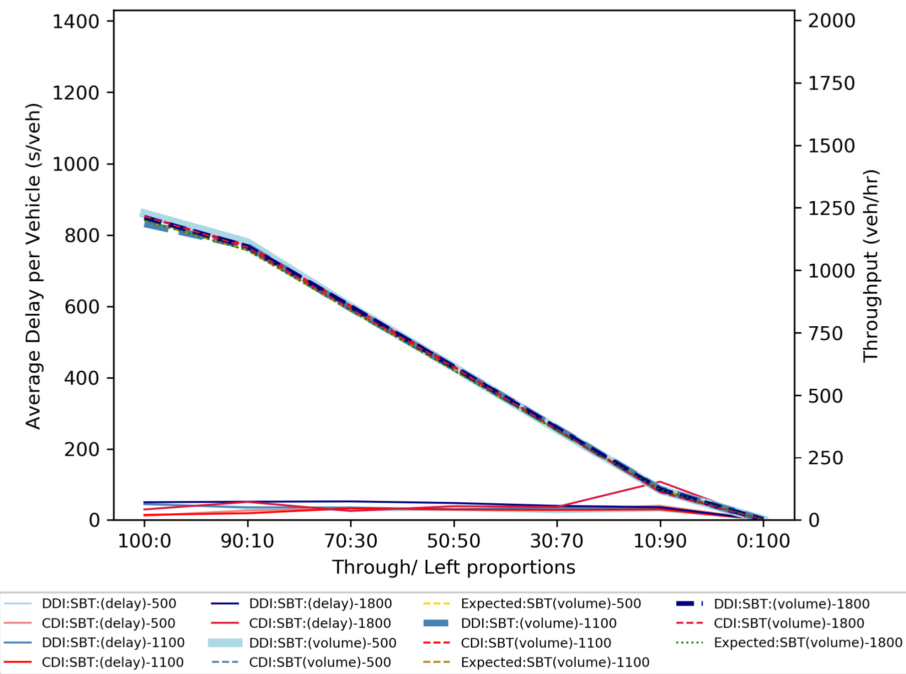

Figure F - 40: DDI and CDI average delay per vehicle and throughput on SBT with cross-street demand of 1500 vph at different off-ramp demands and through/left proportions for LC3

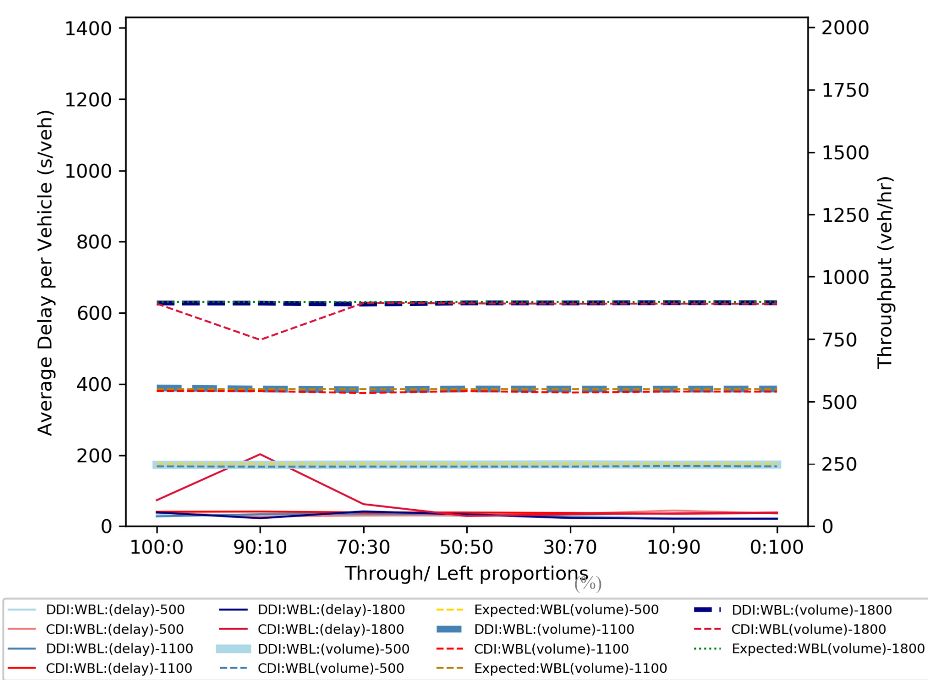

Figure F - 41: DDI and CDI average delay per vehicle and throughput on WBL with cross-street demand of 1500 vph at different off-ramp demands and through/left proportions for LC3

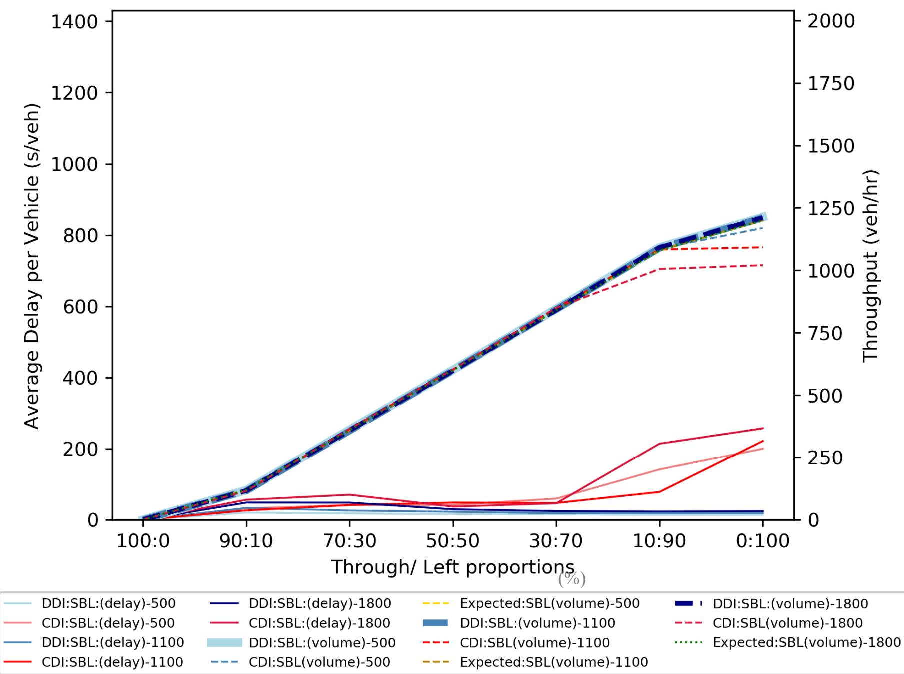

Figure F - 42: DDI and CDI average delay per vehicle and throughput on SBL with cross-street demand of 1500 vph at different off-ramp demands and through/left proportions for LC3

F.3.2 Cross-Street Demand: 2100 vph

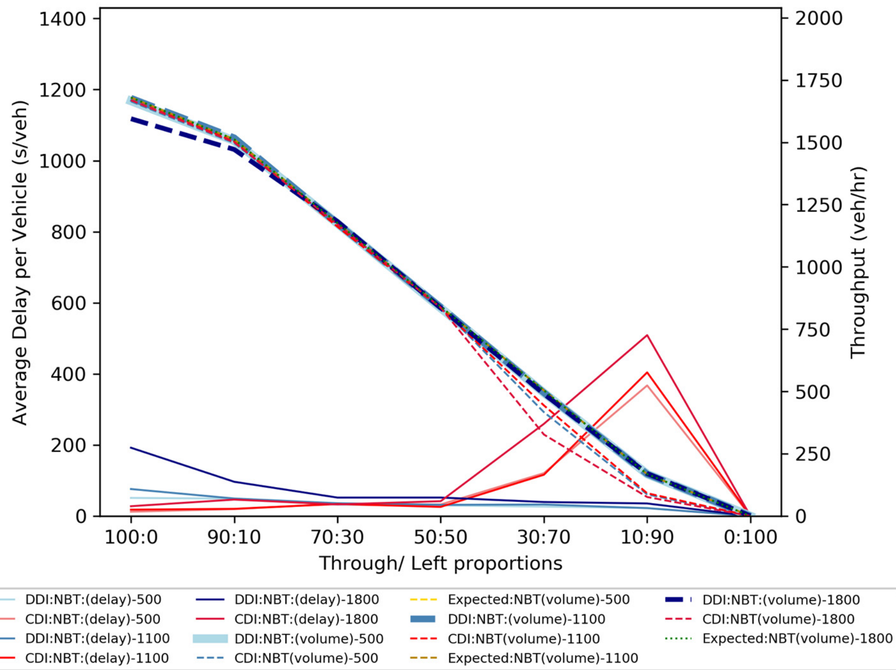

Figure F - 43: DDI and CDI average delay per vehicle and throughput on NBT with cross-street demand of 2100 vph at different off-ramp demands and through/left proportions for LC3

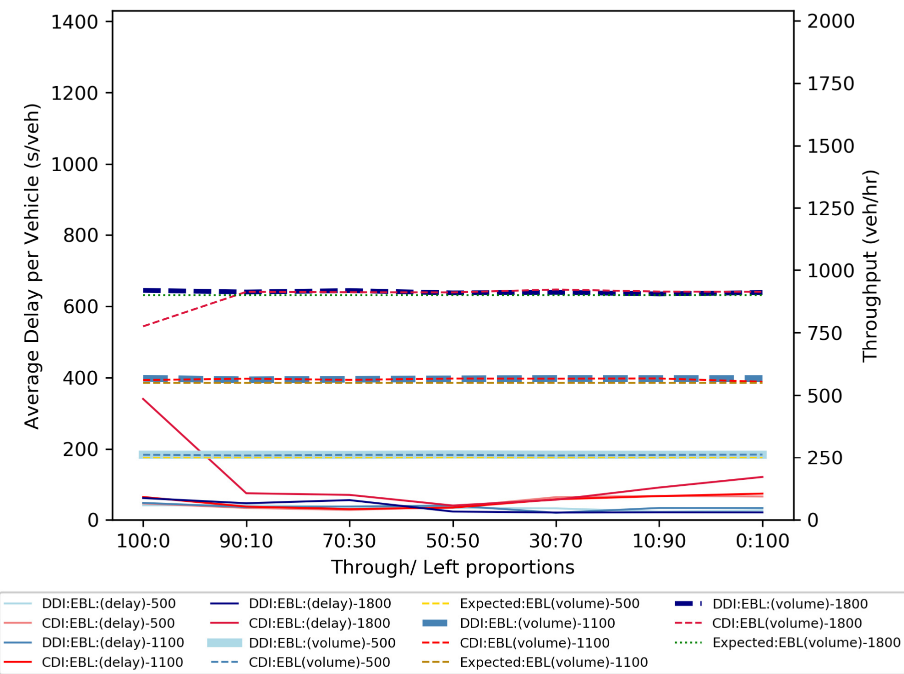

Figure F - 44: DDI and CDI average delay per vehicle and throughput on EBL with cross-street demand of 2100 vph at different off-ramp demands and through/left proportions for LC3

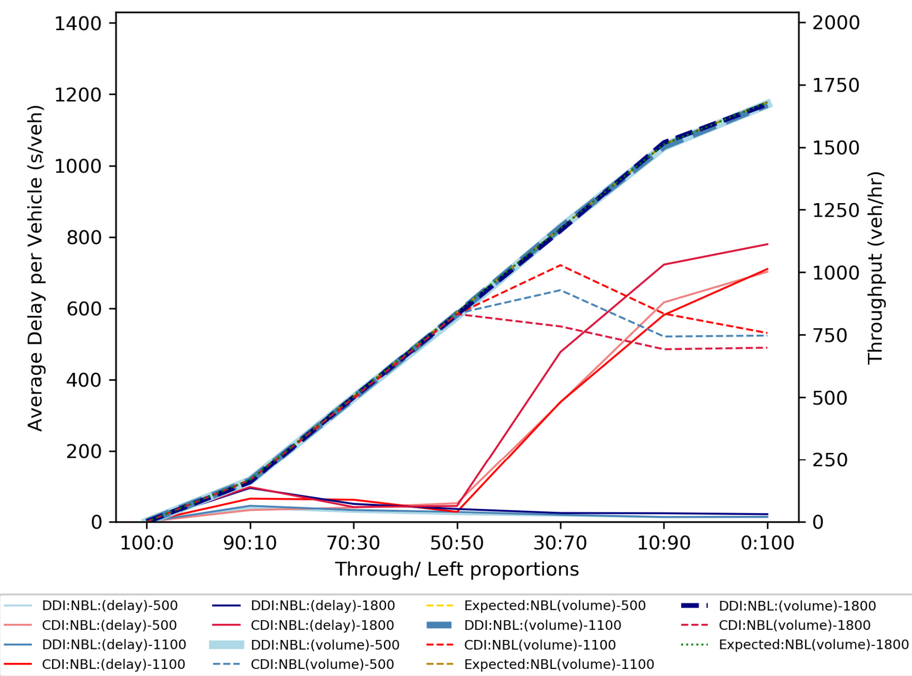

Figure F - 45: DDI and CDI average delay per vehicle and throughput on NBL with cross-street demand of 2100 vph at different off-ramp demands and through/left proportions for LC3

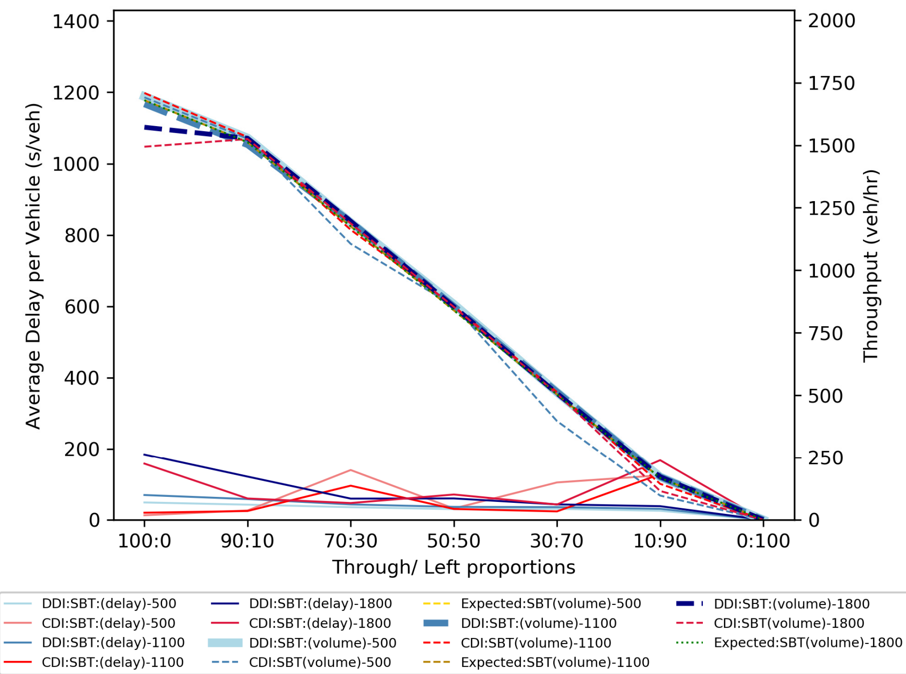

Figure F - 46: DDI and CDI average delay per vehicle and throughput on SBT with cross-street demand of 2100 vph at different off-ramp demands and through/left proportions for LC3

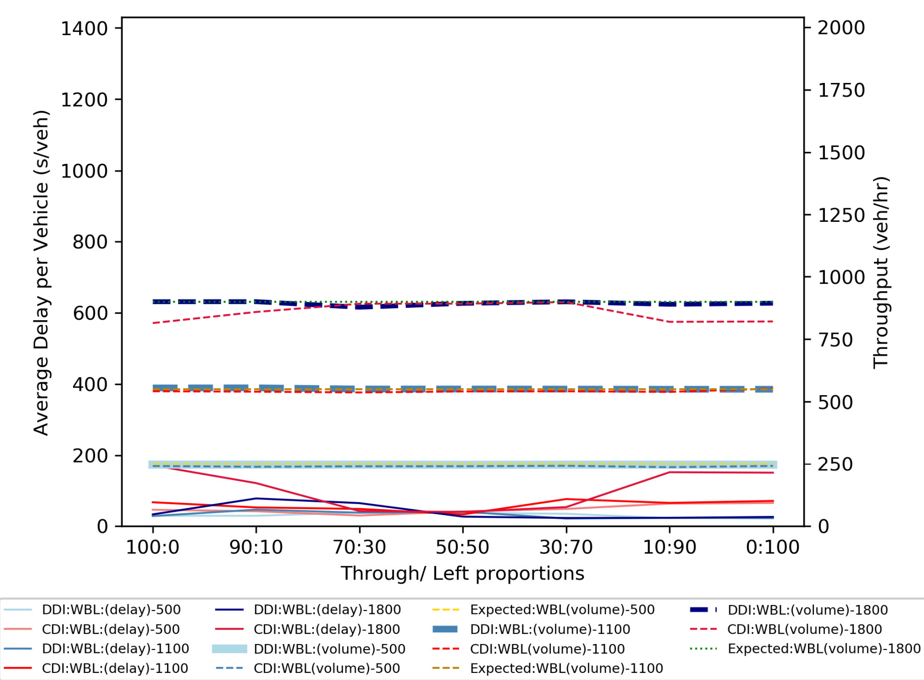

Figure F - 47: DDI and CDI average delay per vehicle and throughput on WBL with cross-street demand of 2100 vph at different off-ramp demands and through/left proportions for LC3

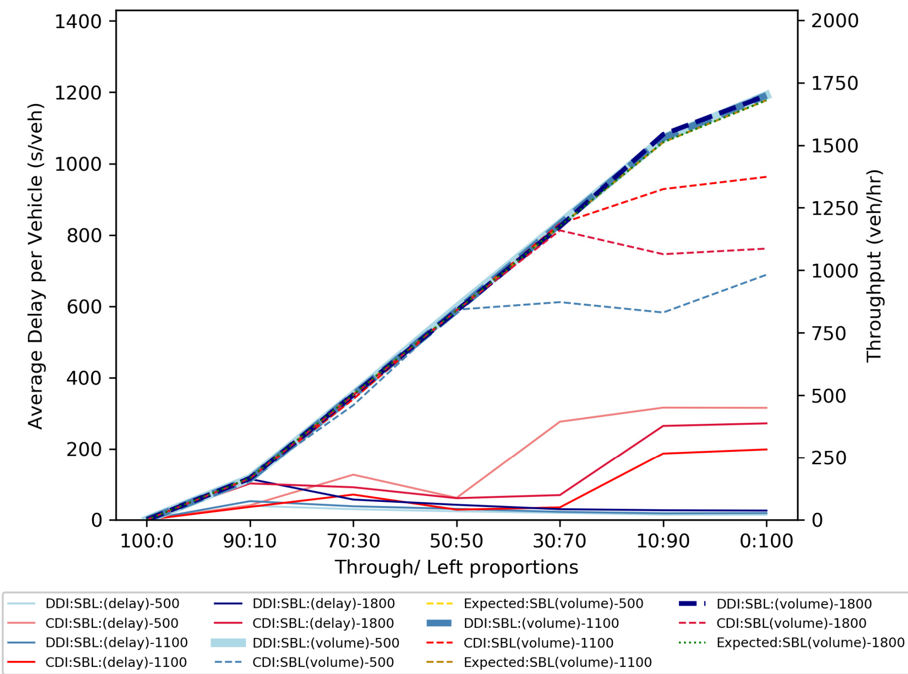

Figure F - 48: DDI and CDI average delay per vehicle and throughput on SBL with cross-street demand of 2100 vph at different off-ramp demands and through/left proportions for LC3

F.3.3 Cross-Street Demand: 2500 vph

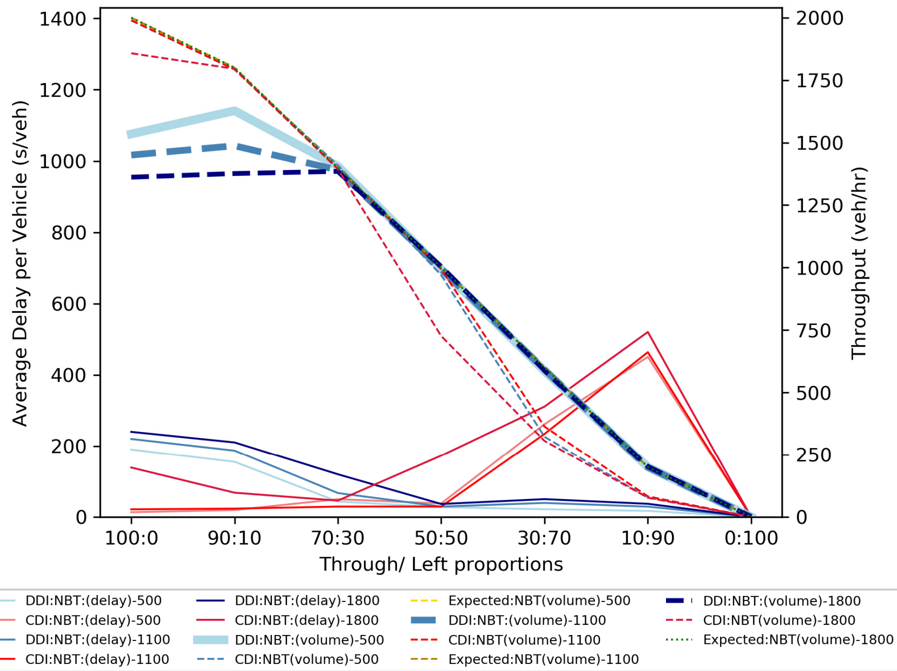

Figure F - 49: DDI and CDI average delay per vehicle and throughput on NBT with cross-street demand of 2500 vph at different off-ramp demands and through/left proportions for LC3

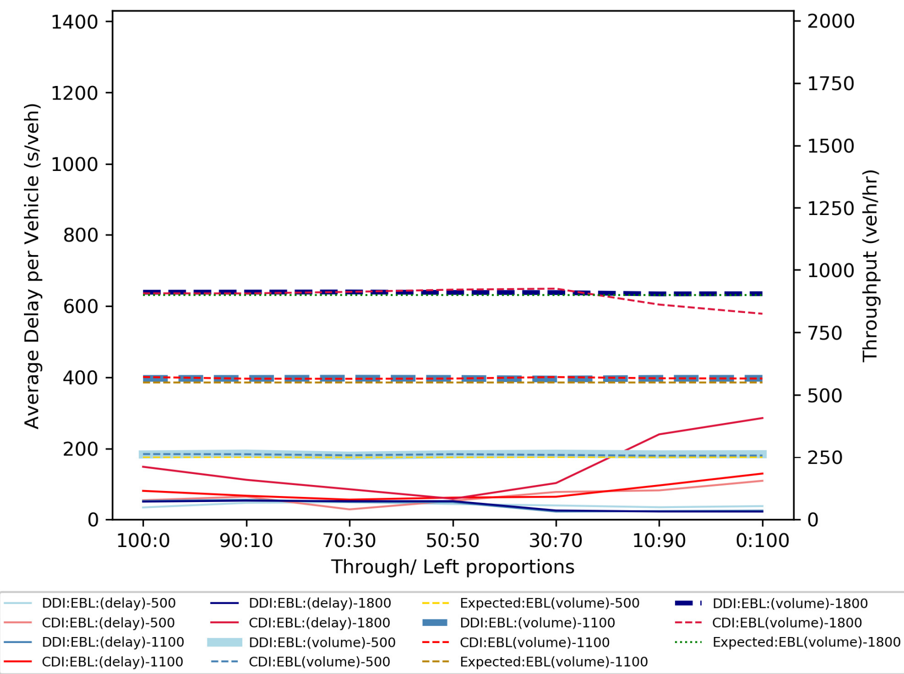

Figure F - 50: DDI and CDI average delay per vehicle and throughput on EBL with cross-street demand of 2500 vph at different off-ramp demands and through/left proportions for LC3

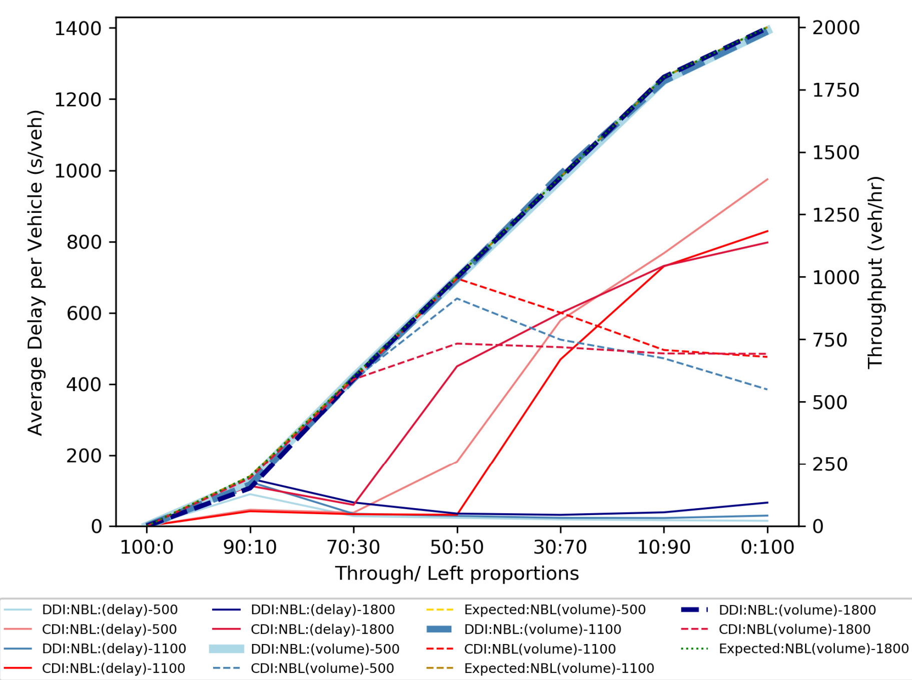

Figure F - 51: DDI and CDI average delay per vehicle and throughput on NBL with cross-street demand of 2500 vph at different off-ramp demands and through/left proportions for LC3

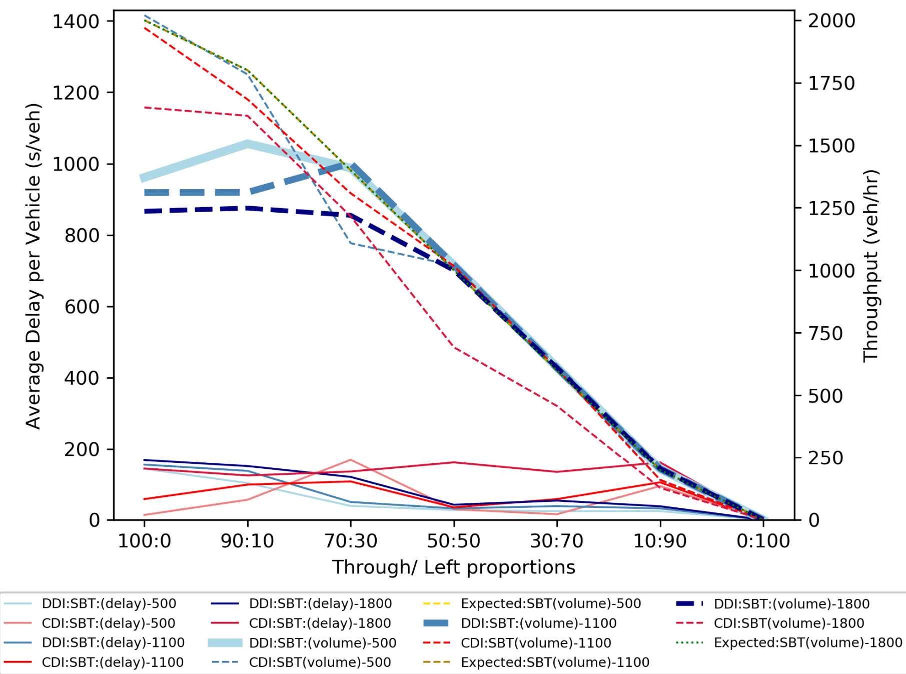

Figure F - 52: DDI and CDI average delay per vehicle and throughput on SBT with cross-street demand of 2500 vph at different off-ramp demands and through/left proportions for LC3

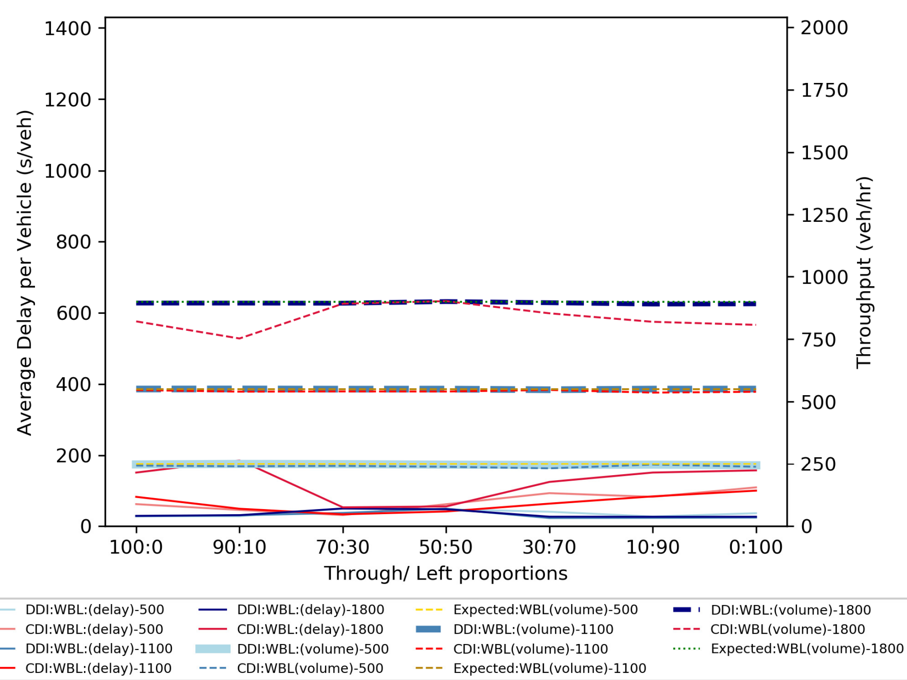

Figure F - 53: DDI and CDI average delay per vehicle and throughput on WBL with cross-street demand of 2500 vph at different off-ramp demands and through/left proportions for LC3

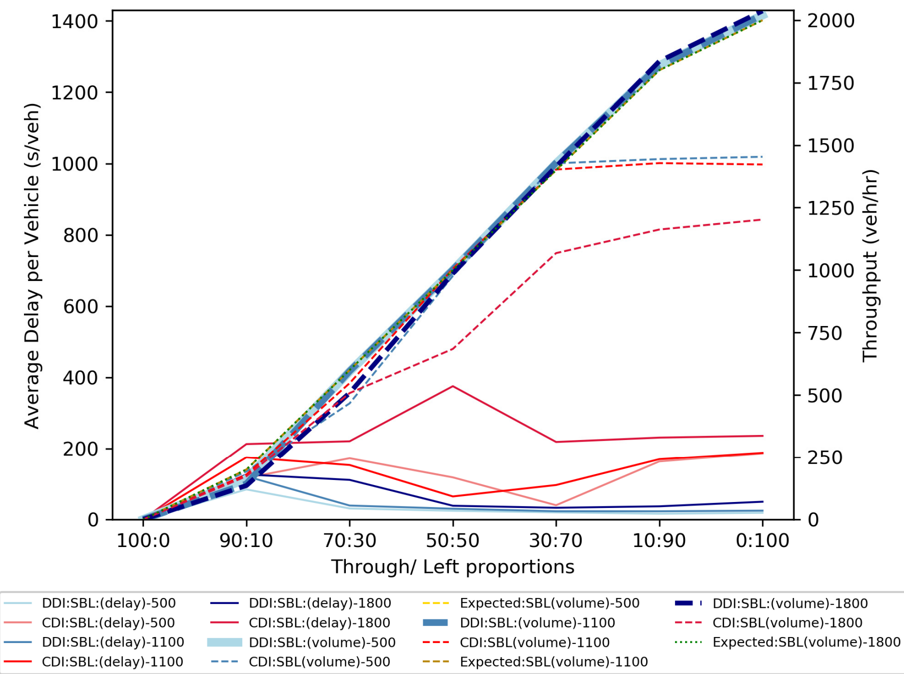

Figure F - 54: DDI and CDI average delay per vehicle and throughput on SBL with cross-street demand of 2500 vph at different off-ramp demands and through/left proportions for LC3